

A Thesis Submitted for the Degree of PhD at the University of Warwick

Permanent WRAP URL:

<http://wrap.warwick.ac.uk/161646>

Copyright and reuse:

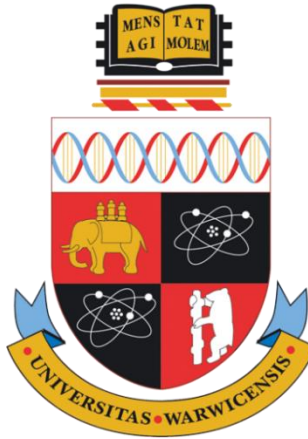
This thesis is made available online and is protected by original copyright.

Please scroll down to view the document itself.

Please refer to the repository record for this item for information to help you to cite it.

Our policy information is available from the repository home page.

For more information, please contact the WRAP Team at: wrap@warwick.ac.uk



Development of Methodology and Test Platform for Local Energy System Analysis and Optimal Operation

by

Songshan Guo

Thesis

Submitted to The University of Warwick

For the degree of

Doctor of Philosophy

In the subject of

Engineering

University of Warwick

Coventry, CV4 7AL

June 2021

Table of Contents

TABLE OF CONTENTS.....	I
ACKNOWLEDGEMENTS.....	IV
DECLARATION.....	V
ABSTRACT.....	VI
LIST OF ABBREVIATION.....	VIII
LIST OF FIGURES.....	X
LIST OF TABLES.....	XIV
CHAPTER 1 INTRODUCTION.....	1
1.1 Background and Motivation	2
1.2 Research Objectives.....	5
1.3 Thesis Structure	6
1.4 Publication and Presentations	9
CHAPTER 2 LITERATURE REVIEW.....	10
2.1 Introduction of Power System Evolution and Revolution.....	11
2.1.1 The Driving Force of Power System Evolution and Revolution.....	12
2.1.2 Evolution of Electricity Market with the Evolution and Revolution of Power Systems	15
2.2 Internet of Things (IoT) Technology for Power System.....	17
2.3 Challenges and Solutions Presenting in Local Energy System.....	21
2.3.1 Modelling and Simulation Methods of Local Energy System	21
2.3.2 Automating Industrial Challenges and Solutions in Local Energy System.....	25
2.3.3 Techno-Economic Assessment in Local Energy System.....	26
2.4 Forecasting Methods in Local Energy System.....	29
2.4.1 Load Forecasting	29
2.4.2 Generation Forecasting.....	30
2.5 Uncertainty Management.....	32
2.5.1 Probabilistic methods	32
2.5.2 Scenarios generation.....	35
2.6 Scheduling Optimisation Algorithm	37
2.7 Relation with my work.....	40
2.8 Summary.....	42
CHAPTER 3 DEVELOPMENT OF IOT AND HIL CO-SIMULATION PLATFORM FOR LOCAL ENERGY SYSTEM STUDY AND ANALYSIS.....	44
3.1 Introduction.....	45
3.2 Current Challenges of HIL and IoT Techniques in LES Simulation	46
3.2.1 HIL Techniques and Challenges in LES simulation	46

3.2.2	IoT Techniques and Challenges in LES Simulation	49
3.3	The Development of Co-Simulation System	50
3.3.1	IoT System Integration	51
3.3.2	Implementation of Time Synchronization	53
3.3.3	IoT System Security	55
3.3.4	Data Compression	56
3.3.5	Simulator Development.....	60
3.4	Cases Study.....	64
3.4.1	Case Study of Simulator	64
3.4.2	Case study of Co-Simulation System	68
3.5	Summary.....	73
CHAPTER 4 OPTIMAL SCHEDULING OF CHP-BASED ENERGY SYSTEM		75
4.1	Introduction.....	76
4.2	Uncertainties of Energy Supply and Demand.....	76
4.2.1	Demand Uncertainties	77
4.2.2	Supply Uncertainties.....	78
4.3	Modelling of CHP-based Energy System	79
4.3.1	Introduction of CHP-Based Energy System	79
4.3.2	Problem Formulation and System Modelling	80
4.4	Scenarios Generation for Scheduling Optimisation.....	85
4.5	Case Study	87
4.5.1	Test System	87
4.5.2	Scenarios Generation.....	91
4.5.3	Optimal Operation Strategies for Different Scenarios	92
4.5.4	Sensitivity Analysis of the Impact of Battery Capacity	101
4.6	Summary.....	102
CHAPTER 5 TECHNO-ECONOMIC STUDY OF SOLAR ENERGY INTEGRATION TO LOCAL ENERGY SYSTEM.....		104
5.1	Introduction.....	105
5.2	Modelling of Local Energy System	105
5.3	Introduction of UoW Power System.....	112
5.3.1	Power Distribution System.....	112
5.3.2	Current Solar PV Installation in UoW	113
5.3.3	Current Balance Mechanism of Power Flow in UoW.....	114
5.4	Techno-Economic Study of Solar PV Integration.....	117
5.4.1	Correlation Analysis.....	118
5.4.2	Analysis of Extended Solar PV Integration	119
5.5	Impact of Solar PV Integration on Current UoW Power System.....	128
5.5.1	Modelling of UoW Power Distribution Network.....	128
5.5.2	Results and Analysis.....	130
5.6	Summary.....	137

CHAPTER 6 STUDY ON LOCAL ENERGY SYSTEM WITH A P2P TRADING MECHANISM.....	140
6.1 Introduction.....	141
6.2 Hierarchical P2P Architecture	142
6.2.1 Unstructured Hierarchical P2P Architecture.....	142
6.2.2 Structured Hierarchical P2P Architecture.....	143
6.2.3 Hybrid Hierarchical P2P Architecture.....	145
6.3 P2P Electricity Trading Mechanism	146
6.4 Two-layer P2P Trading Architecture in Local Energy System.....	148
6.5 Case study	152
6.5.1 Convergence Verification.....	153
6.5.2 Study of Trading Mechanism in Local Energy System	154
6.6 Summary.....	163
CHAPTER 7 CONCLUSIONS AND FUTURE WORK	164
REFERENCE.....	168

Acknowledgements

I would like to thank my Ph.D. supervisor, Professor Jihong Wang. I am heartily thankful for her continuous support throughout the process of this research. Professor Jihong Wang offered her help in the development of the quasi-steady model and various optimisation strategies for local energy system. She guided me to different approaches for resolutions of research difficulties and strength my confidence to be persistent in accomplishing goals.

I would like to thank Dr Nan Jia for providing a support on my research work. I wish to thank Mark Jarvis and Joel Cardinal for opening the access to university meter data and providing the financial support to do the techno-economic analysis of solar integration. From the Power and Control Systems Research Lab, I would like to thank my colleagues including Dr Mark Dooner, Dr WeiHe, Dr Decai Li and Dr Dacheng Li for their support, suggestions and friendship throughout my time here.

I would also like to thank my entire family for their emotional and financial support from China. I also owe deepest gratitude to my wife, Clare. Clare had made UK homelike for me. Finally, I offer my regards and blessings to all of those who have supported me in any respect during the completion of the research.

Songshan Guo

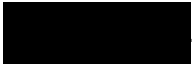
June 2021

Declaration

I hereby declare that the material in this thesis has not been submitted for a higher degree at any other university. This thesis entirely contains research work carried out by Mr Songshan Guo under the supervision of Professor Jihong Wang, unless references are given.

Some parts of this thesis were included in the following published papers:

Songshan Guo, Jihong Wang,” The Modelling and Optimization of Distributed Network Based on Source-Limit Infrastructure,” Applied Energy Symposium: MIT A+B, May 22-24,2019.

Signed.......... (Candidate) Date..... June 2021.....

Abstract

In 2018, UK achieved 33% of its power generation from renewable energy (not including nuclear) and the wind power generation reached 38% on 9th Dec 2019. However, transportation and heating sectors almost remain unchanged compared with 20 years ago. Therefore, to achieve the UK government goal of “net zero emission by 2050”, the three coupled energy sectors of electrical power, transportation and heating must be examined in an integrated systemic way. The challenges of systemically evaluating the local energy system includes the modelling and simulation of coupled energy sectors, the plan and optimization of combined energy system and the innovative power trading mechanism. To address these challenges, this thesis focuses on analysis and optimisation of local energy system and its cooperation with heat supply and local power generation. The main contributions of the thesis are summarized as follows.

The work starts from development of a co-simulation system for local energy systems by combining the Internet-of-Things (IoT) and Hardware-in-the-Loop (HIL) techniques. This provides a platform to test and verify various methods and analysis. The platform takes the advantages of the capability HIL to be able to conduct mixed mathematical and physical modelling study. With the support of IoT system, the simulation/test platform can bring massive real-operation data to the model which extended the power of the test platform.

Using the campus energy system data, scheduling optimisation of Combined Heat and Power (CHP) based local energy system is conducted which is to reduce the energy cost while the system is subject to energy demand and supply uncertainties. A combined scenario generation method is proposed to enable Probability Density Function (PDF) was handled and discretized conveniently. A scheduling multi-objective linear programming problem is formulated with the consideration of practical constraints to minimize the energy cost by avoiding importing electricity from grid at the high tariff period and the optimisation of CHP plant operation can reduce natural gas consumption which is achieved with adding electrical energy storage to the system.

Techno-economic analysis is conducted to explore whether it is economic and technical viable to have solar PV integration with the existing CHP power supply and

what the optimal capacity is for a system with the known CHP power generation capacity. The study also investigates how the solar integration impact on the existing power distribution network. The work has its significance to LES planning, design and management. The study will use Warwick University campus energy system data acquired from data server of co-simulation system for analysis and strategy development.

A P2P electricity trading mechanism with hierarchical P2P architecture is proposed with the aim to enhance revenue of prosumers by applying a game theory in pricing competition. This trading mechanism is to motivate prosumers to actively take part in the proposed architecture of trading. Finally, a few cases studies are used to verify the proposed electricity trading mechanism.

List of Abbreviation

ABC	Artificial Bee Colony
ACF	Auto Correlation Function
ACO	Ant Colony Optimisation
AI	Artificial Intelligence
AMI	Advanced Metering Infrastructure
ARIMA	Auto-Regressive Integrated Moving Average
ARMA	Auto Regressive Moving-Average
CoAP	Constrained Application Protocol
DERs.	Distributed Energy Resources
DHT	Distributed Hash Table
DNO	Distributed Network Operator
DNO	Distributed Network Operator
ELVTF	IEEE European Low Voltage Test Feeder
EPS	Electrical Power System
FiT	Feed in Tariff
GA	Genetic Algorithms
HIL	Hardware In Loop
HuT	Hardware under Test
ICT	Information and Communication Technologies
IGDT	Information Gap Decision Theory
IoT	Internet of Things
LES	Local Energy System
MAPE	Mean Absolute Percentage Error
MC	Monte Carlo
MCS	Monte Carlo Simulation
MGO	Micro-Grid Operator
MGs	Micro Grids
MILP	Mix-Integer Linear Problem
MINLP	Mixed Integer Non-Linear Programming
MODA	Multi-Objective Dragonfly Algorithm
MOGA	Multi-Objective Genetic Algorithm

MPS	Multi-Power System
MQTT	MQ Telemetry Transport
NWP	Numerical Weather Prediction
OS	Operating system
PACF	Partial Auto Correlation Function
PDF	Probability Distribution Function
PMUs	Phasor Measurement Units
PSO	Particle Swarm Optimisation
RWM	Roulette Wheel Mechanism
SCADA	Supervisory Control And Data Acquisition
SGAM	Smart Grid Architecture Model
SOC	State of Charge
SSANN	Sub-Structured Artificial Neural Network
SSL	Secure Socket Layer
SVM	Support Vector Machine
TLS	Transport Layer Security
UoW	University of Warwick
XMPP	Extensible Messaging and Presence Protocol

List of Figures

Fig. 2.1 The landscape of power systems (past vs. future) [20].....	12
Fig. 2.2 The LCOE for projects and global weighted average values for CSP, solar PV, onshore and offshore wind, 2010–2022 [27]	14
Fig. 2.3 Impact of digitalisation on electricity sector assets [37].....	15
Fig. 2.4 Areas that IoT can make difference	18
Fig. 2.5 Relationship between EPOCHS' components [80]	22
Fig. 2.6 Residential and industrial subnetworks of distribution system interfaced with DERs [84].....	24
Fig. 2.7 Classification of model based on spatial and temporal resolution.....	32
Fig. 2.8 Classification of probabilistic methods.....	33
Fig. 2.9 Processing of generating different scenarios	36
Fig. 2.10 Flow chart of branch-and-cut algorithm	38
Fig. 3.1 Controller HIL simulations	47
Fig. 3.2 Example of PHIL	47
Fig. 3.3 Example of PHIL with multi-timescale	48
Fig. 3.4 Architecture of co-simulation system	51
Fig. 3.5 IoT world forum reference model [135]	52
Fig. 3.6 IoT hardware devices	53
Fig. 3.7 Time synchronization mechanism	54
Fig. 3.8 Security list in IoT system	55
Fig. 3.9 IoT security architecture	56
Fig. 3.10 Edge gateway mode	58
Fig. 3.11 Structure of hybrid simulator	61
Fig. 3.12 Two synchronization scheme.....	62
Fig. 3.13 Discharging/charging efficiency of inverter	62
Fig. 3.14 Communication architecture of hybrid simulator	64
Fig. 3.15 European low voltage test feeder [142]	65
Fig. 3.16 Local energy system for case study	66
Fig. 3.17 Distribution of load demand	67
Fig. 3.18 Reference bid price	67
Fig. 3.19 Clearing price and capacity.....	68
Fig. 3.20 Scheduling of battery management.....	68

Fig. 3.21 Architecture of co-simulation for case study	69
Fig. 3.22 Diagram of power co-simulation	69
Fig. 3.23 Battery storage system in the UoW	70
Fig. 3.24 Control outputs (hardware vs. simulator)	71
Fig. 3.25 Connection node of battery system.....	72
Fig. 3.26 Node load profile and battery scheduling	72
Fig. 3.27 Node voltage	73
Fig. 4.1 Diagram of CHP-based energy system	79
Fig. 4.2 Flowchart of hybrid scenario generation method	87
Fig. 4.3 Single line diagram of test distribution system.....	88
Fig. 4.4 Electricity efficiency of each CHP unit	89
Fig. 4.5 Part load efficiency of grouped CHP	90
Fig. 4.6 half-hourly historical data from Jan 2018 to Jan 2019	91
Fig. 4.7 Scenarios by using scenred technology (half-hourly).....	92
Fig. 4.8 Probability distribution of each scenario	93
Fig. 4.9 Operation cost distribution of each scenario.....	94
Fig. 4.10 Results of optimal electricity scheduling.....	97
Fig. 4.11 Results of optimal heat scheduling	100
Fig. 4.12 Difference in operation cost (fix-step vs.variable-step).....	101
Fig. 4.13 Annual operation cost of the energy system in different cases.....	102
Fig. 5.1 Equivalent distribution system with or without zero impedances	106
Fig. 5.2 Flow chart of hybrid Newton Raphson method.....	111
Fig. 5.3 One-line diagram of distribution system	111
Fig. 5.4 Diagram of the University campus power distribution system.....	113
Fig. 5.5 Diagram presenting the installed solar panels network	114
Fig. 5.6 Capacity of potential solar installation in each sector	114
Fig. 5.7 Load demand vs. CHP electrical power generation.....	116
Fig. 5.8 Solar generation for Year 2018.....	116
Fig. 5.9 Electricity bought from the grid (November)	117
Fig. 5.10 Solar generation vs. Load demand.....	119
Fig. 5.11 Purchased energy from grid (248 kW solar vs. 4.2 MW solar)	121
Fig. 5.12 Energy distribution (exporting to grid).....	121
Fig. 5.13 Import electricity from grid based on different scenarios (daily)...	122
Fig. 5.14 Distribution of export electricity based on different scenarios.....	123

Fig. 5.15 Cost breakdown for the solar system [166]	124
Fig. 5.16 Cost assumption for the solar system [166].....	124
Fig. 5.17 Import electricity in different scenarios (half hourly).....	126
Fig. 5.18 Simulation architecture of Warwick distribution network.....	129
Fig. 5.19 Example of load profile for various nodes.....	130
Fig. 5.20 The placement of solar generation system.....	131
Fig. 5.21 Power import with and without solar power generation.....	131
Fig. 5.22 Total solar output of the node_70360	132
Fig. 5.23 Power losses of distribution system.....	133
Fig. 5.24 11kV voltage profiles on different nodes-base	133
Fig. 5.25 11 kV voltage profiles on different nodes-with solar installation...	133
Fig. 5.26 400V voltage profiles on different meters-base.....	134
Fig. 5.27 400V voltage profiles on different meters-with solar installation .	134
Fig. 5.28 The placement of solar generation systems	135
Fig. 5.29 Power input of the main substation.....	136
Fig. 5.30 Power losses of distribution system.....	136
Fig. 5.31 11 kV voltage profiles on different nodes-with solar installation...	137
Fig. 5.32 400V voltage profiles on different meters-with solar PV installation	137
Fig. 6.1 Architecture of hierarchical P2P	142
Fig. 6.2 Architectire of Gnutella v0.6	143
Fig. 6.3 Architecture of vertical hierarchical P2P	144
Fig. 6.4 Architecture of horizontal hierarchical P2P.....	145
Fig. 6.5 Architecture of hybrid hierarchical P2P	146
Fig. 6.6 Game theory approaches and optimisation solutions.....	147
Fig.6.7 Two-layer P2P trading system	148
Fig. 6.8 Diagram of three-stage steps.....	150
Fig. 6.9 PDT vs. τ for fixed assumption	153
Fig. 6.10 PDT vs. τ for different variances	154
Fig. 6.11 Load curves of consumers	155
Fig. 6.12 Variance for load curves	155
Fig. 6.13 Curves of solar generation	156
Fig. 6.14 Curves of wind generation.....	157
Fig. 6.15 Working schedule of EV chargers and Battery systems.....	157

Fig. 6.16 Mean and variance in different networks.....	158
Fig. 6.17 P_{P2P} in different MG markets	159
Fig. 6.18 P_{P2P} vs τ & η in gateway layer.....	161
Fig. 6.19 Total revenues of different MGs: 1-layer P2P system vs 2-layer P2P system.....	163

List of Tables

Table 3-1 SVD compression results.....	59
Table 4-1 System components data.....	88
Table 4-2 Parameters of fitting curve.....	90
Table 4-3 Parameters of modelling for scheduling optimisation	90
Table 4-4 Battery capacity levels for sensitivity analysis	102
Table 5-1 Pearson's Correlation Coefficient and representative strengths.....	118
Table 5-2 Correlations between different parameters	119
Table 5-3 Scenarios of solar installation	122
Table 5-4 Export electricity in different scenarios.....	123
Table 5-5 Payback years of investment.....	125
Table 5-6 Payback years of the investment.....	126
Table 5-7 Payback years of the investment of hybrid systems	127
Table 5-8 Payback years of the investment of the hybrid system.....	128
Table 6-1 Number of participants from each MG in gateway layer.....	159

Chapter 1

Introduction

1.1 Background and Motivation

Energy sector is now facing great challenges in meeting the continuous growth in energy demand and the green-gas emission reduction target. It is predicted that the global energy demand will increase from 13.8 billion tonnes oil equivalent (toe) in 2016 to 19.3 billion toes in 2040 [1]. If “business as usual” continues in energy sector, CO₂ emissions would increase from 32.1 billion tonnes to 42.7 billion tonnes per year, which conflicts with the COP 21 Paris agreement (2015) emission target [2]. According to the Department for Business, Energy and Industrial Strategy’s (BEIS) latest energy trends data, renewables’ share of electricity generation was 47% during the quarter, up from 35.9% in the first quarter of 2019 [3]. However, transportation and heating sectors almost remain unchanged compared with 20 years ago. Therefore, to achieve the UK government goal of “net zero emission by 2050”, the three coupled energy sectors of electrical power, transportation and heating must be examined in an integrated systemic way. The transition moving towards to sustainable energy through the accelerated adoption of clean energy technologies and energy efficiency practice requires the engagement multifaceted factors from scientific, financial, industrial, and public-policy communities. As illustrated in Fig.1.1 [4], the transition is influenced by complex coupling factors, including government policies, investment, technology progress and innovation, and environmental restrictions and people.

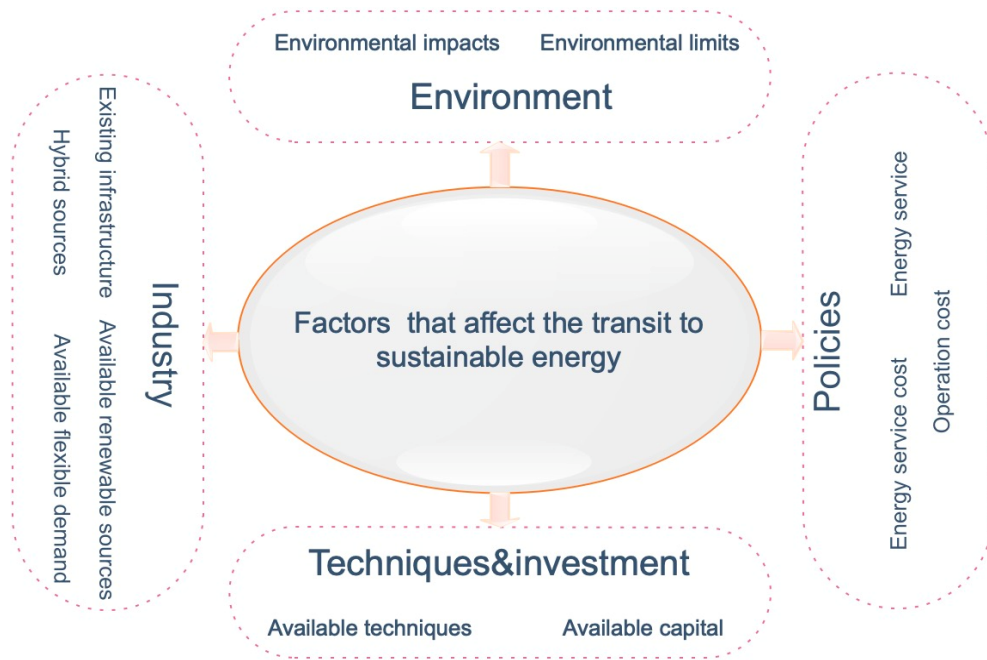


Fig. 1.1 Illustration of factors affecting the progress towards sustainable energy [4]

To address the decarbonisation challenges, it is essential to consider the whole energy process including production, conversion, delivery and consumption. The thesis focuses on analysis and optimisation of power systems at the distribution network level and its co-operation with heat supply and local power generation. Power system is currently experiencing great changes and transformation, that is, it is moving from one-way power flow to two directional power flow. Also, Smart Grid was proposed 15 years ago [5] to introduce the new concept to enable electricity consumers having active roles in electrical system management. The main trend of changes is summarised as follows:

1) Rapidly increased penetration of distributed electricity power generation

With the increase of local power generation such as solar, bio-fuel and CHP, the electricity power flow at the distribution level becomes bi-directional and the consumers are no longer pure electricity users since they can generate power and feed power to network [6]. This transformation generates great impact onto power system operation and makes the power system from transmission to distribution more difficult to plan ahead in terms of optimal operation [7]. For example, it is hard to predict the load demand due to its coupling with local generation and various uncertain variables associated with it. The power system operation and management become more complex; meanwhile, this also brings new

opportunities to the power system management [8]. Local generation, electricity storage and flexible load can participate the power system operation to reduce the power flow congestion, delay investment of over headlines and provide urgent power need to enhance the power system resilience. So, the challenging task is how to encourage local generation from green energy sources and also de-risk uncertainties caused by distributed power generation.

2) Urgent demand on intelligent data communication and management mechanisms

With the need of more and more decentralised electricity power management, the coordination of the distributed system and power grid (transmission and distribution) requires reliable, efficient and secured data communication and management mechanism and platform ([9],[10]). It is found that this is one of the most active areas in technology innovation and entrepreneur emerging. Although the implementation of those communication infrastructures is growing rapidly in terms of data volume and processing power, it is immature and requires much research effort for innovation and development[11].

3) Evolution of DNO to DSO

With increases of small-scale local power generation from renewable power sources, more consumers become prosumers and actively participate in demand side management. To accommodate the power flow management changes, the electricity market is undergoing reform aiming to provide prosumers an innovative system/platform. Virtual Power Plant (VPP) emerged with the transformation which aggregates the distributed generation and flexible load into a recognizable quantity to have its significance in electricity market[12]. Aggregation of smaller generation and load brings more prosumers to electricity market and generate another dimension of flexibility. In addition to aggregation, some local energy trading concepts are also proposed, such as peer to peer (P2P), to allow the independence of prosumers to interact with their local peers, which encourages “generating locally and consuming locally”[13]. As mentioned earlier, it is urgent to reduce CO₂ emission from heating and transportation. So, the integrated approach for local energy systems to coordinate electricity, heating and transportation becomes inevitable. The current Distribution Network Operators (DNO) has to extend the role to cope with the complexity caused by local

generators, local energy trading and coordination wider perspective of power systems. Therefore, DNO is evolving to Distributed System Operator (DSO). DSO will be in the front line to deal with flexible demand and operate networks with synthesising Dispatchable Resources (DR) to ensure local power system optimal operation and formulate VPP to support grid optimal operation [14].

4) Pushing for electricity market reform

In recent years, UK policy in the electricity market reform helps reduce the capital cost and attract investment to potentially risky new renewable power industries [15]. The current reformed electricity market policy is still not able to cope with the complexity of electricity and power sectors [16]. The electric power system had been implemented following a business model of vertically integrated monopoly management for a long time. The core of this reform was to decompose main functions of power generation, transmission and distribution into independent entities in commercial operations, to commercialise electricity power, electric quantity, transmission services as well as auxiliary services in order to realise calculate accurately via electricity price as far as possible, to measure all kinds of operations of power system by economic scale.

On the other hand, the reform needs to examine the current subsidy policies. The current Contracts for Difference scheme is the government's main mechanism for supporting low-carbon electricity generation, the Department for Business, Energy & Industrial Strategy said the fourth round of the contracts for difference scheme in late 2021 would aim to double the capacity to 12 gigawatts of renewable energy compared to the 5.8GW at the previous auction in 2019 [17]. With renewable energy volumes increase, the power generation is not constant in either time or space, so the need will be less for subsidy and more for pricing which is capital-efficient but better reflects system value.

1.2 Research Objectives

The thesis will address the challenges faced by the power system evolution and reform and aims to explore new optimal solutions for local energy system with multi-energy sources. The work of this thesis is helpful to deliver a greener, zero carbon

electricity system at a lower cost to consumers. A key focus is enabling whole system flexibility through the distributed system which we operate, unlocking the opportunities of distributed power sources, storage. The aim will be achieved via the following specified objectives:

- 1) To develop a co-simulation system for verification and validation of optimal scheduling and electrical trading mechanism in local energy system. The co-simulation system aims to provide a generic, scalable, yet easily customized solution for power hardware-in-loop simulation.
- 2) To investigate the optimal operation planning via techno-economic analysis of multi-energy source systems. Extensive studies will be conducted to develop optimal operation strategy for a combined heating and electrical energy system with further analysis on optimal capacity analysis of battery energy storage integration.
- 3) To analyse the optimal integration of solar PV to the existing energy system and investigate its impact on current local energy system via techno-economic analysis. Also, the impact arising from solar PV integration on distribution power network voltage will be analysed.
- 4) To investigate the design of an electricity trading mechanism at the local energy system level. Peer-to-Peer (P2P) electricity trading business model that emerged as a platform-based scheme aiming to encourage the integration of distributed power sources is proposed. With P2P electricity trading, prosumers can share the benefits with the communities that they belong to, further encouraging the consumption and deployment of distributed power sources.

1.3 Thesis Structure

The structure of this thesis is as follows:

Chapter 2 reviews the evolution of power system, the driving factors of the revolution, challenges and techniques to address these challenges in power system. The evolution and revolution of power system is introduced and these factors, government policies, investment, technology progress and innovations, and people are driving these changes. In return, the revolution of electricity market is necessary with the revolution of power system. IoT techniques reviewed in this chapter are

playing an impotent role in this process. However, the evolution and revolution of power system also brings new and different challenges including modelling of power system, control and optimization and techno-economic analysis. To address the challenges, a few techniques which will be used in following chapters are introduced and reviewed.

Chapter 3 is to build a power co-simulation system of Local power system by combining the IoT techniques and HIL techniques. Taken the advantages of both mathematical and physical models, Hardware-in-the-loop (HIL) simulation becomes a trend in industry. Even though some attempts of improving HIL simulation have been done for the validation and testing of LES, current HIL techniques still meet several challenges as described in chapter3. IoT has the potential to solve the challenges of HIL system, which will be studied in chapter3. to build a power co-simulation system of LES by combining the IoT techniques and HIL techniques. The co-simulation platforms will help to address the uncertainties in UK future energy scenarios, such as the impact of distributed power sources on transmission and distribution system, the stability analysis of distributed power architecture and IoT interface and the verification and validation of smart grid concept.

Chapter 4 focuses on how to optimise the scheduling of CHP-based system by considering the uncertainties of energy supply and demand to achieve a minimum operation cost. The challenges of operation and plan of power system need to be addressed in the process of power system evolution. Innovative power management systems and algorithms have to be developed due to the more and more distributed power system. However, the uncertainties of the electricity, heat load and some intermittent energy sources highly affect the optimal scheduling and planning of power system. a programming model was presented for optimising the annual operation cost in CHP-based energy system with hybrid energy resources under energy demand and supply uncertainties. The future power system includes different types of power sources and most of them are intermittent power sources, this optimization strategy will explore the economic dispatch with the uncertainties of power sources and demand.

The work presented in chapter 5 is to conduct techno-economic analysis to explore whether it is economic and technical viable to have solar PV integration with the existing CHP power supply and what the optimal capacity is for a system with the known CHP power generation capacity. The study is also to investigate how the solar integration impact on the existing power distribution network. The work has its significance to local/regional planning, design and management.

In chapter 6, an introduction of hierarchical Peer-to-Peer (P2P) structure that is commonly used for the large-scale and complex LES is provided. Then, a P2P electricity trading mechanism with hierarchical P2P architecture is proposed with the aim to enhance revenue of prosumers by applying a game theory in pricing competition. In order to balance the pricing between customers and suppliers, the asymptotic Shapley value which is well-known solution and general method for ensuring an equitable division is treated as the core of the coalitional game. This trading mechanism is to motivate prosumers to actively take part in the proposed architecture of trading. Finally, a few cases studies are used to verify the proposed electricity trading mechanism.

Chapter 7 concludes this thesis.

1.4 Publication and Presentations

Publication

Songshan Guo, Mark Dooner, Jihong Wang, Tianming Xu, Guoxiang Lu,” Adaptive Engine Optimisation Using NSGA-II and MODA Based on a Sub-Structured Artificial Neural Network” 23rd International Conference on Automation and Computing (ICAC), pp.1-6,2017.

Songshan Guo, jihong Wang,” The Modelling and Optimization of Distributed Network Based on Source-Limit Infrastructure,” Applied Energy Symposium: MIT A+B, May 22-24,2019.

Wei He, Mark Dooner, Marcus King, Dacheng Li, **Songshan Guo**, Jihong Wang,” Techno-economic analysis of bulk-scale compressed air energy storage in power system decarbonisation,” Applied Energy, Volume 282, Part A, 2020.

Dacheng Li, **Songshan Guo**, Wei He, Marcus King, Jihong Wang,” Combined capacity and operation optimization of lithium-ion battery energy storage working with a combined heat and power plant,” Renewable and Sustainable Energy,2021.

Presentation

Songshan Guo, Jihong Wang,"2018 MPG Annual Student Poster Evening & Prize Giving," IET Birmingham, 2018.

Songshan Guo, Jihong Wang,” CHP Based Local Energy System Living Laboratory - System Analysis and Information and Communication Platform,” International Conference on Digital Image and Signal Processing, April 2019.

Chapter 2

Literature Review

2.1 Introduction of Power System Evolution and Revolution

The evolution and revolution of power system is fundamentally a process of power networks forming and extending in the context of technological innovation and development requirements with support from complementary systems of capital, institutions and information. The first power system was demonstrated by George Westinghouse and William Stanley on 20 March, 1886, with wires strung on trees along the town's walks to light a few buildings [18]. Then, around 300 central generation stations were running to supply AC electricity by 1890. By the 1960s, the power system became very large and highly interconnected, with thousands of generation stations delivering electricity to major load centres via high power transmission lines. However, the supply of electricity, especially at peak times, could not meet the demand, resulting in poor electricity quality, such as power cuts, blackouts and brownouts in some areas from 1970s to 1990s [19]. Towards the end of the 20th century, the necessary redundancy and peaking generators were used to relieve the supply pressure at peak times. These redundant technologies in the power system resulted in high costs to the electricity company, which were passed on to consumers in the form of increased tariffs. In general, for the 20th century power systems, fossil fuel power lends to centralised power systems, requiring long supply lines (rail or pipeline) to provide a constant supply of fuel and significant economies of scale in thermal energy production. These supply lines and huge power plants require enormous concentrations of capital, considering not only power generation but also control and operation of the grid.

Since the early 21st century, the improvement on information communication technology helped resolve the limitation and reduce costs of the power system. The peak power prices are no longer to be averaged out and passed on to all the customers. The track of power consumption of each customer enables more feasible traceability during peak power usage. As a result, small business pays more than the average electricity bill since they consume more electricity during the peak time. In parallel, the concerns over environmental damage from fossil fuel-fired power stations are growing. Massive carbon dioxide which is the main contributor to climate change is released into the atmosphere when fossil fuels are burned. Climate change is a serious environmental threat that may contribute to coastal flooding, more frequent and extreme heat waves, more intense droughts, an increase in the number of severe

storms, and the increased spread of infectious diseases. Furthermore, in some rural areas, the geographical conditions and population density limit the development of central electricity generation. These leads to a desire to use large amounts of renewable energy, such as wind and solar power.

Now, a significant increase in the penetration of small units of distributed generation has been witnessed on electricity networks, motivated by a higher demand of environmental protection and a gradual process of liberalisation on the energy market. The electricity landscape in which we operate is undergoing a period of significant and rapid change as the power system moves away from a historical reliance on large, centralised thermal power generation and price insensitive consumption towards a greater diversity of supply and flexibility of demand than ever before, as shown in Fig.2.1. In the past, electricity flowed from large transmission-connected generation, through passive distribution networks to the end consumer. The future power system will be a sophisticated and intelligent infrastructure, connecting a range of new technologies and more active consumers, while maintaining overall resilience and reliability.

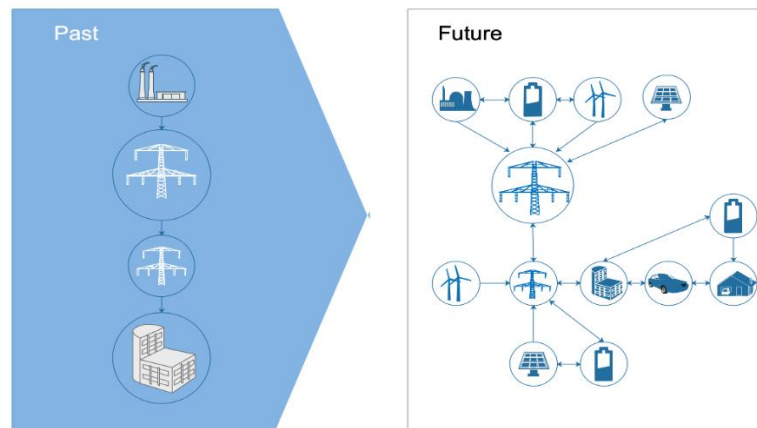


Fig. 2.1 The landscape of power systems (past vs. future) [20]

2.1.1 The Driving Force of Power System Evolution and Revolution

Many current trends are expected to be continuing, bringing more distributed energy, fast charging/discharging storage devices and hybrid generation systems to power

systems. These changes may be driven by the factors including government policies, investment, technology progress and innovations, and people.

- 1) Government policies: - In June 2019, parliament passed legislation requiring the government to reduce the UK's net emissions of greenhouse gases by 100% relative to 1990 levels by 2050 [21]. The actions include improved energy efficiency to reduce electricity demand. Financial support for low carbon technology (Contract for Difference, Renewable Obligation certificate, Frequency response service, grants for new electric vehicles etc.) continues to support changes in these areas. Also, the Paris Agreement signatories have set multinational goals to combat climate change within their own capabilities ([22] [23]). The European Commission launched “A Framework Strategy for a Resilient Energy Union with a Forward-Looking Climate Change Policy” in February 2015 [24]. In October 2014, EU leaders finally agreed on three key targets for year 2030: (1) at least 40% cuts in greenhouse gas emissions (from 1990 levels), (2) at least 27% share for RE, and (3) at least 27% improvement in energy efficiency [25]. In July 2018, the countries of France, Spain and Portugal agreed that there would be a strategic role of interconnections to add value in Europe, to honour commitments related to the Paris Agreement, and to promote convergence between Member States [26].
- 2) The cost reduction of distributed generations: - In most parts of the world, the renewable energy has become the lowest-cost resources for power generation. In 2018, the global Levelised Cost Of Electricity (LCOE) for hydropower, onshore wind were all at the lower-end of the fossil-fuel cost range, so that those technologies competed head-to-head with fossil fuels, even in the absence of financial support (As shown in Fig.2.2). The costs of solar and wind continue to fall; with auction and Power Purchase Agreement (PPA), it predicts that by 2020 or 2022, solar and wind will be highly competitive in electricity market. The global weighted-average LCOE of utility-scale solar PV has fallen by 77% between 2010 and 2018 and cost reductions continue to be driven by both declines in solar PV module prices and balance of system costs. Around 45 GW of new onshore wind was commissioned at a global weighted-average LCOE of USD 0.056/kWh, which was 13% lower than the value for 2017 in 2018 [27]. In

comparison, the LCOE of offshore wind slightly decreased by 1%. For projects to be commissioned in 2020, 77% of the onshore wind project capacity and 83% of the utility-scale solar PV in the IRENA auction and PPA database have costs that are lower than the cheapest fossil fuel-fired power generation option for new generation.

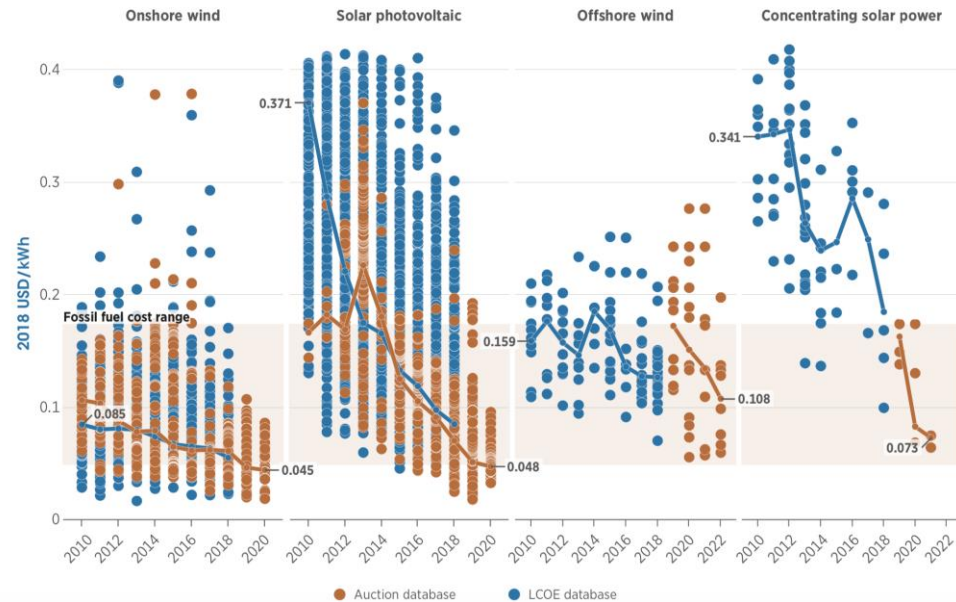


Fig. 2.2 The LCOE for projects and global weighted average values for CSP, solar PV, onshore and offshore wind, 2010–2022 [27]

- 3) Changes of end users' role: - The end users' role is shifting from pure consumers to prosumer with the drive of smart tariff and the innovation of communication techniques. deregulation measures and the rise of digital technologies have empowered consumers to take an active role in managing electricity patterns ([28],[29]). From the customer survey in [30], the majority of end users (80%) indicated that they care about the use of renewable energy. The number of people who is willing to buying the renewable energy is constantly increasing. In addition, more flexible capacity is available for end users with the increase in-home technologies, such as electrical vehicles, battery storage and micro-CHP. This means that end users could provide their flexible capacity directly as flexibility potential, thus being active participants in the energy market [31].
- 4) The advance in digital technology:- The development of digital technology, such as Internet of Things (IoTs) ([32],[33]), Blockchains ([34],[35]) and digital energy currency [36], make the flexible and secured two-way communication feasible in

electrical market. Digital technologies offer an array of opportunities to benefit individual companies, the system suppliers, energy consumers and the environment (Fig.2.3) [37]. It provides the potential to integrate variable energy resources into one control unit via digital sensors and digital information system. In addition, digital techniques are expected to reduce power system costs in different ways: reducing O&M costs; improving network efficiency; reducing unplanned outages and downtime; extending the operational lifetime of assets.

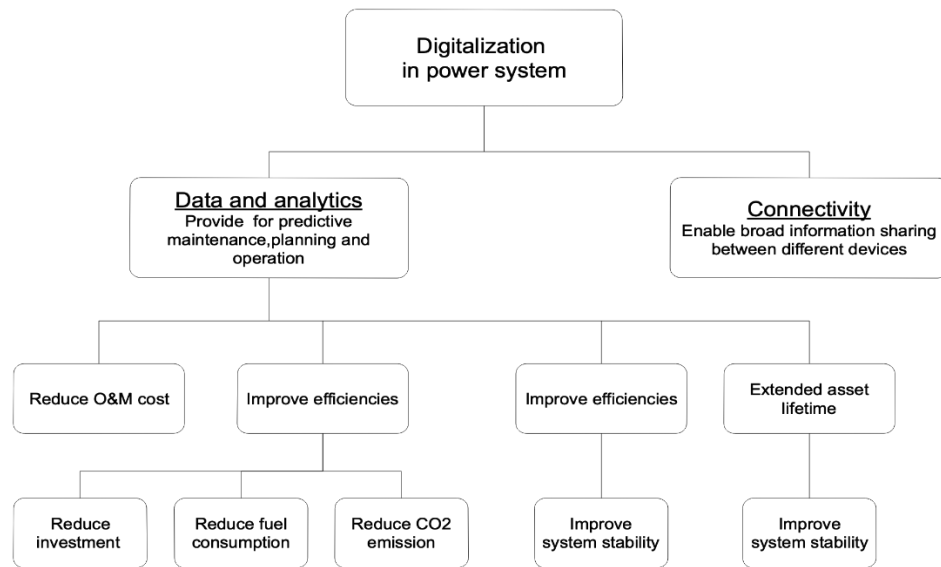


Fig. 2.3 Impact of digitalisation on electricity sector assets [37]

2.1.2 Evolution of Electricity Market with the Evolution and Revolution of Power Systems

Many countries have established electricity markets to regulate the trade of electricity and boost economic efficiency. However, renewable energy resources characteristics, such as production variability and low-predictability, zero marginal-cost of generation, and strong site-specificity, result in multiple technical and economic challenges for the current electricity market [38]. Although traditional passive consumers are becoming ‘prosumers’ — proactive consumers with distributed energy resources, actively managing their consumption, production and storage of energy with the evolution of electricity landscape, it is still an unsolved challenge on how to coordinate vast numbers of distributed energy resources, each

with different owners and characteristics [39]. The individual prosumer and small-scale generators have little impact on the transmission level but on distribution network and the increased cost of complexity of data communication and infrastructure may outweigh the potential benefits. In addition, the risk of market price fluctuations commonly hedges in the large suppliers instead of individual level since individuals' ability to fight risks is weak and cannot be dispersed.

From prosumers' perspective, the benefit can be gained by shifting their flexibilities to become service suppliers. In that case, they can reduce their electricity bill by timely shifting their demand to be in line with the variations of load balance need. However, prosumers who have the potential to participate in the electricity market may let their systems go off-grid if they cannot get benefits or reasonable shared revenues from the distributed power system. In that case, the peak demand still needs to be compensated by the main power network even though most of time the main grid's ability to compensate for peak demand is not used. This is kind of waste of resources for both prosumers and service suppliers. So, coordinating the flexible capacity of each prosumer to reduce the electricity demand and power losses have obvious potential for mitigating the waste of resources. ([40],[41]).

The current prosumers need to buy or sell their electricity via the middle layer (retailers). In that case, prosumers do not know the sources of electricity which may be cheaper than current tariff used or they cannot get the better quotes while they have extra electricity to feed in. Peer-to-Peer (P2P) trading is regarded as a way to bring the benefit to prosumers. P2P electricity trading allows prosumers to trade electricity with other prosumers directly. It is strongly proposed under a collaborative economy principle as the structure that facilitates the exchange of commons amongst all peers [43]. P2P denies a decentralised structure where all peers cooperate with what they have available for commons-based producing, trading or distributing a good or service [42]. P2P trading platforms allow small suppliers to compete with traditional providers of goods and services and get benefits from shared economies [44]. P2P structure may lead to a rethink of the top-down hierarchical structure used for previous grid operation. This new form of market can benefit all participants in the electric power system. The first opportunity is that the introduction of such new market mechanism also creates the possibility of having new business models. Currently, the retail market is lack of competition in many countries, for which the

P2P market mechanism can be a solution [45]. This will lead to retail companies to adapt their roles in the new market. Furthermore, the grid operators or service suppliers can benefit from such a market mechanism by deferring small-scale investment in new lines and equipment. One of the advantages is that grid can be strengthened by all market participants rather than reinforcing the grid via operator's investment [46].

2.2 Internet of Things (IoT) Technology for Power System

The Internet of Things (IoT) is a system of interrelated computing devices, mechanical and digital machines provided with Unique Identifiers (UIs) and the ability to transfer data over a network without requiring human-to-human or human-to-computer interactions [47]. To simplify, the IoT transforms physical objects into smart devices to collect, communicate, monitor and interpret information from their surroundings in real time. In power sector, IoT techniques, underpinning a historic transformation, will lead to a cleaner, more distributed and intelligent power system. Improved availability of data across the whole chains of power system from supply to demand enables the evolution of power system, as shown in Fig.2.4. IoT offers the flexibility between supply and demand with high penetration of various renewable energy resources by using vast quantities of granular data. By using IoT to connect and control load demand, end users can participate in balancing services, which in return assists in maintaining grid stability and reliability. More importantly, IoT technology enables the power system becoming more flexible, increasing the potential of collaboration between the devices and systems, which will help improve energy efficiency, reduce costs, and improve stability.

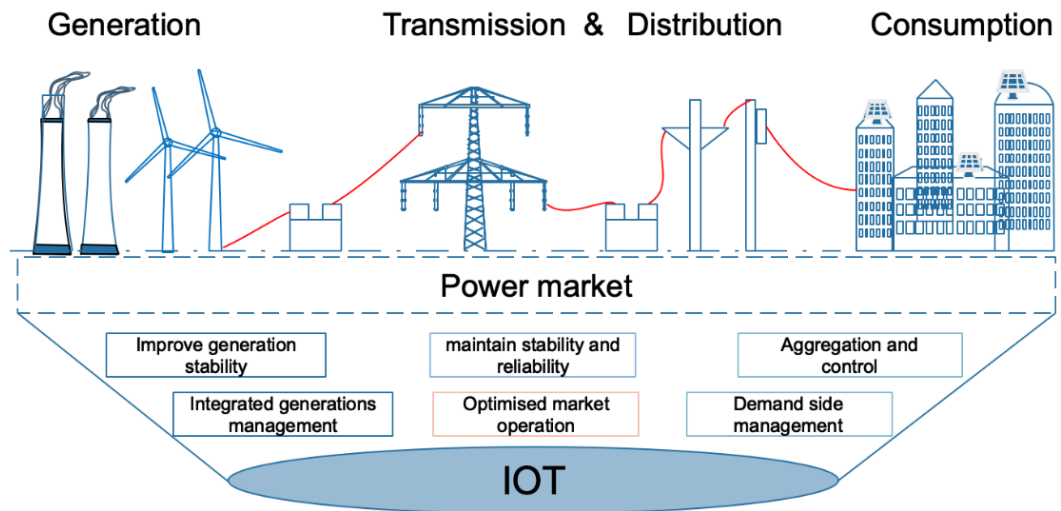


Fig. 2.4 Areas that IoT can make difference

2.2.1.1 IoT in power generation

Reliability, efficiency, minimum environmental impacts, and timely maintenance are the main challenges face by power plants [48]. The aging of power system puts more pressure on those challenging tasks. Especially for large aged power generation stations, it is hard to replace the device in terms of the cost and compatibility. Equipping with IoT facilities will contribute to optimal and safe operation of power generation stations [49]. With data collected via the IoT system, power stations can predict the potential failure via stochastic analysis and then allow the operator to take strategic measures before the failure occurs [50]. IoT systems are able to help to automatically detect the abnormal operations, which helps to minimize the maintenance period and cost. From [51], an existed power plant can save 50 million USD if it is equipped with an IoT system.

Unpredictable power resources, such as solar PV, wind or tide, pose new challenges of power generation intermittence to power systems. IoT enables realising artificial intelligence algorithms throughout the entire power system to manage the intermittence and enables the data transmission from remote stations in real time. The historical generation data together with real-time collected data can improve the forecasting accuracy, which contributes to the flexible management of the power system [52]. In addition, the IoT offers flexibility in choosing between different power resources, such as CHP and Battery [53], solar and battery [54]. Cloud-based IoT makes the online analysis and computing beyond the region limitation so the marginal virtual power plant further improves the flexibility [55].

2.2.1.2 IoT in Power Transmission and Distribution (T&D)

The traditional T&D network faces the challenges in delayed outage response, slow emergency reactions, power losses and impact of DER integration [56]. Integrating IoT technologies can alleviate these challenges. Visualization is vital to the management of T&D network. IoT will offer more intelligent monitoring along with T&D network and provide real-time data in different formats including text, audio, video and photo. In that case, T&D operators can proactively respond to power outage, address the abnormal events and better account for DER integration. T&D network is transmitting from one directional power flow to bi-directional power flow, which brings more challenges for power flow coordination. IoT contributes to alleviate the pressure of congestion due to bi-directional power flow. Furthermore, IoT enables the T&D network to achieve more efficient and reliable operation by coordination between each T&D node. IoT devices and technologies in power T&D networks include smart meters, smart controllers, and various sensors.

2.2.1.3 IoT in power consumption

IoT techniques are the key drivers to promote traditional power networks to be smarter. Firstly, these smart power networks could help the end users to reduce their cost and CO₂ emission. Secondly, the role of consumers is evolving since their power flexibility can participate in power system services, such as demand side response and frequency response. During this process, IoT integrated with computing techniques enables energy efficient communications between microgrid and the main power system. Intelligent IoT sensors that provide customers with meaningful power generation and usage data can help consumers utilize power more efficiently, reduce power wastage, and control costs [57]. Additionally, IoT enables the coordination of power resources and load demand flexibly to improve energy efficiency and reduce cost and emission. Small-scale storage systems can help the end users to reduce their peak power consumption and compensate the fluctuation generated by intermittent resources, such as wind and solar PV. The charging and discharging process of energy storage can be optimised to save energy under the assistance of IoT communication and computing capacity [58].

2.2.1.4 IoT in electricity market

The complexity of the power grid has increased the requirements on the electricity trading market, requiring more flexible transactions and higher real-time performance. As a result, this trading system where energy is traded in shorter increments is more difficult to manage and requires a high level of automation. IoT system can enable the monitoring of remote various generation information and weather information, automatically send instructions based on generation prediction, provide operational data and corrections to operators. Algorithmic trading, or algo-trading, is an emerging method of electricity trading [59]. Algorithmic trading is a method of executing orders using automated pre-programmed trading instructions accounting for variables such as time, price, and volume [60]. It uses auto-computing to deal with large scale transactions, accounting for variables such as time, price and volume to send small slices of the order out to the market over time. Currently, more than 50% of the trades conducted on the German intraday market are algo-trades [61]. Enabled by data collection and a communication system with IoT, algorithms are able to fine-tune positions in response to variable dynamic changes in market prices and changing forecasts, at lower cost than employing teams of human traders.

2.2.1.5 Other impacts of IoT in power system

The McKinsey Global Institute predicts that the total potential economic gain of IoT will be in the range of \$3.9 trillion to \$11.1 trillion per year in 2025 [62]. It is predicted that \$1.3 trillion of value in the electricity value chain from 2016 to 2025 globally by IoT [63]. GE claims its IoT technologies when applied to new coal and gas fired power plants can increase fuel efficiency by 3%, power output by 2%, and reduce unplanned downtime by 5%, operation and maintenance costs by 25%, and fuel consumption during starts by 20% [64]. The deployment of distributed IoTs enables more distributed and green power resources to be connected into power systems, which will help reduce CO₂ emissions [65]. On the other hand, new tools, including blockchain, edge computing paired with smart devices, can facilitate decentralized, peer-to-peer trading in micro-grid. These consequently optimise power flow and reduce power losses, which has a positive impact on the environment. For example, a study of the European market concluded that IoT has the potential to reduce emissions by 113 Mt of CO₂ per year [66].

2.3 Challenges and Solutions Presenting in Local Energy System

2.3.1 Modelling and Simulation Methods of Local Energy System

The power flow of LES is becoming more and more complex due to the penetration of distributed generations. To support the feasible power flow, innovative energy management systems and algorithms have to be developed. Although extensive evaluation on real system is essential in evaluating the performance, it may not be practical to perform these experiments on the actual power grid due to the complexity, safety concerns and the cost implications. To carry out this evaluation, tools that thoroughly cover the need for simulated and validated multi-sources and multiple time scales power system are necessary to prove the control concept.

In recent years, many simulation tools and frameworks have been proposed. EnergyPLAN allows for distributed system modelling and optimisation of a multi-power system to evaluate different scenarios, which is introduced in ([75],[76]). Many researchers studied the interaction and coordination between multi-power sources and variable demand by using GridLAB-D ([77],[78],[79]). The Mosaik framework [80] is a compatible simulation platform in which other models and simulators can be linked together to perform co-simulation.

Due to the complexity of future distributed power systems that includes communication technology, edge computing and bidirectional power flow, the requirement of co-simulation environment (it is unclear about co- parties for simulation) is expected to be the main trend. EPOCHS [80] is a combination of PSLF (commercial electric simulator) with ns-2 (open-source communication-network simulator). This distributed simulation environment was developed to understand the impact of communication system on the distributed power flow. The architecture of EPOCHS is shown in Fig.2.5.

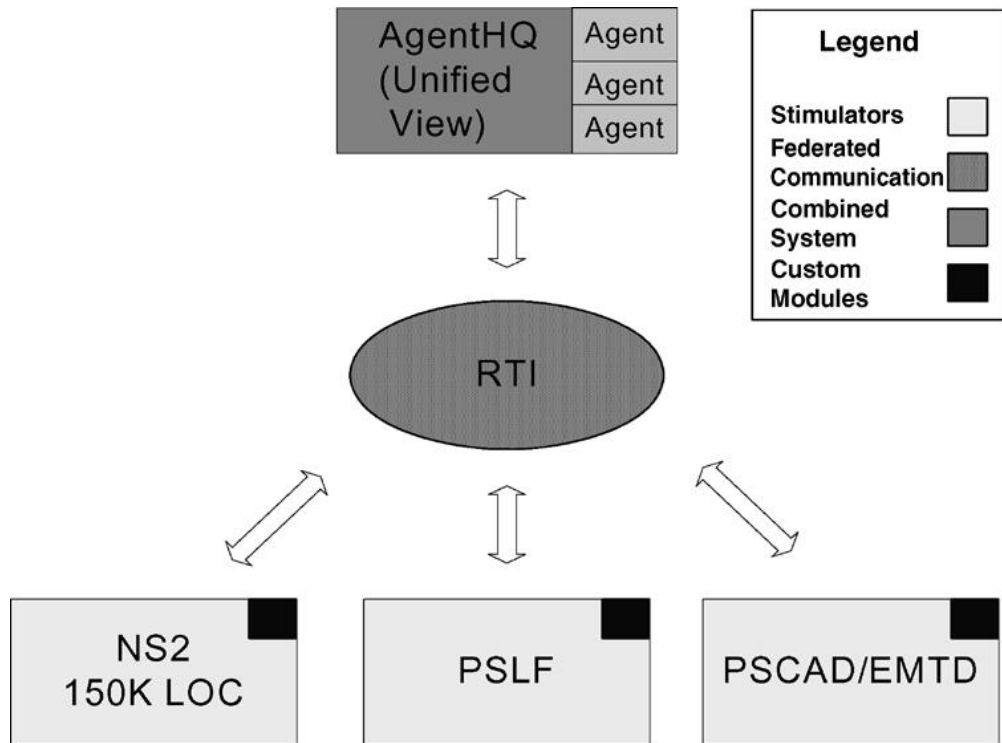


Fig. 2.5 Relationship between EPOCHS' components [80]

EMTDC is a real-time power system simulator with a very detailed electrical model. PSCAD is used to simplify the development of EMTDC schemes. PSLF's simulation engine is very suitable for the study of the time step in milliseconds and the total simulation time in minutes or less. NS2 is a high-quality emulator that can create a variety of communication scenarios. NS2 can simulate the behavior of these protocols under various pressures. For example, when multiple applications share the network and communicate through the same router and communication link, it may be caused by contention for network resources. AgentHQ provides a unified environment to the agent and acts as an agent when the agent interacts with other EPOCHS components. Through it, agents can obtain and set power system values, and can send and receive messages to and from each other. RTI acts as the "glue" between all other components. It is responsible for simulation synchronization and routing communication between EPOCHS components. The time step model is used in EPOCHS, which is one of the simplest component synchronization techniques. In the time stepping model, each component combination will be executed until the preset simulation time is reached. When all alliance members have reached the target synchronization point, these alliance members can interact with each other by

sending messages through RTI. After the joint interaction is over, the RTI selects the time of the next synchronization point, and all simulators continue to execute.

The main contribution is that it is the first time to combine the network simulation with the power system simulation. However, this combination is still hard to be used for Simulation analysis of highly decentralized power systems since it does not consider the computing burden on each component. In addition, it is limited to accurately analyses the characteristics of some components due to simplification of simulation model. Furthermore, no details on routing and availability of the communication link have been considered and analysed in regarding to the power system. Some description of simulation is represented by reduced-order mathematical models, fitted in a purely mathematical fashion. some models may have little or no physical basis. In that case, the role of the simulation is usually to test a proposed system up to the normal design limits and it is hard to reflect the actions of a real system in a complex power system.

The concept of Hardware-in-Loop simulation may provide a way forward [81]. Hardware-in-the-loop simulation techniques can provide a form of rapid prototyping in which we start with a virtual prototype and move in stages towards a real prototype system involving the hardware and software of the final design [82]. Hardware-in-Loop has been used extensively in different power system projects and analysis. The interactions between residential loads and the smart distributed system is evaluated based on smart home Hardware-in-Loop [83]. In this study, a novel co-simulation architecture that integrates PHIL with a larger distribution feeder simulation is proposed. The co-simulation architecture consists of three main components: the hardware, power model, and communication link. Distribution system electrical dynamics and PV Dynamic response are achieved by the power hardware-in-loop system. Power flow, thermal models of the houses, and stochastic patterns of other loads are simulated by GridLAB-D model. Current measurements from the inverters are sent back to GridLAB-D to update the software distribution system model and calculate the power flow of distribution system. The modular architecture allows for the substitution of other power system simulation tools, if desired. Like traditional PHIL simulation, closed-loop bandwidth is a key limitation of simulation accuracy and the types of interactions that can be effectively simulated. Another advantage is

the flexibility of this architecture. The flexibility to support arbitrary distribution feeders is demonstrated. The flexibility is also shown in the ability to physically separate various pieces of the co-simulation. However, the communication between each house is not taken into consideration so it is still hard to simulate the actual data transaction, such as transmission latency and data re-synchronization.

In [84], the co-simulation system is developed to study, implement and validate the new control algorithms. As shown in Fig.2.6, this low voltage distribution system consists of three sub-networks: residential, industrial, and commercial and switches in between can be used for the combination of these sub-networks. In this research, each network is simulated in any one of the available real-time simulators available.

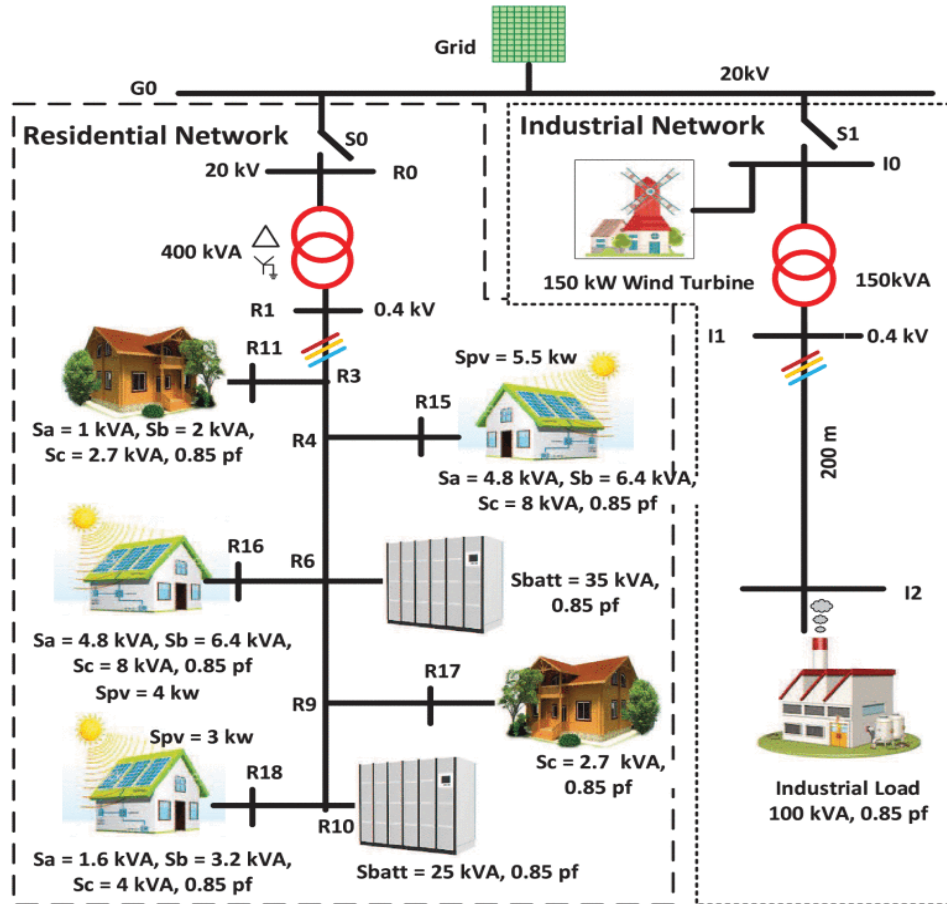


Fig. 2.6 Residential and industrial subnetworks of distribution system interfaced with DERs [84]

This system considers the impact of inter-connection of various subsystems, such as power, control, protection, and communication. Moreover, two communication

methods are compared in terms of latency, jitter and round-trip time to find the proper communication simulation solution. Besides this, the network emulation features which can be utilized to simulate and study the communication related issues in the power is provided in this system. One disadvantage of this system is its complexity, the co-simulation system is built on various isolated components and the interface is not user-friendly. In addition, the co-simulation platform is not compatible with other tools such as electricity market simulator to test and validate new management algorithms.

2.3.2 Automating Industrial Challenges and Solutions in Local Energy System

Automating industrial processes and supervisory control were applied in power acquisition systems in 1990s. This control is a general term for control of many individual controllers or control loops. It refers to a high level of overall monitoring of individual process controllers and gives the operator an overall plant process view, and allows integration of operation between controllers. In this stage, this type of system contributed to the power sector by alleviating the risk of loss of production or blackout. The challenges of these system have low flexibility, low efficiency and high maintenance cost. The old automation system is hard to achieve the transmission of complex and secured data. For example, the old automation system shifted from proprietary to open systems which utilised standard communication protocols. This made it possible to connect third-party peripherals such as printers and disk drives to the system. The addition of the Internet Protocol (IP) also greatly enhanced the communication process. In comparison, with the introduction of the concept of Internet-of-Things (IoT), the automation system is also headed towards much higher levels of complexity and speed, improved security and scalability, and lower costs than ever before.

However, current power systems bearing with high penetration of renewable resources need large amount of real-time data transmission to mitigate the effects of generation uncertainties. In addition, the age of equipment in the power sector and poor maintenance problems can lead to high level of energy losses and unreliability. IoT can contribute to reducing some of these challenges in the management of power plants [86]. By applying IoT system with real-time data communication, edge

devices are able to detect any failure in the operation or abnormal actions, alarming the need for maintenance. This increases reliability and efficiency of the system, in addition to reducing the cost of maintenance. Power balancing between demand and generation is a big challenge due to variability of supply and demand resulting in mismatch in different time scales in intermittent characteristics of solar/wind generation. IoT systems offer the flexibility in balancing generation with demand, which in turn can reduce the challenges of deploying variable renewable energy, resulting in higher integration shares of clean energy and less CO₂ emissions. With the installation of IoT system, a more efficient use of energy can be achieved by using machine-learning algorithms that help determine an optimal balance of different supply and demand technologies [86]. Moreover, IoT has the potential to help the energy sector to transform from a centralised to a distributed, smart, and integrated energy system. This is a key requirement in deploying local, distributed resources as well as turning many small-scale end users of energy into prosumers by empowering local electricity trading [87].

2.3.3 Techno-Economic Assessment in Local Energy System

The technical and economic performance will be affected in distributed LES due to the integration of variable energy sources. One of the challenges in a distributed system with high penetration of distributed energy sources will impact on existing power system connected to. Large-scale of distributed power system connected to grid is proved both a threat and a challenge for maintaining safe and stable operation of electric power systems [89]. Voltage assessment of distributed power systems has been performed using various mathematical formulations collectively known as the voltage stability indices [96]. Most academic literature on the impact of distributed resources has primarily studied a single source ([90],[91],[92],[93]). In these reported researches, location, sizing, number of distributed sources and excited infrastructure determines the voltage stability and power losses. For some weak distributed power systems, storage techniques are commonly used to compensate the negative effect ([94],[95]). However, most studies have been limited to statistical analyses that are yet to be validated by simulations. Furthermore, many of the assumptions are based on the experience of system operators. The experience is not guaranteed to remain valid as the distribution system evolves. Overall, these studies indicate a lack of

holistic assessment methods that are necessary to successfully capture holistic assessment to distributed power system.

Another challenge in the techno-economic assessment of distributed power systems with variable distributed energy sources, energy storage, and demand-side response is the quantitative determination and the coordination of operating reserves. Naturally, the DERs have their restrictions. So, it is essential to assume the flexible capacity that determines its ability to response the generation/load uncertainty or prediction error. One way is to increase the accuracy of load and generation forecasting which directly impacts the flexible capacity and different technologies are used to pursue more accurate results.

Already, the optimal scheduling of energy sources in local energy system has been studied and analysed in different ways. In [97], A two-stage stochastic microgrid energy scheduling model is proposed to optimize the day-ahead energy flow in the first stage while managing the dynamic operations by considering the uncertainties of power sources in the second stage. one of the primary goals of this study is to minimize the operating costs with high reliability, by using a commercial optimization software. The Combined heat and power system is not considered.

The operation strategy of energy system was focused on the interactions between energy system operator by a recursive two-level optimization technique [98]. The proposed model of energy hub uses a thermal model of building to apply demand response not only for electrical loads but also for thermal loads. The stochastic optimization method is used to solve the uncertainty problems. Energy storage systems were also considered to increase the flexibility of energy system. The uncertainty level of long-term supply and demand is much higher than that of short-term supply and demand. In addition, it did not consider the gas system.

In [99], A comprehensive renewable-based hybrid energy system including photovoltaic modules (PV), a wind turbine (WT), battery energy storage modules (BESS), electric vehicle chargers (EV), CHP, and a hydroelectric power plant is proposed, in an attempt to reduce the imbalance and ultimately minimize the cost of the portfolio considering risk factor. However, the environmental factors of the hybrid energy system and how to deal with uncertainty efficiently are not studied.

Generally, many studies [100],[101] have clearly indicated the importance of considering the effect of uncertainties in CHP-based system design. In fact, it is well-known how inherent uncertainties, such as energy demands, energy supply, fuel price fluctuations, regulation, and so on, may affect the potential operation cost /benefits of energy system. In this regard, a robust optimization design method through a case study of a combined heat and power system is proposed [102]. In this study, the uncertainty of load demand of a single representative day is taken into account on a cogeneration system. In [103], it focuses on designing a community-level multi-vector energy system by considering the situation of demand uncertainty regarding insufficient data. A combined energy system plan is proposed in [104], where the Monte Carlo simulation and MILP algorithm are used to deal with the risk management of the uncertainty of fuel cost and discount rate. Taking into account the fluctuation of hourly demand, the operation of CHP system of a building was optimised [105].

In the above studies, long-term uncertainties in energy demand and supply are ignored and typical load and generation data are not considered for the long-term running of CHP systems. However, fluctuations in energy demand over the years may be significant and their effect on overall performance are worth to be specifically evaluated. It would be ideal if the detail scheduling strategy is designed on long-term base. However, there are some challenges: 1) the computation burden is high due to the complexity of system and the large number of data; 2) the optimisation strategy will be affected by the cases that rarely occur or are special; 3) the interconnection of variables among time steps will further increases the variation and complex of system.

The proposed method of thesis divides the long-period data into different scenarios in units of days. Each scenario is divided into different timesteps according to the data interval. In each timestep, the probability of occurrence of a certain data can be calculated according to the distribution of historical data during this timestep or its probability distribution. many scenarios with different occurrence probabilities can be generated for each type of long-term data. For various types of data, these scenarios can be combined again to form new scenarios based on different probability distributions under various types of long-term data. The number of these scenarios

can reach several million and the sum of these scenarios' occurring probabilities is 100%. Some of these scenarios with high occurring probabilities are selected as the reference of scheduling optimisation. The predefined acceptance level will determine the number of selected scenarios and determine the level of characterise long-term data. In addition, the initial value of the state of all devices with storage (electricity storage or heat storage) function in each scenario is equal to value at the end.

2.4 Forecasting Methods in Local Energy System

2.4.1 Load Forecasting

Short term to long term forecasting has become increasingly important because of the restructuring of power systems. However, load forecasting is challenged by data availability and reliability. The load series are complex and exhibits some random factors; the load demand is not only relevant to previous time step on the same day, but also interaction with the same hours on different days [106] below. Load forecasting techniques can be grouped into three main groups: traditional forecasting techniques, modified traditional techniques and soft computing techniques [107].

2.4.1.1 Regression model

Regression is one of the most widely used statistical techniques. It is used to reveal the relationship of load demand and other factors such as weather data, load types. The mathematical model is as follows:

$$P(t) = L(t) + \sum_{i=1}^n k_i r_i(t) + e(t) \quad (2.1)$$

where, $L(t)$ is the standard load at time t ; k_i is a set of varying coefficients, $i = 1, 2, \dots, n$; $r_i(t)$ is an independent influencing factors, $e(t)$ is a random variable.

The prediction accuracy depends on the adequate representation of possible conditions from the historical data. The seasonal load change, annual load growth and daily load change should be considered to increase accuracy of load forecasting. A transformation technique, which consists of a transformation function with

translation methods, is proposed to deal with different factors that affect the load forecasting[108].

2.4.1.2 Auto Regressive Moving Average (ARMA) model

In the implementation of such a model, the operation of difference is employed first such that the stationary time series can be formed. Then, by use of Auto Correlation Function (ACF) and Partial Auto-Correlation Function (PACF), the preliminary order identification of a model is confirmed. In [109], an adaptive ARMA model is developed for load forecasting, in which the available forecast errors are used to update the model. Using minimum mean square error to derive error learning coefficients, the adaptive scheme outperformed conventional ARMA models. The model can be written as:

$$P(t) = \varphi_1 P(t-1) + \dots + \varphi_p P(t-p) + a(t) - \varphi_1 a(t-1) - \dots - \varphi_q a(t-q) \quad (2.2)$$

where, the current value of $P(t)$ is determined by its values at previous periods and the previous values of white noise $[a(t), a(t-1), \dots]$; $\varphi_1, \varphi_p, \varphi_q$ are coefficients. The numbers employed are p and q , respectively.

2.4.1.3 Neural network model

Neural network is widely used in various areas because its ability to learn. Various formulation of neural networks is reported: multilayer perceptron network, self-organizing network and recurrent neural network, etc. Varying number of layers can provide a different level of abstraction to improve the learning ability and task performance[110]. In[111], the long short-term memory recurrent neural network was introduced and the Mean Absolute Percentage Error (MAPE) was obviously improved. A long short-term memory recurrent neural network-based framework was proposed to implement the load forecasting of individual end users[112]. In their work, different machine learning approaches were compared.

2.4.2 Generation Forecasting

Time series model and Numerical Weather Prediction (NWP) models were used for solar irradiance and power forecasting, such as persistence model, Coupled Auto Regressive and Dynamical System (CARDS) model and ANN model[113]. The selection of appropriate forecasting model depends on the forecasting horizon and the available data. Combining the Auto Regressive Integrated Moving Average (ARIMA) and Water-Table Fluctuation (WRF) method using sky images or applying a post processing method were proposed to improve forecasting accuracy[114]. Compared with traditional methods, hybrid approaches have more advantages such as their ability to incorporate stochastic and deterministic forecast. Now, machine learning and data processing techniques are widely used since they can learn and predict data without considering physical model. Closely related to computational statistical analysis, with an input of sample data, a self-adaptive model is built and can analyse, process and predict data using algorithms that are too complex for the human mind. In[115], a solar radiation forecast technique based on fuzzy and neural networks was developed to improve the forecasting accuracy in different sky conditions. Generally, the techniques of forecasting photo-voltaic power generation were classified as[116]:

- Techniques based on satellite images, where the area of cloud and other meteorological changes can be acquired by using meteorological satellite images.
- Using the image analysis techniques to forecast short-term solar irradiance.
- Technologies based on machine learning schemes. ANN and Supporting Vector Machine (SVM) schemes are found to be efficient alternatives for forecasting the global and horizontal solar irradiance and power generation.

The generation forecasting models can be described in Fig.2.7, which shows the classification of forecasting models based on spatial resolution of input data and temporal resolution of output data. In this forecast horizon, the ARIMA models seem to be the most reliable model. They can provide a forecast in a fraction of a second on a personal computer. At longer horizons, the data are dominated by the diurnal cycle. In this case ARIMA models work better. At higher frequency, the data is more dominated by short-term patterns which can be picked up by persistence or ANN.

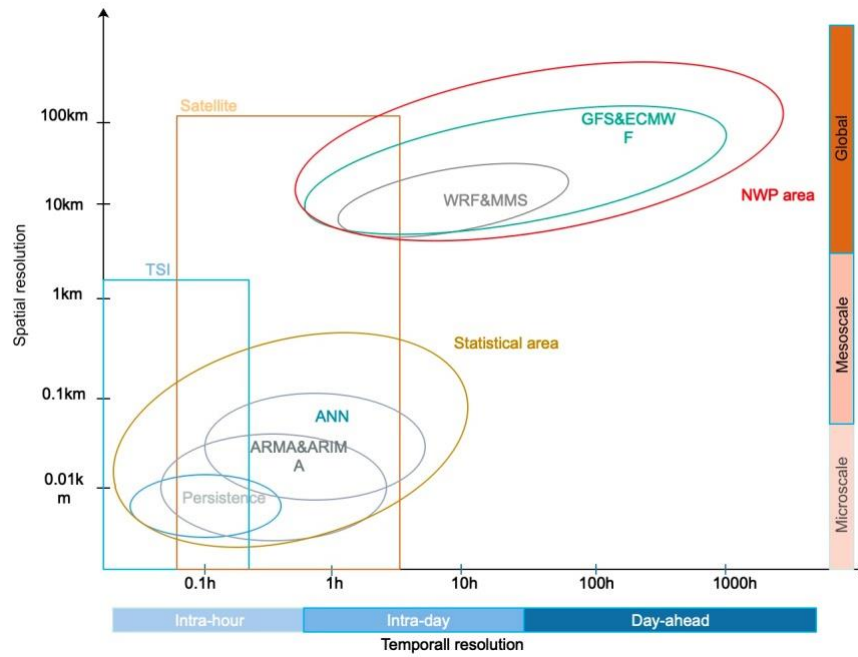


Fig. 2.7 Classification of model based on spatial and temporal resolution

2.5 Uncertainty Management

Uncertainties in load demand and generations are extremely difficult to evaluate since they are highly affected by some stochastic variables. The traditional deterministic approaches in energy system are unavailing to deal with these uncertainties. Hence, different uncertainty modelling techniques have been developed, such as PDF, probabilistic approaches. On the other hand, the coordination of hybrid power sources is commonly studied to mitigate the uncertainties of each power source.

2.5.1 Probabilistic methods

In[117], probabilistic methods (as shown in Fig.2.8) are categorized into two groups: numerical and analytical techniques. Monto Carlo Solution (MCS) is the common and effective methods, which is used when the system is highly nonlinear, complicated and has many uncertain variables[118]. To further increase clarity of the features of uncertainties and reduce computing burden, different types of MCS techniques, such as sequential MCS, non-sequential MCS and pseudo-sequential MCS are utilised for probabilistic uncertainty analysis. Sequential MCS method is more flexible, easy to implement compared with MCS. Non-sequential MCS method

is developed since a system in a combination of components and sampling rate determines its state. It is widely used in risk assessment of power system. pseudo-sequential MCS method is far quicker than MCS.

The weaknesses of MCS method can be listed as follows:

- The computation burden is usually high since it is iterative and needs several evaluations of function.
- The number of simulations needed increases as the degrees of freedom of the solution space increases. Therefore, in order to obtain accurate results, thousands of simulations are usually required.

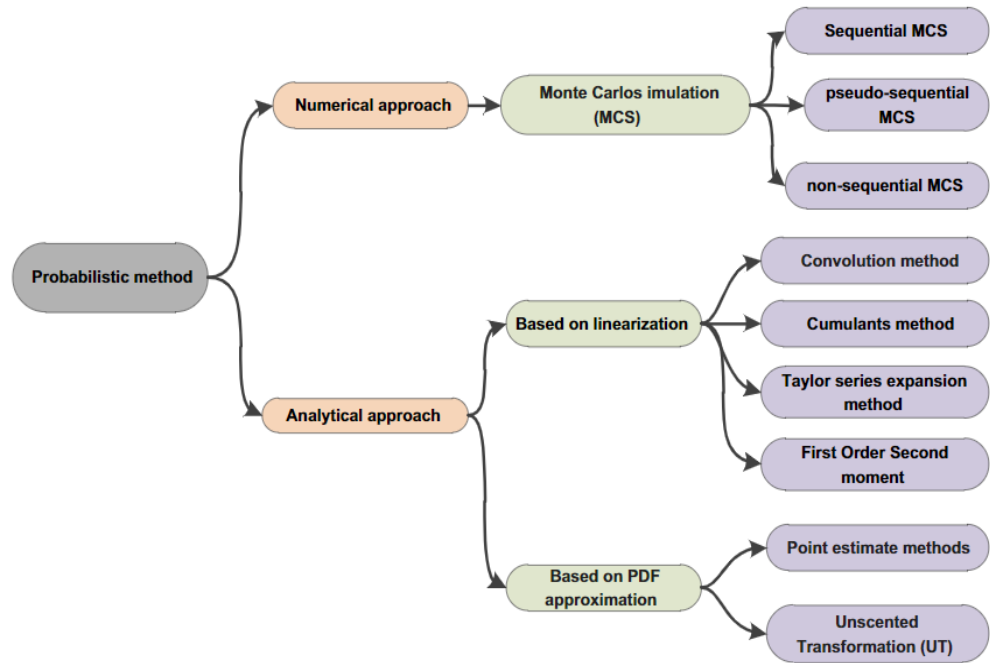


Fig. 2.8 Classification of probabilistic methods

2.5.1.1 Worst case scenario model

Instead of using an explicitly dedicated PDF, the variations of the random variable are defined to a predefined uncertainty set with definite upper and lower boundaries in the worst-case scenario. The level of prediction uncertainty is evaluated by using prediction intervals which has a range with upper and lower limit. The formal definition of prediction interval is given by

$$P_r[L(x) < y(x) < U(x)] = (1 - \alpha) \quad (2.3)$$

where, $L(x)$ and $U(x)$ are the lower and upper limits of function $y(x)$; $1-a$ is the confidence level that the value of $y(x)$ falls between $L(x)$ and $U(x)$.

How to generate the prediction intervals is the key to modelling the uncertainties. The commonly used methods to generate the prediction intervals are Delta, Bayesian and Bootstrap methods. In practice, the narrow prediction intervals with higher coverage probabilities is needed[119]. The limit estimation method is proposed by taking the widths of prediction intervals into consideration. The mathematical definition is defined by

$$B_o = \frac{1}{n_p} \sum_{i=1}^{n_p} \left(\frac{U(x_i) - L(x_i)}{t_{\max} - t_{\min}} \right) \quad (2.4)$$

where, n_p is the number of samples; t_{\max} and t_{\min} are the maximum and minimum values.

2.5.1.2 2m (Point Estimate Method) PEM model

The 2m PEM method takes its importance into consideration. In practice, some of random variables have their real-time values much different than forecasted values. This method transfers these uncertainties into the output variables. the objective function can be stated as

$$S = f(c, z_1, z_1 \cdots z_m) \quad (2.5)$$

where, c is a set of certain variables; $z_i (i = 1, 2 \cdots m)$ are uncertain input variables with probability function.

This method is to find the statistical variation of random variables through the solution set of the deterministic objective function for only a few selected estimated values of random variables. The objective function is evaluated 2m times. Hence, the computation complexity is to be taken into consideration.

2.5.1.3 Cumulant method

Moments and Cumulants method serve a feature extraction from a probability distribution and can avoid complicated convolution computation. The r th moment corresponding to a continuous random variable x is defined as follows:

$$\alpha_r = \int_{-\infty}^{+\infty} x^r dF(x) \quad (2.6)$$

where r is the order of the moment and $F(x)$ is the cumulative probability density function of x .

If X is a discrete random variable and there is a probability for a corresponding component of X , then the r th moment of X is defined as follows:

$$\alpha_r = \sum_{c=1}^{\infty} P_c X_c^r \quad (2.7)$$

On the other hand, cumulants are important features for random variables. The cumulants k_γ can be derived from the moments using recursion in closed forms as follows

$$k_1 = \alpha_1 \quad (2.8)$$

$$k_2 = \alpha_2 - \alpha_1^2 \quad (2.9)$$

$$k_3 = \alpha_3 - 3\alpha_1\alpha_2 + 2\alpha_1^3 \quad (2.10)$$

2.5.2 Scenarios generation

In order to determine the proper Probability Density Function (PDF), the related PDF for each time period is generated through the expected values. Many scenarios can be generated by fitting random variables to the PDFs with equal probability. Fig.2.9 shows the processing of generating different scenarios of the deviations.

The most common type of scenario generation method is Monte Carlo sampling-based scenario generation, where different Monte Carlo based sampling methods give different scenario generation methods. this is one of the most popular scenario generation methods due to its analytical and computational simplicity. The commonly used methods to generate the prediction intervals are Delta, Bayesian and

Bootstrap methods. In [120], The hourly solar irradiance data are used to generate a Beta PDF for each time period.

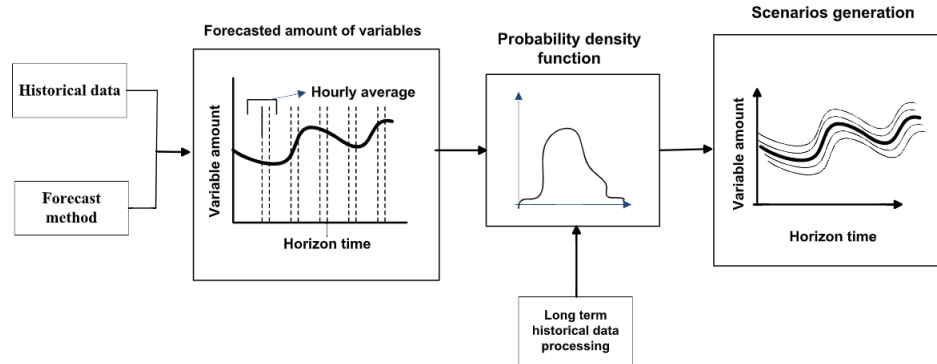


Fig. 2.9 Processing of generating different scenarios

Monte Carlo based scenario generation randomly acquire the sampling according to the probability distribution, so that each sample produces a scenario. In other words, all scenarios have equal probabilities at a given time step. The inverse transform sampling-based scenario generation is commonly used in practice [2-10]. To produce scenarios at given time step in the scenario tree, the inverse cumulative distribution function associated with produced scenarios is needed.

In general, analytical methods reduced the computational complexities of MCS, but they need certain assumptions mathematically to be made, which influence the performance of the methods[121].

[2-10] X. Ma, Y. Sun and H. Fang, "Scenario Generation of Wind Power Based on Statistical Uncertainty and Variability," in IEEE Transactions on Sustainable Energy, vol. 4, no. 4, pp. 894-904, Oct. 2013.

2.5.3 Coordinating of power sources to mitigate system uncertainties

There are different techniques for reducing uncertainties and improving technical and economic advantages in power systems. These techniques were classified into three categories: numerical methods and heuristic methods.

In recent years, Combined Heat and Power (CHP) system is widely applied in distributed energy systems since it is regarded as transition to reduce emission. The coordinative scheduling of distributed sources with CHP is one way to further

increase total energy efficiency [123] and reduce energy cost [122]. In [124], the day ahead CHP unit operation was investigated with the consideration of security of power systems. A integrated grid service that combines electrical-load shifting and flexible heating supply was proposed to improve the operational flexibility of the CHP micro-grid [125]. Normally, complicated coordination challenges are handled on hourly basis by using a specialised power simplex algorithm [126]. A multi-objective model has been built, aiming to coordinate the rated power of the power generation unit (PGU), the capacity of storage unit, the electric chilling ratio and the on-off coefficient [127]. However, these researches focused on the daily or short-term dispatch algorithms which is not consider the uncertainties in different time period. Furthermore, CHP operation constraints are rarely considered in previous research works.

2.6 Scheduling Optimisation Algorithm

The scheduling optimisation problem of energy system is always linear and involves both discrete and continues time variables. The problem can be defined as:

$$\min \{Z=cx + hy : Ax + Gy \geq b, x \in K^n, y \in \mathfrak{R}^p\} \quad (2.11)$$

where, A and G are $m \times n$ matrices; c and h are n -vectors; and b is m -vector.; x, y are variables, where x is the integer variables, $x \in K^n$, and y is the continuous variables, $y \in \mathfrak{R}^p$.

From above problem definition, it is a large-scale mixed integer linear problem with on/off status of operation of equipment and binary variables for selection and continuous variables for system allocation. The MILP method is commonly used to solve mixed integer linear problem because of its rigorousness, flexibility and extensive modelling capability[161]. In addition, the advance in modelling and solution to scheduling formulations leads to its application in large and complex system.

There are many popular MILP algorithms, such as general benders decomposition[162], outer approximation[163], branch-and-bound [164]and branch-and-out[165]. Compared with branch and bound method, branch-and-cut improves the efficiency by using a cutting plane algorithm with a relative time savings of 31%[166]. The processing of general branch-and-cut algorithm can be defined in

Fig.2.10, where z_{lp} is the objective function, z_{best} is the best objective function value known as so far and z_{heur} is the objective function value of a feasible solution delivered by a heuristic. The data preparation is to remove the redundant constraints and establish the classification criteria which is followed by selecting the unevaluated candidates. Then, the function value z_{lp} is generated by LP solver. If $z_{lp} > z_{best}$ the node is fathomed and goes back to selection step. Otherwise, a heuristic is used to generate feasible solution. The violated inequalities are trying to be generated and add these constraints to the formulation of selected candidates if the inequalities can be successfully generated. After generating cuts, we need to define the set of feasible solutions by 0-1 fixed variable. The way of determining the branching variable is to select the one with fractional value closest to 1/2. The generated candidates will be added to unevaluated nodes.

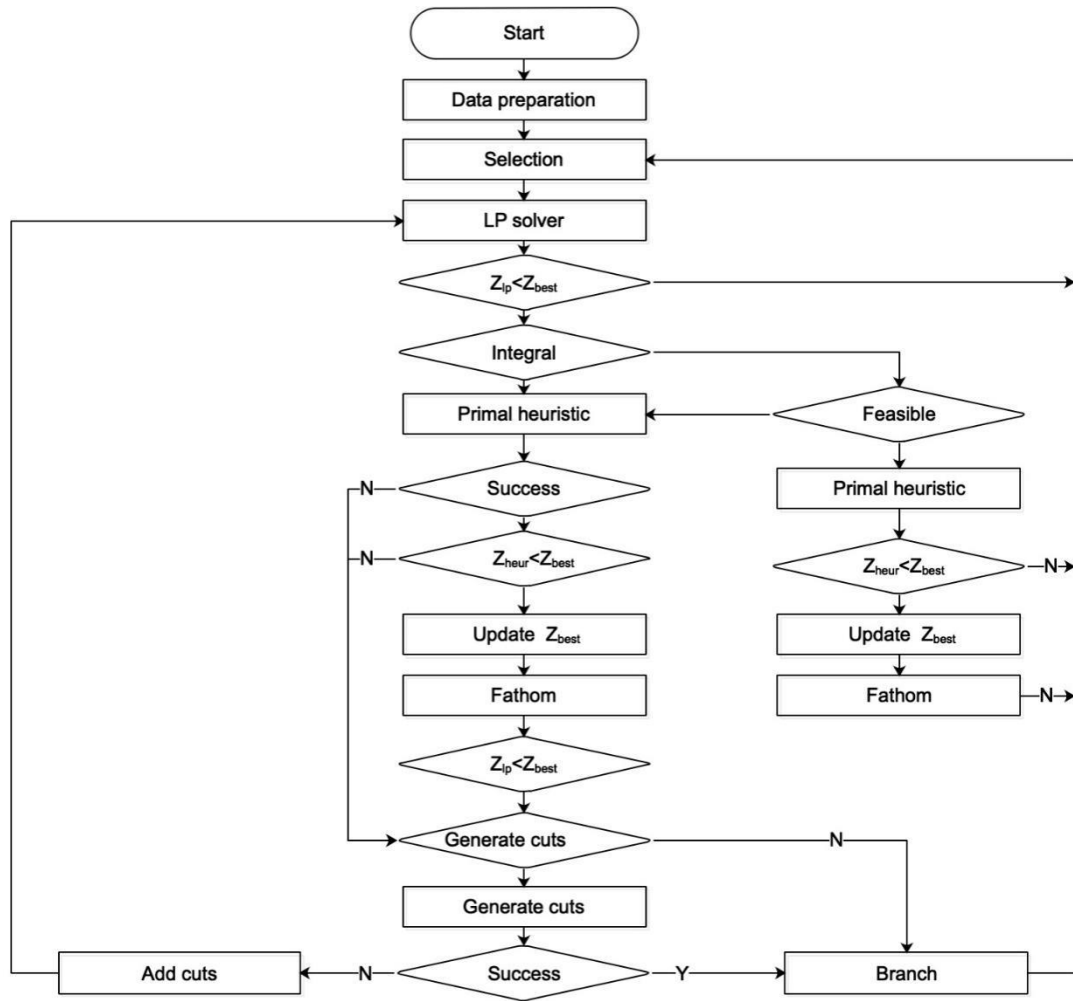


Fig. 2.10 Flow chart of branch-and-cut algorithm

The method proposed in [167] further reduce the computational burden of branch-and-cut method by adding appropriate inequalities into MILP. It is assumed that Q is the set of all feasible solution. From Eq.2.11, MILP may include multiple equivalent solutions, each of them consists of a symmetry group G .

The redundant calculation would be needed to solve unnecessary problems since the equivalent solution is uncertain. In this case, the decision to determine which branch of a bifurcation is taken should be made, which can be regards as symmetry breaking problem. symmetry breaking for solving this constraint satisfaction problems is studied in [168]. One of methods use the idea of adding constraints to a constraint problem in order to remove symmetries. That is, one representative solution is kept in each equivalence branch by breaking symmetry statically. For this static symmetry breaking, the practical application is to impose hierarchical decisions[167]. To make the symmetry breaking theory clear, the example illustrates it as follows:

$$Q = \begin{cases} \{[0,1,0,1]\} \mapsto f_1 = 186 \\ \{[1,0,1,0]\} \mapsto f_2 = 186 \\ \{[0,1,1,0]\} \mapsto f_3 = 196 \\ \{[0,1,1,1]\} \mapsto f_4 = 196 \\ \{[1,0,1,1]\} \mapsto f_5 = 204 \\ \{[1,1,0,1]\} \mapsto f_6 = 204 \\ \{[1,1,1,0]\} \mapsto f_7 = 204 \\ \{[1,1,1,1]\} \mapsto f_8 = 212 \end{cases}$$

A set Q containing 9 feasible solutions for $onoff_{gt}$ (represented as $[onoff_{11}, onoff_{12}, onoff_{21}, onoff_{22}]$) is obtained. The following inequalities proposed in [169] are included into hierarchical constraints:

$$onoff_{1t} \geq onoff_{2t} \forall t \quad (2.12)$$

where, $onoff_{1t}, onoff_{2t}$ are the decision variables.

After the inequality's constraints are applied, the set Q can be reduced into four feasible solutions. The inequalities constraints impose the order on the variables to avoid the calculation of redundant solutions.

$$Q = \begin{cases} \{[1,0,1,0]\} \mapsto f_1 = 186 \\ \{[1,0,1,1]\} \mapsto f_2 = 204 \\ \{[1,1,1,0]\} \mapsto f_3 = 204 \\ \{[1,1,1,1]\} \mapsto f_4 = 212 \end{cases}$$

However, as systems become more interconnected, the performance of Eq.2.12 is not working well. Hierarchy that imposes an order on the binary variables does not work on efficiency varying systems. Therefore, the method in this section proposed a slight improvement on Eq.2.12 with the consideration of the interaction of variables. The improved hierarchical constraints, which adjust the mixed order of symmetry diminishing, can increase the system adaptability. These methods ensure some of the symmetric solutions breaking, while at least one optimal solution keeping.

$$onoff_{gt} \cdot \eta_{gt} \geq onoff_{kt} \cdot \eta_{kt}, \forall g, k, t, \eta_{gt} \quad (2.13)$$

where, $onoff_{gt}$, $onoff_{kt}$ are decision variables; η_{gt} , η_{kt} are adjustable coefficients.

The outline of this proposed algorithm can be written as

- 1) Remove the redundant constraints and establish the classification criteria
- 2) select the unevaluated candidates
- 3) Form the subset
- 4) Apply the diminishing algorithm proposed in Eq.2.13
- 5) Active the lower efficiency variables if needed
- 6) Solve the problems

2.7 Relation with my work

The different co-simulation methods are introduced to simulate the more and more complex distribution system. HIL system is proposed co-simulation architecture since some real electrical components cannot be well simulated the by the virtual simulator. Some researchers are limited to accurately analyses the characteristics of some components due to simplification of simulation model, Also, no details on routing and availability of the communication link have been considered and analysed in regarding to the power system. the communication between each house is not taken into consideration in some studies so it is still hard to simulate the actual

data transaction, such as transmission latency and data re-synchronization. A co-simulation system is developed based on IoT techniques and HIL techniques. The hybrid simulator which is the core in this IoT-based HIL system can simulate both the communication and power networks and generate indication or control signals to each device. The integration of the co-simulation system will be designed by considering time synchronization, system security and data flow power co-simulation system provides a generic, scalable, yet easily customized solution for LES simulation that can support different hardware, high volumes of data exchange between simulator and hardware and several different simulation programs.

In recent years, the smart energy is more flexible with the installation of distributed generator and switchable load. In other words, the overall uncertainty is greatly increased. In addition, the output of some power sources, such as PV system and wind generations, is intermittent, which brings more challenges for the operation. From the literature review, various uncertainties management techniques are introduced. Monte Carlo based sampling methods are used in my study due to its analytical and computational simplicity.

The optimal scheduling problems consist of various decision variables that should be taken into account to achieve optimal solution. Firstly, the load and generation data used for scheduling optimisation are key to the optimisation performance. One is to generate the scenarios based on the historical data and another is to generate the data by using forecasting techniques which is reviewed above. The proposed method of this thesis divides the long-period historical data into different scenarios in units of days. Each scenario is divided into different timesteps according to the data interval. In each timestep, the probability of occurrence of a certain data can be calculated according to the distribution of historical data during this timestep or its probability distribution. Many scenarios with different occurrence probabilities can be generated for each type of long-term data. For various types of data, these scenarios can be combined again to form new scenarios based on different probability distributions under various types of long-term data.

2.8 Summary

From the demonstration of the first power system in 1886 to the beginning of the 21st century, the development of communication systems helped resolve the limit and reduce the cost of power systems, until more and more distributed generations were connected to the grid in modern times. A few factors, such as government policies, investment, technology progress and innovations, and people, have played an active role in the different stages of power system evolution. As one of the important driving forces, the IoT technology drives the power system becoming more flexible, increasing the potential of collaboration between the devices and systems, which will help improve energy efficiency, reduce costs, and improve stability. IoT has a positive impact on the evolution of the power system in terms of power generation, power transmission and distribution, power consumption, electricity market and social impact.

Study of LES usually depends on sophisticated simulation tools due to its complexity and no single mathematical model can fully describes the complexity and dynamics of LES. Taken the advantages of both mathematical and physical models, Hardware-in-the-loop (HIL) simulation becomes a trend in industry. Even though some attempts of improving HIL simulation have been done for the validation and testing of power system, current HIL techniques still meet several challenges as described in chapter3. Based on the overview of IoT technique, IoT has the potential to solve the challenges of HIL system. Chapter3 is to build a co-simulation system for distributed power system by combining the IoT techniques and HIL techniques.

The challenges of operation and plan of power system need to be addressed in the process of power system revolution. Innovative power management systems and algorithms have to be developed due to the more and more distributed power system. However, the uncertainties of the electricity, heat load and some intermittent energy sources highly affect the optimal scheduling and planning of power system. Chapter4 focuses on how to optimise the scheduling of CHP-based energy system by considering the uncertainties of energy supply and demand to achieve a minimum operation cost. Chapter5 will study the planning of distributed power system and its impact on existed power system in terms of techno-economic analysis.

Finally, the changes of power system drive the evolution of electricity market since the particularity of renewable energy, such as the variability and low predictability of production, zero marginal power generation cost, and strong on-site specificity, has brought a series of technical and economic challenges to the current electricity market. In chapter6, Peer-to-Peer (P2P) electricity trading business model that emerged as a platform-based scheme aiming to encourage the integration of distributed power sources is proposed. With P2P electricity trading, prosumers can share the benefits with the communities that they belong to, further encouraging the consumption and deployment of distributed power sources.

Chapter 3

Development of IoT and HIL Co-Simulation Platform for Local Energy System Study and Analysis

3.1 Introduction

Study of Local Energy System (LES) usually depends on sophisticated simulation tools [128] due to its complexity and no single mathematical model can fully describes the complexity and dynamics of LES s. Simulating study of the LES is an essential procedure and process in system design and implementation. Simulation studies allow a variety of scenarios and system configurations to be examined. In simulation studies, the assumptions/hypothesis are made, and the system model needs to be simplified to allow the simulation implementation. It is always a trade-off between the model accuracy, mathematical solvability and simulation realisation so the fidelity of the model is often sacrificed. With the power system's development, power system has rapid increase in integration of renewable energy and becomes more interacting and inseparably coupling with other power systems, for example, heating and electrical vehicle. Therefore, the simulation and modelling approaches face great challenges and new approaches are demanded.

In addition to mathematical modelling and simulation, another approach is physical modelling, that is, building a scale-down real system physical model in the laboratory or workshop to mimic the real-world scenarios. This method may represent the real system more accurately than mathematical model in a certain range of operation. But it is very costly, and space taken. Also, the scale-down version of the system may not be able to represent the full-scale system characteristics. The physical model has also imposed restrictions on fault and extreme operation case test.

Taken the advantages of both mathematical and physical models, Hardware-in-the-loop (HIL) simulation becomes a trend in industry. HIL links the physical model/part of real systems and mathematical simulation into one platform. HIL can embed and engage the real system components or subsystems into the same simulation system to enable validation and evaluation of the design with different real-life dynamic constraints and boundary conditions. The HIL is now becoming a powerful tool for system study when all layers of a system need to be simulated but full hardware approach is not available.

With development of the trial project of the integration of new generation technologies, these generations are commonly allocated in different areas and IoT technology enable their real-time communications. It brings the challenges for HIL

to simulate the system with widely distributed generations: 1) The hardware sampling frequency and the simulation computation burden need to be carefully considered for the purpose of time synchronization; 2) Another challenge is the selection, deployment, monitoring, and analysis of aggregated data in real-time.

To address this challenge, a co- simulation system with the idea of combining HIL techniques with IoT technique is developed in this chapter for techno-economic analysis of LES in the following chapter. The co-simulation system aimed to provide a generic, scalable, yet easily customized solution for LES simulation that can 1) reduce the cost of HIL implementation; 2) support different hardware, including controllers, physical equipment, and physical systems in LES; 3) support high volumes of data exchange between hardware and simulations; and 4) accommodate the use of several different simulation programs.

3.2 Current Challenges of HIL and IoT Techniques in LES Simulation

3.2.1 HIL Techniques and Challenges in LES simulation

The HIL techniques used in power system is generally classified into two types: controller based HIL and PHIL[129]. The first commonly used simulation system is controller HIL, as shown in Fig.3.1. It allows a physical controller hardware to be evaluated with the simulated inputs, such as the inverter controller, battery controller and turbine controller. For this system simulation, the system should run on a digital real-time simulator. The timescale of input is from milliseconds to microseconds. The simulation is updated based on data from the controller, which in turn updates the control signals. Some real actuators are also used to validate the ability of controller to deal with the disturbance from actuators.

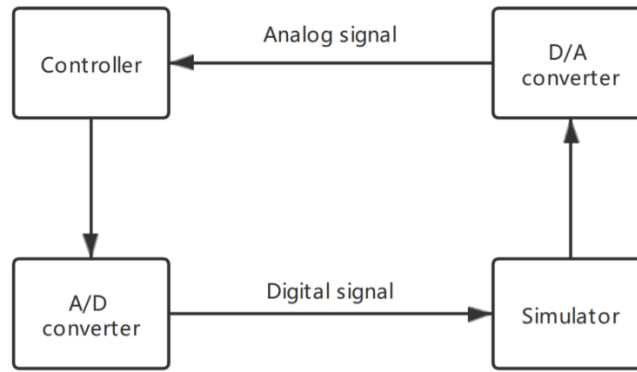


Fig. 3.1 Controller HIL simulations

PHIL simulation involves interfacing actual power hardware to a simulated system to validate the combinational results. An example of PHIL simulation is illustrated by Fig.3.2 [130], in which the Hardware under Test (HuT) is interfaced to a simulated power system through a power amplifier. IoT system with the function of time synchronization and data processing seamlessly couple the power hardware with the simulated environment. Besides, this combinational approach also has more flexibility for varying the surroundings of the HuT compared to the test in pure hardware. The advantage of this method is more practical than simulation since models that capture the full range of realistic behaviour may not exist, and it allows proprietary systems to be tested. Thus, this approach still facilitates a great deal of flexibility for exploring a range of surrounding systems and obtaining experimental data for model development and validation.

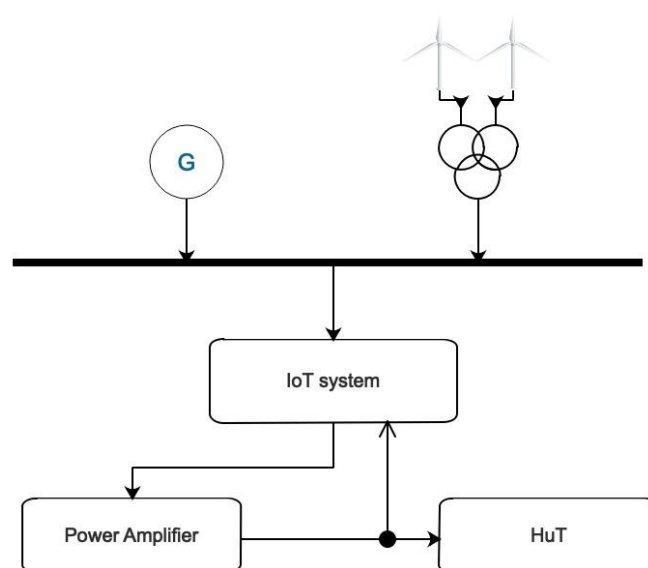


Fig. 3.2 Example of PHIL

For the large LES, the conventional PHIL is hard to meet the computing requirement since the real-time simulators cannot deal with millions of data in microseconds. The timescale of this simulators is from seconds to hours, so the simulation runs on a high-performance computer. The hardware sampling frequency and the simulation computation need to be carefully considered for the purpose of time synchronization. This synchronization procedure should also consider the communication latency between the simulator and the remote hardware. Fig.3.3 shows the example of PHIL with multi-timescale, the data inputs can be from different sources, such as remote devices, online sources. In radial power system, the simulator receive data from different nodes with different time delay and then need to process and synchronize these data. The control command sends commands to each device and formulate the loop control.

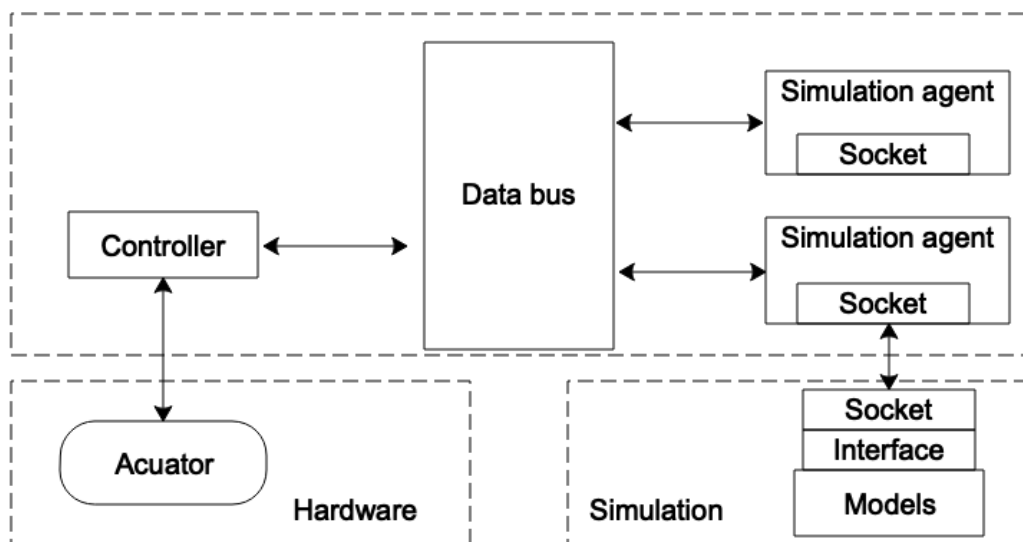


Fig. 3.3 Example of PHIL with multi-timescale

Even though some attempts of improving HIL simulation have been done for the validation and testing of LES ([131]-[132]), current HIL system still have several challenges:

- Challenges of HIL capacity on complex system. The non-linearity and diversity of power system is increasing with the installation of renewable power system. Representing the dynamic characteristics has to be compromised due to the fixed time step and centralised computing burden which will limit the simulation size and transient performance.

- Challenges on testing geographically distributed HuT. In recent years, more and more distributed system is integrated into power system, which brings more challenges to validate the distributed HuT for joint test, considering the stability, latency and synchronicity.
- Challenges on communication of HIL system. The communication network, especially for long geographic distance among distributed HuT may has different delay and signal loss. Millions of data that are produced from each HuT will increase the risk of network congestion and signal loss.
- Lack of a general framework to facilitate the flexibility of the simulation system. Current HIL system is limited to simulate a specific system or network and is not compatible with other simulation systems.

3.2.2 IoT Techniques and Challenges in LES Simulation

The IoT has two key words: “Internet” and “Thing.” The “Internet” can be defined as “The interconnection of HuT in various areas via specific communication protocols” and the “Thing” is “an object that can be widely defined, such as devices and system” Thus, “Internet of Things” semantically means a network of interconnected objects uniquely addressable, based on specific protocol. IoT in local energy system is a huge dynamic network infrastructure of Internet-enabled physical objectives. It contains embedded technologies and all types of information devices such as sensors, actuators, and the Internet to sense, identify, locate, monitor, manage, cooperate, and control of objects/things in physical, digital, and virtual world [133].

IoT can be used to achieve the reliable data transmission via wire or wireless communication network for various parts of power system, including generation, distribution and consumption. For distributed generation, IoT enables the monitoring of generation volume and the potential control of power generation. It is used to acquire the electricity consumption, voltage stability and protection setting in the distribution line. In addition, IoT could properly manage the data flow between the master and slave HuT to mitigate the network congestion.

To achieve technical goals in applying IoT in LES simulation, there are some challenges which need to be addressed. Normally, IoT devices have limited resources and capabilities such as computing capacity, storage and bandwidth, so the compression and aggregation of data is crucial. Delay and packet loss are important parameters that determine the performance of simulation. It degrades system performance and simulation cannot satisfy predetermined requirements if the delay and loss cannot be fixed properly. Furthermore, the standard of IoT device is no clear standard, so developing a general co-simulation system which can be compatible with different IoT devices is a big challenge.

In general, HIL and IoT techniques have their own advantages and disadvantages, but both can be complementary with each other in the following parts:

- The limitation of HIL techniques on complex system can be alleviated by IoT techniques via distributed IoT devices. In other way, the combination of source limited IoT devices can contribute to complex computing work.
- HIL can easily acquire, monitor and dispatch the information via IoT system from distributed HuTs without the geographical limitation.
- The synchronicity of data flow of various devices can be managed and optimised by different level management of IoT techniques and HIL techniques. IoT is responsible for latency monitoring and transmission and HIL is used to synchronise the data flow based on the latency.

In next section, A co-simulation system that combines the HIL and IoT techniques is developed to build a high flexible and stable simulation environment. Firstly, the integration of the co-simulation system will be designed by considering time synchronization, system security and data flow. Then the development and validation of simulator of HIL was introduced to achieve dynamic simulation. Finally, the co-simulation system is verified via cases study.

3.3 The Development of Co-Simulation System

The architecture of co-simulation system is shown in Fig.3.4. The data communication between switchable loads/renewable devices and different types of server is achieved by IoT system. To reduce the burden of communication network,

the data compression techniques is normally used to reduce the data volume. The local server is used to deal with the data and data computing in LES. The online server collects the data from other online sources, such as trading information, energy policy and GPS information. The real-time data exchange between two servers is always running. The heartbeat frame is a way to be used for checking the running status of each server. A virtual simulator is integrated in the local server to simulate the power flow and components. In addition, the data of real components will help the virtual simulation system to improve the accuracy of components simulator by using self-learning techniques.

This simulation system also has the potential to integrate with other devices in the lab, such as RT-lab, hardware simulator. TCP/IP protocols are used for the lab devices and IO card needs to be integrate with the server if sensor signals are to be collected.

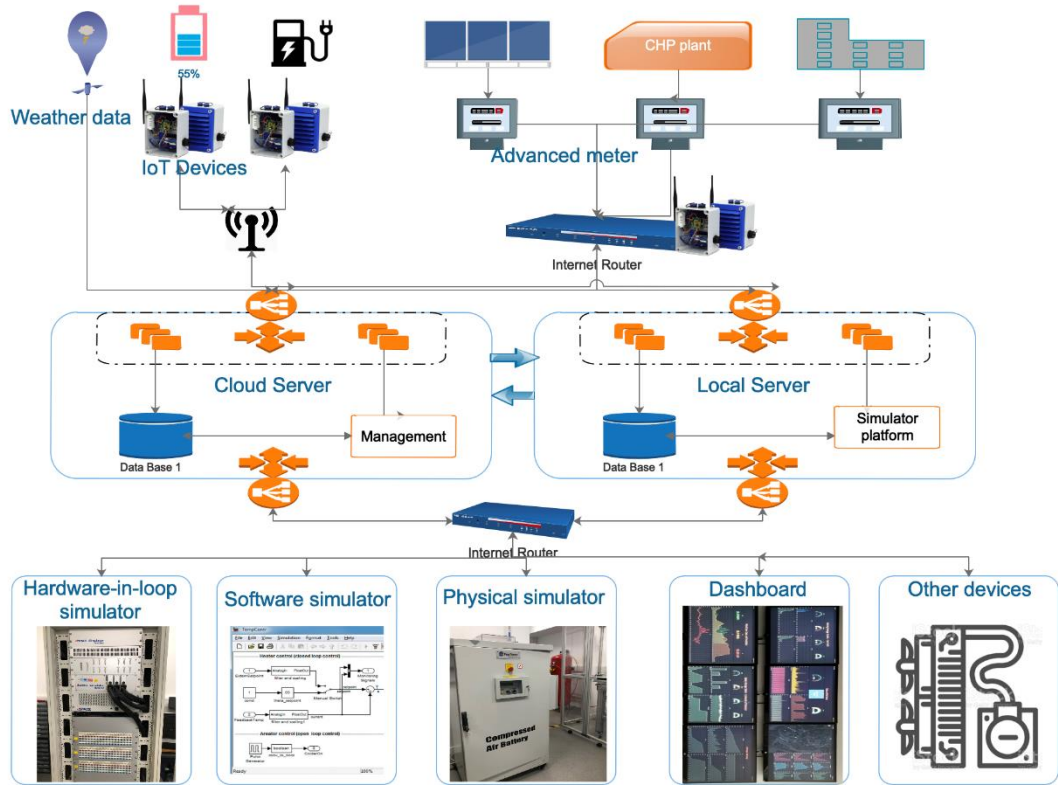


Fig. 3.4 Architecture of co-simulation system

3.3.1 IoT System Integration

The IoT system could be considered as a multiple level system, as shown in Fig.3.5. IoT is a combination of sensors, devices, networks, and software that works together to unlock valuable, actionable data from internet of thing [134]. The IoT system can be defined as seven functional layers: physical device, connectivity, edge computing, data accumulation, data abstraction, application and collaboration.

Fig.3.6 shows the hardware of designed IoT device. Primarily, this module communicates with external sensing devices and server by using WiFi or 4G techniques. The IoT device can receive the control signals from upper server and then implement the control commands. Each network-integrated device is capable of monitoring and reporting its own activity and data. The current research supports the notion that the most promising method of integrating renewable generation resources is realized in LES and recent research is promising increased general reliability and frequency stability through various “smarter” approaches[135].

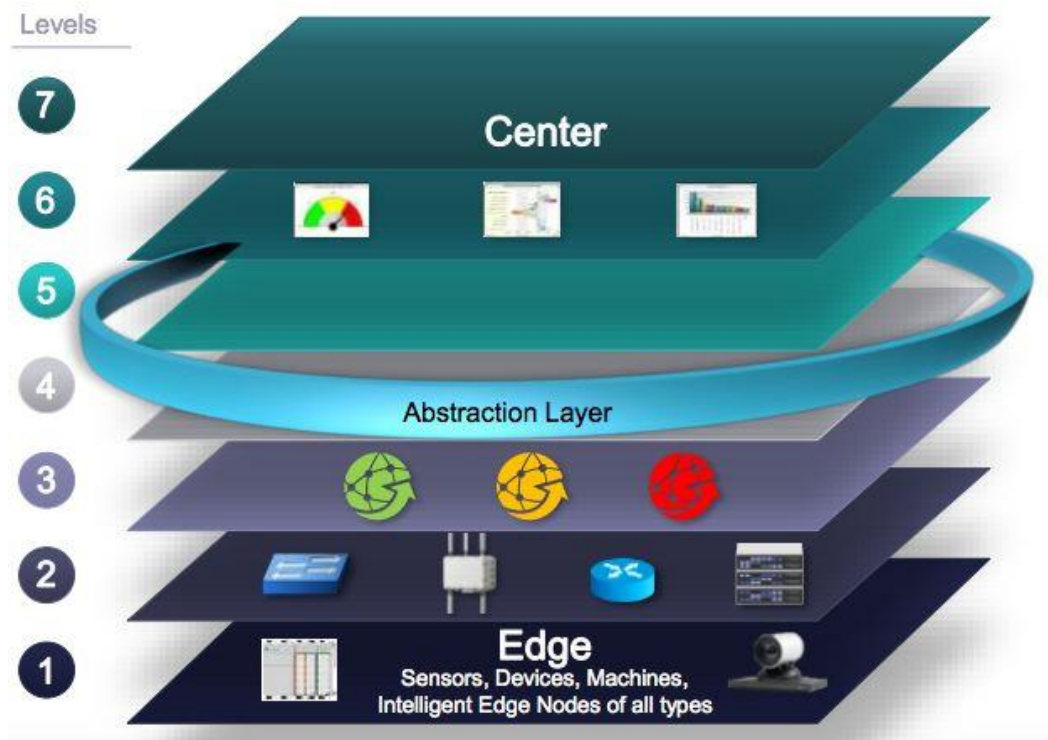


Fig. 3.5 IoT world forum reference model [135]



Fig. 3.6 IoT hardware devices

3.3.2 Implementation of Time Synchronization

The hardware sampling frequency, data transmission delay and simulation computation time need to be carefully considered for the purpose of time synchronization. Let Δt_1 denote the time interval when the data sent from remote hardware to server need to be updated. Let Δt_2 denote the time interval from server to simulator. Time synchronization requires the same intervals between simulator to remote hardware. A mechanism is needed to manage the time interval since the actual simulation time may be different from the $\Delta t_1 + \Delta t_2$. In terms of the stability of IoT system, the computation time can be ignored since the Δt_1 is normally above 1minute. Fig.3.7 illustrates the time synchronization mechanism.

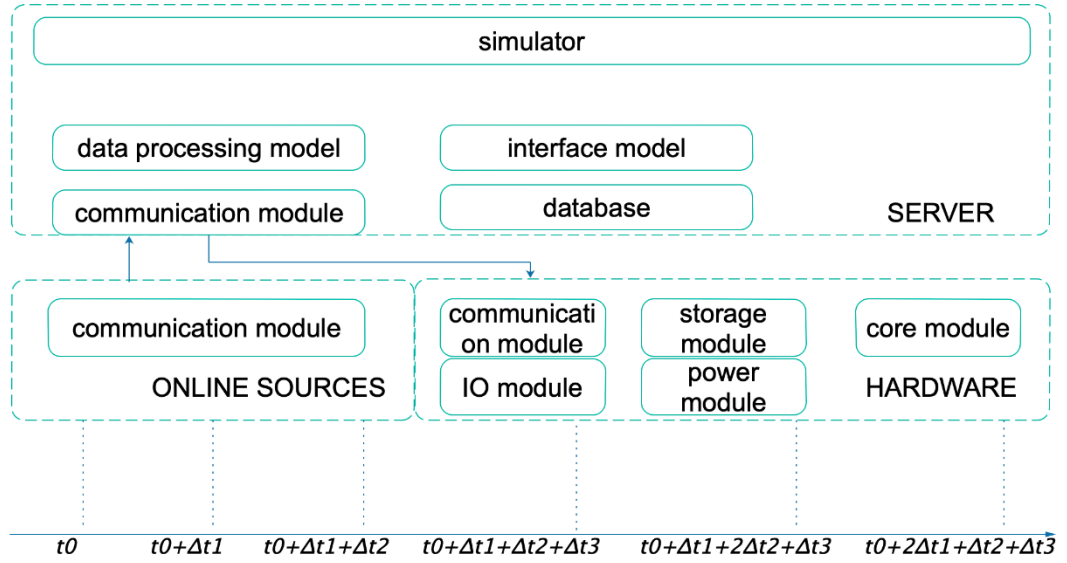


Fig. 3.7 Time synchronization mechanism

The mechanism is implemented with the following sequences of steps:

- 1) At time t_0 when the simulation system starts to work, the system is to initialize the system with predefined initial value and then wait for the inputs.
- 2) The simulator will request the inputs from server storage module. The remote devices and other online inputs scrape the values of the sensed variables from the controller and then publishes the scraped variables to server storage module after waiting t_1 until time $t_0 + \Delta t_1$.
- 3) In time $t_0 + \Delta t_1 + \Delta t_2$, the simulation system starts to run the simulation, the time delay of the stage is set to Δt_3 . It is noted that Δt_3 should be longer than the simulation period.
- 4) The simulation becomes idle after completion of its computation in Step 3 until $t_0 + \Delta t_1 + \Delta t_2 + \Delta t_3$, when the simulation agent sends the control command to the hardware using the remote procedure call.
- 5) Steps 2-4 are repeated for each subsequent hardware in time step Δt to move the simulation forward in time until a specified end time

For the alarm detection, the event-driven mechanism (trigger an action when the fault event occurs). The transmission of alarm signals will not follow the above sequences of steps.

3.3.3 IoT System Security

Common concerns regarding risks focus on security and encryption of data while in transit to and from the server, or in transit from edge devices to and from the devices, along with patching of devices, device and user authentication, and access control. Securing IoT devices is essential, not only to maintain data integrity, but also to protect against attacks that can impact the reliability of devices. As devices can send large amounts of sensitive data through the internet and end users are empowered directly to control a device, the security of “things” must permeate every layer of the solution.

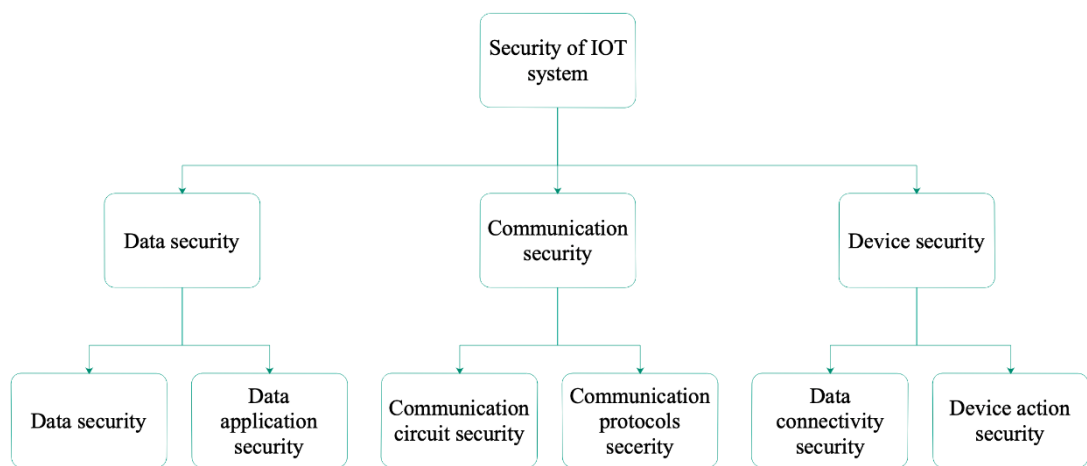


Fig. 3.8 Security list in IoT system

Fig.3.8 shows the security list in different layer. In order to fulfil the code of practice for consumer IoT security. Three leading practices need to be considered to achieve the greatest and most immediate security benefits:

- 1) No default password: many users do not change the default password, which is the main reason of security issues.
- 2) Implement a vulnerability disclosure policy.
- 3) Keep software regularly update software updates need to be easy to implement and not disruptive to the functioning of the devices.

The device gateway acts as an intermediary between connected devices and the cloud services, which allows those devices to exchange the data via MQTT protocol. The MQTT messages are transit over Transport Layer Security (TLS), the succession of

SSL (Secure Sockets Layer). A multi-layer security architecture is applied at each layer of IoT system, as shown in Fig.3.9. In order to connect a new device, this device needs to be authenticated. The most common technique used for authentication is X.509 certificate [136]. For the authorization and access control, the memory of IoT hardware is organized into compartmentalized blocks, resulting in good security levels. The memory protection unit is used to enforce the memory isolation. Forming isolated domains protect sensitive parts of the system, as each part is in different portion of memory. In other words, attacking any section does not violate others.

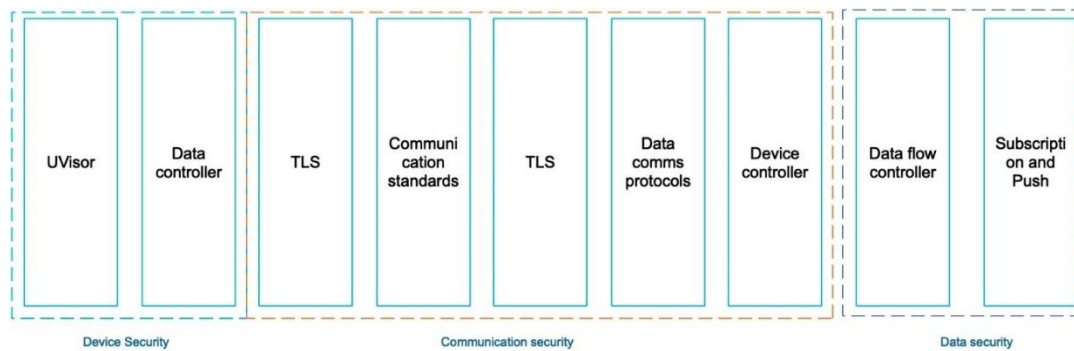


Fig. 3.9 IoT security architecture

All traffic to and from IoT devices is encrypted over SSL/TSL protocol. TLS is used to ensure the confidentiality of application protocols. Furthermore, forward secrecy, a property of secured communication protocols, is supported. It means that a malicious user who learns the private key of an IoT device should not be able to decrypt any communication protected under this key unless learning the temporary key of each session.

A data credibility check mechanism is also used to enhance the data security. For the energy devices, such as solar system, battery system and CHP plant, each variable is corresponding with other variables, which can be described by numerical equations.

3.3.4 Data Compression

In LES, millions of data are produced from smart meter or device system every hour. The ongoing growth in micro-generation is resulting in more small generators scattered geographically throughout a region, as opposed to the traditional model of a centralized energy plant serving a large area. Furthermore, high frequency data processing is necessary in terms of real-time energy flow management. The large

volume of data will help utilities to do things they never could do before such as better understanding the customer behaviour, conservation, consumption and demand, keeping track of downtime and power failures etc [137]. So the data compression technique is used to increase network stability.

The edge gateway mode of data compression infrastructure is applied in power co-simulation system[138], as shown in Fig.3.10, the distributed sensors communicated with gateway and edge computing techniques are applied in the gateway to further reduce the computing burden in cloud layer. [139]proposed lossless compression algorithms for smart meters and compare them to off-the-shelf algorithms by using the Lempel–Ziv–Markov Chain Huffman Coding algorithm. In [140], a dynamic compression technique is proposed, which resulted in CRs that ranged from 6:1 to 11:1. An embedded zero tree wavelet transform-based technique is proposed with regards to the power data compression [141]. However, higher (Compression Ratios) CRs may be required for multiple distributed data transmission and communication. Moreover, there is a lack of research works on the compression of steady-state data in comparison to the compression of waveform signals.

Singular Value Decomposition (SVD) technique is one of commonly used method that is employed for image compression and other related applications [143]. The main motivation of using SVD is to use simple method to achieve good trade-off between data compression and loss of information since the number of singular values is the only parameter that needs to be set. The SVD technique can be used to decompose a matrix M into a product of three matrix as

$$M = U\Sigma V^* \quad (2.1)$$

where, U is an $m \times m$ unitary matrix over K ; Σ is a diagonal $m \times n$ matrix with non-negative real numbers on the diagonal; V is an $n \times n$ unitary matrix over K and V^* is the conjugate transpose of V .

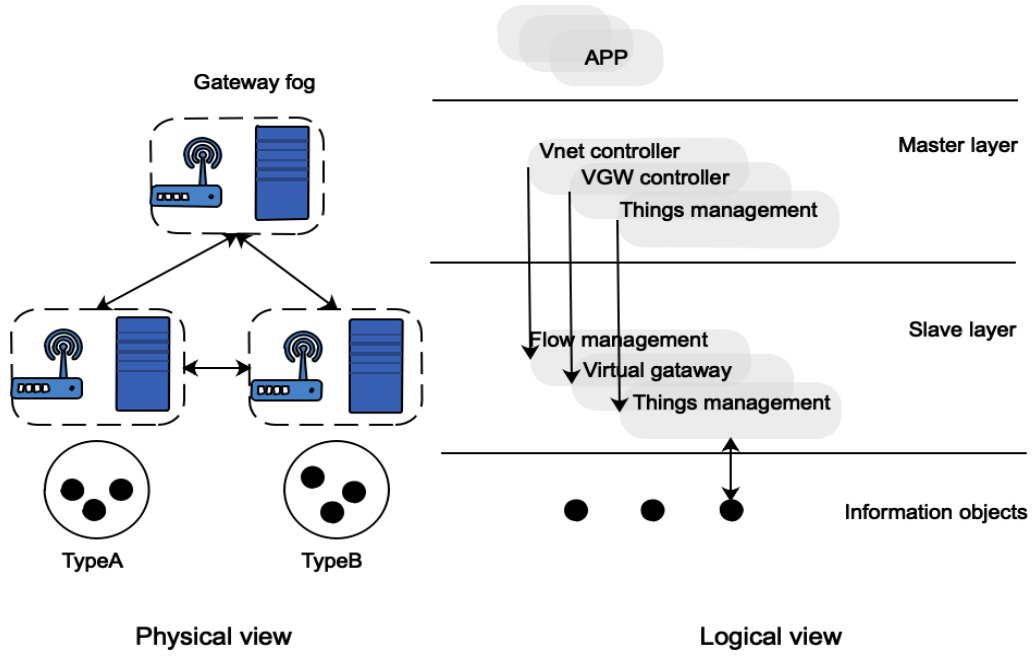


Fig. 3.10 Edge gateway mode

The data from m different sub devices, taken over t time instants, needs to be transmitted to server system. Let the set of these data be put in the form of matrix M which can be written as

$$M^{m \times t} = U^{m \times m} \Sigma^{m \times t} V^{t \times t} \quad (2.2)$$

The data compression of SVD technique is based on the weight of SVs. It means that only a few SVs are non-negligible in real practice. In that case, the approximation of matrix M can be described by keeping the significant SVs of matrix Σ . Assuming p SVs are significant SVs in matrix Σ and let MP denotes the approximated matrix M . MP can be written as

$$MP = U \Sigma' V \quad (2.3)$$

Where each matrix can be written into submatrices as

$$\begin{aligned}
MP &= \begin{bmatrix} MP_{11}^{p \times p} & MP_{12}^{p \times (t-p)} \\ MP_{21}^{(m-p) \times p} & MP_{22}^{(m-p) \times (t-p)} \end{bmatrix} \\
U &= \begin{bmatrix} U_{11}^{p \times p} & U_{12}^{p \times (m-p)} \\ U_{21}^{(m-p) \times p} & U_{22}^{(m-p) \times (m-p)} \end{bmatrix} \\
V &= \begin{bmatrix} V_{11}^{p \times p} & V_{12}^{p \times (t-p)} \\ V_{21}^{(t-p) \times p} & V_{22}^{(t-p) \times (t-p)} \end{bmatrix} \\
\Sigma' &= \begin{bmatrix} \Sigma_{11}^{p \times p} & 0 \\ 0 & 0 \end{bmatrix}
\end{aligned}$$

Data compression ratio is defined as the ratio between the uncompressed size and compressed size. For example, compression ratio=2, means that the volume of the compressed data is 50% of original data. From above assumption, the compression ratio can be written as

$$CR = \frac{m \times t}{(m + t + 1) \times p} \quad (2.4)$$

The core of lossy compression method is to find the good trade-off between the compression ratio and loss of information. The mean absolute error and the mean percentage error are used to evaluate the error between reconstructed data matrix and original matrix. The expression of *MAE* *Mae* and *MPE* are

$$MAE = \frac{1}{m \times t} \sum_{i=1}^m \sum_{j=1}^t |M(i, j) - MP(i, j)| \quad (2.5)$$

$$MPE = \frac{1}{m \times t} \sum_{i=1}^m \sum_{j=1}^t \left| \frac{M(i, j) - MP(i, j)}{X(i, j)} \right| \times 100 \quad (2.6)$$

In our case, Input data acquired from IoT devices for our simulation have been pre-processed using raw data from the estate in University of Warwick. The CR is 5:1 since it is the best trade-off between the CR and loss of information according to the table 2-1.

Table 3-1 SVD compression results

CR	p	MAE	MPE
20	28	0.031	2.41
10	55	0.018	1.45

6.67	84	0.009	1.01
5	111	0.007	0.75
4	138	0.0005	0.61

The process of the transmission of compressed data based on a distributed power system is shown as follows:

- 1) For each distributed controller, the data monitored from sensor/devices is filtered in the local filter module and then stored in the memory of distributed controller as a Metrix M .
- 2) Apply SVD to obtain the matrices U , Σ and V .
- 3) Based on a value of p chosen to achieve a given CR, form submatrices
- 4) Then, compressed data is transported from distributed controller to a central server.
- 5) Reconstructing the M of each distributed controller by computing MP and evaluate the loss of information.
- 6) Preparing the reconstructing data for the simulation platform.

3.3.5 Simulator Development

The hybrid simulator is the core in this power co-simulation system since it can simulate both the communication and energy networks as well as supporting signals exchange. Fig.3.11 illustrates the structure of hybrid simulator and has the following functions:

- 1) Simulation of distributed power flow.
- 2) Simulation of electric components, such as generations, loads and transformers.
- 3) A self-learning function module to improve the accuracy of components simulation.
- 4) Integration of network simulation based on NS-3.
- 5) An energy management system to manage distributed sources.

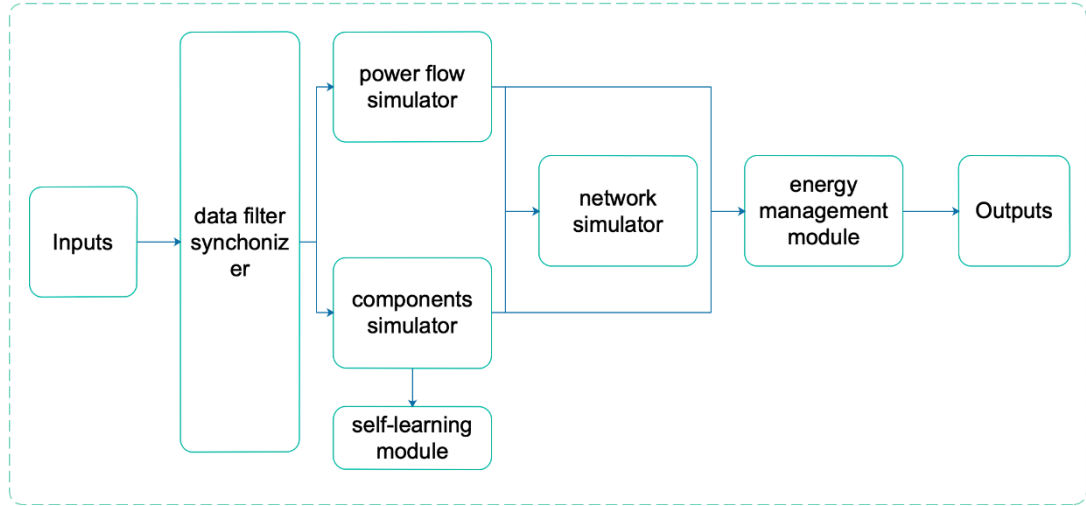


Fig. 3.11 Structure of hybrid simulator

For the simulation of power system, GridLAB-D models define the network through elements such as transformers, meters, lines, loads and generators. However, not all elements need to be simulated in different projects since some real elements are to be taken for the HIL simulation. So, switchable function will be needed to select different modules and the data from real devices will be used in the self-learning module.

NS-3 [144] is a discrete event network simulation platform mainly developed for educational purposes and experiments on Internet-based environments. The goal of the NS-3 is to develop a preferred, open simulation environment for networking research: it should be aligned with the simulation needs of modern networking research and should encourage community contribution, peer review, and validation of the software. NS-3 uses Mercurial as a source code management system and Waf for building the source code libraries.

Then, a broker is needed between electrical power simulator and network simulator. FNCS [145] is proposed in our simulator since it able to support integration with one or other simulators in conjunction with a communication network simulator, such as MATLAB, MATPower and EnergyPlus.

Time management and synchronization is especially challenging for the power system with multiple time scales. To solve this, a two-synchronization scheme is used to achieve on-time delivery as shown in Fig.3.12. Step1 synchronization is executed when all simulators are fully implemented at time t and then this synchronization

time t' is calculated. During the period, all data generated at time t will be delivered to the network simulator. Step2 is delivered at time t' and it is noted that the time period of network simulation should lower than t' . During the phase any messages are to be delivered.

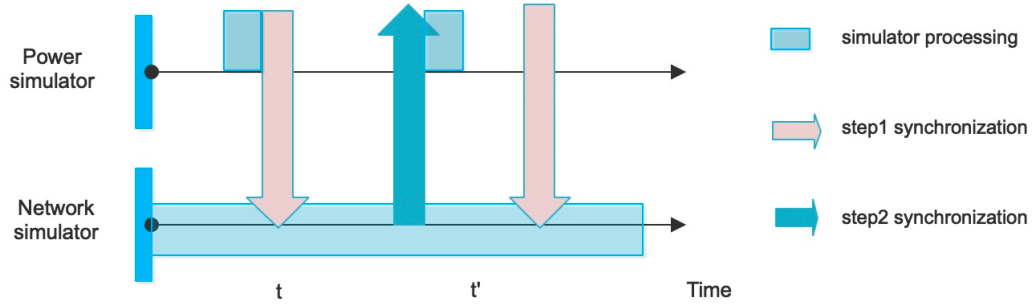
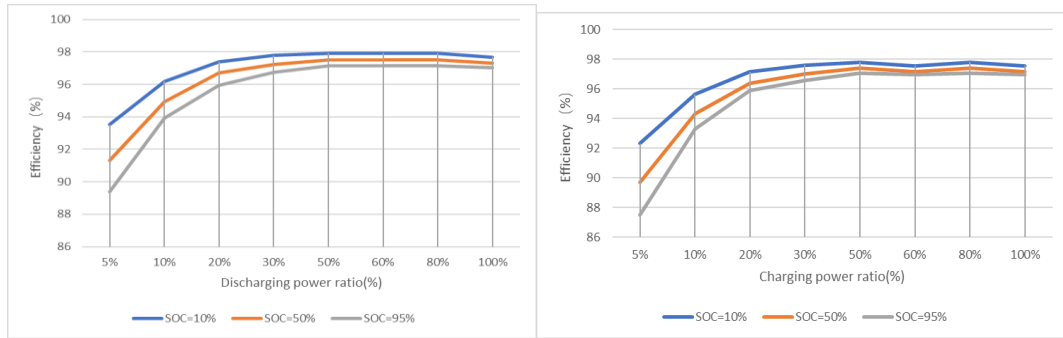


Fig. 3.12 Two synchronization scheme

The battery model is of rebuilt of GridLAB-D battery model by considering the self-discharging and the inverter efficiency curve. From the real data, the efficiency of inverter is determined by the SOC and charging/discharging power as shown in Fig.3.13. The inverter efficiency is close to its upper value when the discharging/charging power gets close to 35% of rated power.



a) Discharging efficiency

b) charging efficiency

Fig. 3.13 Discharging/charging efficiency of inverter

The SOC at the time t during the processes of charging, discharging and self-decay can be obtained by the following equation.

$$\begin{cases} \text{Charging: } SOC_t = SOC_{t-1} + \frac{P_{ch}\eta_{in}\Delta t}{C_b} \\ \text{Discharging: } SOC_t = SOC_{t-1} - \frac{P_{dis}\Delta t}{\eta_{in}C_b} \\ \text{Self-decay: } SOC_t = SOC_{t-1} - k_{de}\Delta t \end{cases} \quad (2.7)$$

where, P_{dis} and P_{ch} refer to the charging and discharging power, respectively; C_b is the capacity of the battery; k_{de} is the self-decay rate; and Δt is the time interval. It is assumed that the SOC delay of every minute is determined by the following equation. it is also one of the parameters that is to be updated.

$$k_{de} = (0.001 + (SOC_{ini} - 10) \times 0.0001) / 60 \quad (2.8)$$

For the lithium-ion battery, the equation of impact of aging on battery capacity can be represented as

$$Q(n) = \begin{cases} Q_{bol} - \varepsilon(n) \cdot (Q_{bol} - Q_{eol}) & n \neq 0 \\ Q(n-1) & n = 0 \end{cases} \quad (2.9)$$

where, Q_{bol} is battery maximum capacity in Ah, at the beginning of life; Q_{eol} is battery maximum capacity in Ah at the end of life; $n = bT_h$, T_h is half-cycle duration in s .

$$\varepsilon(n) = \begin{cases} \varepsilon(n-1) + \frac{0.5}{N(n-1)} \left(2 - \frac{DOD(n-2) + DOD(n)}{DOD(n-1)} \right) & n \neq 0 \\ \varepsilon(n-1) & n = 0 \end{cases} \quad (2.10)$$

where, DOD is battery depth-of-discharge (%) after a half-cycle duration.

$$N(n) = H \left(\frac{DOD(n)}{100} \right)^{-\xi} \cdot \exp \left(-\varphi \left(\frac{1}{T_{ref}} - \frac{1}{T_a(n)} \right) \right) \cdot (I_{ave}^{dis}(n))^{-\gamma_1} \cdot (I_{ave}^{ch}(n))^{-\gamma_2} \quad (2.11)$$

where, H is cycle number constant; ξ is exponent factor for the DOD; φ is Arrhenius rate constant for the cycle number; I_{ave}^{dis} is average discharge current in A during a half cycle duration; I_{ave}^{ch} is average charge current in A during a half cycle duration;

γ_1 is exponent factor for the discharge current; γ_2 is exponent factor for the charge current.

3.4 Cases Study

3.4.1 Case Study of Simulator

This case is used to verify the performance of developed simulator. As shown in Fig.3.14, this simulator is to simulate the electricity trading process and electricity management based on the electricity price. This simulator includes the information transmission via network simulator, the simulation of power system via GridLAB-D and the energy management system. The communication connection between each simulator/management system is built via a FNCS broker, so each independent simulator/management system can complete its own simulation/control based on the information from other simulators/management system.

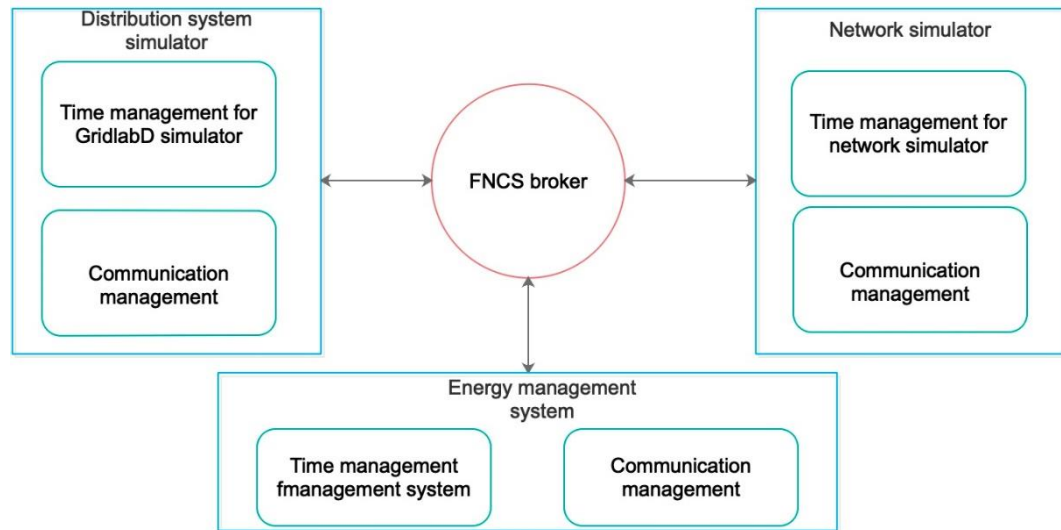


Fig. 3.14 Communication architecture of hybrid simulator

The distribution system simulator is developed based on the IEEE European Low Voltage Test Feeder ELVTF, as shown in Fig.3.15. This is a low-voltage power system based on a distribution system with a fundamental frequency of 50 Hz. The feeder is connected to the Medium Voltage system through a transformer at a substation. The transformer steps the voltage down from 11 kV to 416 V. The medium voltage node is modelled as a voltage source and appropriate impedance. The transformer at the substation is rated 4MVA (import)/1MVA (export), rated

voltage 11/0.416kV with delta/grounded-wye connection. The 25 solar systems and 10 battery systems are randomly installed in different nodes to simulate the distributed energy sources.

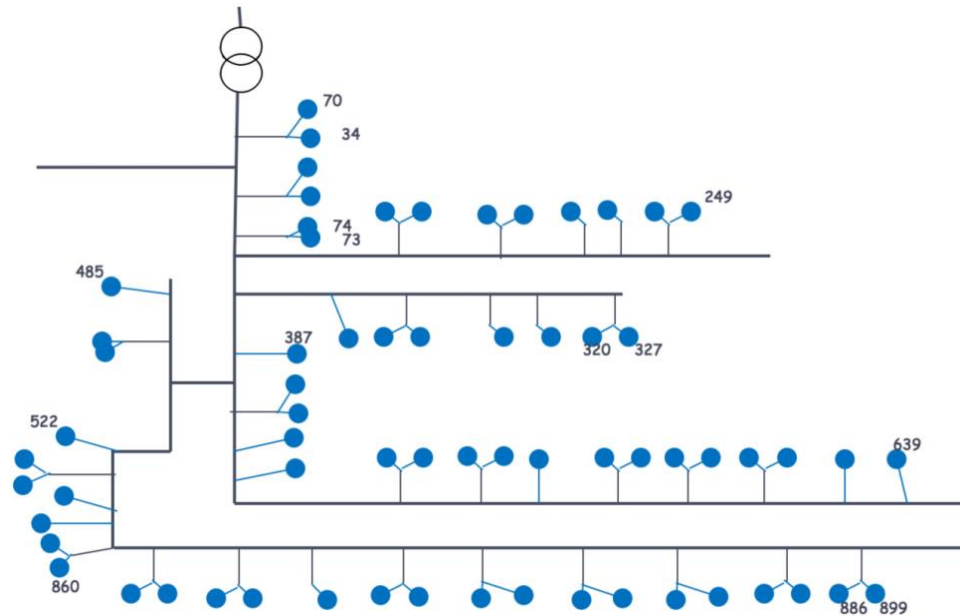


Fig. 3.15 European low voltage test feeder [142]

The data, such as metering information, transaction information, weather data, is transmitted to the network simulator or energy management system. The Carrier-Sense Multiple Access (CSMA) protocol is used in the network simulator since CSMA tries to reduce the frequency of these collisions and provide a plan at the same time on how to proceed if a collision does occur. time delay is set to 2ms for simulating transmission latency. The power controller will send the control command to the controllable components via broker after dealing with the input data from distribution simulator. A basic transaction process is also simulated to verify the information exchange between each node.

The case study will demonstrate a real case of transactive control, exchanging market price, control command and bids through a simulated network, as shown in Fig.3.16. The distributed simulator consists of 100 houses. Some of these houses take part in a transactive market where they send bidding information to an auction agent. A price signal broadcasts back to the participating houses based on the bidding information. The power controller which is responsible for controlling the working status of 10 battery systems installed in user's houses will manage these batteries according to

the system demand and signal price. The information is communicated through the NS-3 by realistically considering messages delay. Each node is given an IP address and later map the IP addresses to names given to each house in the GridLAB-D model. The NS-3 model routes the message appropriately, realistically delaying its transmission, and then the FNCS application instance running on the destination node in the network reads the message once it arrives and sends it back to the FNCS broker so it can be sent back to the destination simulator. The simulator will run on Dell T640 server including 16 cores per processor, 64G memory and 2T storage disk.

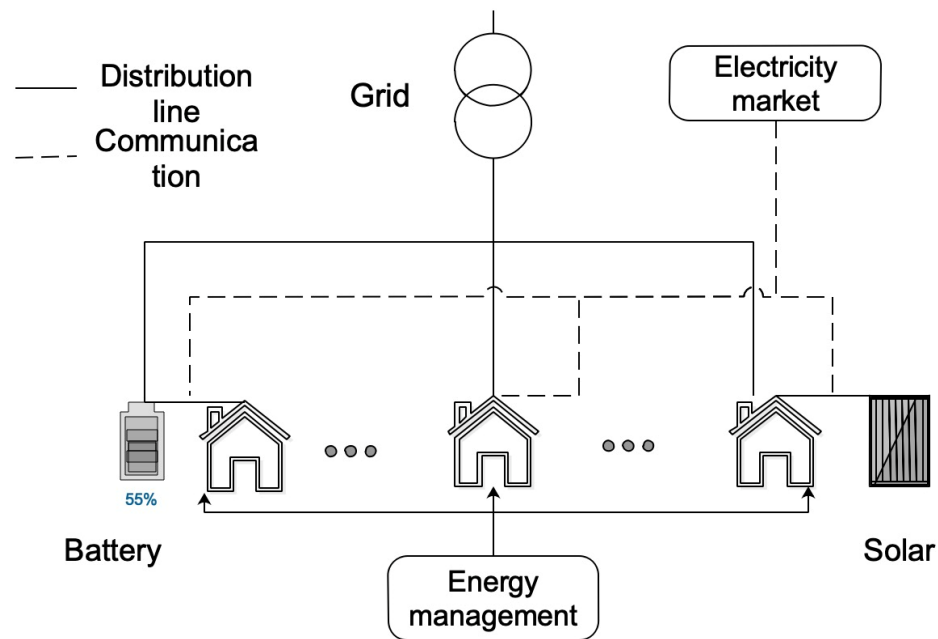


Fig. 3.16 Local energy system for case study

The main substation transformer is defined as a reference property that the value of which represents the total demand of the market and it is used to estimate the unresponsive buyers. In our case, we assumed that the allowable bid price and bid capacity are limited to £1.2 and 720 kW respectively. Fig.3.17 shows the distribution of total load in one day. The reference bid price should be bid at predefined margin, as is shown in Fig.3.18. In this case, the parameters, such as market ID, average price, standard price deviations and clearing price are subscribed to hybrid simulator via FNCS broker. The power controller schedules the battery working based on the current clearing price.

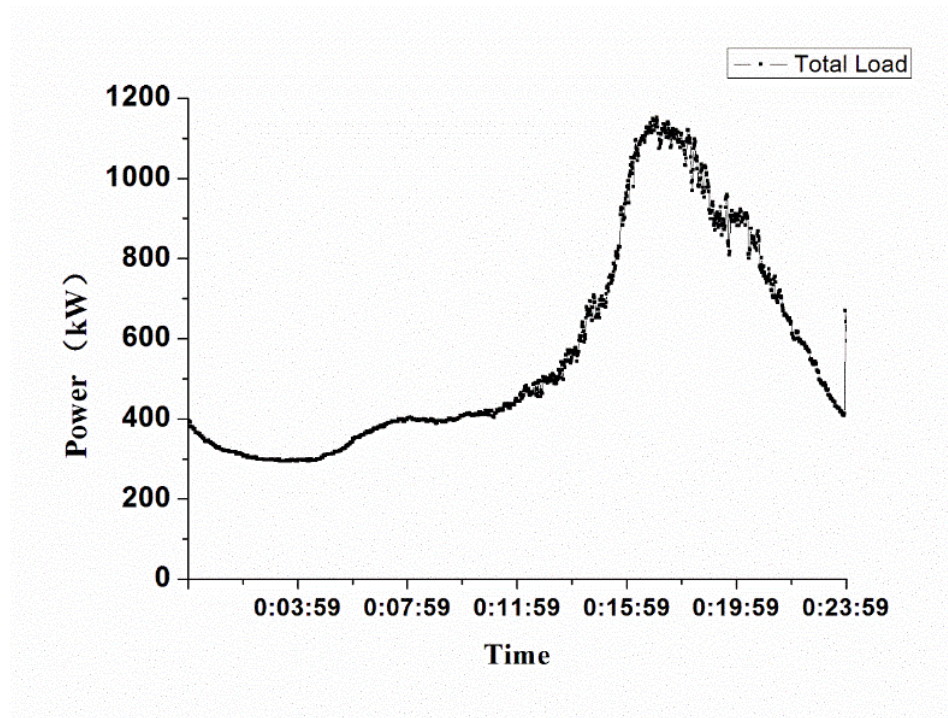


Fig. 3.17 Distribution of load demand

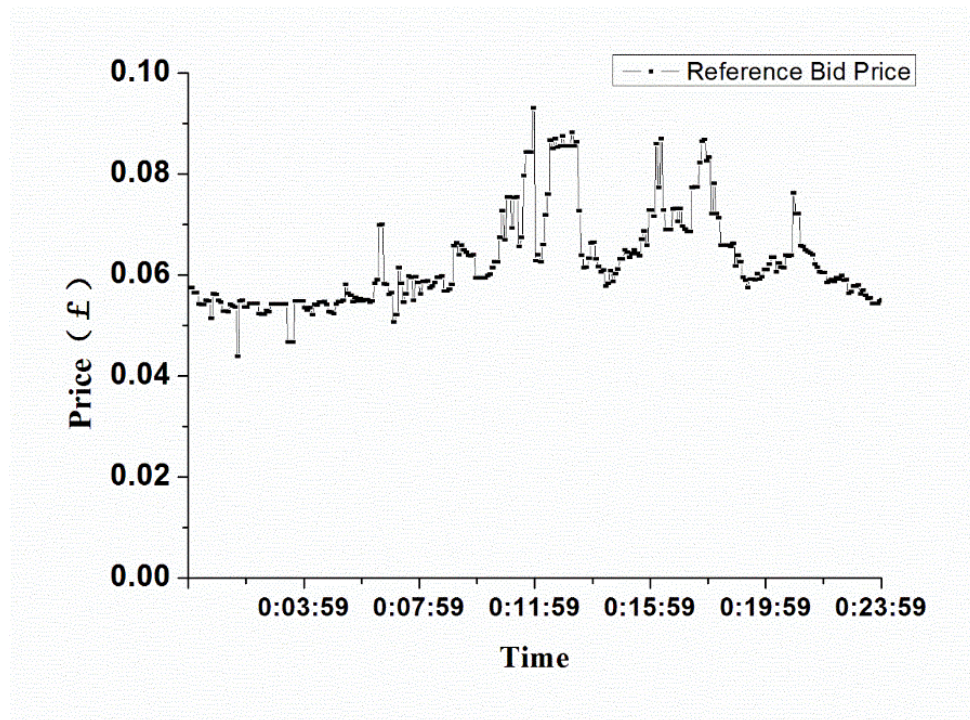


Fig. 3.18 Reference bid price

Fig.3.19 represents the clearing price and clearing capacity in hybrid simulator. The clearing price is close to reference price when the bid capacity is below the capacity limit. The clearing price is up to maximum price limit when bid capacity gets up to 720 kW. After the energy management system received the clearing price from FNCS

broker, the scheduling signals are generated and sent back to distribution simulator via FNCS broker. Fig.3.20 shows the working scheduling of one battery system. To verify the process of data transmission, the simple control strategy is that system is charging when the price is low, and the system is discharging when the price is high.

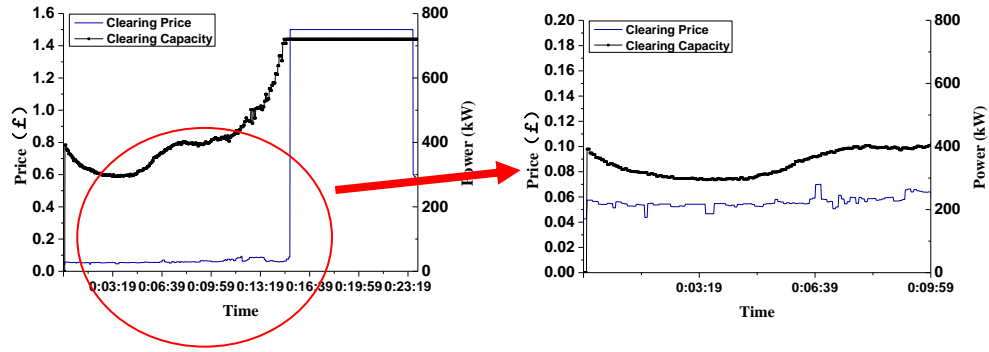


Fig. 3.19 Clearing price and capacity

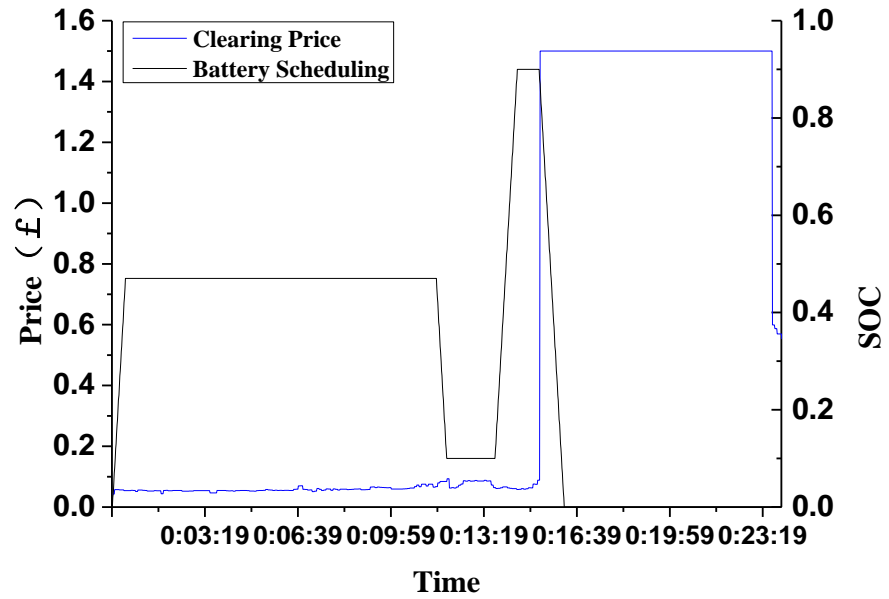


Fig. 3.20 Scheduling of battery management

3.4.2 Case study of Co-Simulation System

This case study introduces a novel co-simulation architecture that integrates IoT techniques & HIL techniques. As shown in Fig.3.21, the battery system is located in remote area with the integration of inverter and the server locates in the lab. The purpose of this case is to compare the performance of the inverter simulator with that

of actual inverter then control the battery scheduling according to the management power balance in the LES simulator.

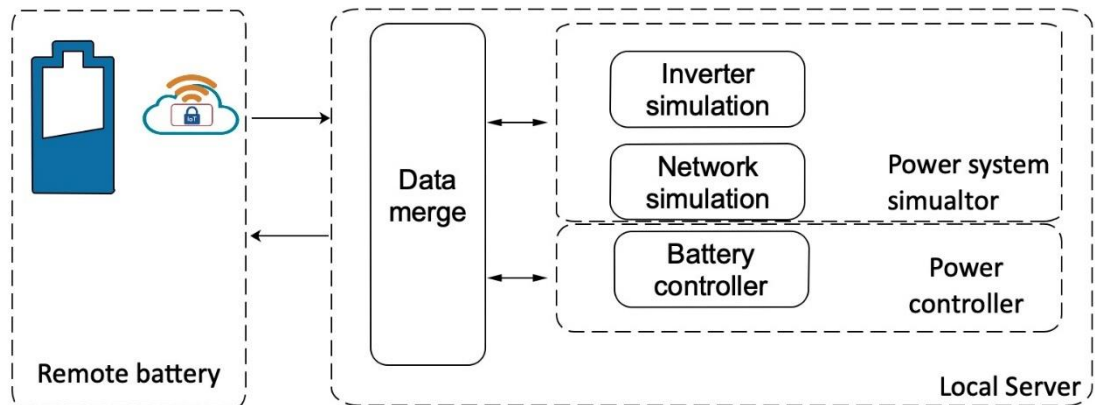


Fig. 3.21 Architecture of co-simulation for case study

As shown in Fig.3.22, there are three main parts in this co-simulation structure: hardware, simulator and distribution simulator. The distribution simulator that simulates the European low-level test feeder generates a point of connection, which is connected to a physical battery system. The battery system works in a constant current mode, in which the system is controlled by using voltage magnitude and frequency as references. The local simulator control signal is updated at 1-kHz sample frequency of real-time model, which is much faster than the 1-Hz updates from data transmission and distribution simulator.

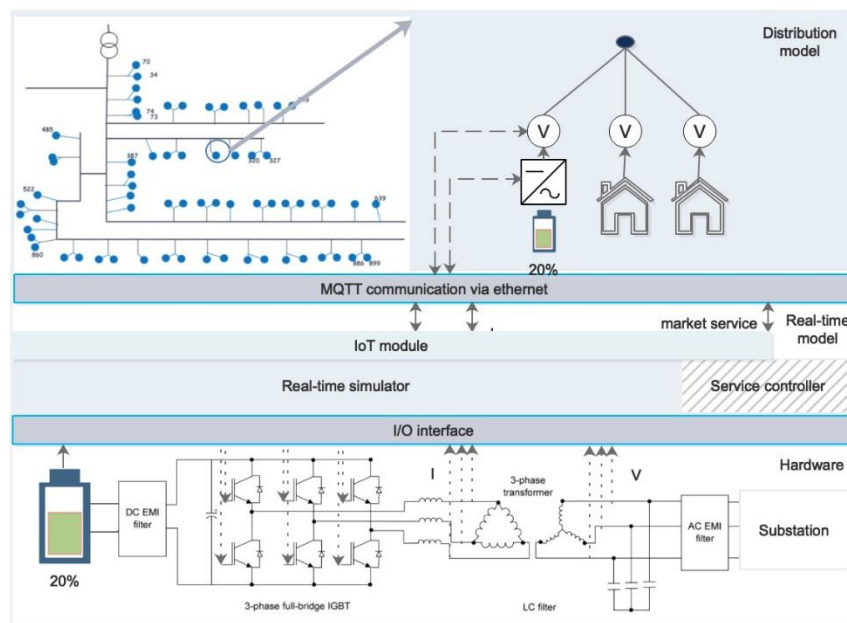


Fig. 3.22 Diagram of power co-simulation

Simulating the DC interaction of battery inverter is implemented by using hybrid simulator to enable testing battery inverter under controlled State of Charge (SoC) and power of battery. The simulator controller is used to control the inverter. At the same time, the signals, such as inverter DC voltage, SoC and system current, are transmitted to simulator via IoT system. By constantly modifying the charging/discharging power based on simulated varying conditions and real response of inverter, this configuration help the distribution simulator to improve the accuracy of simulation of battery inverter system.



Fig. 3.23 Battery storage system in the UoW

This co-simulation system is validated in different ways. The battery inverter model itself is validated through the real battery system installed around sports centre of UoW (as shown in Fig.3.23). It is a 50kW battery system with 35 kWh Li-ion battery installation. Fig.3.24 shows the results of the power step-up test in the real system and the simulation platform. In the real battery system, the control strategy of battery inverter is based on the PID controller. The overshoot during the step test is hard to avoid even though these parameters are optimized during the product commissioning. In comparison, the quasi-steady model used in the virtual simulation model is difficult to accurately simulate the real reactions of battery inverter. However, the simulator can simulate the operation of battery system very well in most of conditions.

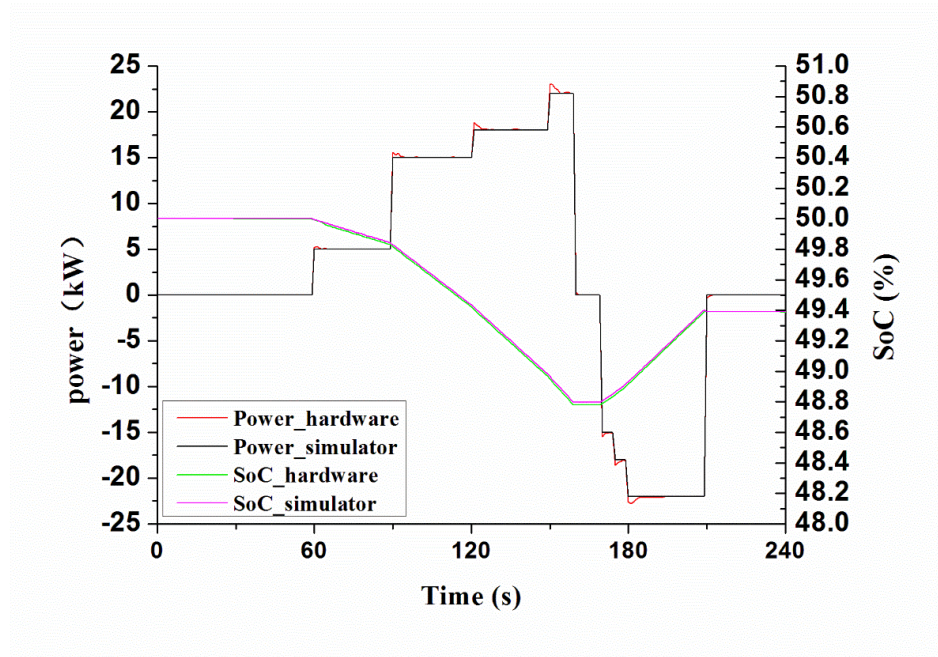


Fig. 3.24 Control outputs (hardware vs. simulator)

To validate the power co-simulation platform and evaluate system-level impacts by using the existing distribution feeder model, one of nodes of the European low-level test feeder is connected to battery simulator as shown in Fig.3.25. The inputs of battery simulator are from the real battery system via IoT system. In this case, the battery simulator will generate the charging/discharging command based on the load profile in the distribution simulator. The simulator will send charging command to hardware when the load of connection node is below the setting value. The hardware will receive the discharging power from simulator when the load of connection node is above setting value. The aim of this algorithm is to keep the load in a stable status. The output signals from hardware are regard as inputs of simulator to analyse the impact to the distribution system.

Fig.3.26 shows the load profiles and battery information in connection node before and after the battery system is connected. The data for the platform validation is randomly intercepted certain pieces (680s) of data in a day. As for the battery scheduling, negative value represents a charging mode of battery while a positive value represents a discharging mode. As shown in Fig.3.27, the peak load of connection node reduces from 10 kW to 3.8 kW. After the battery is introduced, load fluctuations reduce from 10 kW to 1.8kW and voltage stability is improved around this connection node. Although the load fluctuation of this node is reduced, in fact,

after the battery is used, the node voltage slightly increases by 0.4V. That is because the voltage of this node is mainly affected by the voltage and load of other nodes. The reduction of fluctuation of this node does not affect the overall load fluctuation, so the voltage at this node rarely changes. The time round-trip delay between simulator and hardware is around 0.2s and the reaction of simulator has around 1s time delay compared with the real reaction of hardware. The dynamics of this power co-simulation architecture are mainly limited by the combination of communication latency and frequency of signals sampling.

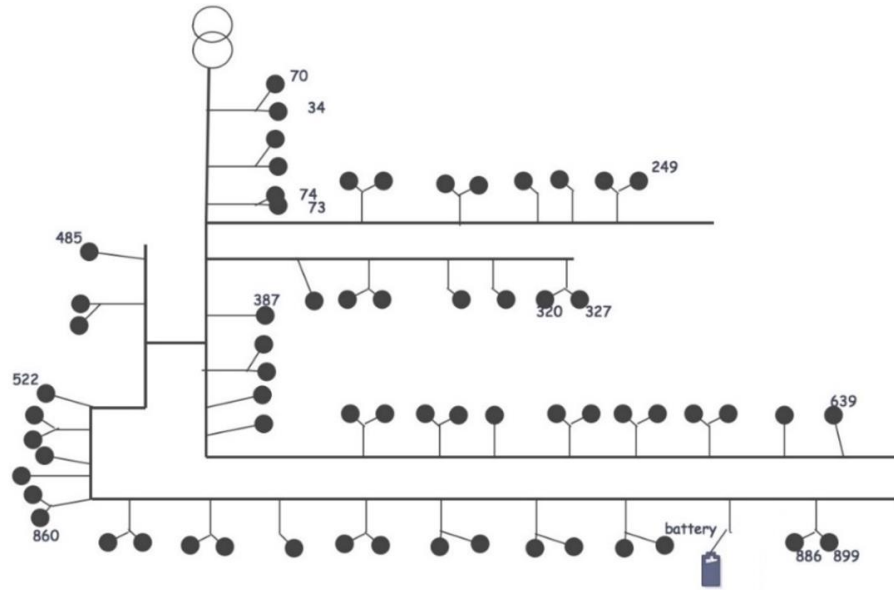


Fig. 3.25 Connection node of battery system

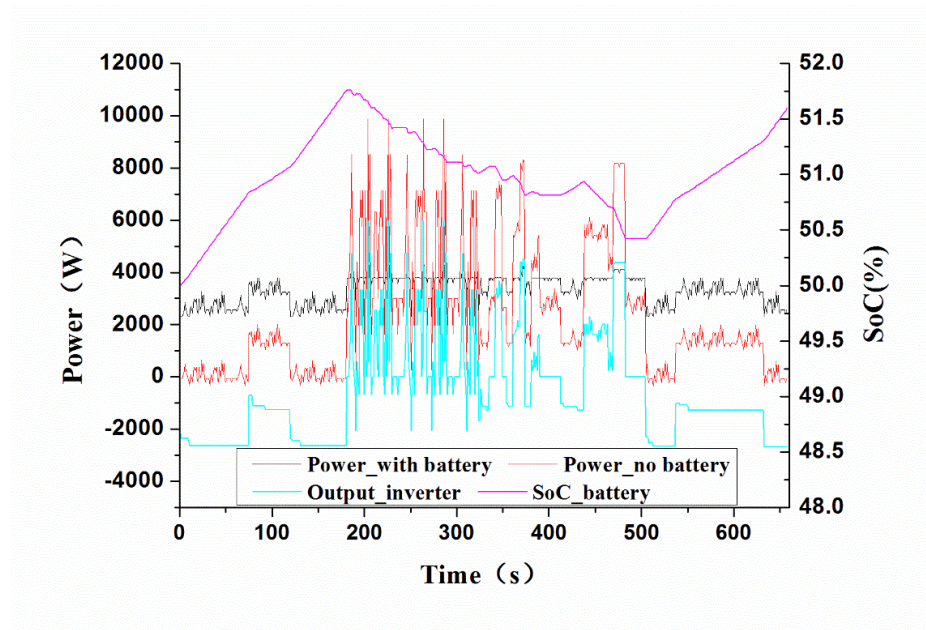


Fig. 3.26 Node load profile and battery scheduling

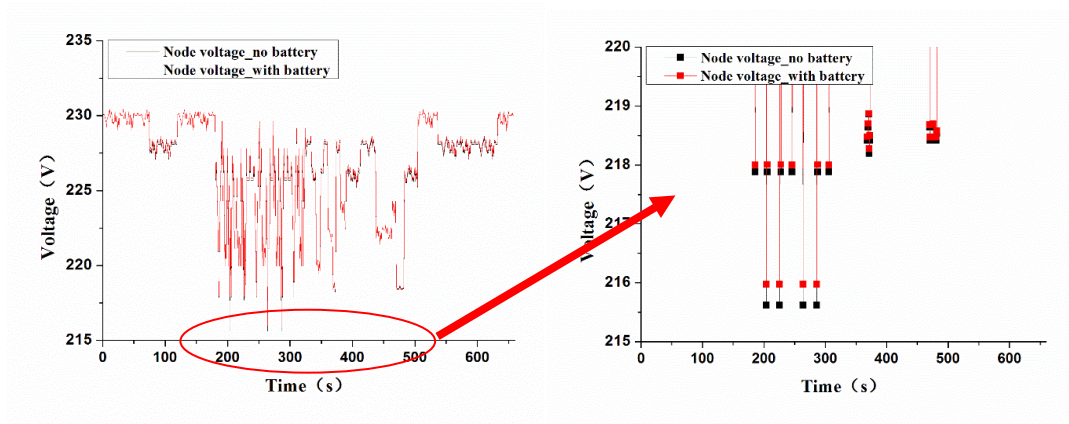


Fig. 3.27 Node voltage

3.5 Summary

The different co-simulation methods are introduced to simulate the more and more complex distribution system. HIL system is proposed co-simulation architecture since some real electrical components cannot be well simulated the by the virtual simulator. PHIL allows a physical controller hardware to be evaluated with the simulated inputs, such as the inverter controller, battery controller and turbine controller. The main parts of PHIL architecture that need to be concerned, such as time synchronization, IoT communication and security are introduced in this chapter. The hardware sampling frequency, data transmission delay and simulation computation time have been carefully considered for the purpose of time synchronization. The device gateway acts as an intermediary between connected devices and the cloud services, which allows those devices to exchange the data via MQTT protocol. The MQTT messages are transit over Transport Layer Security (TLS), the succession of SSL (Secure Sockets Layer). A multi-layer security architecture is applied at each layer of IoT system. A co-simulation system is developed based on IoT techniques and HIL techniques. The hybrid simulator which is the core in this IoT-based HIL system can simulates both the communication and power networks and generate indication or control signals to each device. the integration of the co-simulation system will be designed by considering time synchronization, system security and data flow power co-simulation system.

This platform aims to provides a generic, scalable, yet easily customized solution for LES simulation that can support different hardware, high volumes of data exchange between simulator and hardware and several different simulation programs.

The co-simulation system studied in this chapter will work as the foundation for other researches which contents will be mentioned in subsequent chapters. The system supports the research in subsequent chapters in various aspects stated below:

- 1) Data service: the co-simulation system contains a comprehensive data acquisition function, information collected will work as a supportive data for scheduling optimization of energy system, techno-economic analysis of solar integration and design of P2P trading mechanism discussed in following chapters;
- 2) Simulation of LES: the modeling and scheduling of LES discussed in chapter 4 are based on this co-simulation system, while the LES model developed in Chapter 5 further extended on the foundation of co-simulation system.
- 3) Operating platform: the purpose of the simulation-system is to provide a flexible and compatible environment for different LES research.

Chapter 4

Optimal Scheduling of CHP-based Energy System

4.1 Introduction

In recent years, more attention was paid to the requirements of improving energy utilization efficiency and addressing environmental problems. In addition, some new techniques, such as solar PV, CHP and energy storage, are becoming more economic viable for the perspective of investment. In many cases, various generation technologies are used or combined in one particular energy system with integration of thermal and electrical energy storage units. The different units of the combined system operation cost are traditionally optimised separately with no coordination. In that case, the system does not work optimally from system perspective, which in turn increases the system operation cost. Operation scheduling is crucial for system reliability and efficiency while considering the coupling relationship among these units and their interactions of different states. The challenges are presented

- The smart energy is more flexible with the installation of distributed generator and switchable load. In other words, the overall uncertainty is greatly increased. In addition, the output of some power sources, such as PV system and wind generations, is intermittent, which bring more challenges for the operation.
- The optimal scheduling problems consist of various decision variables that should be taken into account to achieve optimal solution. However, optimising these variables brings more computational difficulty and is time-consuming.

In this chapter, the optimal scheduling strategy of CHP-based combined energy system is investigated. Firstly, the mathematical model is built to simulate the energy balance of this combined system. Then, the load and supply scenarios are introduced under the consideration of uncertainties to analyse annual operation cost. The following would find the optimal strategy of system scheduling to reduce annual operation cost. Finally, the test results are analysed.

4.2 Uncertainties of Energy Supply and Demand

The operation scheduling of combined energy system is influenced by the actual values of energy supply and demand which are determined by various factors such as weather and user behaviour. Uncertainties always remains for future energy supply

and demand as the true values of future energy supply and demand remain unknown. Such uncertainties make it difficult for a design of the long-term optimal scheduling strategy. Firstly, the uncertainties bring the difficulty in historical data selection, the data processing based on a single year data is different with that of multi-year data; Secondly, the uncertainties of supply and demand will dramatically affect the results of prediction and optimisation. So, the uncertainty management is necessary for developing a representative scheduling strategy. Different methods can be used for the uncertainties management: analytical equations ([146]-[147]), statistical/machine-learning techniques [150] and hybrid models ([151]-[154]).

4.2.1 Demand Uncertainties

To achieve a sensible solution, several sources of demand side uncertainties should be taken into consideration. When taking the uncertainties in electrical demand, thermal demand and cooling demand into account, it is assumed that each of them follows normal distribution [155]. To be simplify, these distributions are independent between each other. Thus, the Probability Density Function (PDF) of electrical demand, thermal demand and cooling demand can be respectively represented by

$$f(ED) = \frac{1}{\delta_{ED}\sqrt{2\pi}} e^{-\frac{(ED-\mu_{ED})^2}{2\delta_{ED}^2}} \quad (4.1)$$

$$f(TD) = \frac{1}{\delta_{TD}\sqrt{2\pi}} e^{-\frac{(TD-\mu_{TD})^2}{2\delta_{TD}^2}} \quad (4.2)$$

$$f(CD) = \frac{1}{\delta_{CD}\sqrt{2\pi}} e^{-\frac{(CD-\mu_{CD})^2}{2\delta_{CD}^2}} \quad (4.3)$$

where, $f(ED)$, $f(TD)$, $f(CD)$ are the probability density function of electrical demand, thermal demand and cooling demand, respectively; μ_{ED} , μ_{TD} , μ_{CD} are sample mean of electrical demand, thermal demand and cooling demand; δ_{ED} , δ_{TD} , δ_{CD} are the sample variance of electrical demand, thermal demand and cooling demand; ED , TD , CD are the sample values for electrical demand, thermal demand and cooling demand.

Markov chain modelling is an autoregressive process which are normally used to generate synthetic sequences for modelling stochastic data [148]. Markov chain modelling is based on the construction of a transitional probability matrix where the transition from one discrete state to another discrete state is represented in terms of its probability [149]. Firstly, the first order Markov chain model process the current state and calculate the probability of going to next state. The second order Markov chain model calculate the next state by comparing two previous states with the current one. Markov chain model is suited to modelling systems where the current state of a sequence is highly correlated to the state immediately preceding it and where a large sample size of data exists. For the demand side uncertainties, the uncertainties are determined by the user's behaviour and activities requirement, the correspondence between each state are ignored in our case.

4.2.2 Supply Uncertainties

A statistical approach is applied to forecast solar radiation. Beta PDF (as shown in Eq.4.4) is used to model the probability distribution of solar generation since Beta distribution is proved to be the better model to describe the probability distribution of solar radiation ([156]-[157]).

$$f(x) = \begin{cases} \frac{\Gamma(\alpha + \beta)}{\Gamma(\alpha)\Gamma(\beta)} x^{(\alpha-1)} (1-x)^{(\beta-1)} & 0 \leq x \leq 1 \\ 0 & \text{otherwise} \end{cases} \quad (4.4)$$

Where, $f(x)$ is the probability density function of solar generation, x is the sample value of solar generation, and α, β are the parameters calculated from historical sample data of solar generation, as shown in Eq.4.5

$$\begin{aligned} \alpha &= \mu \left(\frac{\mu(1-\mu)}{\delta} - 1 \right) \\ \beta &= (1-\mu) \left(\frac{\mu(1-\mu)}{\delta} - 1 \right) \end{aligned} \quad (4.5)$$

where, μ is the sample mean and δ is the sample variance of solar generation.

4.3 Modelling of CHP-based Energy System

4.3.1 Introduction of CHP-Based Energy System

A schematic diagram of a typical CHP-based energy system is shown in Fig.4.1. The energy system consists of two subsystems: heat subsystem and electricity subsystem. The heat subsystem contains gas boiler, gas-fired engine, absorption chiller and thermal storage. While the power subsystem includes gas-fired engine, solar PV system and electricity storage. In addition, the power subsystem can import or export the electricity via the external Distribution Network Operator (DNO) distribution system, which means the CHP-based energy system is directly connected with the main grid. The DNO will charge the electricity usage according to the primary meter installed on the DNO main switch room. The thermal storage and electricity storage are integrated to balance the energy flow.

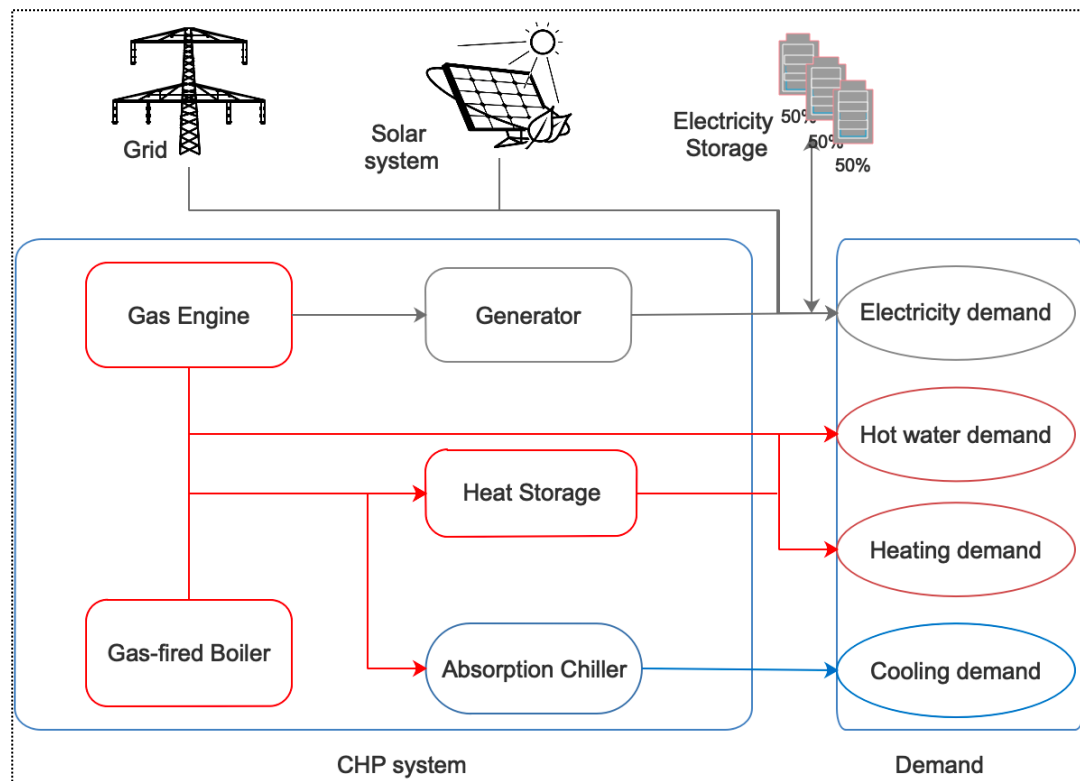


Fig. 4.1 Diagram of CHP-based energy system

As an important component of energy system, CHP generates electricity and provides recoverable heat simultaneously. The energy efficiency of CHP has big impact on system energy efficiency, so a curve fitting model is used to simulate the CHP

electricity efficiency in various power outputs. In [158], the CHP efficiency (as shown in Eq.4.6) curve can be represented by a third-degree polynomial fitting function for electricity curve.

$$\eta_{iCHP}^{ele} = a_1 r_i^3 + a_2 r_i^2 + a_3 r_i + a_4 \quad (4.6)$$

Where, η_{iCHP}^{ele} is the electricity efficiency of CHP unit i ; r is the ratio between actual power and rated power; a_1, a_2, a_3, a_4 are coefficients that need to be identified.

Normally, more than one CHP unit is integrated into energy system to meet the electricity and heat demand. So, the efficiency of CHP system is determined by the efficiency of each CHP unit. The CHP efficiency can be written as

$$\eta_{CHP}^{ele} = \frac{\sum_{i=1}^N \eta_{iCHP}^{ele}}{N} \quad (4.7)$$

where, η_{CHP}^{ele} is the CHP efficiency; η_{iCHP}^{ele} is the electricity efficiency of CHP unit i ; N is the number of CHP units.

The gas-fired boiler is used to convert gas to heat and then conducted to the surrounding water. Concerning the thermal storage, there are some heat storage system fitted around CHP house to store heat in buffering the thermal demand variations.

For the electricity storage system, the amount of energy stored at the battery system can relieve the peak demand of electricity import from main grid. In addition, the battery system can help reduce the electricity bill by considering the Time of Use (ToU) price.

4.3.2 Problem Formulation and System Modelling

4.3.2.1 Problem formulation

The objective of optimal operation of energy system is to minimize the operational cost. The operation cost consists of gas bill and electricity bill. The decision variables include the amount of natural gas consumed; electrical energy imported from main grid. The objective function is formulated as follows:

$$OC_{sce} = \min(\sum_t ((p_{gas}(t) \cdot G_{gas}(t) + p_{elec}(t) \cdot E_{grid}(t))) \quad (4.8)$$

where, OC_{sce} is the object function of operation cost of each scenario; $p_{elec}(t)$ and $p_{gas}(t)$ are the unit purchase price of electricity and natural gas price; $E_{grid}(t)$ is the energy imported from main grid at timestep t , it equals to $E_{grid}(M_{sup}, M_{dem}, t)$, where M_{dem} and M_{sup} are the indication of energy demand and supply.; $G_{gas}(t)$ is the consumed natural gas at timestep t .

The gas consumption consumed by boiler and gas-based engine can be formulated as

$$G_{gas}(t) = \frac{H_{CHP}^{Boil}(M_{dem}, t)}{(\eta_{boil} \cdot LHV_{ngas})} + \frac{H_{CHP}(M_{dem}, t)}{(\eta_{CHP}^{th} \cdot LHV_{ngas})}, \forall M_{dem}, M_{sup}, t \quad (4.9)$$

where, $G_{gas}(t)$ is gas consumption consumed by boiler and gas-based engine; η_{boil} is heat efficiency of gas-fired boiler; LHV_{ngas} is lower heat value of natural gas.

In this case, the long-term operation scheduling optimisation is characterised by the combination of various independent scenarios. After we get the optimal result for each scenario, the long-term optimisation objectives are the sum of each scenario function.

$$OC = \sum OC_{sce} \quad (4.10)$$

4.3.2.2 modelling of energy balance

To satisfy the given load demand, electricity, domestic hot water, and space heating and cooling energy balances are formulated in the following. For electricity, the sum of the load demand must be satisfied by the sum of the electricity provided by CHP, PV, power grid, and electrical storage

$$E_{dem}(M_{dem}, t) + E_{ES}^{Ch}(M_{dem}, t) = E_{CHP}^{Eng}(M_{sup}, t) + E_{PV}(M_{sup}, t) + E_{ES}^{Dis}(M_{sup}, t) + E_{grid}(M_{sup}, M_{dem}, t), \quad \forall M_{dem}, M_{sup}, t \quad (4.11)$$

where, $E_{dem}(M_{dem}, t)$ is the load demand; $E_{ES}^{Ch}(M_{dem}, t)$ and $E_{ES}^{Dis}(M_{sup}, t)$ are the battery charging and discharging energy during timestep t ; $E_{CHP}^{Eng}(M_{sup}, t)$ represents the electricity generated by CHP during timestep t ; $E_{PV}(M_{sup}, t)$ is the energy provided by solar PV system during timestep t ; $E_{grid}(M_{sup}, M_{dem}, t)$ is the energy imported/exported from/to grid; M_{dem} and M_{sup} are the indication of energy demand and supply.

The thermal demand must be satisfied by the thermal energy provided by CHP, gas-fired boiler, and thermal storage:

$$\begin{aligned} H_{dem}(M_{dem}, t) + H_{TES}^{Ch}(M_{dem}, t) = & H_{CHP}^{HD}(M_{sup}, t) + H_{CHP}^{Boil, HD}(M_{sup}, t) \\ & + H_{TES}^{Dis}(M_{sup}, t), \quad \forall M_{dem}, M_{sup}, t \end{aligned} \quad (4.12)$$

where $H_{dem}(M_{dem}, t)$ is the heat demand during timestep t ; $H_{TES}^{Ch}(M_{dem}, t)$ and $H_{TES}^{Dis}(M_{sup}, t)$ are thermal charging and discharging energy during timestep t ; $H_{CHP}^{HD}(M_{sup}, t)$ represents the heat generated by CHP during timestep t ; $H_{CHP}^{Boil, HD}(M_{sup}, t)$ is the heat energy generated from gas-fired boiler during timestep t .

For the cooling balancing, the demand must be satisfied by the thermal energy provided by CHP and gas-fired boiler:

$$C_{dem}(M_{dem}, t) = [H_{CHP}^{CD}(M_{sup}, t) + H_{CHP}^{Boil, CD}(M_{sup}, t)] \times \eta_{CoP}, \quad \forall M_{dem}, M_{sup}, t \quad (4.13)$$

where, η_{CoP} is the Coefficient of Performance (CoP) of absorption chiller; $C_{dem}(M_{dem}, t)$ is the cooling demand during timestep t ; $H_{CHP}^{CD}(M_{sup}, t)$ and $H_{CHP}^{Boil, CD}(M_{sup}, t)$ are energy provided by CHP and boiler for absorption chiller during timestep t .

4.3.2.3 Gas-fired boiler

The total thermal supply of boiler is subdivided to meet the demand of heat demand, and the demand of cooling through the absorption chillers[158]:

$$H_{CHP}^{boil}(M_{dem}, t) = H_{CHP}^{Boil, HD}(M_{sup}, t) + H_{CHP}^{Boil, CD}(M_{sup}, t), \quad \forall M_{dem}, M_{sup}, t \quad (4.14)$$

where, $H_{CHP}^{boil}(M_{dem}, t)$ is the total demand of gas-fired boiler during timestep t .

4.2.3.4 Energy balance of CHP

The total heating rate recovered is subdivided to meet the demand of domestic hot demand, and the demand of space cooling through the absorption chillers[158]:

$$H_{CHP}(M_{sup},t) = H_{CHP}^{CD}(M_{sup},t) + H_{CHP}^{HD}(M_{sup},t) + H_{TES}^{Ch}(M_{dem},t), \forall M_{dem}, M_{sup}, t \quad (4.15)$$

where, $H_{CHP}(M_{sup},t)$ is the heat energy provided by CHP.

The heating rate recovered from the CHP system is formulated as:

$$H_{CHP}(M_{dem},t) = E_{CHP}^{Eng}(M_{sup},t)\eta_{CHP}^{th} / \eta_{CHP}^{ele}, \forall M_{dem}, M_{sup}, t \quad (4.16)$$

where, η_{CHP}^{th} is the thermal efficiency of CHP system; η_{CHP}^{ele} is the electricity efficiency of CHP system during timestep t ; $E_{CHP}^{Eng}(M_{sup},t)$ is the electricity generated by gas engine during timestep t .

4.3.2.5 Energy storage

For the thermal storage system, it is assumed that the source of heat is only from the CHP generation. The amount of storage energy at the beginning of timestep t equals to the non-dispatched energy stored during timestep $t-1$, plus the energy flow. The thermal storage can be expressed as

$$H_{TES}(t) = H_{TES}(t-1) + (H_{TES}^{Ch}(M_{dem},t) - H_{TES}^{Dis}(M_{sup},t)), \forall M_{dem}, M_{sup}, t \quad (4.17)$$

where, $H_{TES}(t)$ is the stored heat during timestep t ; $H_{TES}(t-1)$ is the stored heat during timestep $t-1$.

Similarly, the electricity storage is formulated as

$$E_{ES}(t) = E_{ES}(t-1) + (E_{ES}^{Ch}(M_{dem},t) - E_{ES}^{Dis}(M_{sup},t)) \cdot D_t, \forall M_{dem}, M_{sup}, t \quad (4.18)$$

where, $E_{ES}(t)$ is the stored electricity during timestep t ; $E_{ES}(t-1)$ is the stored electricity during timestep $t-1$.

4.3.2.6 Inequality constraints

For most of the energy devices of the energy system, the common constraint is the capacity constraint. The energy rate provided by each energy device is limited by its minimum and maximum values.

$$\begin{aligned}
E_{CHP}^{Eng,LL}(M_{sup},t) &\leq E_{CHP}^{Eng}(M_{sup},t) \leq E_{CHP}^{Eng,HL}(M_{sup},t) \\
E_{ES}^{Ch,LL}(M_{dem},t) &\leq E_{ES}^{Ch}(M_{dem},t) \leq E_{ES}^{Ch,HL}(M_{dem},t) \\
E_{ES}^{Dis,LL}(M_{sup},t) &\leq E_{ES}^{Dis}(M_{sup},t) \leq E_{ES}^{Dis,HL}(M_{sup},t) \\
H_{TES}^{Ch,LL}(M_{dem},t) &\leq H_{TES}^{Ch}(M_{dem},t) \leq H_{TES}^{Ch,HL}(M_{dem},t) \\
H_{TES}^{Dis,LL}(M_{sup},t) &\leq H_{TES}^{Dis}(M_{sup},t) \leq H_{TES}^{Dis,HL}(M_{sup},t) \\
H_{CHP}^{boil,LL}(M_{dem},t) &\leq H_{CHP}^{boil}(M_{dem},t) \leq H_{CHP}^{boil,HL}(M_{dem},t)
\end{aligned} \tag{4.19}$$

where, $E_{CHP}^{Eng,LL}(M_{sup},t), E_{CHP}^{Eng,HL}(M_{sup},t)$ are the lower and upper limit of CHP generation; $E_{ES}^{Ch,LL}(M_{dem},t)$ and $E_{ES}^{Ch,HL}(M_{dem},t)$ are the lower and upper charging limit of electricity storage ; $E_{ES}^{Dis,LL}(M_{sup},t)$ and $E_{ES}^{Dis,HL}(M_{sup},t)$ are the lower and upper discharging limit of electricity storage ; $H_{TES}^{Ch,LL}(M_{dem},t), H_{TES}^{Ch,HL}(M_{dem},t)$ are the lower and upper charging limit of thermal energy storage; $H_{TES}^{Dis,LL}(M_{sup},t), H_{TES}^{Dis,HL}(M_{sup},t)$ are the lower and upper discharging limit of thermal energy storage $H_{CHP}^{boil,LL}(M_{dem},t), H_{CHP}^{boil,HL}(M_{dem},t)$ are the lower and upper limit of gas-boiler generation.

The ramping limit of each CHP unit should be satisfied.

$$E_{CHP}^{Eng,RLL} \leq E_{CHP}^{Eng}(M_{sup},t) - E_{CHP}^{Eng}(M_{sup},t-1) \leq E_{CHP}^{Eng,RHL} \tag{4.20}$$

where, $E_{CHP}^{Eng,RLL}, E_{CHP}^{Eng,RHL}$ are the lower and upper step limit for CHP generation.

Different initial status and final stage of CHP-based energy system will affect the optimisation results. In practice, system operator normally makes the final status is same as initial status to reduce the control uncertainty. In our case, it is assumed that initial stored energy of thermal storage and electricity storage is equal to final stored energy for both system, which is shown as

$$\begin{aligned}
E_{ES}(t=0) &= E_{ES}(t=T) \\
H_{TES}(t=0) &= H_{ES}(t=T)
\end{aligned} \tag{4.21}$$

where, $E_{ES}(t=0)$ is the stored electricity at initial timestep; $E_{ES}(t=T)$ is the stored electricity at the end timestep T ; $H_{TES}(t=0)$ is the stored heat at initial timestep; $H_{ES}(t=T)$ is the stored heat at the end timestep T .

4.4 Scenarios Generation for Scheduling Optimisation

The short-term scheduling strategy make it difficult to achieve the reduction of operation cost which is normally evaluated on annual base. It would be ideal if the detail scheduling strategy is designed on long-term base. However, there are some challenges: 1) the computation burden is high due to the complexity of system and the large number of data; 2) the optimisation strategy will be affected by the cases that rarely occur or are special; 3) the interconnection of variables among time steps will further increases the variation and complex of system; The weather of different years will affect the pattern of energy supply and demand, which brings the challenges for data selection.

The proposed method divides the long-period data into different scenarios in units of days. Each scenario is divided into different timesteps according to the data interval. In each timestep, the probability of occurrence of a certain data can be calculated according to the distribution of historical data during this timestep or its probability distribution. Taking the solar generation data as an example, we have one-year solar generation data, 365 historical data is acquired at timestep 1(00:00-00:30). It is assumed the distribution follows standard probability distribution so the parameters of standard distribution equations can be calculated. As a result, the occurrence probability is calculated. Many scenarios with different occurrence probabilities can be generated for each type of long-term data. For various types of data, these scenarios can be combined again to form new scenarios based on different probability distributions under various types of long-term data. The number of these scenarios can reach several million and the sum of these scenarios' occurring probabilities is 100%. Some of these scenarios with high occurring probabilities are selected as the reference of scheduling optimisation. The predefined acceptance level will determine the number of selected scenarios and determine the level of characterise long-term data. In addition, the initial value of the state of all devices with storage (electricity storage or heat storage) function in each scenario is equal to value at the end.

As the dimension of PDF increases, the proposed scenario method [159] cannot handle these scenarios efficiently. A revised scenario generation method is introduced, where various PDF can be handled and discretized conveniently. In

addition, this method further improves the computing efficiency by using Roulette wheel Mechanism (RWM). Fig.4.2 shows the flowchart of this proposed method. The main process is summarized as follows:

- The parameters of PDFs for solar radiation, and demand are obtained using based on half-hourly historical data. These continuous PDFs are sliced into several segments for each timestep;
- According to the PDFs of supply side and demand side, discretize the PDF into different intervals. Monte Carlo Simulation (MCS) which is a sampling technique is utilised to generate the scenarios. For the scenario generation, the first step consists in randomly generating a set of scenarios, taking into account the intrinsic autocorrelation of the half-hourly historical data. Then in the second step, a subset of the scenarios previously generated is chosen according to the forecasting error. Finally, the scenarios are selected to the set of scenarios obtained in the second step;
- The total number of these scenarios generated by using MCS maybe over thousand. Excellent computing performance and longer period time will be needed for optimising large number of scenarios. In addition, the probability of some scenarios' occurrence is almost zero which means such scenarios could never happen. In general, scenario reduction is a probabilistic way of retaining the representative scenarios. We aim to preserve most of the characteristics from the original set in the reduced set. One class of methods include forward selection and backward reduction-based greedy algorithms [152]. With the introduction of an optimization platform called GAMS, Nicole adapted their method in a routine called SCENRED which made use of state-of-art optimization solvers for even more improved computational performance [153]. The SCENRED [160], which uses Fast Backward + Forward methods to reduce the scenario, is proposed. The algorithms exploit a certain probability distance of the original and the reduced probability measure. A trade-off needs to be achieved by considering scenario probabilities and distances of scenario values.

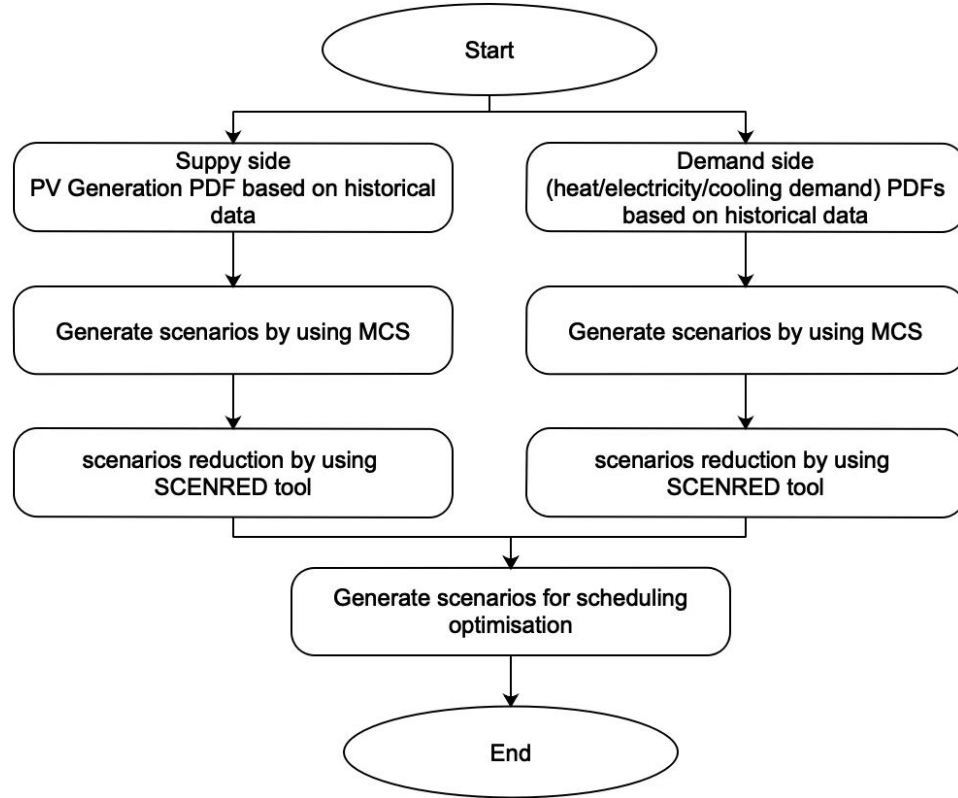


Fig. 4.2 Flowchart of hybrid scenario generation method

- After each set of reduced scenarios is generated, all these scenarios should be arranged and combined to obtain all possible scenarios and calculated their probabilities. If variable A is independent with variable B, the simultaneous occurring probability of A and B can be expressed as

$$P(AB) = P(A) \cdot P(B) \quad (4.22)$$

where, $P(AB)$ is the occurring probability of A and B; $P(A)$ is the occurring probability of A; $P(B)$ is the occurring probability of B.

4.5 Case Study

4.5.1 Test System

In this section, a simulated system based on UoW energy system is employed to verify the proposed model and method. As shown in Fig.4.4, the model consists of two CHP systems at node 70121, two 10MW solar panel systems at node 70244 and 70338 separately, one thermal storage is connected at node 70104 to store the heat generated by CHP system with 20MWh storage capacity and one 4MW/8MWh

battery electrical system. The CHP plant at the University of Warwick (UoW) consists of 3 CHP units, each generating 1.4 MW of electrical power and 1.8 MW of thermal power with a total electrical power generation of 4.2 MW and thermal power production of 5.4 MW. The CHP units adopt the reciprocating gas engine system 1370 GQMA provided by Cummins, which is composed of reciprocating methane gas engine, alternator, generator and control system. Concerning the thermal storage, there are four 10.5 m tall water reservoirs to store 400 tons of hot water in the case of low thermal demand. The detail is shown in Table 4-1.

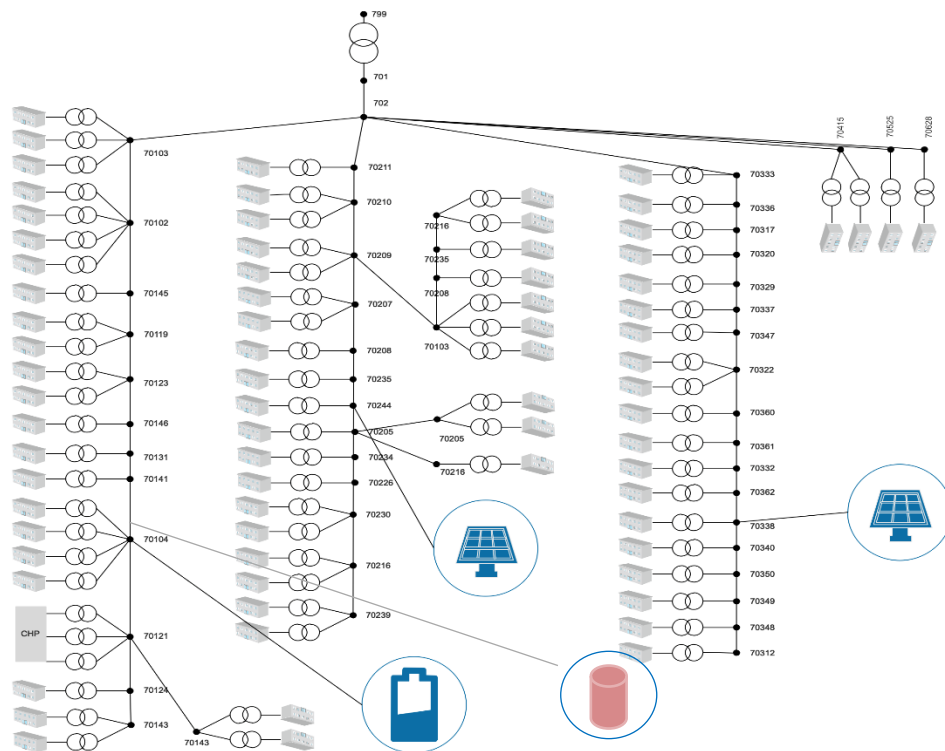


Fig. 4.3 Single line diagram of test distribution system

Table 4-1 System components data

Components	Number	Size (MW)	Capacity (MWh)
Boiler	3	6.8	
CHP units	3	1.4	
CHP units	2	2	
Battery system	1	4	8
Solar system	2	10	
Thermal storage	1		20
Absorption chiller	1	2	

The parameter of third-degree polynomial fitting function for the electricity efficiency curve is shown in Table 4-2 according to Eq.4.6. Its performance curve of each CHP unit is shown in Fig.4.4 [170]. According to the torque curve of gas-fired engine, the system efficiency is lower at the partial load and it increases to high value when the load is above 50% of rated load. The efficiency curve (calculated in Eq.4.7) of all CHP units is shown in Fig.4.5. The efficiency curve is fluctuating since it is determined by the load distribution. When the one unit can meet the system requirement so the efficiency follows efficiency of one unit; when system needs two or more units to work, the efficiency curve will be the calculated by considering two efficiency curves. The calculated efficiency curve is non-linear since the efficiency curve of each unit is non-linear.

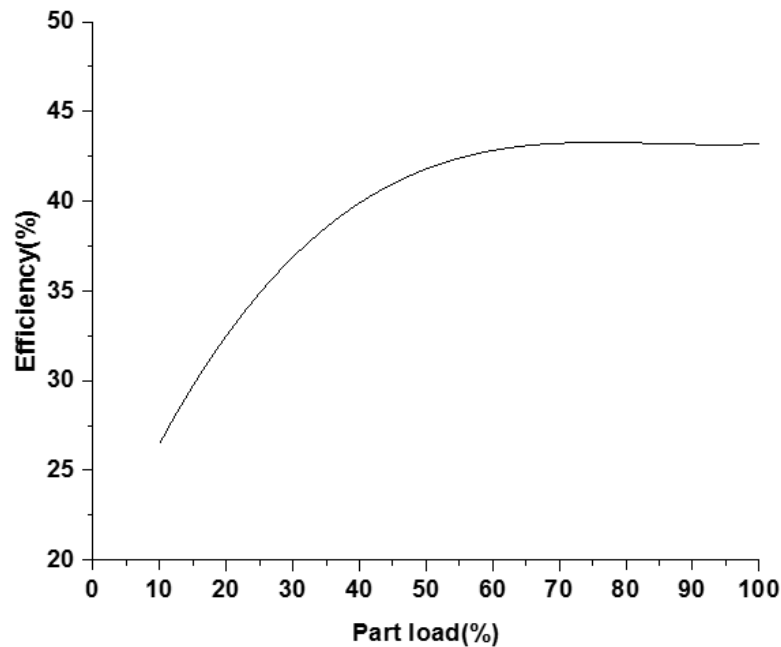


Fig. 4.4 Electricity efficiency of each CHP unit

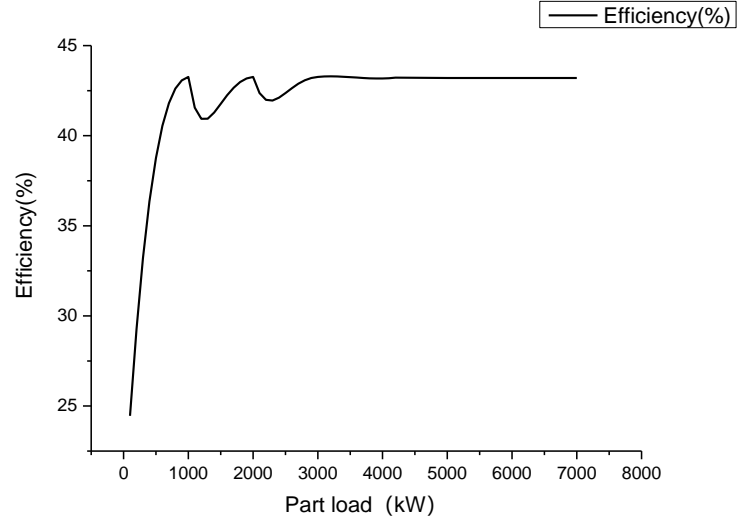


Fig. 4.5 Part load efficiency of grouped CHP

Table 4-2 Parameters of fitting curve

a_1	a_2	a_3	a_4
0.0000414	-0.01056	0.88786	18.6361

The operation cost is determined by the gas and electricity prices. The electricity tariff is given time-of-use tariff, which is acquired from the DNO. For the gas price[171] , the fixed price is used (4p/kWh). A two-period time-of-use tariff is adopted in this section according to the bill of university electricity bill clarification, which means that customer is charged at off-peak tariff (12p/kWh) for any electricity consumed during hours 21–16, and a peak tariff (17/kWh) during hours 16–21.

Table 4-3 shows the parameters used for scheduling optimisation of the CHP-based Energy System. The conversion coefficients are from the manufacture specification.

Table 4-3 Parameters of modelling for scheduling optimisation

Parameter	Value	Unit
η_{CoP}	1.35	
η_{CHP}^{th}	0.437	
η_{boil}	0.9	
LHV_{ngas}	47.141	MJ/kg
$E_{ES}(t = 0)$	5000	kWh
$H_{TES}(t = 0)$	10000	kWh
$E_{CHP}^{Eng,LL}(M_{sup}, t)$	0	kWh

$E_{CHP}^{Eng,HL}(M_{sup},t)$	1000	kWh
$E_{ES}^{Ch,LL}(M_{dem},t)$	0	kWh
$E_{ES}^{Ch,HL}(M_{dem},t)$	2000	kWh
$E_{ES}^{Dis,LL}(M_{sup},t)$	0	kWh
$E_{ES}^{Dis,HL}(M_{sup},t)$	2000	kWh
$H_{TES}^{Ch,LL}(M_{dem},t)$	0	kWh
$H_{TES}^{Ch,HL}(M_{dem},t)$	2500	kWh
$H_{TES}^{Dis,LL}(M_{sup},t)$	0	kWh
$H_{TES}^{Dis,HL}(M_{sup},t)$	2500	kWh
$H_{CHP}^{boil,LL}(M_{dem},t)$	0	kWh
$H_{CHP}^{boil,HL}(M_{dem},t)$	1000	kWh
$E_{CHP}^{Eng,RLL}$	0	kWh
$E_{CHP}^{Eng,RHL}$	700	kWh

4.5.2 Scenarios Generation

After the MCS is used to generate, the supply side consists of 100 scenarios related to solar generation based on the half-hourly data from January of 2018 to January of 2019 from the co-simulation system developed in chapter3. Each scenario contains 48 timesteps (half-hourly). The demand side contains 100 scenarios related to energy demand (electricity demand, heat demand, cooling demand) based on the half-hourly data (shown as Fig.4.6).

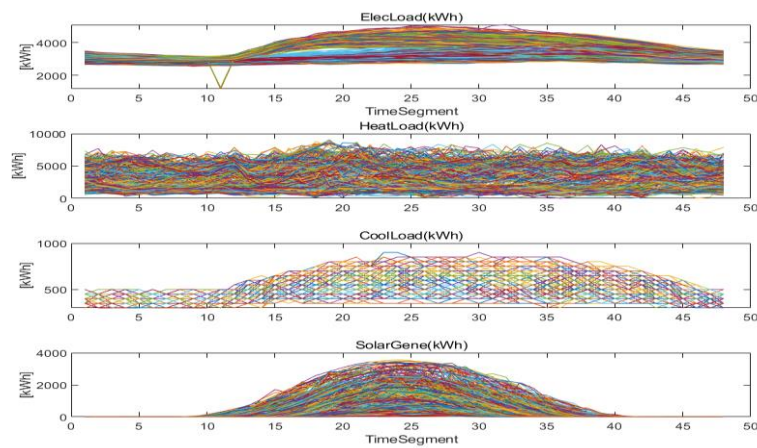


Fig. 4.6 half-hourly historical data from Jan 2018 to Jan 2019

After the SCENRED is used to reduce the number of scenarios, twenty best scenarios are separately generated for energy demand and supply, as shown in Fig.4.7. To evaluate the optimisation algorithm in various scenarios with reasonable computation time, the scenarios of energy demand is combined with the scenarios of energy supply one by one, and finally the scenarios for scheduling optimisation are generated. In this case, this optimisation problem involves 400 scenarios with total 112500 constraints.

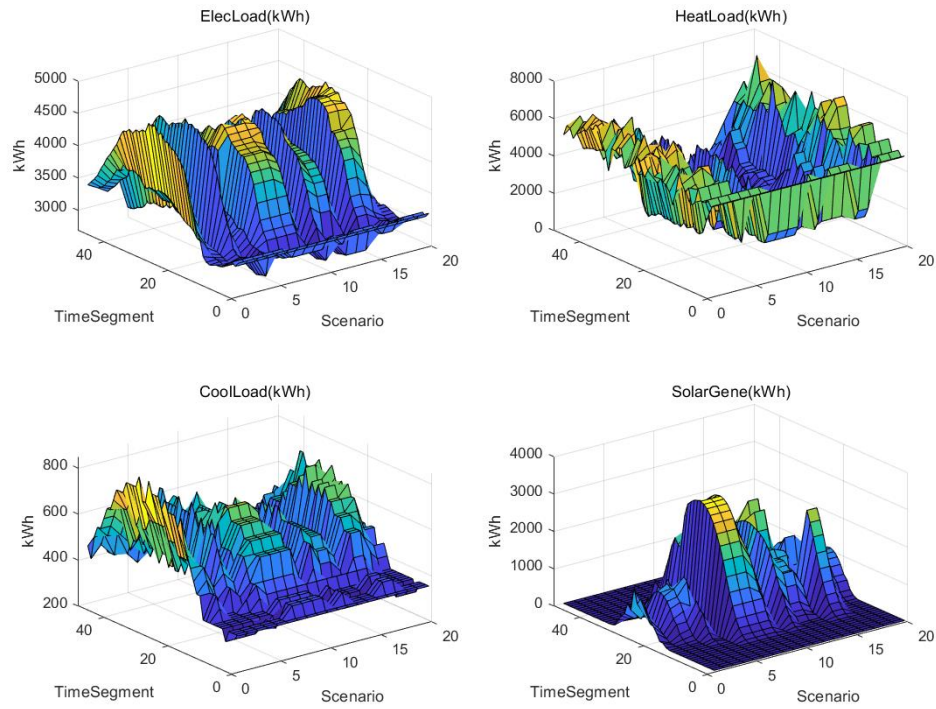


Fig. 4.7 Scenarios by using scenred technology (half-hourly)

4.5.3 Optimal Operation Strategies for Different Scenarios

Normally, CHP plants can only be run in a finite number of configurations, thus making the delivered power a quantized variable. Here, it is assumed each CHP unit is limited to five different configurations (defined as fix-step CHP output): 0% rated capacity, 25% rated capacity, 50% rated capacity, 75% rated capacity and 100% rated capacity. The variable-step CHP output where there is no limit of five configurations is also to be considered for the scheduling optimisation. Then, the results of operation cost of CHP-based energy system are compared and analysed with two different configurations (fix-step CHP output and variable-step CHP output).

4.6.3.1 Operation strategies with fix-step CHP output

The scheduling strategy of energy system with fix-step CHP output were analysed. The probability of each scenario was shown in Fig.4.8, in which 20 demand scenarios and 20 generation scenarios were selected to analyse the energy scheduling strategies under the optimal operation cost. 400 scenarios were generated since both demand scenarios and generation scenarios were independent with each other. The highest occurrence probability scenario was at scenario 381 where the probability was around 0.04260.

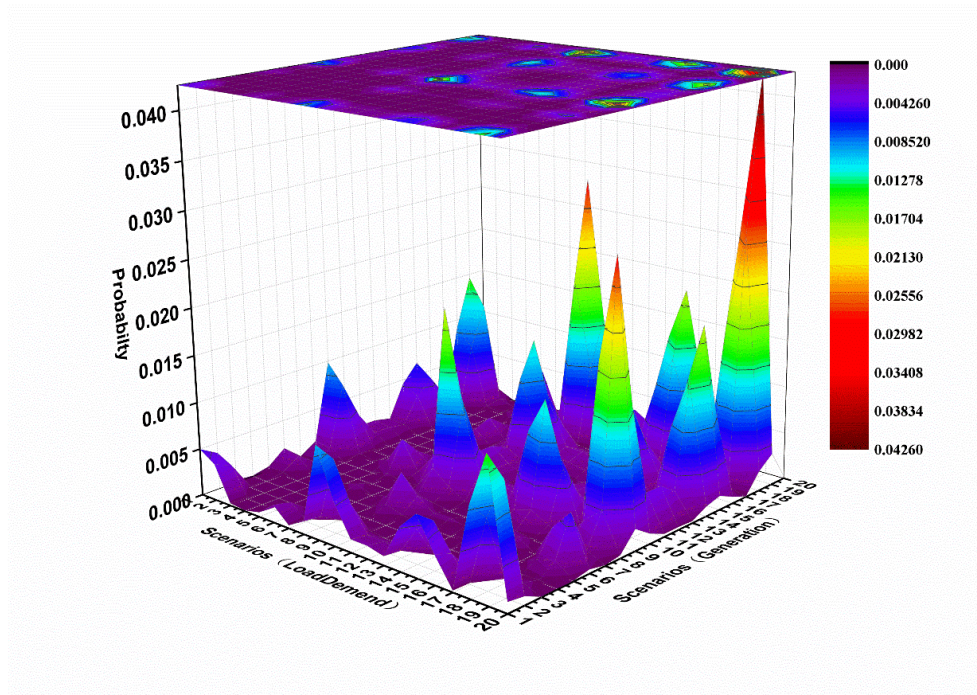


Fig. 4.8 Probability distribution of each scenario

The operation cost of each scenario based on Eq.4.8 was shown in Fig.4.9. The operation cost of different scenarios ranges from £ 9,450 to £ 23,900. The annual operation cost was calculated by considering the scenario occurring probability and each scenario operation cost, which was formulated in Eq.4.25. The annual cost was £ 5,615,764, and the daily average operation cost was £ 15,385. Such costs include purchasing electricity and gas.

$$OC_{year} = \frac{365}{400} \cdot \sum_{i=1}^N (OC_{sce}(i) \cdot \rho(i)) \quad (4.23)$$

where OC_{year} is annual operation cost, $OC_{sce}(i)$ is the operation cost at scenario i ; $\rho(i)$ is the occurring probability of scenario i .

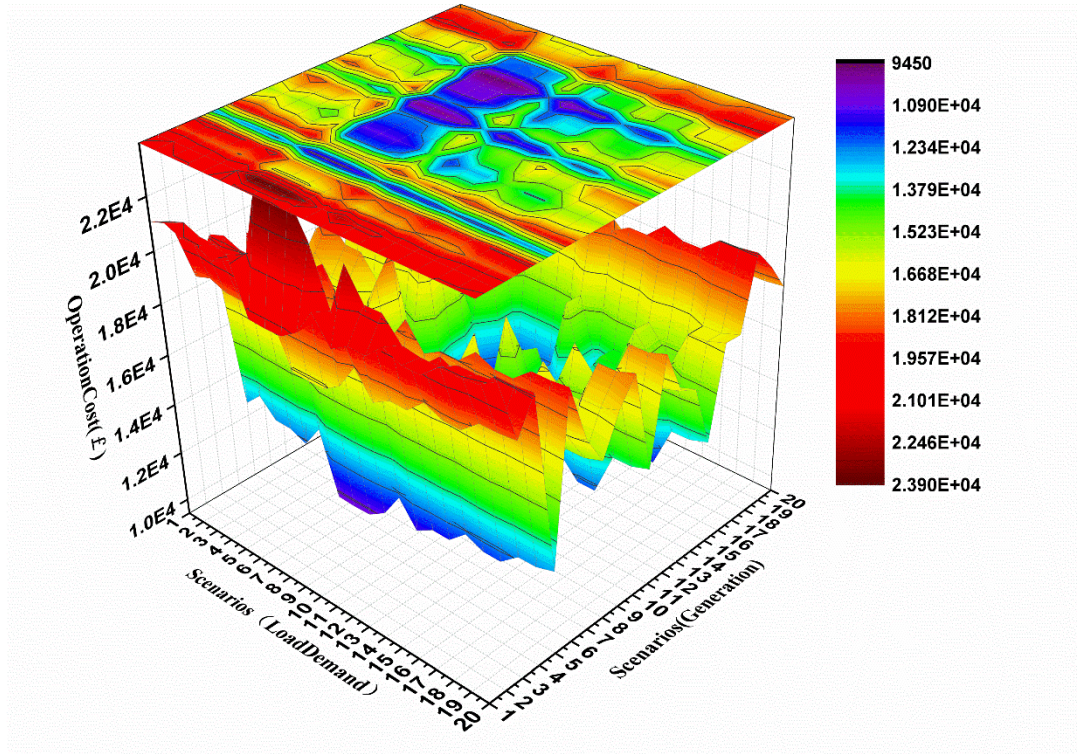
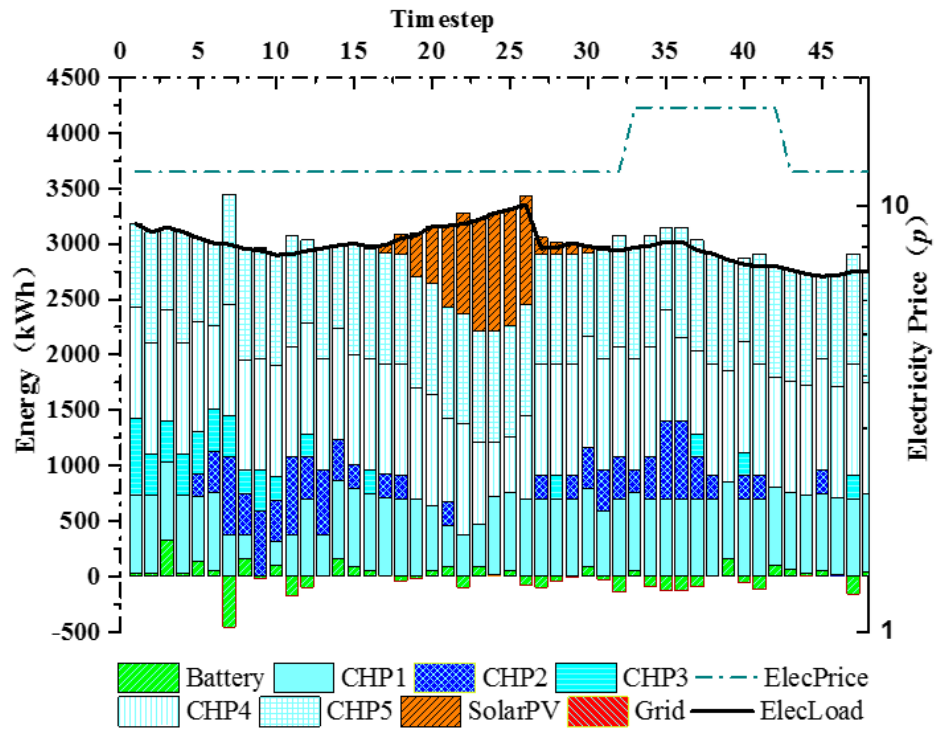


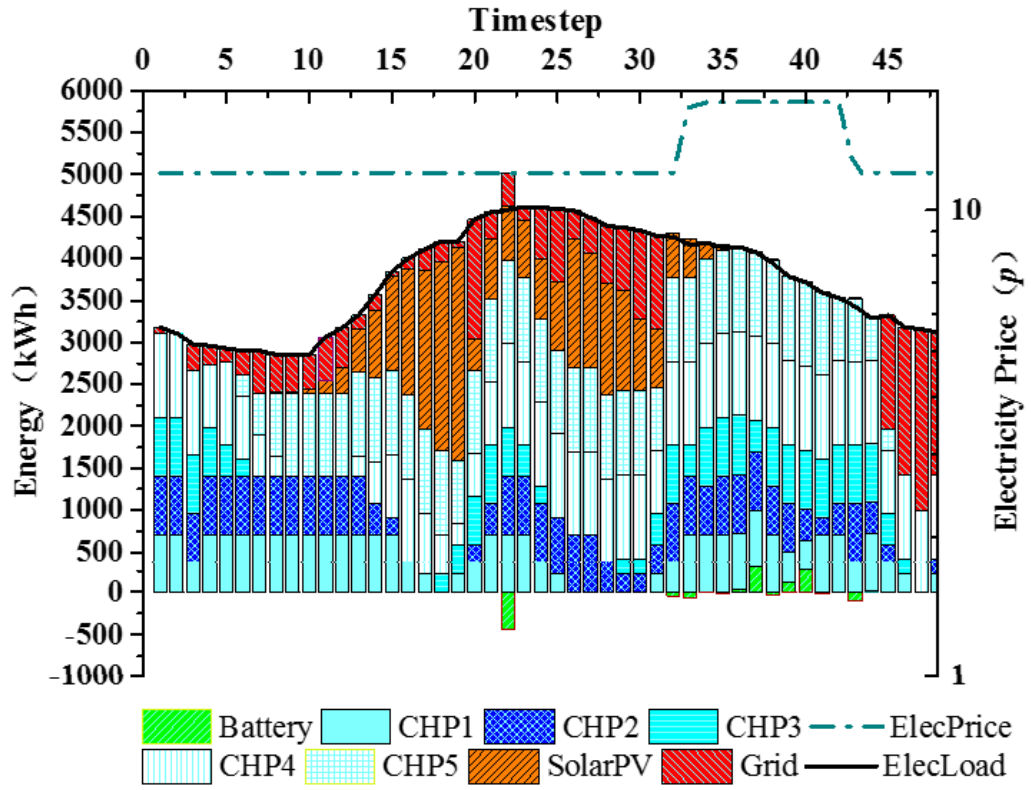
Fig. 4.9 Operation cost distribution of each scenario

Fig.4.10 showed the half-hourly optimisation results of four scenarios that selected from 400 scenarios: the electricity power provided by CHP and battery system, the electricity power from grid, the electricity power generated by solar PV system, and the electricity load demand. From Fig.4.10a, CHP system mainly contributed the electricity energy since the PV generation was at low level and thermal demand was higher. In this case, CHP system was most economic energy source by working at high power. In Fig.4.10b, the electricity demand was larger than the capacity of generators, so CHP-based energy system needed to buy electricity energy from main grid. it was obvious that the operation of this energy system was sensitive to the grid price variation, since the electricity price from grid was higher than the gas price and battery cycling price in both peak and off-peak price. In addition, the price from grid was still higher than that of other electricity sources. In Fig.4.10c, the surplus energy generated from solar PV system was stored in battery or exported to grid for free since it is assumed that there is no (Power Purchase Agreement) contract with DNO for the electricity export. The battery storage was used to absorb the surplus energy

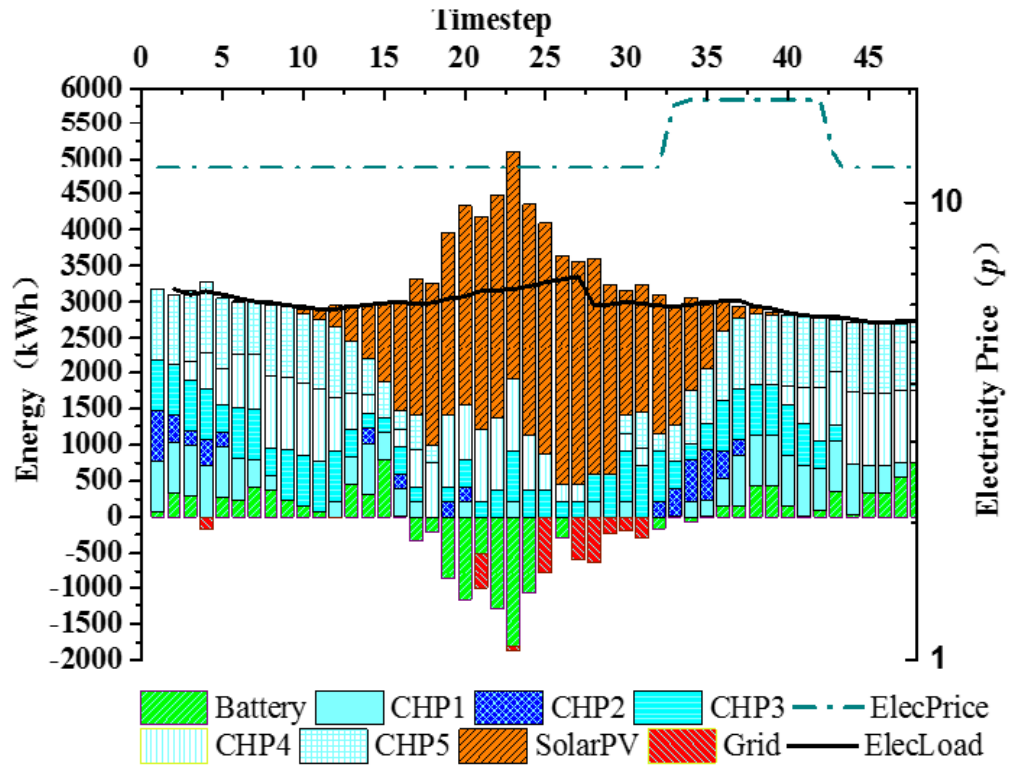
or do the electricity peak-shifting to reduce the total operation cost. However, electricity was delivered to grid for free in some timesteps due to the limitation of capacity of battery storage. The operation cost is higher if the electricity generated by the CHP export to grid. In Fig.4.10d, the electricity from grid mainly contributes to the electricity demand since the thermal demand is lower during this period. It was noted that the initial energy stored in battery system should be equal to the end energy stored in battery system. In this case, there were some forced charging processes in some timesteps.



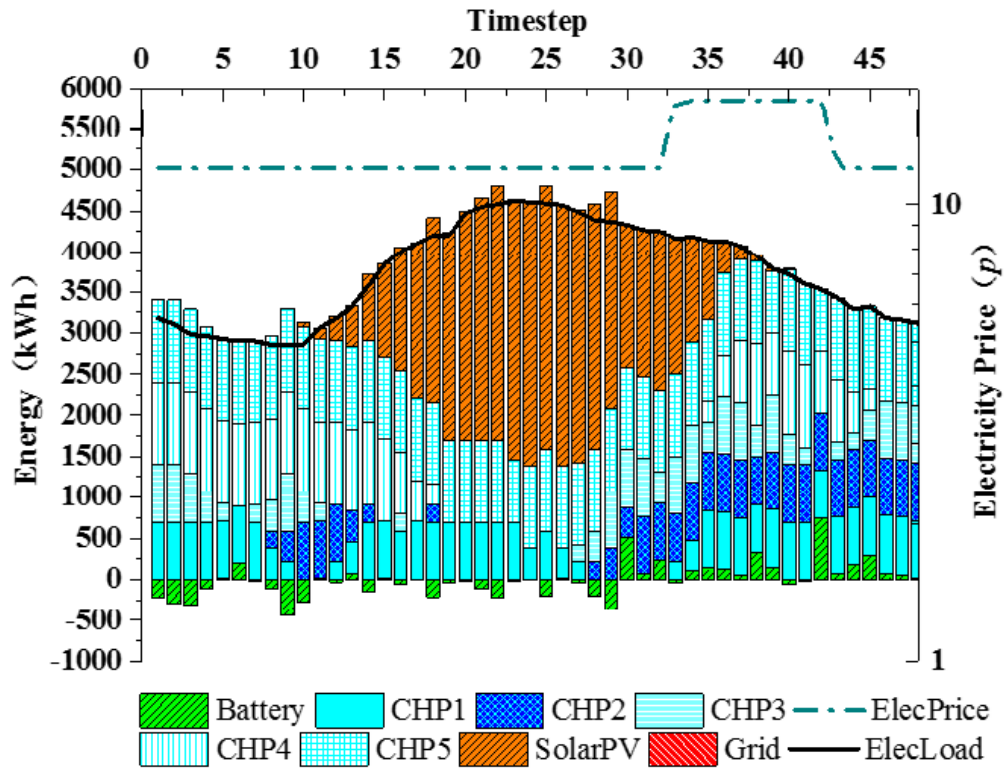
a



b



c

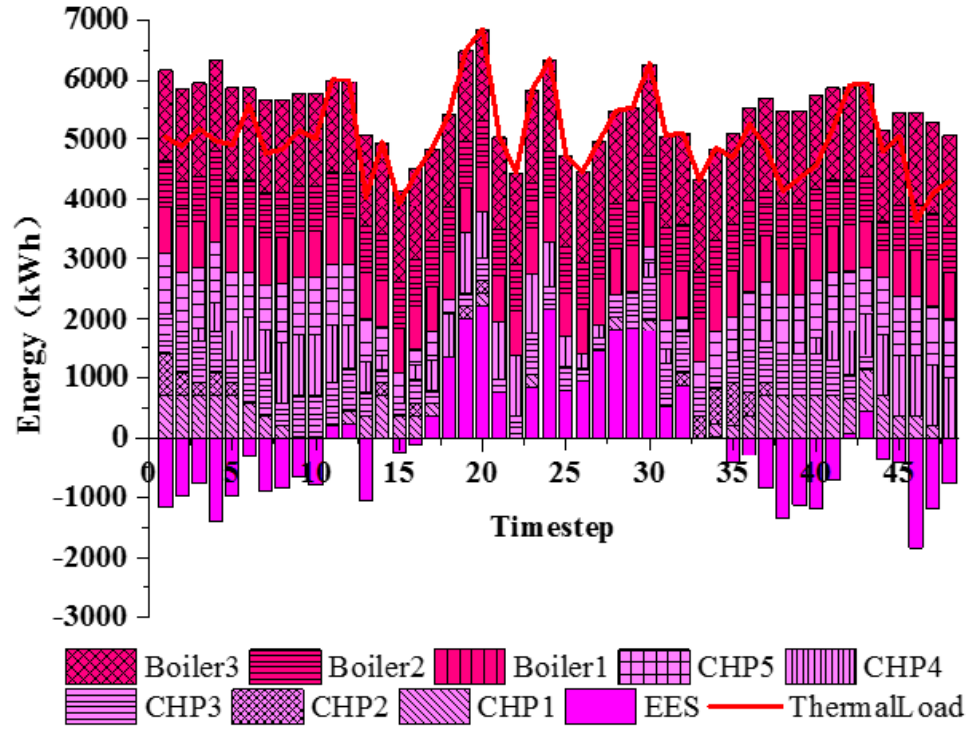


d

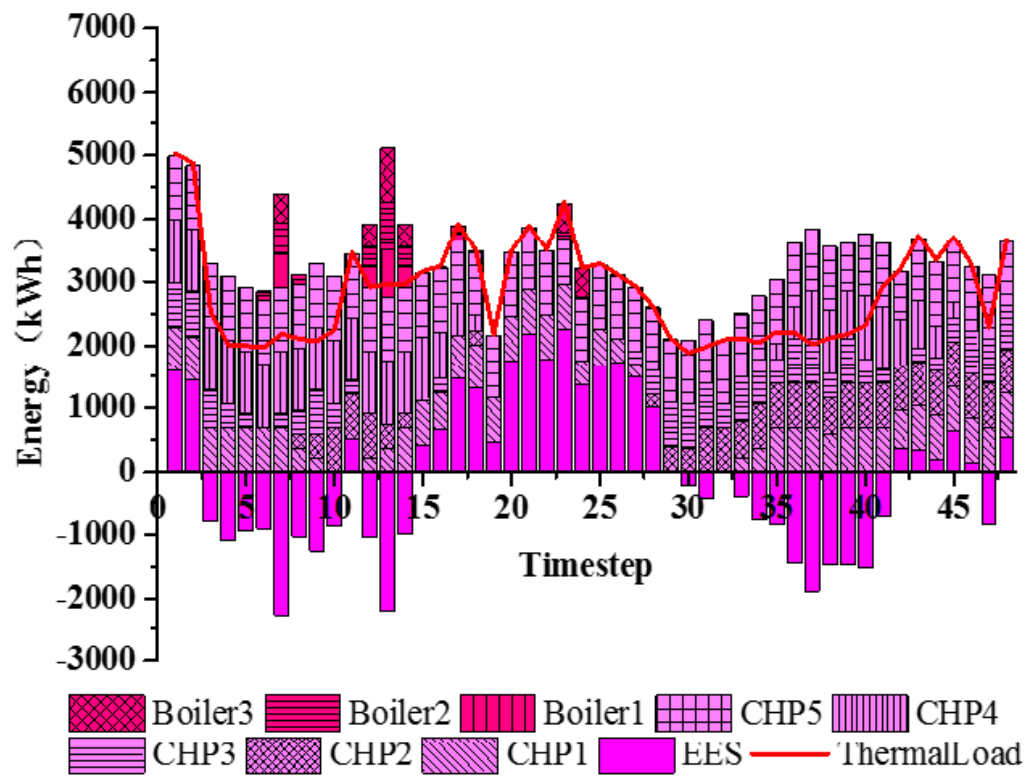
Fig. 4.10 Results of optimal electricity scheduling

Fig.4.11 showed the thermal demand (heat demand and cooling demand) for four scenarios selected from 400 scenarios: thermal rate from thermal storage, thermal rate provided by boiler. Load demand and thermal demand jointly affected CHP operation and 6.8 MW gas-fired boilers provided heat energy which was used to provide heat and drive the absorption chiller to generate the cooling energy. In Fig.4.11a, CHP units and boiler units both provided the energy in the heavy thermal demand. There was surplus energy from CHP units in the processing of operation optimisation, the reasons are: 1) To economically meet the electricity demand, CHP would generate extra heat; 2) CHP worked in discrete working point which led to extra heat generation; 3) Extra heat was needed to be stored in thermal storage to compensate the heat gap in the following timesteps. In the case of light thermal load, the heat from CHP units fully met the thermal and the thermal storage acted as a peak shifting function as shown in Fig.4.11b. In Fig.4.11c, only one CHP unit worked at rated capacity under large amount of PV electricity export. As a result, the thermal demand could not be met even though all boiler units were at maximum export, so thermal storage system was discharging heat to the energy system to compensate the

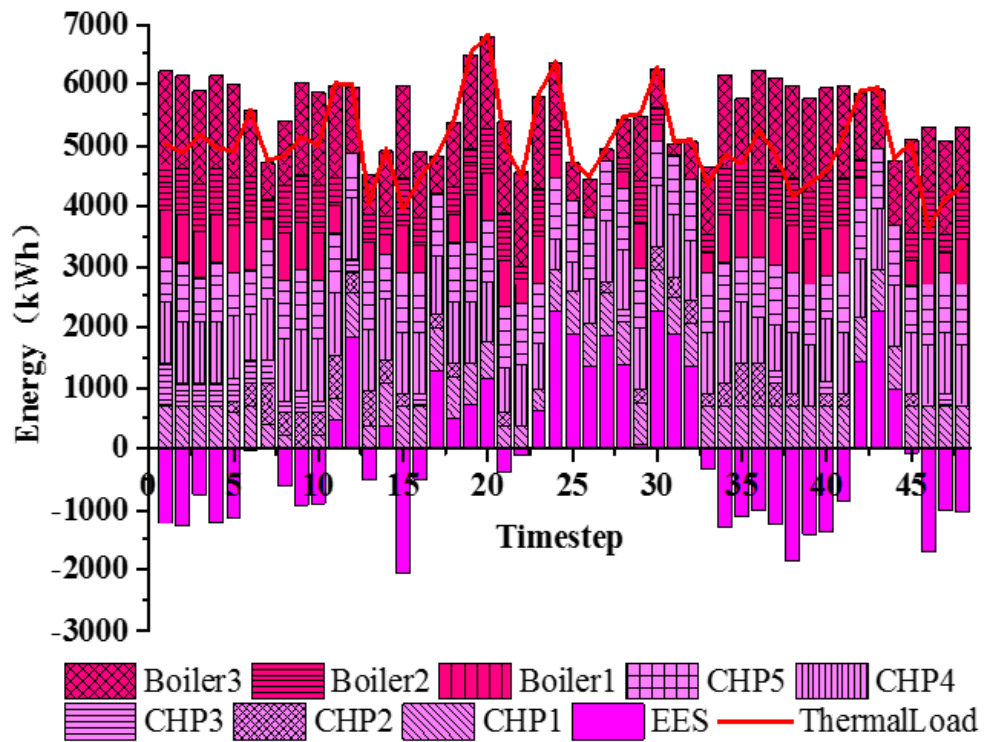
energy gap from timestep 16 to timestep 32. Similar to battery storage system, the initial energy stored in thermal storage system should be equal to the energy stored in thermal storage at the end. In this case, the forced charging processes was needed from timestep 33 to timestep 48. In Fig.4.11d, the boiler units were needed to provide the heat to the CHP-based energy system in some timesteps compared with the scheduling results in Fig.4.11b.



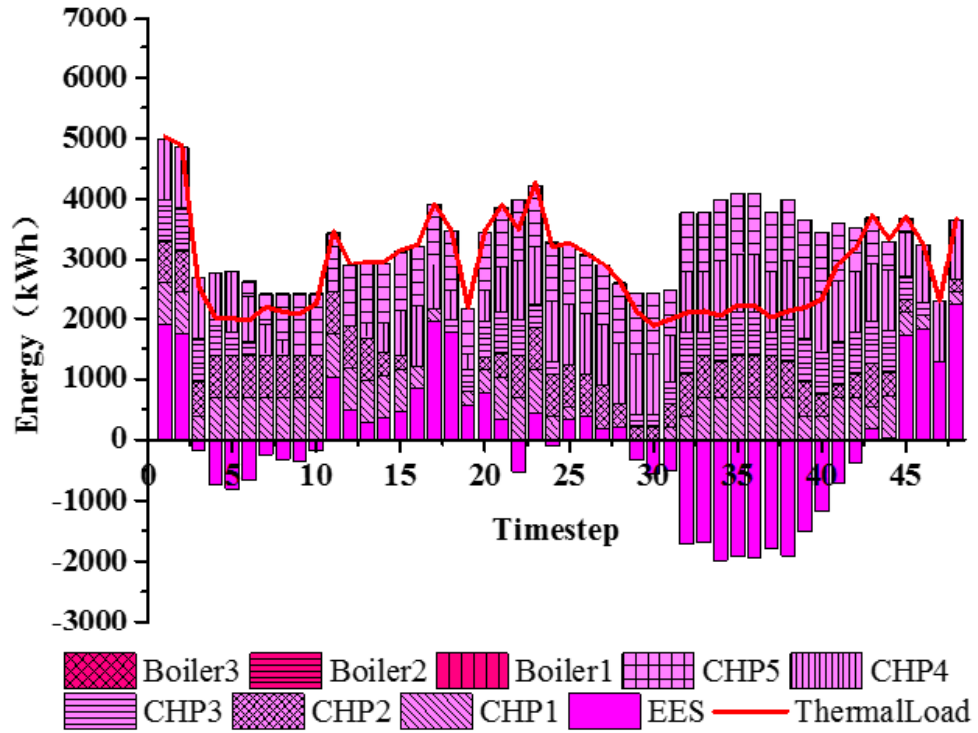
a



b



c



d

Fig. 4.11 Results of optimal heat scheduling

4.6.3.2 Operation strategies with variable-step CHP output

The scheduling strategies of the CHP-based energy system with variable-step CHP output were analysed and compared to that of fix-step CHP output. Firstly, the operation cost was compared under the same scenarios for different CHP outputs. Fig.4.12 showed the distribution of difference in operation cost (operation cost of variable-step minus the operation cost of fix-step). The difference in operation costs ranged from -£ 0.17 to -£ 2.075 so the operation cost of variable-step case is slight lower than that of fix-step case. The annual operation cost is £ 5,615,200 in variable-step case while this figure is £ 5,615,764.

The reasons for the small differences in the results optimized by different methods can be summarized as: The fixed-step optimisation algorithm means the output of each CHP unit is discrete points, such as 5% rated power, 25% rated power, 50% rated power. From the efficiency calculation equation, the efficiency is determined by the CHP output. If the CHP output is higher than 50% of rated power, the efficiency of CHP unit reaches to peak point. For the variable-step algorithm, the output of CHP unit can be changed from 0 to rated power. 1) If the demand is higher,

which means each CHP should generate more power (50%), so even though the optimal parameters are slightly different, the optimisation result is similar;2) If the demand is lower, some CHP units may work at high power output and others work at lower or even no output. In this case, the variable-step algorithm has a certain advantage compared to fix-step algorithm since variable-step algorithm can set any value of CHP output. But the object of this optimisation is to reduce the operation cost, it is a way to ensure the CHP units work at higher efficiency area;3) In this system, 5 CHP units are installed to supply the electricity and heat. In other words, the CHP system has a certain flexibility to coordination within these 5 CHP units. As a result, the advantage of variable-step algorithm is not obvious.

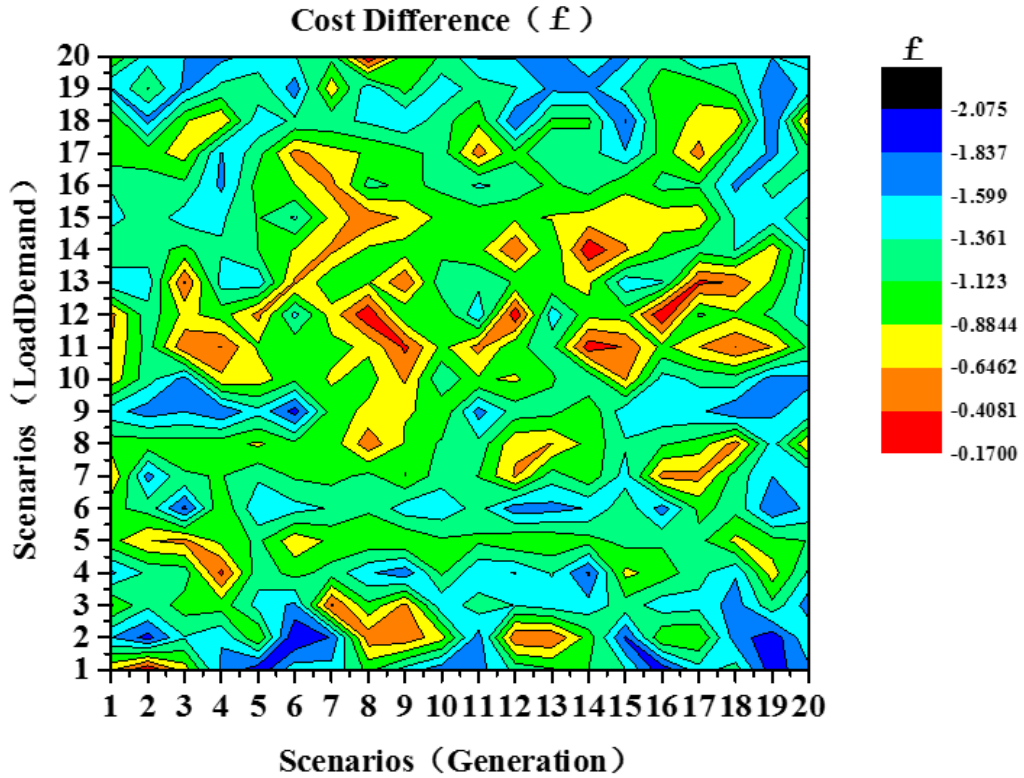


Fig. 4.12 Difference in operation cost (fix-step vs.variable-step)

4.5.4 Sensitivity Analysis of the Impact of Battery Capacity

A sensitivity analysis was carried to investigate the impact of battery capacity on the scheduling algorithms of this energy system and economic performance. Table 4-4 showed the analysis cases for this sensitivity analysis, where one extreme case was considered (no battery installation).

Table 4-4 Battery capacity levels for sensitivity analysis

Cases	1	2	3	4	5
Battery power (MW)	0	2	3	4	5
Capacity (MWh)	0	4	6	8	10

The annual operation cost of the whole system with different levels of battery capacity was shown in Fig.4.13. As compared with current case (4 MW/8 MWh battery), the annual operation cost increased as the installed battery capacity decreased. The minimum annual operation cost, equal to £ 5,615,237, is reached when the maximum battery was installed. Conversely, the maximum annual energy cost, equal to £ 5,677,716, was reached when no battery was installed. the expected annual operation cost increased about 1.2 % compared with base case (4MW/8MWh) in the absence of battery.

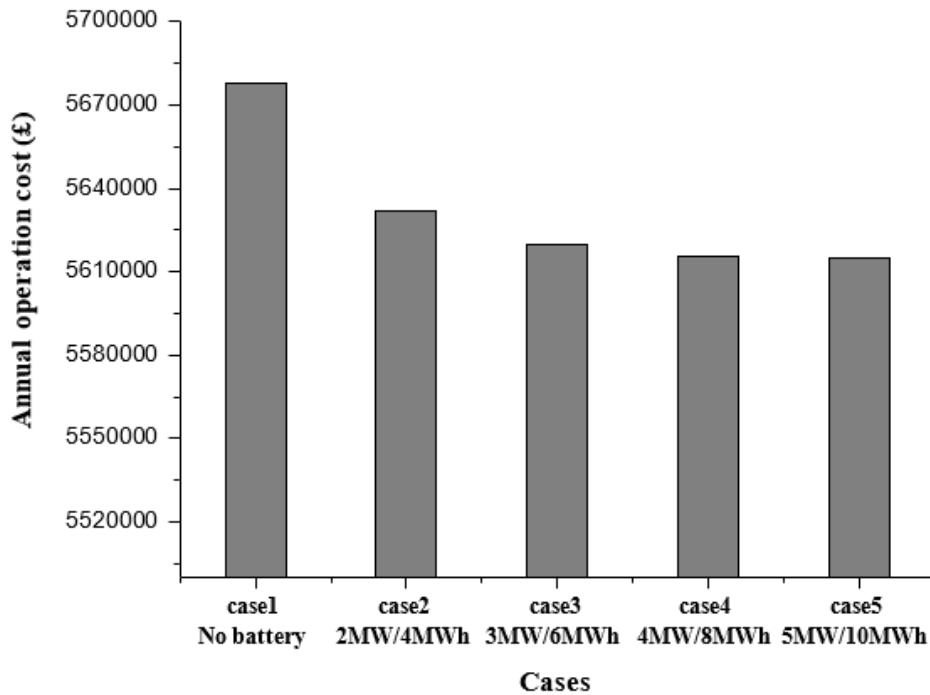


Fig. 4.13 Annual operation cost of the energy system in different cases

4.6 Summary

In this chapter, a programming model was presented for optimising the annual operation cost in CHP-based energy system with hybrid energy resources under energy demand and supply uncertainties. To solve these uncertainties, A combined scenario generation method was introduced, where various PDF was handled and

discretized conveniently. Then, SCENRED, which used Fast backward forward methods to reduce the scenarios, is proposed. A scheduling multi-objective linear programming problem was formulated with the consideration of practical constraints to minimize the energy operational cost, which included the electricity import cost from the main grid, cost of consumed natural gas, as well as the battery running cost, while satisfying time-varying demand.

In the case study, the simulated model in co-simulation system was implemented, with half-hourly load demand and derived supply from historical data. The annual operation cost was evaluated by considering the probability density and operation cost of each scenario. The annual cost was £ 5,615,764, and the daily average operation cost was £ 15,385 in fix-step CHP output case. Then, the operation cost was compared for different CHP configurations (fix-step/variable-step CHP output). The difference in annual operation cost is small since the difference ratio of operation cost is only 0.01 %. In addition, a sensitivity analysis was carried out to investigate the impact of battery penetration on the economic performances of the CHP-based energy system, showing that, in the absence of battery, the expected annual operation cost increased about 1.2 % compared with base case (4MW/8MWh).

Chapter 5

Techno-Economic Study of Solar Energy

Integration to Local Energy System

5.1 Introduction

With more strict emission regulations, more regional energy systems emerge which aims to achieve self-sufficient energy supply. One typical combination is Combined Heat and Power (CHP) with, solar PV power generation assembly in the UK. In many cases, CHP plants have already installed in the region and the system has been used to supply heating demand and generate power meanwhile. CHPs are normally operating in thermally led mode[172], so power generation is fluctuating with thermal energy demand changes. In many situations, the region needs to import electrical power from the grid in warm days. This provides the potential to equip solar PV on site in a cost-effective manner.

The work presented in this chapter is to conduct techno-economic analysis to explore whether it is economic and technical viable to have solar PV integration with the existing CHP power supply and what the optimal capacity is for a system with the known CHP power generation capacity. The study is also to investigate how the solar integration impact on the existing power distribution network. The work has its significance to LES planning, design and management. The study will use Warwick University campus energy system data acquired from data server of co-simulation system for analysis and strategy development.

5.2 Modelling of Local Energy System

To gain a better understanding to the impact of renewable energy integration, the simulation study of LES is performed while the full capacity of solar PV power generation is considered. This model of LES is developed on power co-simulation system in chapter 3 and the power simulator is to be improved so that it can be used for the analysis of power losses and voltage stability in LES. The model is integrated into GridLAB-D simulation and analysis tool that has good compatibility with other coding language.

The solver of power flow is Newton Raphson Power Flow (NRPF)solver [173] which are commonly used when all the buses are PQ buses. This method will guess all unknown variables, such as voltage magnitude and angel at load bus and load bus at the initial stage. Then, a Taylor Series [174] is written for each of the power balance equations included in the system of equations. The result is a linear system of

equations. However, when PV buses exist, the performance of the method will be affected. In addition, many branches in a power distribution system have very low impedance. In order to use admittance matrix-based approaches, basic NRPF arbitrarily assigns small non-zero impedances, which makes the analysis ill-conditioned and not easy to converge. An approach is proposed to handle the zero-impedance branches and avoid convergence problems resulting from those small impedance branches[175]. Only non-zero impedance buses are considered while constructing the bus admittance matrix. The zero impedance branches are represented though associated buses. Fig.5.1 shows an example construction of an equivalent distribution system with or without zero impedances.

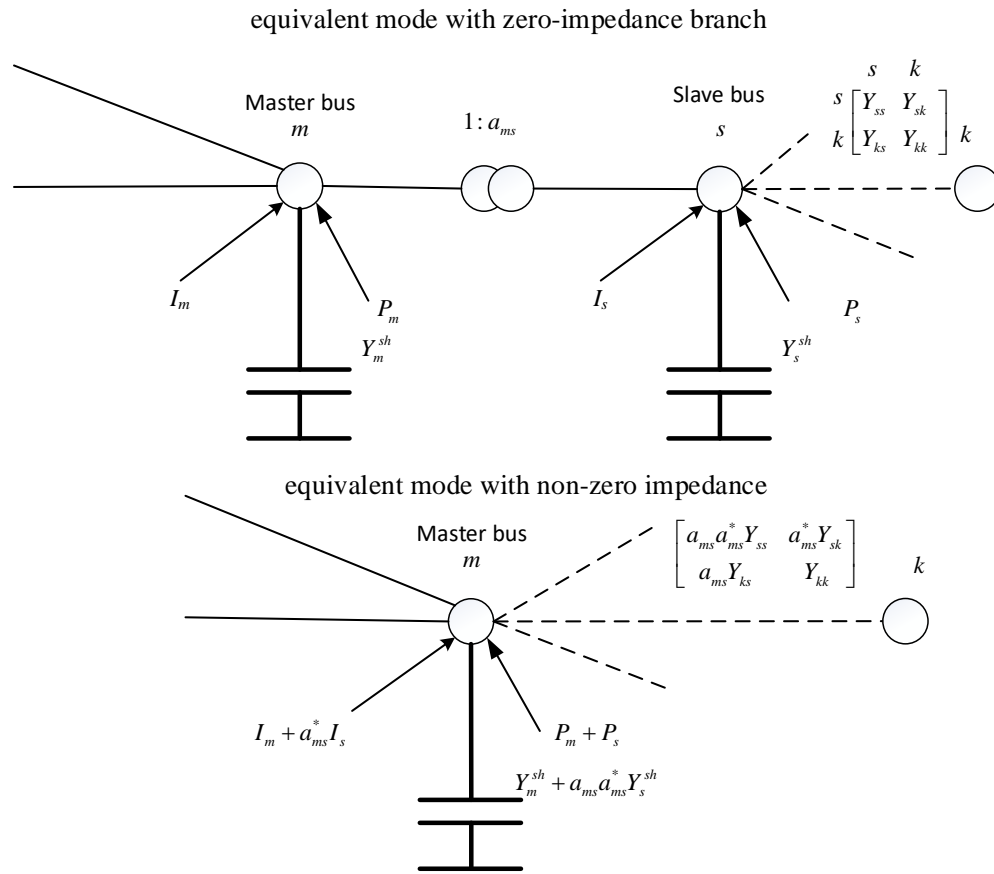


Fig. 5.1 Equivalent distribution system with or without zero impedances

The branch admittance matrix between bus s and bus k is given by

$$\begin{bmatrix} Y_{ss} & Y_{sk} \\ Y_{ks} & Y_{kk} \end{bmatrix} \quad (5.1)$$

where, Y_{ss} and Y_{kk} are the self-admittances; Y_{sk} and Y_{ks} are the mutual admittances; bus m provides an injected complex current I_m , an injected complex power P_m and a compensator with admittance Y_m^{sh} . The bus s provides an injected complex current I_s , an injected complex power P_s and a compensator with admittance Y_s^{sh} .

In the equivalent model, the zero-impedance branch and bus s are removed. The branches connected to bus s are reconnected to bus m . The admittance matrix between bus m and bus k can be given by

$$\begin{bmatrix} a_{ms} a_{ms}^* Y_{ss} & a_{ms}^* Y_{sk} \\ a_{ms} Y_{ks} & Y_{kk} \end{bmatrix} \quad (5.2)$$

where, a_{ms}^* is the conjugate of zero-impedance branch ratio; The self-admittance at bus m is determined by the product of self-admittance at bus s in the model and the square of the zero-impedance branch ratio; The mutual admittance for bus m to k is the product of the conjugate of the zero-impedance branch ratio and mutual admittance for bus s to k in the original system; The mutual admittance for bus k to bus m is the product of the zero-impedance branch ratio and mutual admittance for bus k to bus s in the original model.

The current at the bus s is multiplied by the conjugate of the zero-impedance branch ratio to add to the master bus m and the equivalent current at bus m is

$$I_m + \sum_{s \in M} a_{ms}^* I_s \quad (5.3)$$

Similarly, the power and shunt compensation admittance can be given by

$$P_m + \sum_{s \in M} P_s \quad (5.4)$$

$$Y_m^{sh} + \sum_{s \in M} a_{ms} a_{ms}^* Y_s^{sh} \quad (5.5)$$

For the power-flow solver, both current and power mismatch method are proposed. The PQ buses equation is developed based on current mismatches whereas PV buses equations are based on power mismatches. The complex current and power mismatch at a given bus k are given by [177]

$$\Delta I_k = \frac{P_k^{sp} - jQ_k^{sp}}{E_k} - \sum_{i=1}^n Y_{ki} E_i \quad (5.6)$$

$$\Delta P_k = P_k^{sp} - \sum_{i=1}^n |V_k| |V_i| (G_{ki} \cos \delta_{ki} + B_{ki} \sin \delta_{ki}) \quad (5.7)$$

where, E_k is the complex conjugated voltage phase at bus k ; E_i is the voltage phasor at bus i ; P_k^{sp} and Q_k^{sp} are specified active and reactive power at bus k ; $Y_{ki} = G_{ki} + jB_{ki}$: bus admittance matrix element; B_{ki} is the susceptance of the n^{th} bus admittance, G_{ki} is the conductance of the n^{th} bus admittance. V_i and V_k are the voltage at bus i and bus k respectively.

The P_k^{sp} and Q_k^{sp} can be calculated by using the difference between power from generator and power from load.

$$P_k^{sp} = P_{G(k)} - P_{L(k)} \quad (5.8)$$

$$Q_k^{sp} = Q_{G(k)} - Q_{L(k)} \quad (5.9)$$

where, $P_{G(k)}$ and $Q_{G(k)}$ are active and reactive powers of generator for bus k ; $P_{L(k)}$ and $Q_{L(k)}$ are active and reactive powers of loads for bus k ; $P_{L(k)}$ and $Q_{L(k)}$ can be modelled in polynomial form[178]:

$$P_{L(k)} = P_{0k} (a_p + b_p V_k + c_p V_k^2) \quad (5.10)$$

$$Q_{L(k)} = Q_{0k} (a_q + b_q V_k + c_q V_k^2) \quad (5.11)$$

where:

$$a_p + b_p + c_p = 1 \quad (5.12)$$

$$a_q + b_q + c_q = 1 \quad (5.13)$$

In Eq.5.8-Eq.5.13, the Jacobian matrix is used to represent the power and current mismatches flow method through NRPF method[179].

$$\begin{bmatrix} \Delta I_{m1} \\ \Delta I_{r1} \\ \vdots \\ \Delta P_k \\ \vdots \\ \Delta I_{mn} \\ \Delta I_{rn} \end{bmatrix} = \begin{bmatrix} \frac{\partial I_{m1}}{\partial V_{r1}} & \frac{\partial I_{m1}}{\partial V_{m1}} & \dots & \frac{\partial I_{m1}}{\partial \delta_k} & \dots & \frac{\partial I_{m1}}{\partial V_{rn}} & \frac{\partial I_{m1}}{\partial V_{mn}} \\ \frac{\partial I_{r1}}{\partial V_{r1}} & \frac{\partial I_{r1}}{\partial V_{m1}} & \dots & \frac{\partial I_{r1}}{\partial \delta_k} & \dots & \frac{\partial I_{r1}}{\partial V_{rn}} & \frac{\partial I_{r1}}{\partial V_{mn}} \\ \vdots & \vdots & \vdots & \vdots & \vdots & \vdots & \vdots \\ \frac{\partial P_k}{\partial V_{r1}} & \frac{\partial P_k}{\partial V_{m1}} & \dots & \frac{\partial P_k}{\partial \delta_k} & \dots & \frac{\partial P_k}{\partial V_{rn}} & \frac{\partial P_k}{\partial V_{mn}} \\ \vdots & \vdots & \vdots & \vdots & \vdots & \vdots & \vdots \\ \frac{\partial I_{mn}}{\partial V_{r1}} & \frac{\partial I_{mn}}{\partial V_{m1}} & \dots & \frac{\partial I_{mn}}{\partial \delta_k} & \dots & \frac{\partial I_{mn}}{\partial V_{rn}} & \frac{\partial I_{mn}}{\partial V_{mn}} \\ \frac{\partial I_{rn}}{\partial V_{r1}} & \frac{\partial I_{rn}}{\partial V_{m1}} & \dots & \frac{\partial I_{rn}}{\partial \delta_k} & \dots & \frac{\partial I_{rn}}{\partial V_{rn}} & \frac{\partial I_{rn}}{\partial V_{mn}} \end{bmatrix} \begin{bmatrix} \Delta V_{r1} \\ \Delta I_{m1} \\ \vdots \\ \Delta \delta_k \\ \vdots \\ \Delta V_{rn} \\ \Delta V_{mn} \end{bmatrix} \quad (5.14)$$

where, ΔI_m is real part of current mismatch at the bus n ; ΔI_{mn} is imaginary part of current mismatch at the bus n ; ΔP_k is active power mismatch at bus k ; ΔV_m represents the real part of the voltage at bus n ; ΔV_{mn} represents the imaginary part of the voltage at bus n ; $\Delta \delta_k$ represents the phase angle at bus k .

At the bus k of PQ bus, the derivation of diagonal elements can be written as

$$\frac{\partial I_{mk}}{\partial V_{rk}} = B_{kk} - a_k \quad (5.15)$$

$$\frac{\partial I_{mk}}{\partial V_{mk}} = G_{kk} - b_k \quad (5.16)$$

$$\frac{\partial I_{rk}}{\partial V_{rk}} = G_{kk} - c_k \quad (5.17)$$

$$\frac{\partial I_{rk}}{\partial V_{mk}} = -B_{kk} - d_k \quad (5.18)$$

where a_k, b_k, c_k, d_k can be shown as

$$a_k = \left[\frac{Q'_k (V_{rk}^2 - V_{mk}^2) - 2P'_k V_{rk} V_{mk}}{V_k^4} + \frac{V_{rk} b_p P_{0k} V_{mk} + b_p Q_{0k} V_{mk}^2}{V_k^3} + c_q Q_{0k} \right] \quad (5.19)$$

$$b_k = \left[\frac{P'_k (V_{rk}^2 - V_{mk}^2) + 2Q'_k V_{rk} V_{mk}}{V_k^4} - \frac{b_p Q_{0k} V_{mk} V_{rk} + b_p P_{0k} V_{rk}^2}{V_k^3} - c_p P_{0k} \right] \quad (5.20)$$

$$c_k = \left[\frac{P'_k (V_{rk}^2 - V_{mk}^2) - 2Q'_k V_{rk} V_{mk}}{V_k^4} + \frac{b_p Q_{0k} V_{mk} V_{rk} - b_p P_{0k} V_{mk}^2}{V_k^3} - c_p P_{0k} \right] \quad (5.21)$$

$$d_k = \left[\frac{Q'_k (V_{rk}^2 - V_{mk}^2) - 2P'_k V_{rk} V_{mk}}{V_k^4} + \frac{V_{mk} b_p P_{0k} V_{mk} - b_q Q_{0k} V_{rk}^2}{V_k^3} - c_q Q_{0k} \right] \quad (5.22)$$

where:

$$P'_k = P_{G(k)} - P_{0k} a_p \quad (5.23)$$

$$Q'_k = Q_{G(k)} - Q_{0k} a_q \quad (5.24)$$

The off-diagonal elements are formulated as

$$\frac{\partial I_{mk}}{\partial V_{ri}} = B_{ki} \quad (5.25)$$

$$\frac{\partial I_{mk}}{\partial V_{mi}} = G_{ki} \quad (5.26)$$

$$\frac{\partial I_{rk}}{\partial V_{ri}} = G_{ki} \quad (5.27)$$

$$\frac{\partial I_{rk}}{\partial V_{mi}} = -B_{ki} \quad (5.28)$$

For the PV buses, the derivation of diagonal elements at bus k can be written as

$$\frac{\partial P_k}{\partial \delta_k} = -V_k \sum_{\substack{i=1 \\ i \neq k}}^n (G_{ki} \sin \delta_{ki} - B_{ki} \cos \delta_{ki}) \quad (5.29)$$

The off-diagonal elements are formulated as

$$\frac{\partial I_{mk}}{\partial \delta_k} = V_k (G_{kk} \cos \delta_k - B_{kk} \sin \delta_k) \quad (5.30)$$

$$\frac{\partial I_{rk}}{\partial \delta_k} = -V_k (G_{kk} \cos \delta_k + B_{kk} \sin \delta_k) \quad (5.31)$$

$$\frac{\partial P_k}{\partial V_{mi}} = V_k (G_{ki} \sin \delta_k - B_{ki} \cos \delta_k) \quad (5.32)$$

$$\frac{\partial P_k}{\partial V_{ri}} = V_k (G_{ki} \sin \delta_k + B_{ki} \cos \delta_k) \quad (5.33)$$

Fig.5.2 shows the flow chart of hybrid NRPF algorithm.

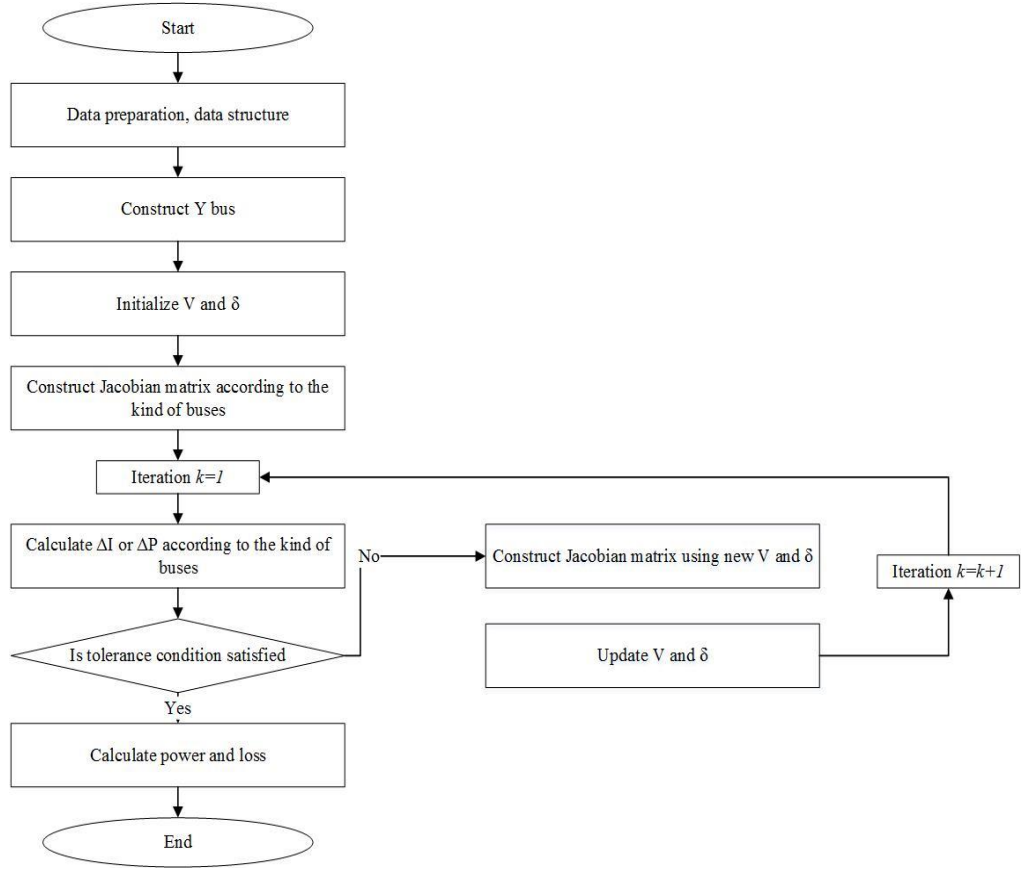


Fig. 5.2 Flow chart of hybrid Newton Raphson method

Fig.5.3 represents the one-line diagram of buses $m1$ and $m2$. The amount of power that can be transmitted through the lines is limited by several factors, including the material itself and the temperature. This limitation is observed as a decrease in power transmission from the source to the destination, called power loss.

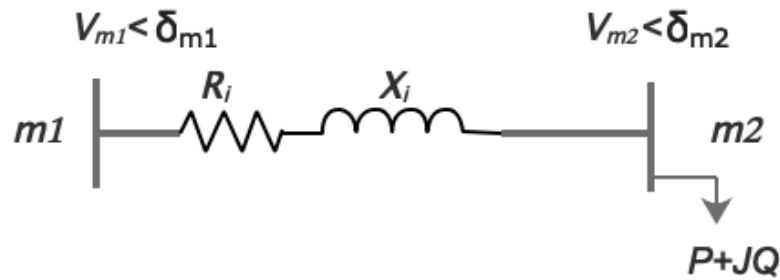


Fig. 5.3 One-line diagram of distribution system

The power loss of the LES is an important criterion in evaluating a network, which can be formulated by:

$$P_{loss} = \sum_{i=1}^N R_i \times \frac{(P_{m2}^2 + Q_{m2}^2)}{V_{m2}^2} + j \sum_{i=1}^N X_i \times \frac{(P_{m2}^2 + Q_{m2}^2)}{V_{m2}^2} \quad (5.34)$$

where P_{loss} is the total network loss, P_{m2} and Q_{m2} are the active and reactive loads at bus $m2$. V_{m2} is the voltage phasor of the buses $m2$. R_i and X_i are the resistance and reactance of the branch i .

In order to analyse the impact of photovoltaic systems on the existed power system, the data of simulated load demand is formulated in Eq.5.35. To simplify the simulation system, the impact of CHP on the power network has not been taken into consideration.

$$S_{ld} = D_{tld} - D_{chp} \quad (5.35)$$

where S_{ld} is the simulated load demand, D_{tld} is the historical data of the electricity demand, D_{chp} is the historical data of CHP electricity generation.

5.3 Introduction of UoW Power System

5.3.1 Power Distribution System

The UoW power system studied in this chapter has an 11kV bus ring that delivers the electrical power to all the electricity end users/buildings. In addition to delivering power generated from the CHP, the electricity distribution network is connected to a main substation sitting on UoW campus which is owned by the Distribution Network Operator (DNO). Fig.5.4 shows the architecture of distribution system in UoW. Each substation transforms the supply voltage from 11 kV to 400 V for end users.

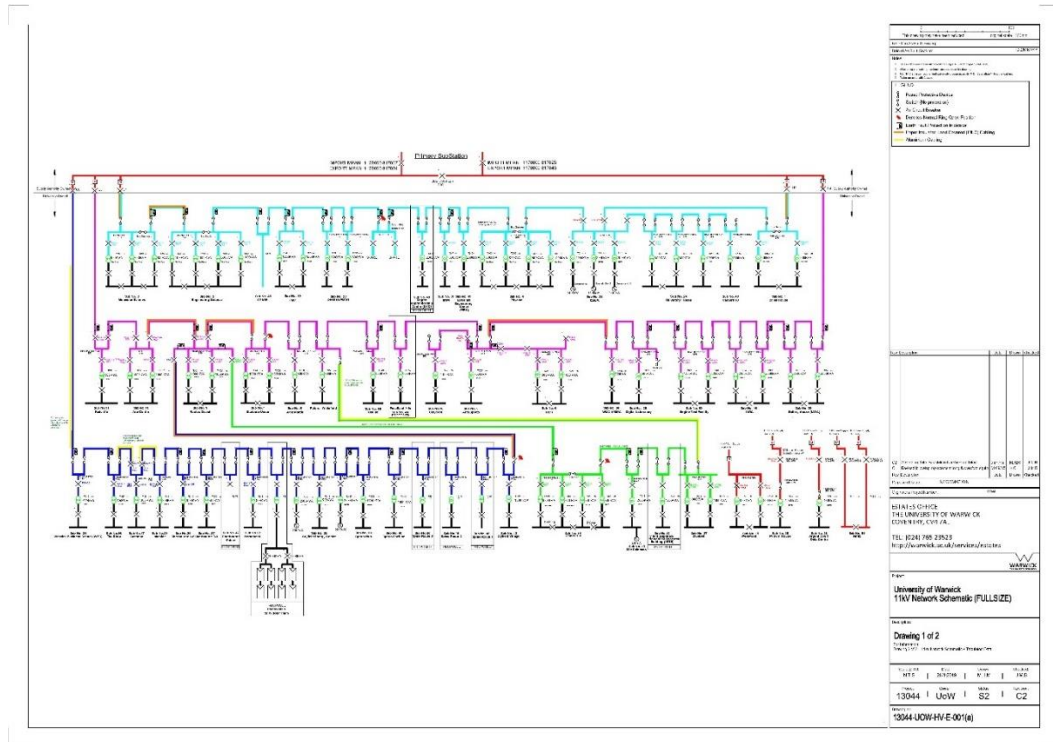


Fig. 5.4 Diagram of the University campus power distribution system

5.3.2 Current Solar PV Installation in UoW

The solar PV panels are installed on various campus rooftops, producing electricity and feeding to the system via the local substations. By 2018, the rated power of solar PV on campus is 248 kW, which is rather small in terms of the campus electrical load demand. A schematic diagram of the university's photovoltaic system installations is depicted in Fig.5.5.

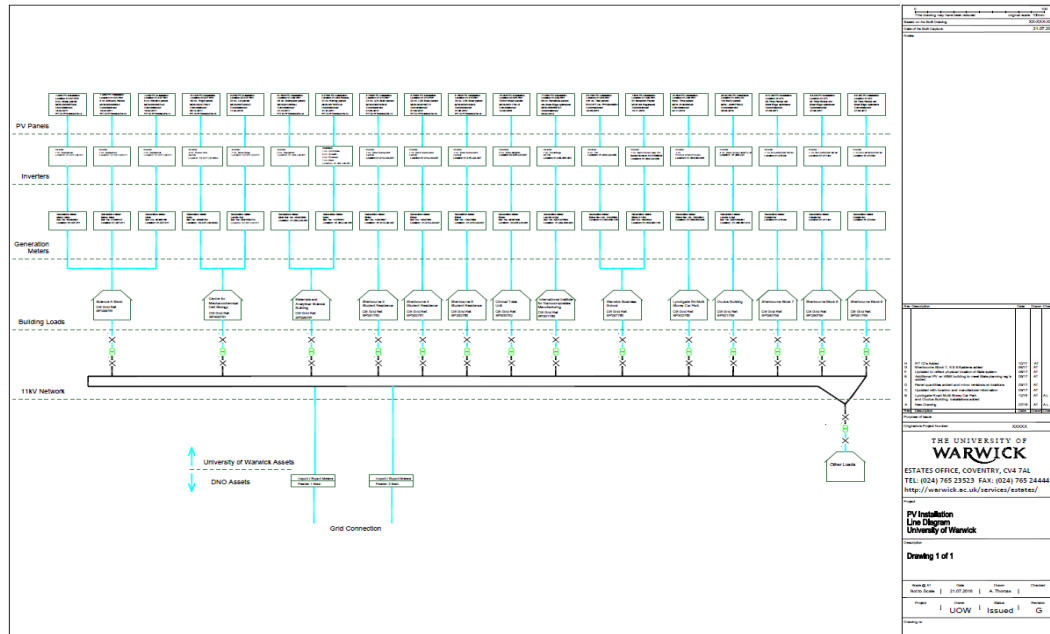


Fig. 5.5 Diagram presenting the installed solar panels network

With the trend of increase in electricity demand, the potential for installation of more rooftop solar PV panels is investigated by Stavropoulos in 2018 [180]. The study has derived the total university existing building roof areas and identified the effective areas for PV installation. The potential capacity of solar installation of each building tops is estimated and illustrated in Fig.5.6. From the analysis, it is found that the rated peak power from total solar PV installation could reach 3.87 MW, which may need approximately 13,042 PV panels.

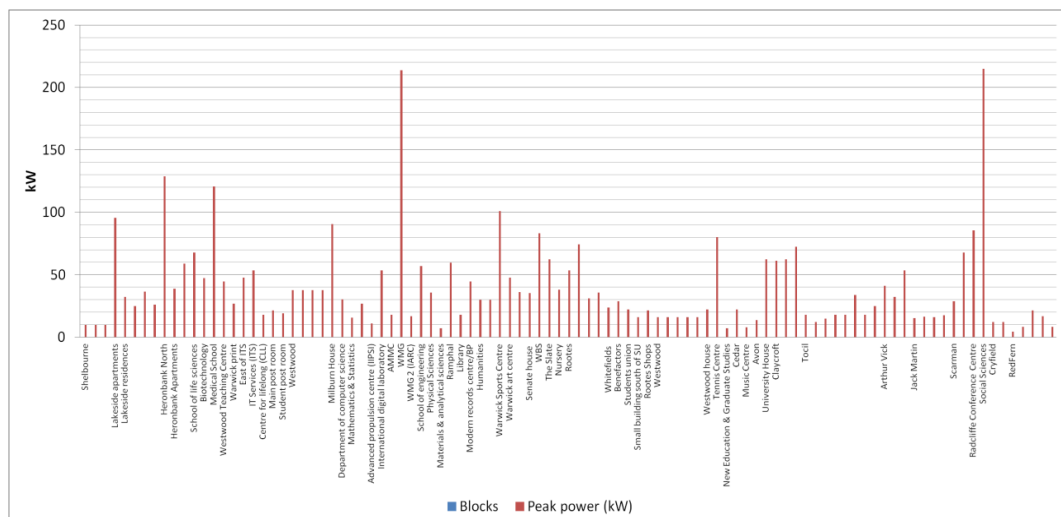


Fig. 5.6 Capacity of potential solar installation in each sector

5.3.3 Current Balance Mechanism of Power Flow in UoW

The UoW's power metering data is recorded and archived to the power co-simulation system every 30 minutes. The data includes all the metered substations and feeders around the campus as well as the virtual meters for both thermal and electrical load. This study considers the electricity demand, CHP generation, electricity import and solar generation. Historical data analysis is conducted, which covers the data sets of the total electric demand and total CHP generation stored for the last year (01.01.2018 to 01.01.2019).

The total electrical consumption and CHP power generation (illustrated in Fig.5.7) in 2018 are 61,272,655 kWh and 37,457,691 kWh, respectively. For solar generation, the total generation is 177,681 kWh as shown in Fig.5.8. 61.4 % of the UoW's annual electrical energy consumption is from onsite power sources for 2018, such as CHP plant and Solar PV panels. Compared with the period of 2015, the figure is lower as over 80 % electricity consumption were from on-campus generation in 2015 [181]. Currently, the solar generation compared with the total load demand is still very small and the power generation from CHP is relatively low in summer between May and October since the CHP plant is running on thermal led mode and the heat demand is low in those months. The gap between the load demand and electricity power generation is becoming larger for the month from May to October. So, UoW needs to buy more electricity from the grid to fill the gap.

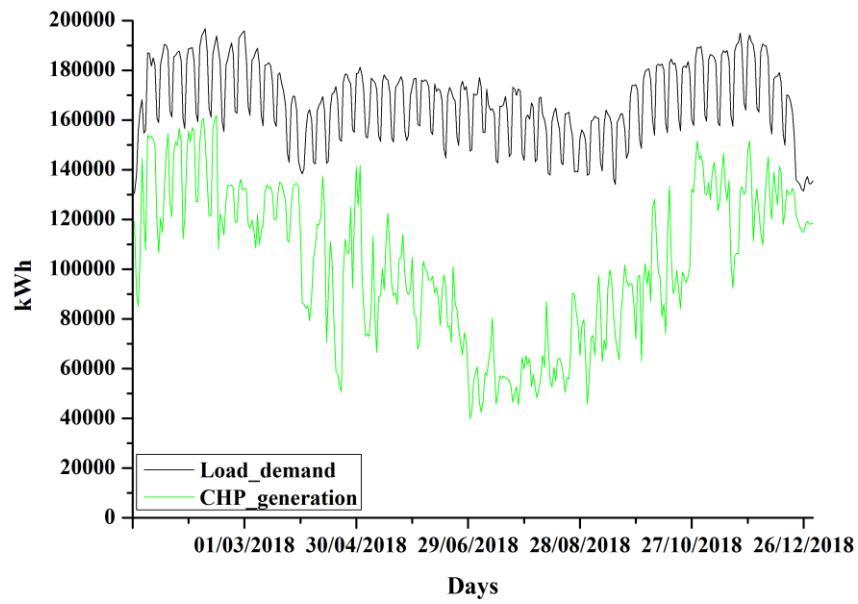


Fig. 5.7 Load demand vs. CHP electrical power generation

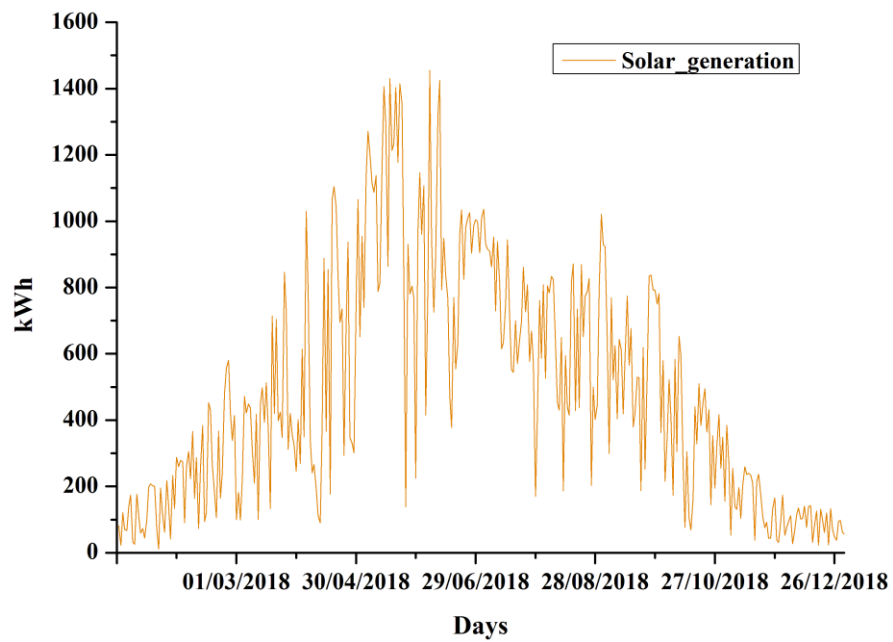


Fig. 5.8 Solar generation for Year 2018

The gap between the demand and electricity generation of onsite sources is varying with time and Fig.5.9 shows the gap variation over one week. In most cases, the load demand is higher than the onsite power generation so purchasing electricity from grid

is needed. The negative value indicates the electricity export to the grid when CHP generates the surplus electricity. If the gap can be filled by on-campus clean energy power generation source, the reduction in electricity purchase may save the UoW energy bill and reduce CO₂ emission. The next section will perform the analysis of the potential for more solar PV installation and integration on campus.

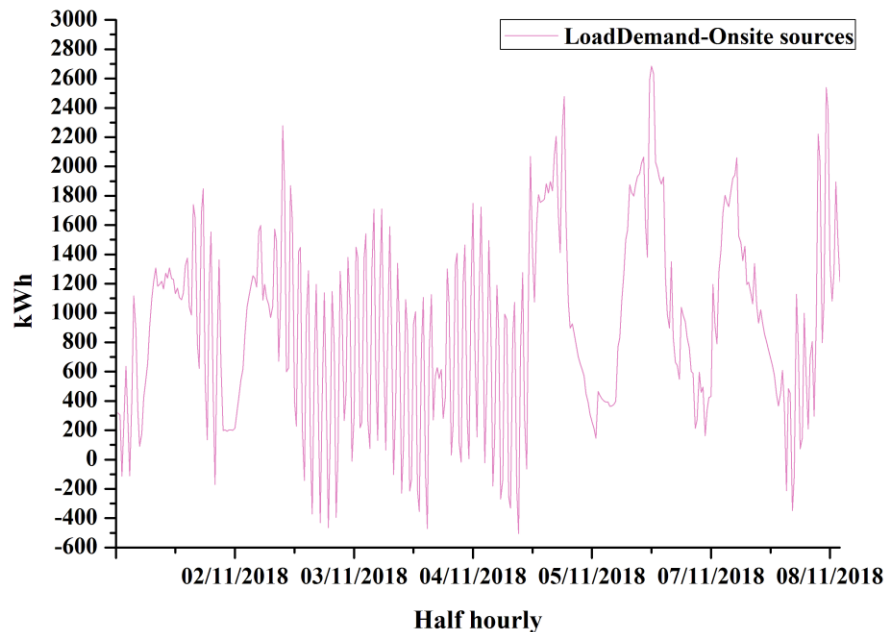


Fig. 5.9 Electricity bought from the grid (November)

5.4 Techno-Economic Study of Solar PV Integration

Increasing solar power generation is one of the potential options to accommodate the campus energy demand growth in a greener way. It is clear that the UoW has suitable space for solar PV installation. However, there are many factors which are unknown:

- What is the potential capacity the university can accommodate?
- What is the optimal installation capacity to have the maximum gains financially and environmentally?
- What impact does the massive solar PV generation integration impose onto the existing campus energy system?

In this section, the following studies are reported: i) identification of the correlations between solar generation and load demand; ii) techno-economic study for PV

integration potential on campus; iii) the impact analysis with different hypotheses for solar PV installation.

5.4.1 Correlation Analysis

One goal of integrating solar PV system is to compensate the power gap between generation and demand. If the generation curve is consistent with demand curve, this generation source is easy to be integrated into original system. Correlation analysis is a method of statistical evaluation used to study the strength of a relationship between two, numerically measured, continuous variables. To examine the correlation between solar power generation and load demand, Pearson's Correlations Coefficient (PCC) [182] is used. PCC provides a measure of the strength of a linear association between two variables, with the results varying from the range of -1, representing a perfect negative linear correlation, to 1, which represents a perfect positive linear correlation. Zero value of a PCC indicates that there is no linear relationship. A further breakdown of the value representation is given in Table 5-1.

Table 5-1 Pearson's Correlation Coefficient and representative strengths

PCC	Correlation Strength
$ \rho = 0$	indicates that both variables are not linearly related
$0:00 < \rho < 0:09$	no correlation
$0:10 < \rho < 0:25$	a small linear correlation
$0:26 < \rho < 0:40$	a medium linear correlation
$0:41 < \rho < 1:00$	a strong linear correlation
$ \rho = 1$	a perfect positive/negative linear correlation

The study uses the data from the historical record, including solar generation, distributed load demand and electricity generation from the CHP based on the co-simulation system. It is expected to exhibit linear relationships between the chosen solar outputs and electrical demand. No documented outages are recorded during the period of the study and the standard deviations of all variables are within the expected limits.

The results are shown in Table 5-2, where $\rho_{LD\&Solar}$ represents the PCC between the solar power generation and the load demand and $\rho_{(LD-CHP)\&Solar}$ represents the PCC between the solar power generation and the electricity purchase/import from the grid. It can be seen that the correlation factors between the solar generation and

the load demand are strong in most of months. For example, as shown in Fig.5.10, the solar generation gets to its peak when the load demand is high.

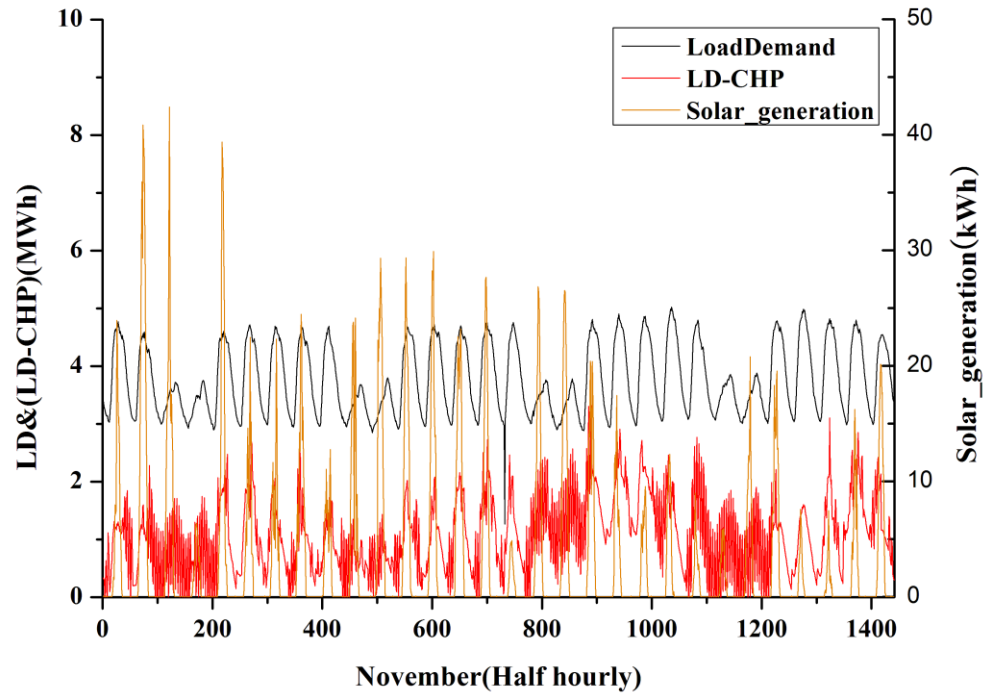


Fig. 5.10 Solar generation vs. Load demand

Table 5-2 Correlations between different parameters

Month	1	2	3	4	5	6	7	8	9	10	11	12
$\rho_{LD\&Solar}$	0.45	0.45	0.50	0.56	0.59	0.72	0.73	0.66	0.61	0.48	0.39	0.35
$\rho_{(LD-CHP) \&Solar}$	0.27	0.41	0.42	0.52	0.48	0.57	0.64	0.46	0.45	0.38	0.28	0.28

From the above analysis, it can be seen that all the data exhibit the positive PCC level and the high PCC numbers are shown for May, June, July and August. In general, the thermal energy demand is low, and the weather has longer duration of daytime with more sunshine for those four months in the UK. It leads to a positive sign in extending the solar PV capacity which could be one way to reduce dependence on the import energy from the grid and lower the cost.

5.4.2 Analysis of Extended Solar PV Integration

5.4.2.1 Potential capacity of campus rooftop solar PV installation

Stavropoulos [180] through his project has analysed the potential future installation of solar PV panels while all the available building rooftops of the university are considered. Stavropoulos' study obtained the total effective area and orientation of the University's campus roof-tops; then the potential installation capacity is calculated in association with the suitable areas. Based on the evaluation, the potential capacity of rooftop solar installation is 4.2 MW. The solar PV generation is calculated by using the historical data of current 248 kW solar PV generation as shown in Eq.5.36. The Load demand data and CHP electricity generation data used in this analysis is from the historical data for the period of 01/01/2018- 01/01/2019

$$E_{t,as} = \frac{E_{t,his}}{P_{re,rated}} P_{po,rated} \quad (5.36)$$

where, $E_{t,as}$ is the estimated solar generation at time step t with the assumed rated solar generation capacity $P_{po,rated}$; $E_{t,his}$ is the historical solar generation data with the installed solar generation capacity, $P_{re,rated}$.

From the above analysis, the total solar generation can be increased from 177,681 kWh to 3,020,667 kWh for the time period considered if all the suitable spaces used for solar installation. In this case, the proportion of self-generated electricity increased by 5 % to 66 % based on the electricity demand in 2018-19. Due to the nature of solar generation, the peak generation of solar system is from May to October, during which the gap between the load demand and the power generation from CHP is relatively higher than the rest of the year. Therefore, the electricity from solar system may fill the gap well. Fig.5.11 shows the difference of electricity purchased from grid after and before the 4.2 MW solar system is installed. From the comparison, it is clear that the mean electricity purchased from the grid is reduced 12,000 kWh per day from April to October. The half-hourly data of the purchased electricity from the grid is shown in Fig.5.12 after the 4.2 MW rooftop solar system is installed. Compared with the daily data, there are a few points where the electricity is fed back to the grid. The total number of these points is 273 and these points are distributed in 50 days. The total electricity exported to grid is 50.09 MWh. The total number is 160 and the total export electricity is 36.63 MWh before the 4.2 MW solar system is installed. 2 % of solar electricity is fed back to the grid with 4.2 MW solar generation in this year.

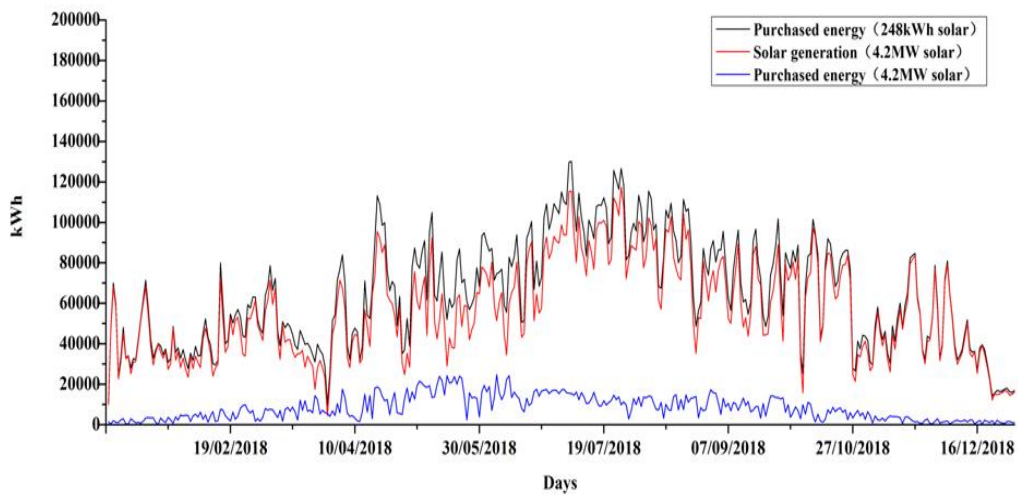


Fig. 5.11 Purchased energy from grid (248 kW solar vs. 4.2 MW solar)

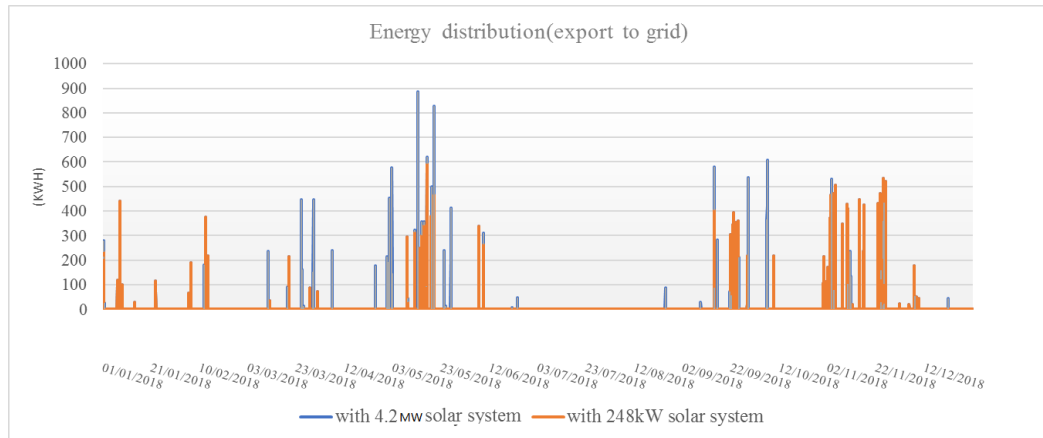


Fig. 5.12 Energy distribution (exporting to grid)

5.4.2.2 Optimisation of the sizing of solar system

In this subsection, the optimal sizing of solar system is studied aiming to reduce the imported electrical energy from the grid. From the above subsection, the lower limit used is 4.2 MW. The upper limit is chosen as 20 MW since the peak power demand is assumed to be 14.6 MW in 2030 and the total solar system conversion efficiency is 73 %. According to the 2020 carbon emission management plan of UoW, It is assumed that the ratio of the UoW's annual energy consumption from onsite power sources should be above 70 % and the power sources should be renewable energy. So, the lower limit should be above 10.3MW (the ratio is 70.3 % after the calculation

based on load demand in 2018). Six random sized solar system between 10 MW to 20 MW are chosen for comparison, as shown in Table 5-3.

Table 5-3 Scenarios of solar installation

Scenarios	1	2	3	4	5	6
Solar power rating (MW)	11.2	12.4	13.6	14.9	17.4	19.8

In Fig.5.13, the electricity imported from the grid does not reduce from November to February although the solar power rating increased from 11.2 MW to 19.8 MW. From March to 15th of June, different scenarios highly affected the imported electricity. The energy fed back to the grid increased with the increment of capacity of solar installation in this period. For example, the maximum export electricity is 60,000 kWh on 17th of May in scenario 6. In comparison, the export electricity was around 10,000 kWh on the same day for the scenario 1. Generally, scenario 6 is the better scenario if the period between 1st of May and 15th of June is not considered.

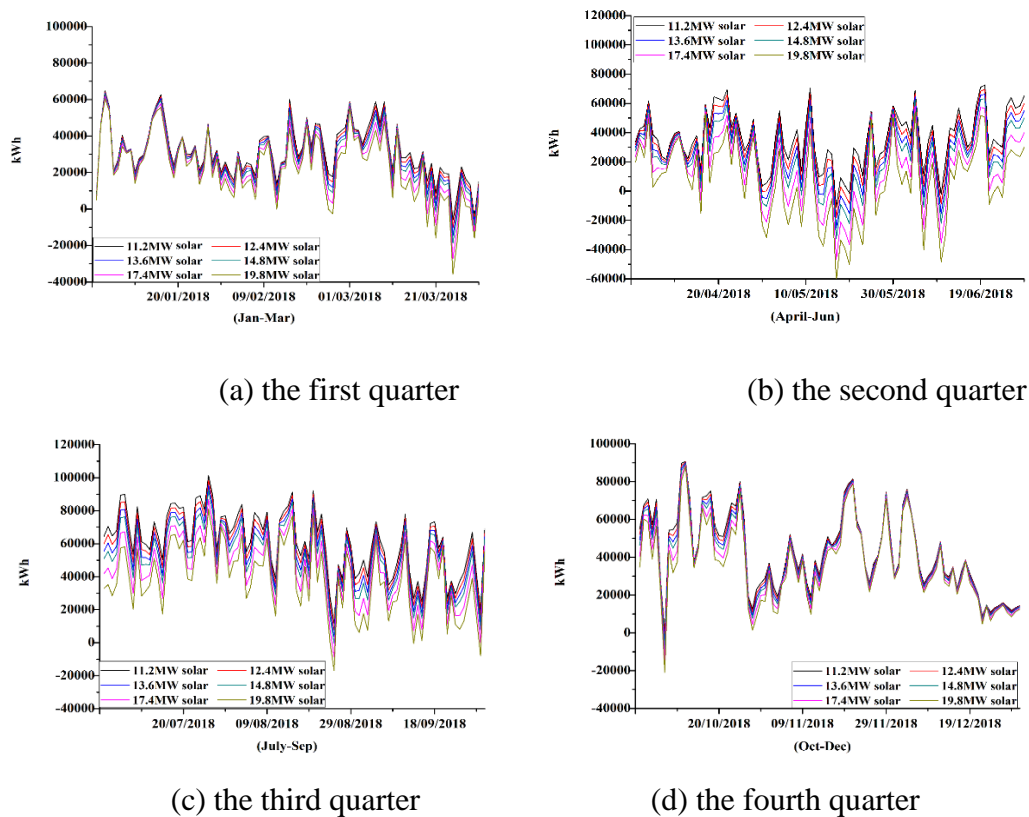


Fig. 5.13 Import electricity from grid based on different scenarios (daily)

Table 5-4 Export electricity in different scenarios

Scenario	1	2	3	4	5	6
Export electricity (kWh)	942,346.7	1,310,172	1,736,721	2,210,559	3,289,515	4,512,237
Days of export electricity	6	9	13	18	27	46

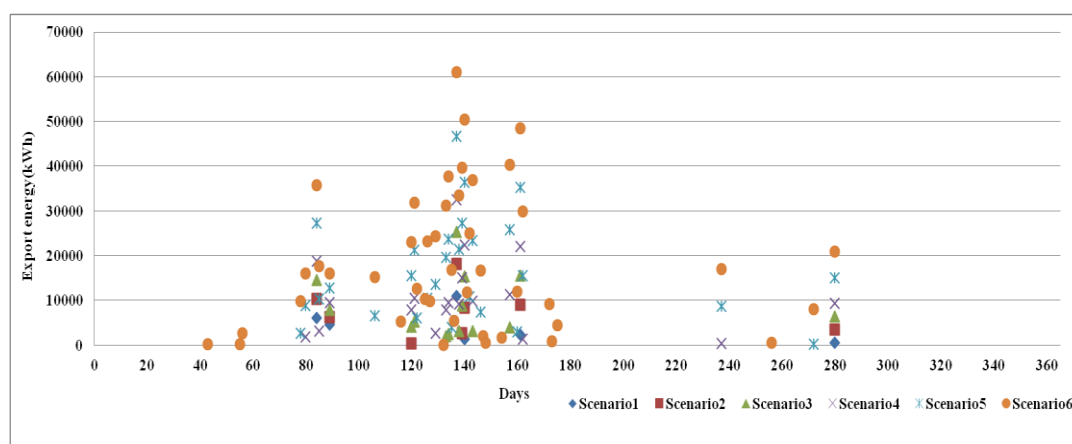


Fig. 5.14 Distribution of export electricity based on different scenarios

The daily export electricity is listed in Table 5-4 and the power distribution of one year is shown in Fig.5.14. From the distribution of export electricity, there are 46 days when the campus generates more electricity and feeds back to the grid. The number of days of electricity export for scenario 1-scenario 5 are 6, 9, 13, 18 and 27, respectively. The scenario 1-scenario 3 could be considered as the proper solutions if the days of electricity export are limited to 15 days.

5.4.2.3 Economic analysis of solar PV integration

The cost breakdown of the solar PV is illustrated in Fig.5.15 [184]. The Solar Trade Association (STA) provides a clear estimate of how utility-scale solar cost in comparison with a residential and commercial roof-top solar PV cost, as shown in Fig.5.16. For the large scale of ground-mounted solar PV plants over 5 MW, the cost of installation is significantly lower than the residential rooftop systems. The different cost scenarios that are from £1,000,000/MW to £1,200,000/MW are used to calculate the payback year of the investment. The calculation is under the assumption that all the solar generation is consumed by demand and the prices for the solar generation is from 0.07 £/kWh to 0.10 £/kWh in 2015 [176].

Cost breakdown for solar plant

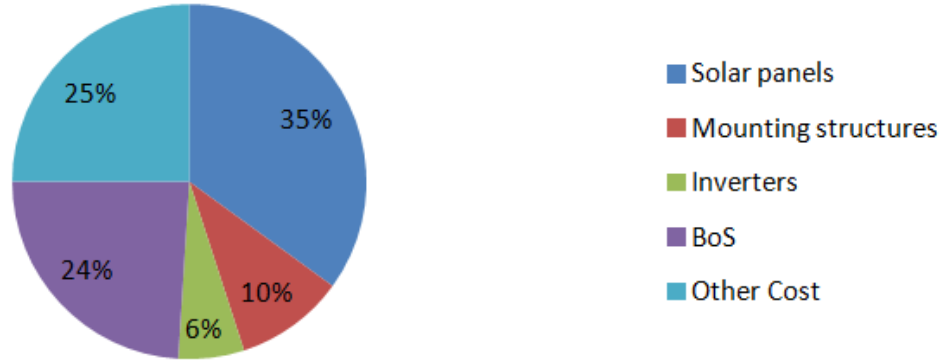


Fig. 5.15 Cost breakdown for the solar system [166]

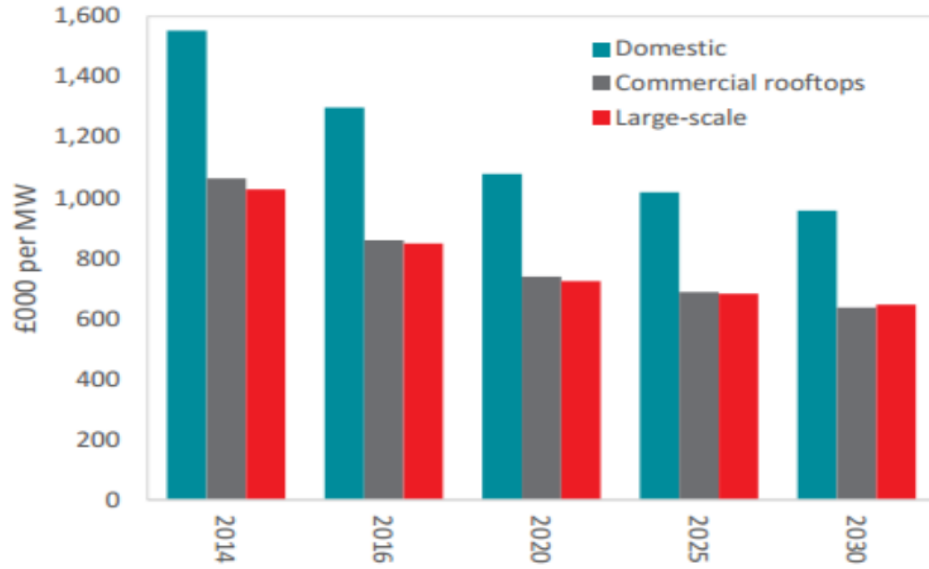


Fig. 5.16 Cost assumption for the solar system [166]

Table 5-5 shows the payback year with different assumptions of installation cost and solar energy price. The best case of payback time is 13.9 years and the worst case is 23.8 years. Normally, the lifetime of solar system is estimated to be 25 years, so the payback time is normally less than the solar lifetime period.

For the calculation of CO₂ emission, Eq.5.37 is adopted, where e_{co_2} is the weight of reduction of CO₂ emission, E_{solar} represents the total energy generation in 25 years, ζ is the coefficient of CO₂ generation and has the value of 365 g/kWh for CCGT power plant [183]. In the worst case, the CO₂ emission reduction can be 2,860 tons within the solar PV panel lifetime of 25 years.

$$e_{co_2} = E_{solar} \zeta \quad (5.37)$$

Table 5-5 Payback years of investment

Price (£/kWh) Cost (£/MW)	0.07	0.08	0.09	0.10
1000000	19.86	17.38	15.45	13.90
1050000	20.86	18.25	16.22	14.60
1100000	21.85	19.12	16.99	15.29
1150000	22.84	19.99	17.77	15.99
1200000	23.84	20.86	18.54	16.69

Fig.5.16 shows that the large-scale solar system is more economic, and the campus has enough space to install the large-scale utility type of solar PV panels but need to identify the feasible space and location.

The following subsection will calculate the payback year based on the large-scale solar system. The ratio of solar energy usage is calculated based on the load profile and solar power generation in 2018. To calculate the cost and benefit of installation of solar PV panels, the following assumptions are made:

- The benefit of export energy is negative since the University does not have the export license, but the transmission fee and capacity fee need to be paid by UoW.
- The price of the solar PV generation is 0.08 £/kWh
- The solar PV panels are installed on the farmland assuming that the cost of solar PV investment is 700000 £/MW [185]

The payback year is calculated as: the investment of solar panel investment is divided by the benefit of solar generation. Table 5-6 shows the payback years for different scenarios. The best case is 13.9 years and the worst case is around 18 years. The difference of payback years is mainly affected by the ratio of onsite usage of solar energy.

Table 5-6 Payback years of the investment

Solar power rating (kW)	11200	12400	13600	14900	17400	19800
Solar export (kWh)	942346.7	1310172	1736721	2210559	3289515	4512237
Solar used (kWh)	7053310	7573891	8035748	8450316	9148173	9702263
Installation cost (£)	7840000	8680000	9520000	10430000	12180000	13860000
Payback years	13.89	14.33	14.81	15.43	16.64	17.86

The half hourly data of export energy is shown in Fig.5.17 for different scenarios. To absorb the export electricity on UoW, the energy storage system may be considered. The power rating of storage system is estimated around 2 MW and the capacity would be around 5 MWh for Scenario 1 and Scenario 2. The power rating of energy storage system is predicted to be around 4 MW and the capacity would be around 8 MWh for Scenario 3 and Scenario 4. The power rating of the energy storage system is estimated around 8 MW and the capacity could be around 16 MWh for Scenario 5 and Scenario 6.

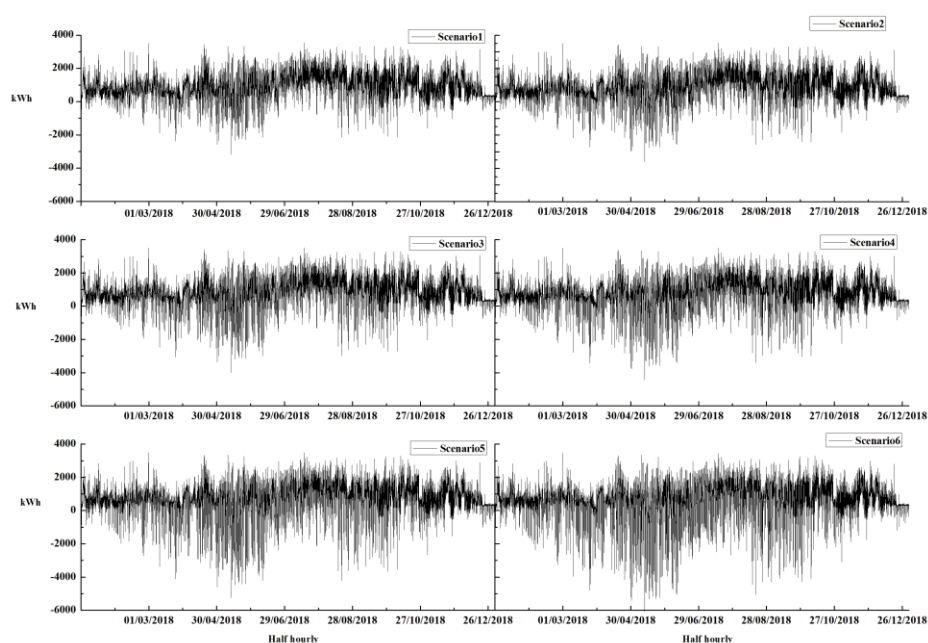


Fig. 5.17 Import electricity in different scenarios (half hourly)

Then the battery storage system is considered to optimise the power flow. The installation cost of Lithium Nickel Manganese Cobalt Oxide (NCM) battery is 400 £/kWh [186]. It is assumed that 95 % of the electricity from the PV's external output

to the grid is stored in the battery. Then, at the peak of the power consumption, taking the conversion loss, 80 % of this energy is fed back into the onsite network. The Table 5-7 shows the payback year of hybrid system. Generally, the payback year is prolonged by 2 years after storage system is integrated. It is noted that the battery lifetime is not considered.

Table 5-7 Payback years of the investment of hybrid systems

Battery capacity (kWh)	5000	5000	8000	8000	16000	16000
Battery cost (£)	2000000	2000000	3200000	3200000	6400000	6400000
Solar power rating (kW)	11200	12400	13600	14900	17400	19800
Solar export (kWh)	47117.3	262034.4	86836.1	442111.8	164475.8	902447.4
Solar used (kWh)	7948538.9	8622028.1	9685632.7	10218763.2	12273212	13312053
Installation cost (£)	7840000	8680000	9520000	10430000	12180000	13860000
Payback years	15.47	15.48	16.42	16.67	18.92	19.02

Table 5-8 shows the payback year of the hybrid system if the lifetime of battery system is considered. The lifetime of battery is 10 years since the State of Health (SoH) cannot meet the storage requirement after ten years. The cost of the battery system increased by extra 50 % and the payback years are prolonged by 3 years after the storage system is installed.

Table 5-8 Payback years of the investment of the hybrid system

Battery capacity (kWh)	5000	5000	8000	8000	16000	16000
Battery cost (£)	3000000	3000000	4800000	4800000	9600000	9600000
Solar power rating (kW)	11200	12400	13600	14900	17400	19800
Solar export (kWh)	4117.3	26034.4	8836.1	44111.8	16475.8	90447.4
Solar used (kWh)	7948538.9	8622028.1	9685632.7	10218763.2	12273212	13312053
Installation cost (£)	7840000	8680000	9520000	10430000	12180000	13860000
Payback years	17.05	16.93	18.48	18.63	22.18	22.03

From the above analysis, the 11.2MW solar system is recommended based on the campus current power flow and its operation. It is not economically viable to consider installing battery storage if it is used purely for supporting solar power generation and utilization. Certainly, the benefits of battery energy storage installation should be analysed in a broad content of LES beyond supporting solar power only.

5.5 Impact of Solar PV Integration on Current UoW Power System

5.5.1 Modelling of UoW Power Distribution Network

When large-scale solar PV generation is connected to a power system, the power system structure will migrate from single power radial network into weak-link network of Multi-distributed power generation. Large capacity of Distributed Generation (DG) integration in a power system will impact on feeder's voltage, short circuit current, active and reactive power flow and other system characteristics. DG integration will decrease transmission power on the feeder and the feeder will need to support DG output reactive power, so load node voltage along the feeder will be raised. The level of voltage raising is linked closely with DG location and the size of the total capacity.

Fig.5.18 shows the architecture of UoW radial distribution system used in the simulation study. The main substation between node_799 and node_701 provides the electricity energy to distributed loads. The voltage of primary substation is 132kV. Node_701 is a metering point that can monitor the total import/export energy. There are 3 feeders in node_702 where three branches are connected.

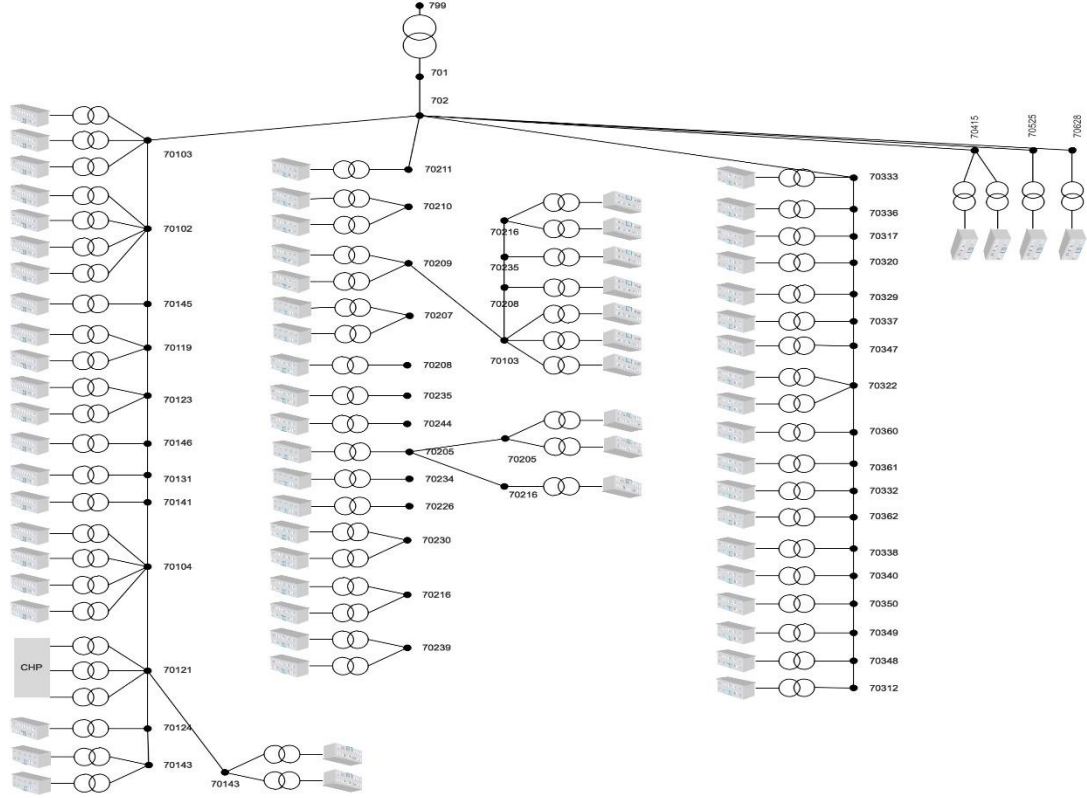


Fig. 5.18 Simulation architecture of Warwick distribution network

Based on the power co-simulation system developed in chapter3, the simulated UoW power distribution system is integrated into simulation platform of co-simulation system. The substation takes the three-phase unbalanced power solution seen at the substation node, calculates the average power on the phases, and writes this average to the load property in the parent node. For other nodes in this distribution system, the ZIP load is connected to each node and the value of load is simulated based on the acquired load metering data of UoW in co-simulation system. Fig.5.19 shows the load profile of some nodes at random 48 hours. The maximum electricity demand is 30 kW and the lowest demand of one user is close to 1 during some period.

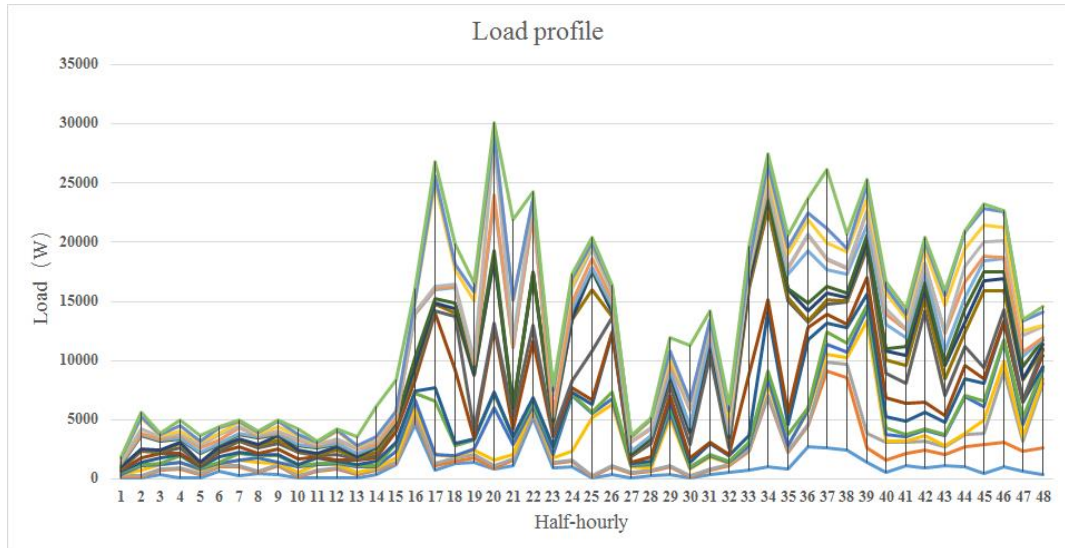


Fig. 5.19 Example of load profile for various nodes

5.5.2 Results and Analysis

Following the analysis presented in [180], 4.2 MW solar PV capacity can be accommodated by the current campus rooftop. In this study, it is assumed that the total solar PV power generation is connected to the substation of the node_70360 as shown in Fig. 5.20. The worst-case scenario is used to analyse the impact on distribution network. Fig. 5.21 shows the half-hourly total power input to distribution load demand before (base) and after the 4.2 MW solar PV is installed. The minimum and peak power of the main substation are 6.6 MW and 16.3 MW, respectively. During the period from 7:00 to 17:00, the import power is dramatically reduced since the solar PV generates electrical power to this distribution system. Fig. 5.22 shows the solar power generation of that day. The radiation data is obtained from the campus weather station on 2nd July 2017.

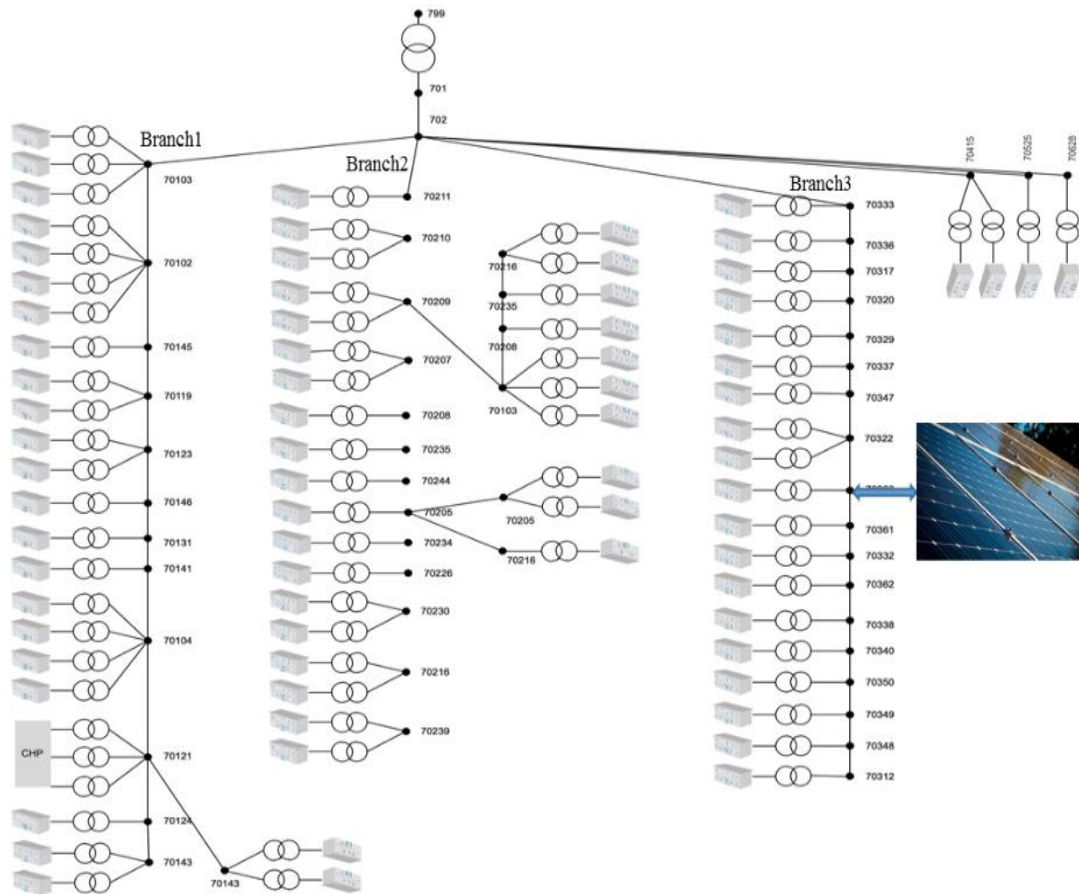


Fig. 5.20 The placement of solar generation system

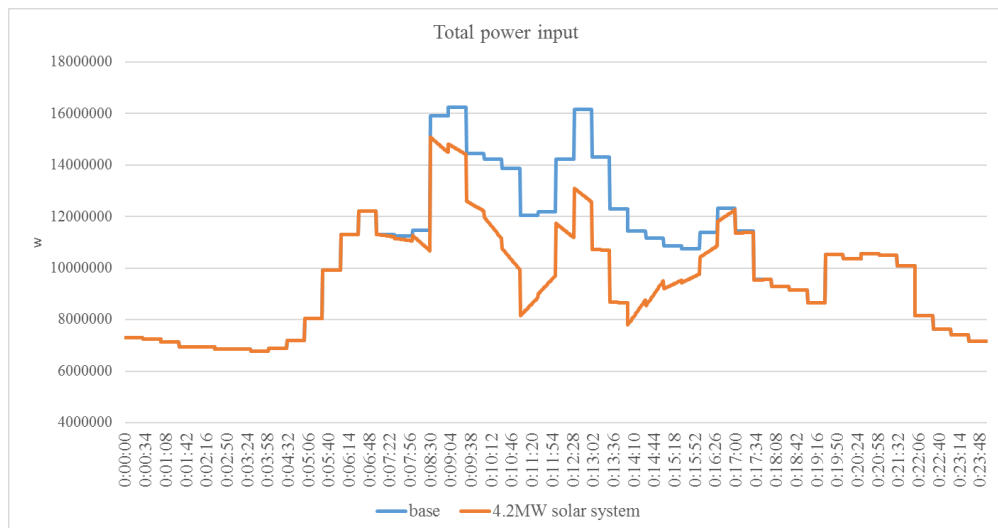


Fig. 5.21 Power import with and without solar power generation

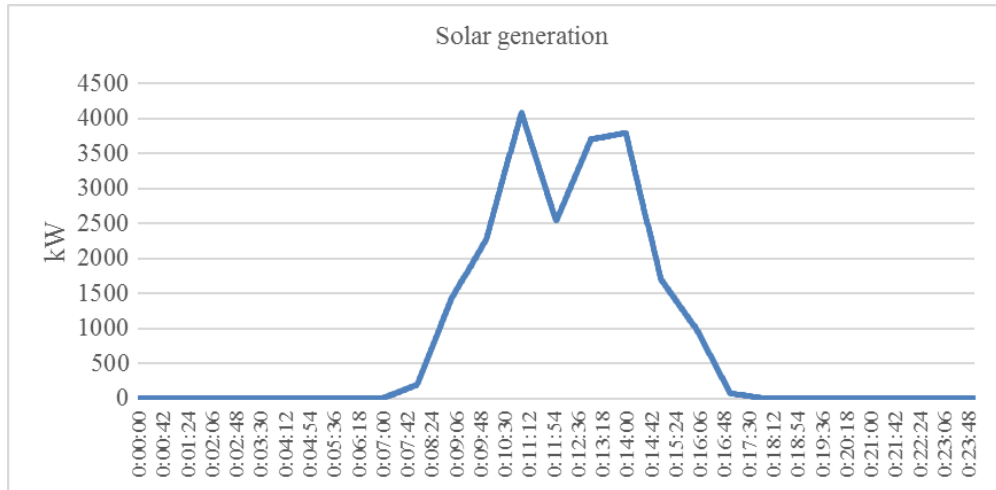


Fig. 5.22 Total solar output of the node_70360

In Fig.5.23, the one-day energy losses are around 500 kWh which is calculated by the difference of power import in different conditions. The total energy losses are reduced by 10 % to 450kWh after the solar system is installed. Fig.5.24 and Fig.5.25 compare the 11kV voltage profiles of various nodes in different time segments. The voltage on Branch 1 and Branch 2 is kept the same before and after the solar system is installed since the solar system is installed on Branch 3 only. In the radial distribution system, the voltage gradually decreases as the node moves away from the initial feeder. The voltage of node_70360 increases by around 100V at 12pm, when the solar system generates more power compared with other time segments. It is obvious that the node voltage of Branch 3 is higher than the voltage of other branches. As a result, the 4.2 MW solar system highly affects the node voltage in the connected branch. It is clear that the voltage is still within the allowed voltage variation limit (6 % of rated voltage).

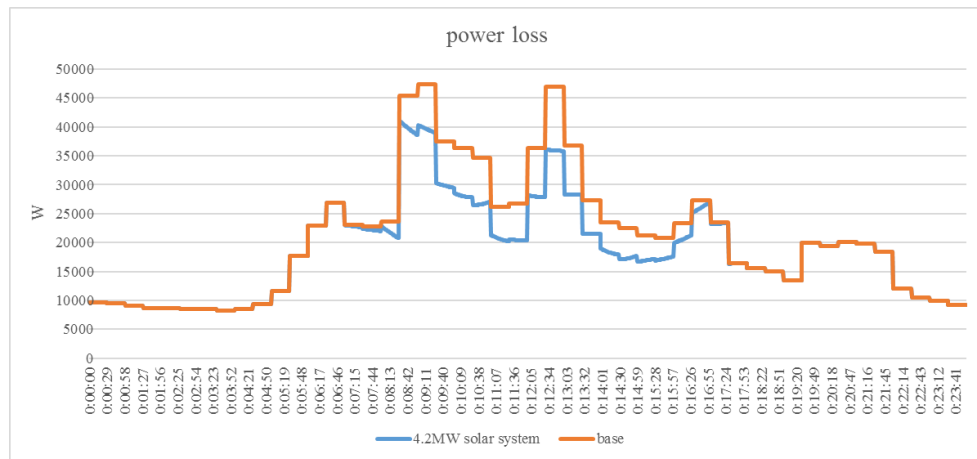


Fig. 5.23 Power losses of distribution system

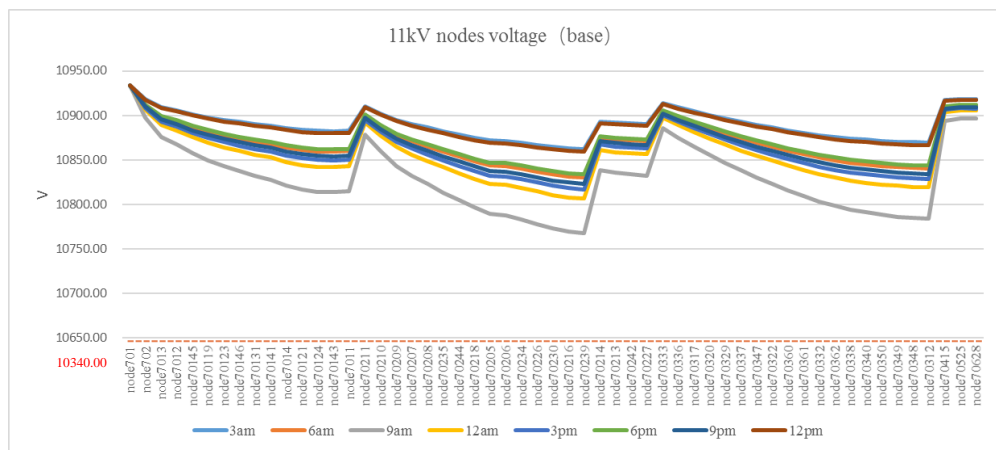


Fig. 5.24 11kV voltage profiles on different nodes-base

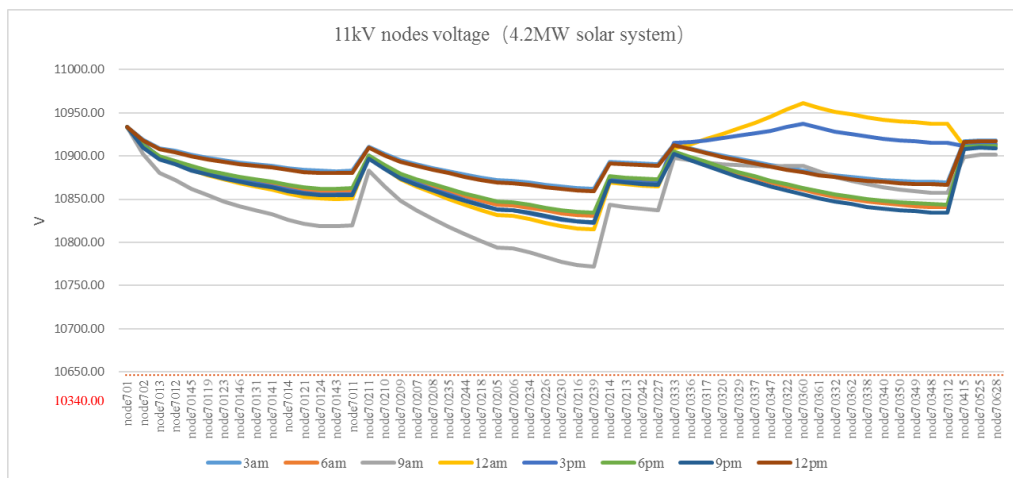


Fig. 5.25 11 kV voltage profiles on different nodes-with solar installation

The profiles of low voltage are shown in Fig.5.26 and Fig.5.27 to compare the voltage before and after the solar system installation. The voltage of meter_1101 is much lower than other meters since the load demand is higher and the transformer is slightly overload during some time segments. After the solar system is installed, the voltage of meter_90360 and meter_100360 gradually increases with the increment of solar generation. Both meter_90360 and meter_100360 are connected to the second segment of 11kV/400V transformer. The voltage of other meters in the same branches also increases by around 4V. The voltage drops of meter_90362 is improved because of the installation of solar system.

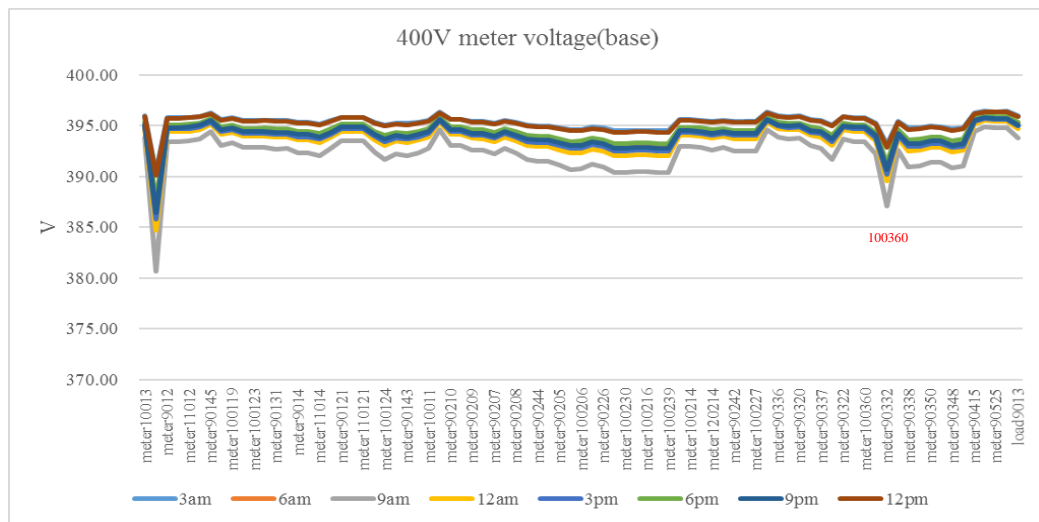


Fig. 5.26 400V voltage profiles on different meters-base

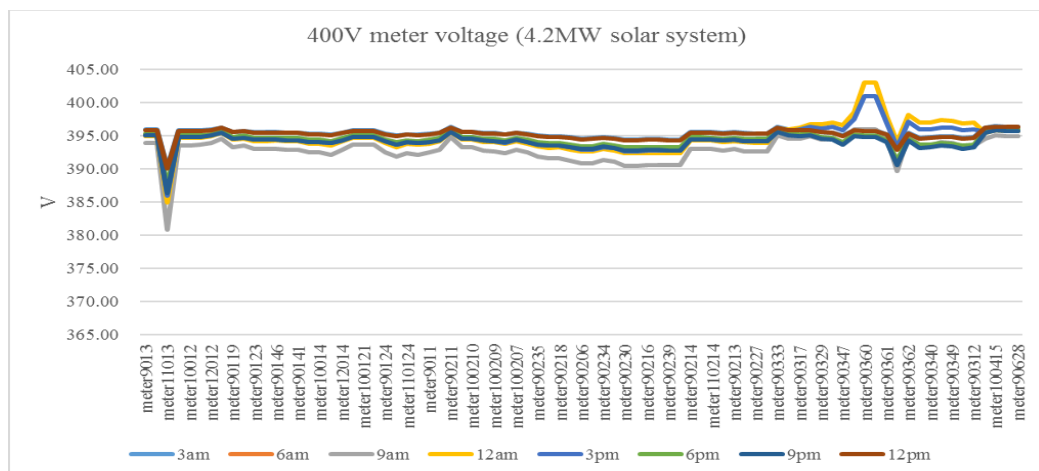


Fig. 5.27 400V voltage profiles on different meters-with solar installation

From the study conducted in Section 5.3, the 11.2MW pure solar installation capacity is recommended in terms of cost and benefit balance. The following subsection will analyse the impact of 11.2MW solar integration on the distribution network. The first 5.6 MW solar system is still installed at node_70360 of Branch 3, and the second 5.6 MW solar system is connected to node_70244 of Branch 2 as shown in Fig.5.28.

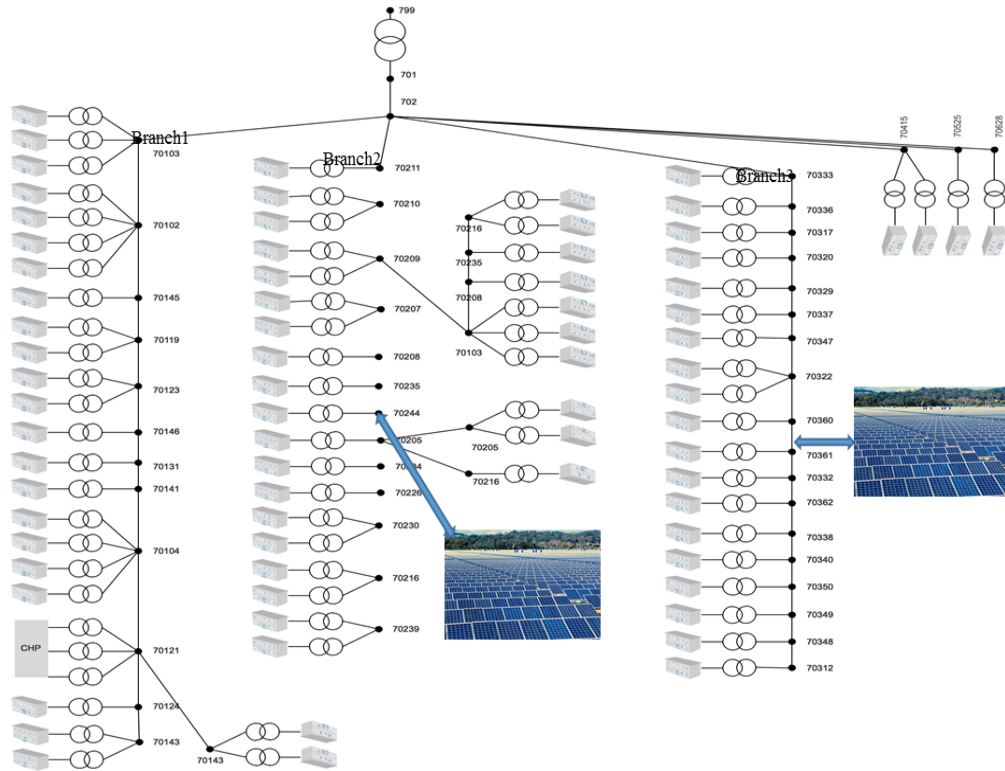


Fig. 5.28 The placement of solar generation systems

In Fig. 5.29, the daily total electricity import is further reduced from 249 MWh to 203 MWh compared with the base model after two 4.2 MW solar system is installed. The peak load demand reduces from 16.2 MW to 13.7 MW. In comparison, the total energy loss reduces by 25 % to 367kWh, as shown in Fig.5.30.

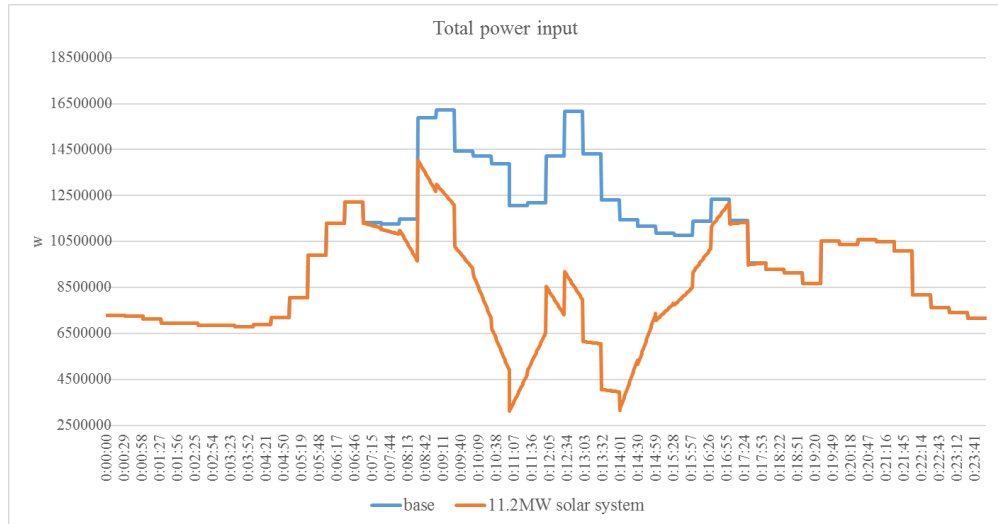


Fig. 5.29 Power input of the main substation

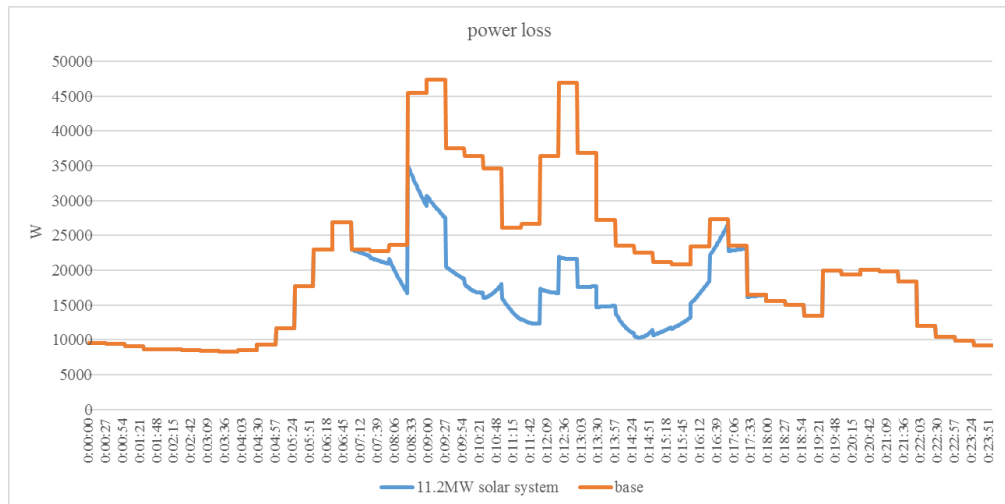


Fig. 5.30 Power losses of distribution system

The distribution of medium and low voltage profiles is shown in Fig.5.31 and Fig.5.32, respectively. In Fig.5.31, the dashed line is the voltage profiles in different time segment, the solid line is the voltage profiles after the 11.2 MW solar system is engaged online. The voltage profiles are nearly same during the period from 21:00 to 6:00, during which, there is no electrical power generated from the solar PV system. The voltage increment of Branch 2 and Branch 3 is different although the capacity of solar system is same since the load demand and architecture of each branch is different. From the above analysis, the installation of solar PV improves the stability of current power distribution system.

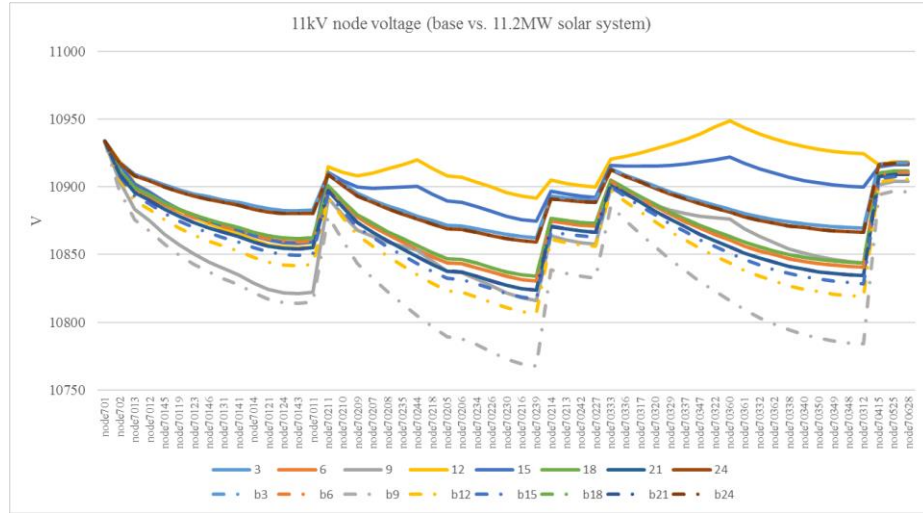


Fig. 5.31 11 kV voltage profiles on different nodes-with solar installation

In Fig.5.32, it can be seen that the obvious increase of voltage in the meter_70244 and meter_70360. It indicates that the solar system will also cause the voltage increase at the low voltage system. The voltage of the nearby meters is also affected but the difference is not obvious.

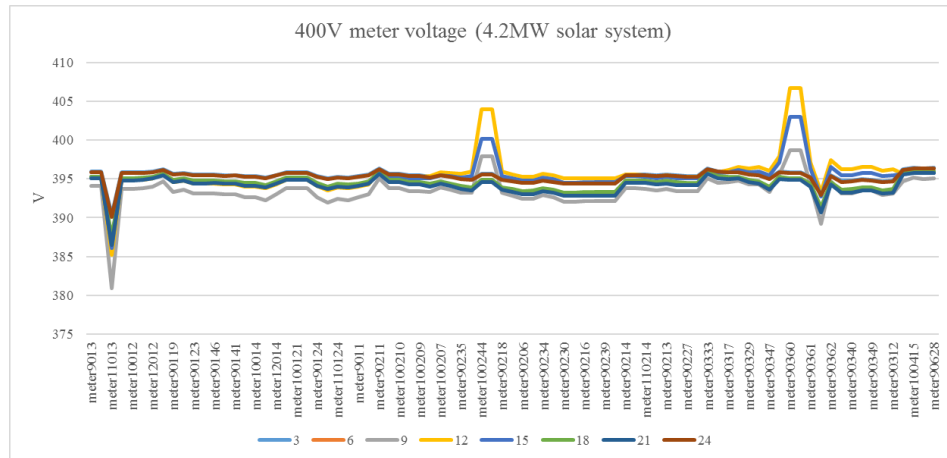


Fig. 5.32 400V voltage profiles on different meters-with solar PV installation

5.6 Summary

The analysis clearly shows the correlation between the load demand, CHP power output, solar PV generation and electricity purchase profiles. The correlations can be summarized into:

- i) the gap between the CHP power generation and the load demand is associated with weather tightly as its operation is the thermal-lead algorithm; in winter, the gap is smaller, and the gap is much greater in summer;
- ii) the solar power generation profiles are highly correlated to the electrical power import from the grid; in the rich radiation days, more electrical power is purchased at the moment, in line with solar PV generation. The quantified correlation analysis results are shown in Table 5-2. Therefore, the data correlation analysis convinces that the solar integration has potential reduce the power import to reduce the University electricity bill and cut the University carbon footprint.

The installation capacity and economic analysis are then performed. The study showed that the current campus rooftop areas can accommodate 4.2 MW solar PV panel installation with the potential of capacity increase when more new buildings are commissioned in use. The payback years for 4.2 MW to 20 MW range of rooftop solar system investment is then analysed based on the current market condition and values and the results indicate that the payback time is between 14 to 24 years depending on the solar energy price and installation cost.

Further investigations are made into the installation of larger utility scale ground solar PV systems. Different appropriate sizes of solar units are chosen for comparison. The installation cost for utility solar PV is relatively small compared to rooftop solar system, so the large solar plant should be considered if the installation space is available. The payback year can be reduced by 5 years compared with the rooftop installation.

In the case that the surplus energy of solar system is produced and fed to the grid for free, the energy storage system may be an option. The payback years are studied and compared, which shows that the payback years of hybrid system is much longer than the solar PV installation alone without batteries.

From the study case, the 11.2 MW pure solar installation capacity is recommended in terms of cost and benefit. With the evolution of the campus and energy usage variations, the optimal installation capacity can be changed.

After the solar PV power generation integration, the decrease of transmission power on the feeder and support of solar output reactive power makes load node voltage along the feeder will be raised. This voltage and power loss are studied and analysed. The results are presented in Section 5.5, which can provide the supporting information in planning and design.

In general, the effect on the distribution system as a result of solar PV integration is positive. The proposed capacity of solar system improves the voltage stability and reduces the total power losses on the campus power distribution system. The power losses reduce by 10 % with the introduction of 4.2 MW solar system and reduce by 24 % with the installation of 11.2 MW solar system. The location of solar system will highly affect the curve of branch voltage.

Chapter 6

Study on Local Energy System with a P2P Trading Mechanism

6.1 Introduction

As described early, the power system has seen more and more distributed or local generation connected at the distribution level. Management and operation such as blended central and local generation power systems lead to the changes in electricity market and the supply chain. Consumers are becoming prosumers as they produce electrical energy and also consume electrical energy at the local level. This will reduce the dependence on the main grid and can optimize their energy usage at the local level which may lead to cost reduction. With this change, one new element appears in electricity market – prosumers. This pushes electricity market reform and new mechanisms and electricity trading methods are under exploration.

In the traditional electricity trading model, if the producers of electricity are producing excess electricity, they often sell the electricity directly to the power company. However, the problem is that power companies often buy electricity at low prices and then sell them to users at high prices, which creates inequality in energy transactions. The sell price includes transmission fee, distribution fee, operators' revenues, purchase price and power losses fees so it is high than purchase fee. In recent years, Peer-to-Peer (P2P) electricity trading business model that emerged as a platform-based scheme aiming to encourage the integration of distributed power sources is proposed. With P2P electricity trading, prosumers can share the benefits with the communities that they belong to, further encouraging the consumption and deployment of distributed power sources. Furthermore, P2P electricity trade has the potential to reduce the cost and reliance on the main grid.

In this chapter, an introduction of hierarchical P2P structure that is commonly used for the large-scale and complex LES is provided. Then, a P2P electricity trading mechanism with hierarchical P2P architecture is proposed with the aim to enhance revenue of prosumers by applying a game theory in pricing competition. In order to balance the pricing between customers and suppliers, the asymptotic Shapley value which is well-known solution and general method for ensuring an equitable division [187] is treated as the core of the coalitional game. This trading mechanism is to motivate prosumers to actively take part in the proposed architecture of trading. Finally, a few cases studies are used to verify the proposed electricity trading mechanism.

6.2 Hierarchical P2P Architecture

P2P networks can be classified as structured and unstructured P2P networks. Hierarchical P2P systems utilize more than one level hierarchy to distribute the overlay nodes, multiple options can be taken by each level, either structured or unstructured. The hierarchical P2P [188] can be classified into three categories: unstructured, structured and hybrid, as shown in Fig.6.1.

Unstructured hierarchical P2P systems utilize unstructured topology at each layer. Structured hierarchical P2P systems utilize only structured topology at each layer. Hybrid hierarchical P2P systems combine unstructured and structured overlay topology in its hierarchy. In our case, hybrid hierarchical P2P systems utilize structured overlay topology at its upper level while utilizing unstructured overlay topology at its lower level.

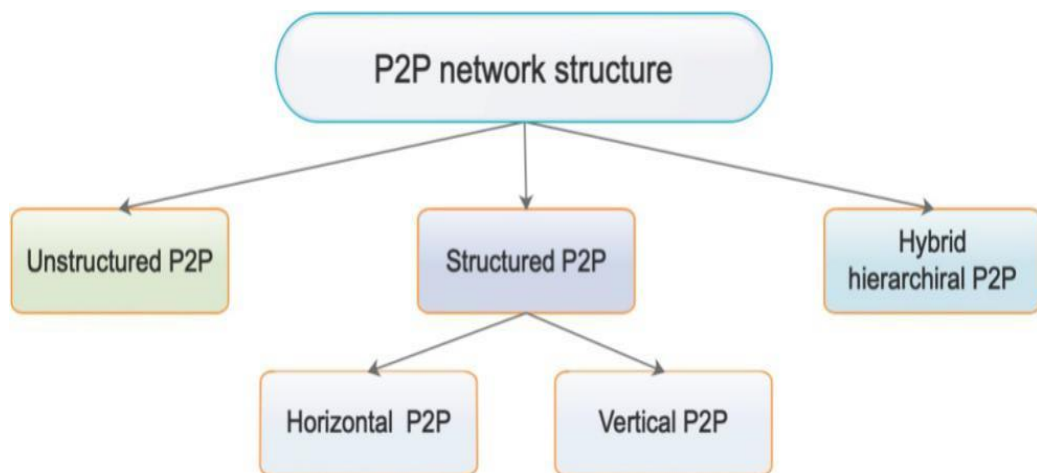


Fig. 6.1 Architecture of hierarchical P2P

6.2.1 Unstructured Hierarchical P2P Architecture

An unstructured P2P network is formed when the overlay links were established arbitrarily. It means peers establish connections randomly with each other instead of restricted by any fixed restrictions. In an unstructured P2P network with various peers inside, if a peer wants to find another peer in this P2P network, the query must be flooded through the network in order to find peers who have the information of desired peer. Prosumer's communication regarding energy demand, availability, distance, price and tariff take place in a P2P fashion[189]. One of the advantages of

this unstructured model is the results of good performance and reduction of latency since the prosumers communicate with each other directly. However, there is no guarantee that flooding will find a peer that carried the desired information since there is no correlation between a peer and the its carried information. Moreover, flooding may also cause network congestion. Most of the popular P2P networks, such as Gia [191]and Gnutella[190] , are unstructured. They are decentralized and unstructured. The aggregate system capacity for Gia is three to five orders of magnitude better than that of Gnutella.

Gnutella v0.6 [190] employs a two-layer hierarchy, as shown in Fig.6.2. Peers are categorized into leaf and ultrapeer. A leaf peer only maintains connection with its own ultrapeer, while an ultrapeer maintains connections to its own leaf peers, as well as to the other ultrapeers from the overlay, and acts as proxy for its connected leaf peers. In the procedure of resource lookup, leaf peers are only responsible for initiating lookup requests and receiving correlated lookup response. At the ultrapeer layer, the flooding-based mechanism is utilized to forward the lookup request.

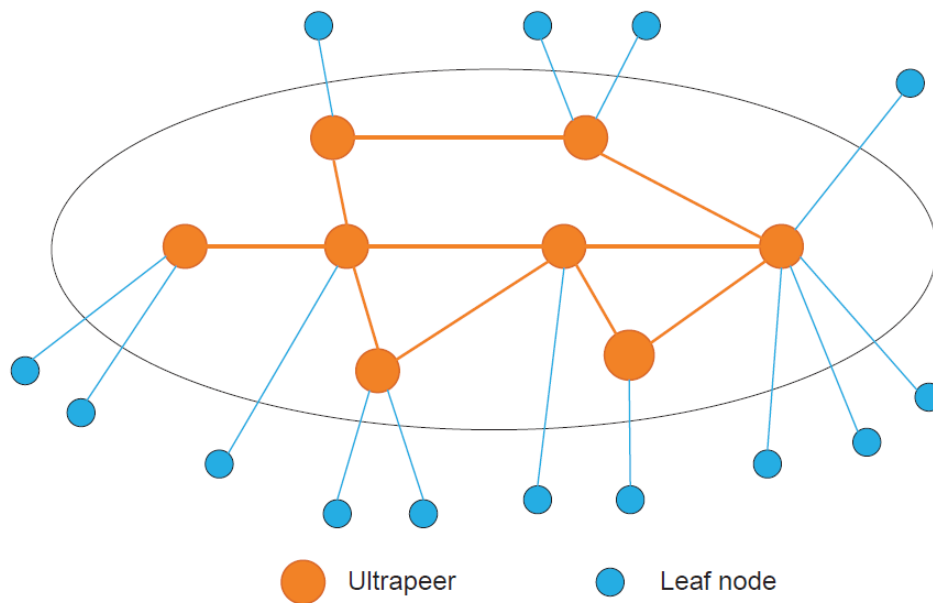


Fig. 6.2 Architectire of Gnutella v0.6

6.2.2 Structured Hierarchical P2P Architecture

The structured P2P network organizes peers into a specific structure by using a technique[192]. Under such a structure, whenever a peer wishes to search for some data, it can determine the peer who is responsible for the data and then directs the search towards the responsible peers. Due to the use of Distributed Hash Table (DHT), structured networks have efficient message routing, but suffer from high maintenance overhead.

A framework for the vertical hierarchical P2P [193] is shown in Fig.6.3. Peers are clustered into different groups and the messages are routed to the destination cluster using inter-cluster overlay, and then routed into designation peer through intra-cluster overlay. There is at least one super (powerful) peer which is selected in terms of reliability, computing ability and connectivity. The normal peer chooses to join one cluster based on the proximity.

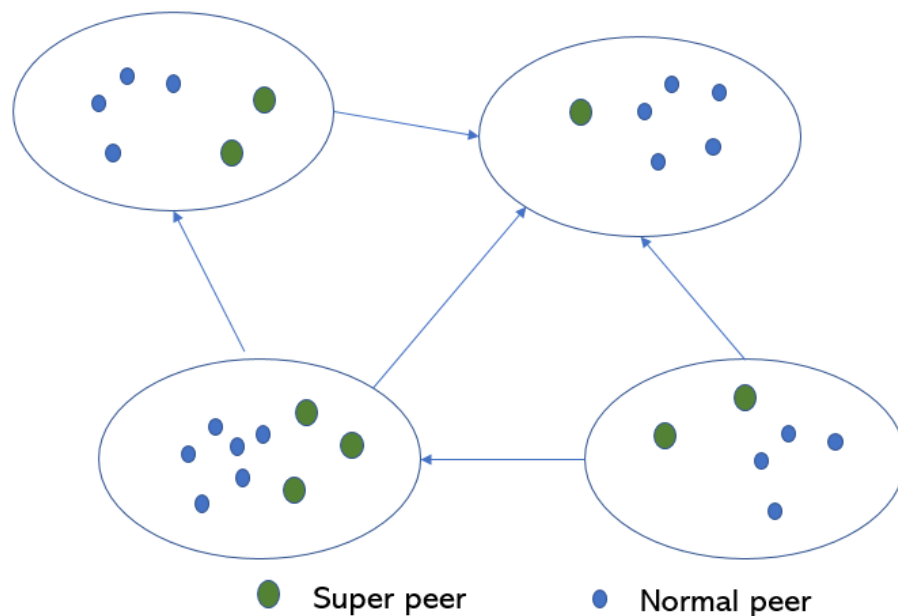


Fig. 6.3 Architecture of vertical hierarchical P2P

A framework for the horizontal hierarchical P2P[194] is shown in Fig.6.4. A cluster of host computers participate in an overlay as a single peer. The query is routed from cluster to cluster as a flat DHT algorithm does until it gets to the destination cluster. In the intra-cluster, the multicast service mechanism which transmits the data from one single source to multiple destinations is used to reach the destination peer

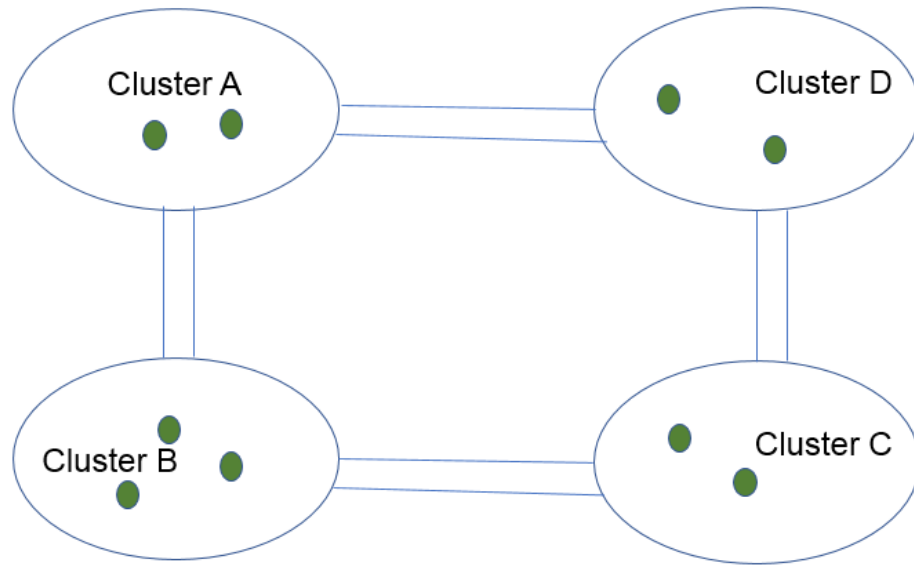


Fig. 6.4 Architecture of horizontal hierarchical P2P

6.2.3 Hybrid Hierarchical P2P Architecture

Hybrid hierarchical P2P system combines unstructured and structured overlay topologies in their hierarchies in order to utilise the benefits from both ends farthest. A hybrid P2P system is proposed to make use of the advantages of both structured and unstructured P2P networks[195]. One of the hybrid infrastructures is combining flooding technique and DHT structured search technique. It shows that Gnutella is effective for locating highly replicated items. As shown in Fig.6.5, the root layer consists of clusters which are constructed using local network and each cluster contains a dedicated gateway peer. All the gateway peer consists of gateway layer. Furthermore, additional random connections are achieved by utilising a random walk algorithm.

In this part, a hierarchical P2P structure that integrates the scalability of structured overlay network with the connection flexibility of unstructured overlay networks is proposed. A core structured network is used in gateway layer, which forms the backbone of the hybrid system, while MG layer is an unstructured P2P network. The MG layer consists of many MG peers and a gateway peer (A0, B0, and C0). Each gateway peer is identified by a Gateway ID (GID), which is the gateway's ID in the core network, and a MG Peer ID (MGPID), which is the peer's ID in the MG.

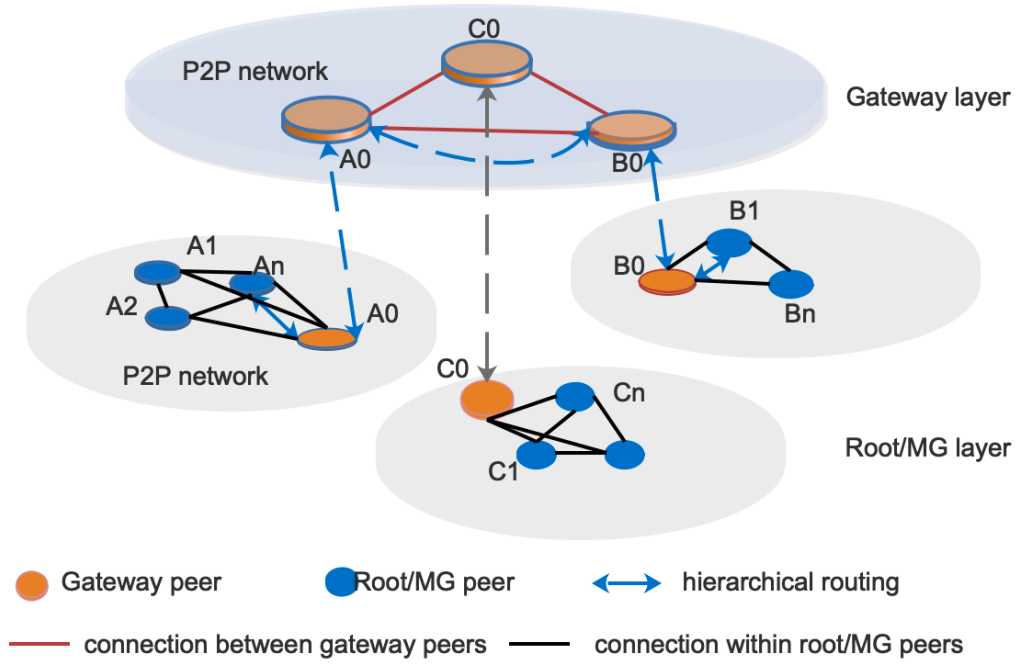


Fig. 6.5 Architecture of hybrid hierarchical P2P

6.3 P2P Electricity Trading Mechanism

Electricity trading approaches are becoming increasingly important in the development of the energy sharing in LES due to the need to meet energy demand considering the intermittent supply of LES. Human factors need to be taken into considerations such as rationality, motivation, and environmental friendliness in decision makings. game theory-based approach is proposed since it provides an analytical and conceptual framework with a set of mathematical tools to analyse optimization problems with several objective function[196]. Game theory is a mathematical and signal processing method [197] that analyses strategies in competitive circumstances where a choice made by one prosumer depends on the actions of others. Fig.6.6 shows the game theory approach and some optimization solution techniques. There are two basic types of games in game theory: non-cooperative game and cooperative game.

A non-cooperative game is a game where decisions made by prosumers did not rely on nor interfered by the coordination and communication occurred between prosumers, however, it does not mean that prosumers did not coordinate or communicate at all. The Nash equilibrium is the most popular solution concept of the non-cooperative game $\{(S_i)_{i \in N}, (f_i)_{i \in N}, N\}$. S_i is set of player i 's strategies,

$i = 1, 2, 3 \dots N$, f_i is player i 's payoff as a function of the strategies. The Nash equilibrium is a vector of actions x^* , such that $f_i(x^*) \geq f_i(x_i, x_{-i}^*)$, $\forall i \in N$, where $x_i = (x_1, \dots, x_N)$. When the inequality above holds strictly (with $>$ instead of \geq) for all prosumers and all feasible alternative strategies, then the equilibrium is classified as a strict Nash equilibrium. Otherwise there is exact equality between x_i^* for some of the players the equilibrium is classified as a weak Nash equilibrium. In addition, it is key to select an efficient and desirable Nash equilibrium from multiple Nash equilibrium as the solution.

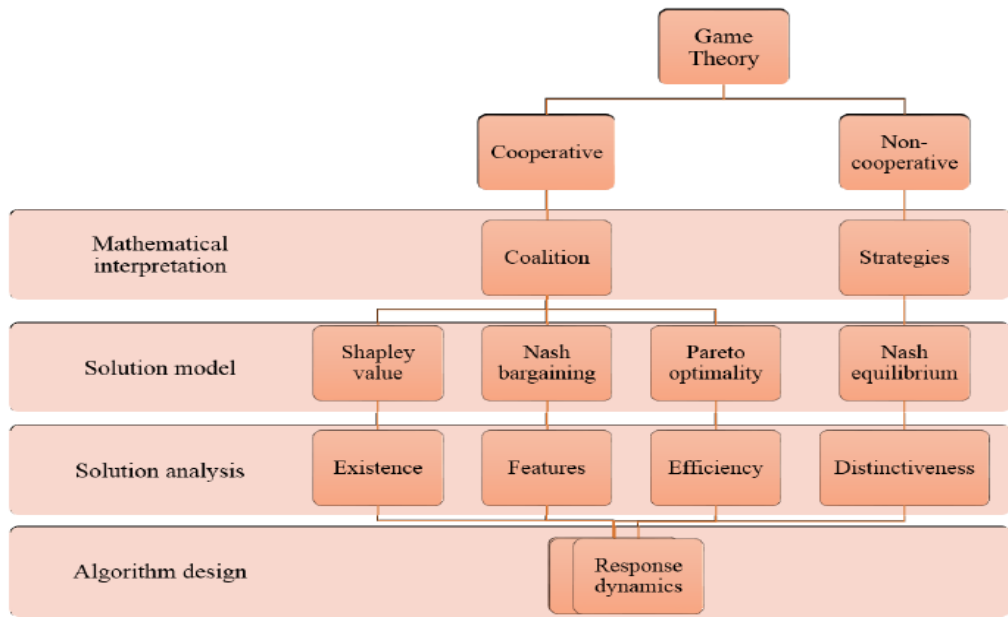


Fig. 6.6 Game theory approaches and optimisation solutions

In a cooperative game, players with similar objective functions can communicate amongst themselves to form a coalition. The benefit of such cooperation is shared among themselves. Cooperative game is typically described by a characteristic function v . It focuses on the prediction of coalitions formed, joint actions taken by the group and the resulted collective payoffs. The approach of characteristic function is considered more general and robust in comparison to the non-cooperative model. Given a coalition of prosumers $S \in \{1, \dots, N\}$, $v(S)$ is the sum of payoffs. Under circumstances of fierce competition, the Shapley value had been often used by the cooperative game theory as a predictive concept.

It is shown that with the cooperation among LES and ESS owners, the problem of intermittent supply can be alleviated [199]. This will further reduce the need for large energy storage systems and provide cost savings for the prosumers participating in the cooperation. In that case, many researchers use the cooperation theory to solve the electricity trading problem.

6.4 Two-layer P2P Trading Architecture in Local Energy System

The trading system supported and investigated by this chapter is depicted in Fig.6.7. This system consists m numbers of connected Micro-Grids (MGs), named as N_i , where i ranged from 1 to n . The MGs are integrated energy systems consisting LES and multiple electrical loads. The loads can be divided into uncontrollable and controllable loads within clearly defined electrical boundaries. The P2P network is used for the communication of trading data and controlling data. The system aims to benefit all participants in MG where they would be able to purchase or sell electricity freely, as well as participating the electricity trading activities in gateway layer. The EMS of the MG is to collect the potential trading contract, as well as managing the MG system and verifying the contract. The contracts will be released once it is found valid by the EMS. Surplus or deficit energy supplied in comparison to actual demand will then be calculated by the EMS and continue its outstanding electricity trading in the gateway layer.

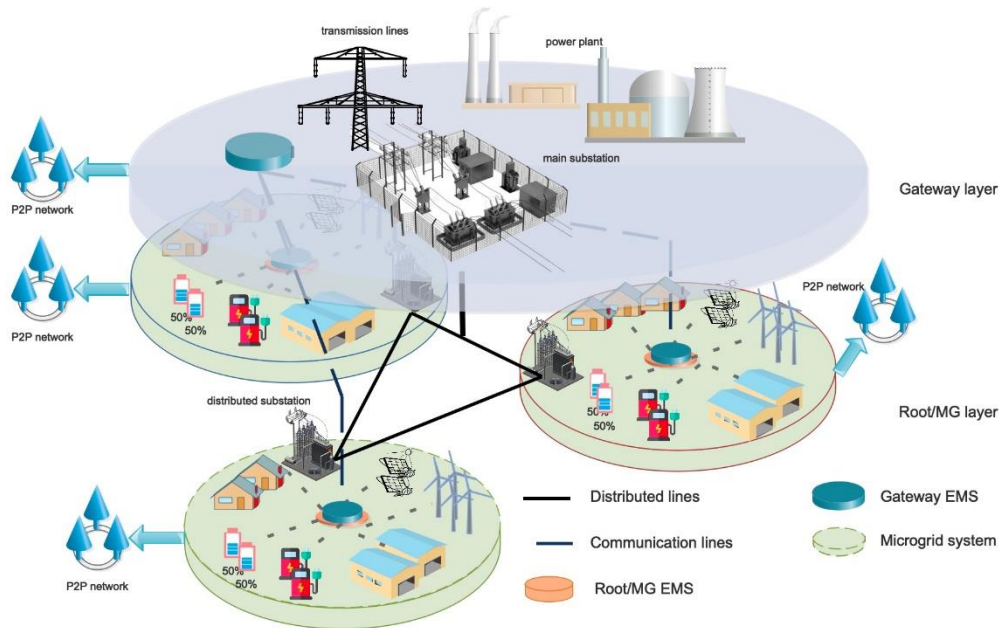


Fig.6.7 Two-layer P2P trading system

To simplify the complexity of an electricity trading system, only Real-Time Market (RTM) is considered in this chapter. The MG peers shall submit potential electricity capacity before the timing of $t+1$ (t is the continuous time in a half hour). The predictive algorithm by using ARIMA prediction model) is used to predict the energy demanded and generated for the period from time t to time $t+1$. For example, we normally use ARIMA [198] model to predict the potential capacity of solar generation by using the historical generation data and weather data. Each peer can submit a pair (s, p) , where s is the energy units and p are the price margin (the minimum price the peer is willing to get or the maximum price that peer is willing to pay). In this case, this approach is beneficial for both sellers and buyers since they enhance the flexibility of electricity trading.

Each buyer or seller of MG can be regarded as a local peer, the gateway peer is one of local peers, but it has the capacity to take high computing tasks. In contrast, other local peers have the limited capacity and cannot take complex tasks. After the completion of electricity trading in MG, the total capacity of electricity demand or supply will be calculated by its gateway peer. The gateway peer will then take part in gateway-layer P2P trading with its calculated surplus or deficit energy demand. The gateway peer will submit the number of trading units according to the number of peers rather than the minimum bidding unit in the purpose of increasing efficiency. The hierarchical routing between two MGs is shown in Fig.6.5. Peer An seeks deals with other peers in other MGs since it does not deal with any peers in the MG where it belongs. On An's behalf, gateway peer A0 participates into the P2P trading in gateway-layer and reach a deal with B0 who is acting on B1's behalf. All contract information will be recorded in gateway peer due to its strong computing and storing capabilities. In the circumstances of unbalancing supply and demand of electricity, the surplus or deficit has to be compensated by taking part in the RTM. Generally, the trading process can be divided to three-stage steps which should be cleared before the RTM is cleared. A diagram of three-stage steps is shown in Fig.6.8.

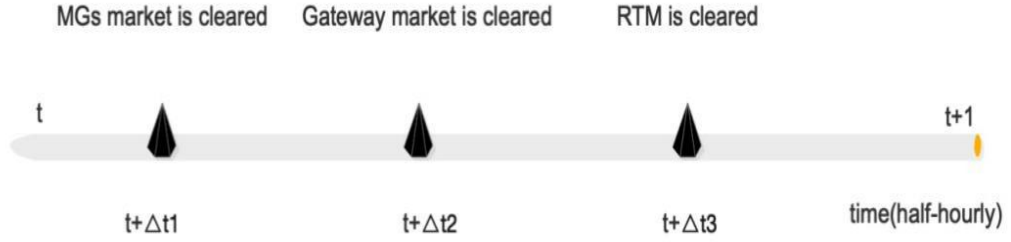


Fig. 6.8 Diagram of three-stage steps

The cooperative game proposed in this chapter as it increases overall revenue of all prosumers in comparison to the competitive approach. we define N as the set of prosumers and $R(\cdot)$ is the monetary profit of two-layer LES (shown as Fig.6.7). Let $\dot{N}_{ils} \subset N_s$ and $\dot{N}_{ilb} \subset N_b$ be arbitrary subsets of sellers and buyers of MG i , respectively; N_b, N_s are the set of sellers and sellers. let $\dot{N}_{igws} \subset \dot{N}_{ils}$ and $\dot{N}_{igwb} \subset \dot{N}_{ilb}$ ($\dot{N}_{igws} \cap \dot{N}_{igwb} = 0$) be the unscheduled arbitrary subsets of sellers and buyers of i gateway peer layer, respectively. P_{bDAM} is the purchase price from grid in Day Ahead Market (DAM) and P_{sDAM} is the selling price to grid in DAM. S_j and B_k are the amount of electricity supplied/demanded. Therefore, $V(\dot{N})$ can be expressed as

$$\begin{aligned}
 V(\dot{N}) &= V\left(\sum_{i=2}^n \dot{N}_{igws} \cup \sum_{i=2}^n \dot{N}_{igwb}\right) \\
 &= \sum_{i=2}^n (P_{sDAM} [\sum_{j \in \dot{N}_{gws}} S_j - \sum_{k \in \dot{N}_{gwb}} B_k]^+) \\
 &\quad - \sum_{i=2}^n (P_{bDAM} [\sum_{k \in \dot{N}_{gwb}} B_k - P_{iss} \sum_{j \in \dot{N}_{gws}} S_j]^+)
 \end{aligned} \tag{6.1}$$

All prosumers shall be considered while allocating revenue through calculation from the Shapley value (Eq.6.1) in the proposed system. Shapley value is a means to capture the average marginal contribution of a player. Obviously, the way to do it would be to consider all possible coalitions of N players. Therefore, the computational complexity will be considered rather significant. The Asymptotic Shapley value is proposed in [200] to reduce the computational complexity. It had been advised that the use of Asymptotic Shapley value is considered justify in cases that the number of prosumers is large [200].

We assume that a prosumer i in local P2P network j who want to trade an amount of φ during the period of t . φ can be either negative or positive, corresponding to seller and buyer. Let random variable S_j and B_j be the amount of electricity supplied/demanded during the period t for network j . The means of S_j and B_j are denoted by μ_{jS} and μ_{jB} respectively. Their variances are denoted by σ_{jS}^2 and σ_{jB}^2 respectively. Finally, the Shapley value can be calculated as

$$\Phi_{\varphi}(j) = \begin{cases} P_{jlp} \varphi & \kappa < 1 \\ P_{jup} \varphi & \kappa > 1 \\ \left(\frac{P_{jup} + P_{jlp}}{2} + \frac{P_{jlp} - P_{jup}}{2} \bullet \frac{1}{\sqrt{\pi}} \int_0^1 \int_{\frac{-\sqrt{\ell}\tau}{\sqrt{2}\eta}}^{\frac{\sqrt{\ell}\tau}{\sqrt{2}\eta}} e^{-\ell^2} d_{\ell} \right) \varphi & \kappa = 1 \end{cases} \quad (6.2)$$

where P_{jup} and P_{jlp} are maximum and minimum price limit of MG j , respectively.

Let $(\mu_{jS}N_{jS} - \mu_{jB}N_{jB})/\sqrt{N_j} \rightarrow \tau$ as $N_{jS}, N_{jB}, N_j \rightarrow \infty$, $\mu_{jS}N_{jS}/\mu_{jB}N_{jB} \rightarrow \kappa$ and

$$\eta = \sqrt{(\mu_{jB}\sigma_{jS}^2 + \mu_{jS}\sigma_{jB}^2)/(\mu_{jB} + \mu_{jS})}$$

The stability of the asymptotic Shapley value had been discussed in [201]. The price of electricity, P_{p2p} , could be used to allocate the revenue for each prosumer. To make the two-layer P2P network more stable, the total revenue should be fairly allocated to the prosumers by adjusting the P_{p2p} . Otherwise the prosumer's revenue from P2P network may be less than the revenue generated from DAM. As a result, these prosumers will not take part in the P2P network. We use the core concept to allocate the revenue among prosumers fairly, which cannot be further improved by dividing the grand coalition into subsets. Prosumers can share the revenue by adjusting the price of electricity in local P2P network j , shown as

$$P_{P2P}(j) = \begin{cases} P_{jlp} & \kappa < 1 \\ P_{jup} & \kappa > 1 \\ \left(\frac{P_{jup} + P_{jlp}}{2} + \frac{P_{jlp} - P_{jup}}{2} \bullet \frac{1}{\sqrt{\pi}} \int_0^1 \int_{\frac{-\sqrt{\ell}\tau}{\sqrt{2}\eta}}^{\frac{\sqrt{\ell}\tau}{\sqrt{2}\eta}} e^{-\ell^2} d_{\ell} \right) & \kappa = 1 \end{cases} \quad (6.3)$$

The number of prosumers, i.e., N_{jB} and N_{jS} , is finite and the κ is not known in asymptotic regime. In this case, we use the boundary of $P_{P2P}(j)$ to calculate $P_{P2P}(j)$ when $\kappa \neq 1$. For example, when $\kappa > 1$, $(\mu_{jS}N_{jS} - \mu_{jB}N_{jB})/\sqrt{N_j} \rightarrow \infty$ and $P_{P2P}(j)$ is close to P_{jlp} .

The core mentioned above is based on open market, which means that the government will not provide any subsidies with purposes to promote any specific kind of energy generation, such as renewable energy [202]. In such case, $P_{sDAM} < P_{bDAM}$ may allow the core to divide revenue in a feasible way.

After MG market is cleared, the gateway peer starts the bidding in gateway layer. Let random variable S and B be the total amount of unbalanced electricity supply/demand of distribution network j during the period t . Moreover, the means of S and B are denoted by μ_S and μ_B respectively. Their variances are denoted by σ_S^2 and σ_B^2 respectively. So, $\tau = (\mu_S N_S - \mu_B N_B)/\sqrt{N}$ and $\eta = \sqrt{(\mu_B \sigma_S^2 + \mu_S \sigma_B^2)/(\mu_B + \mu_S)}$. The trading price in gateway-layer network can be calculated as

$$P_{P2P} = \left(\frac{P_{sDAM} + P_{bDAM}}{2} + \frac{P_{sDAM} - P_{bDAM}}{2} \cdot \frac{1}{\sqrt{\pi}} \int_0^1 \int_{\frac{\sqrt{\ell}\tau}{\sqrt{2}\eta}}^{\frac{\sqrt{\ell}\tau}{\sqrt{2}\eta}} e^{-\ell^2} d_\ell \right) \quad (6.4)$$

6.5 Case study

In this section, the convergence of the revenue equations and the trading results of proposed distributed network are investigated. Firstly, we will verify the convergence of Eq.6.3 by adjusting the ratio of the total amount of electricity supplied by the seller to the total amount of electricity consumed by the buyer. Then, we investigated the trading procedures in the proposed two-layer P2P (as shown in Fig.6.7) power network structure and the difference of pricing scenario in various MGs. At the end, we will look at the changes of overall revenue between every single peer whose trade remained outstanding in MG to trade in gateway layer by themselves and packing them as a single peer to process the trade in the gateway layer

6.5.1 Convergence Verification

In practice, the ratio of the average amount of electricity supplied by the seller to the average amount of electricity consumed by the buyer is not equal in most of the times. Therefore, this section will verify the convergence of P_{P2P} . Let $\mu_s = 3.3, \sigma_s^2 = 12$, $\mu_B = 2.7, \sigma_B^2 = 10$. The cost of demand and price of production in West Midlands of UK [203] were adopted in our assumption: $P_{jlp} = 4.5p / kWh$, $P_{jup} = 14.2p / kWh$. As shown in Fig.6.9, the P_{P2P} converges to its asymptotic value. When the average electricity supply is smaller than electricity demand: $\tau < 0$, the revenue bias towards the sellers and it converges to P_{jup} as τ decrease. When $\tau < 0$, the revenue $P_{P2P} = 9.35p / kWh$. Then, we keep $\mu_s = \mu_B = 3$ and change the variances from 12 to 36. From Fig.6.10, we observed that the speed of convergence decreased with the increase of σ_s^2 and σ_B^2 . In other words, the variation of τ will decrease when the variances of electricity supply and demand increase.

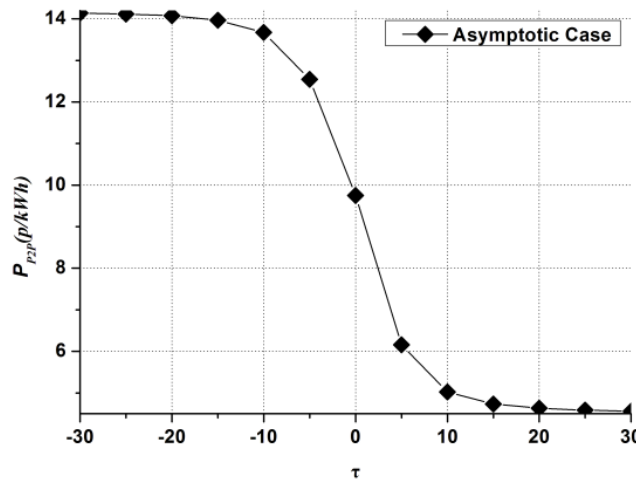


Fig. 6.9 PDT vs. τ for fixed assumption

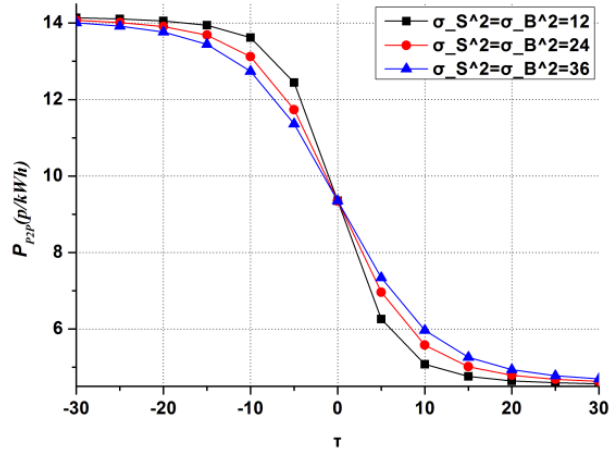


Fig. 6.10 PDT vs. τ for different variances

6.5.2 Study of Trading Mechanism in Local Energy System

6.5.2.1 Data inputs

In this section, a two-layer P2P trading network is simulated: the gateway layer and local layer. The gateway layer is physically connected with three MGs: A, B, and C, as shown in Fig.6.7. There are 54 consumers in each MG used in each MG. The load curves of 54 consumers are shown in Fig.6.11. Some consumers' load demand shows a relatively flat pattern while others fluctuate significantly. The variance, $\sigma_b^2(t)$, of the load curves is depicted in Fig.6.12. It was observed from the mean value of load profiles that the peak load happened during the period from 8am to 11pm. and 18 pm to 22pm. The difference of variances became obvious due to the significant peak value of some loads.

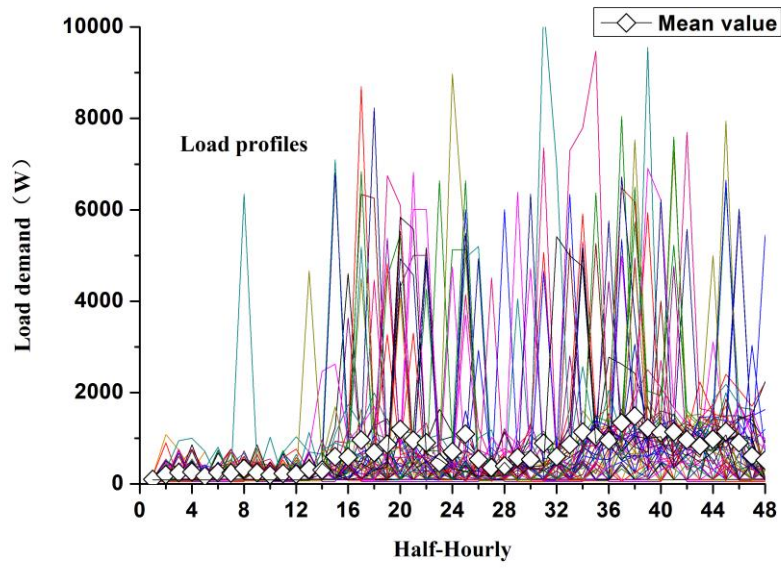


Fig. 6.11 Load curves of consumers

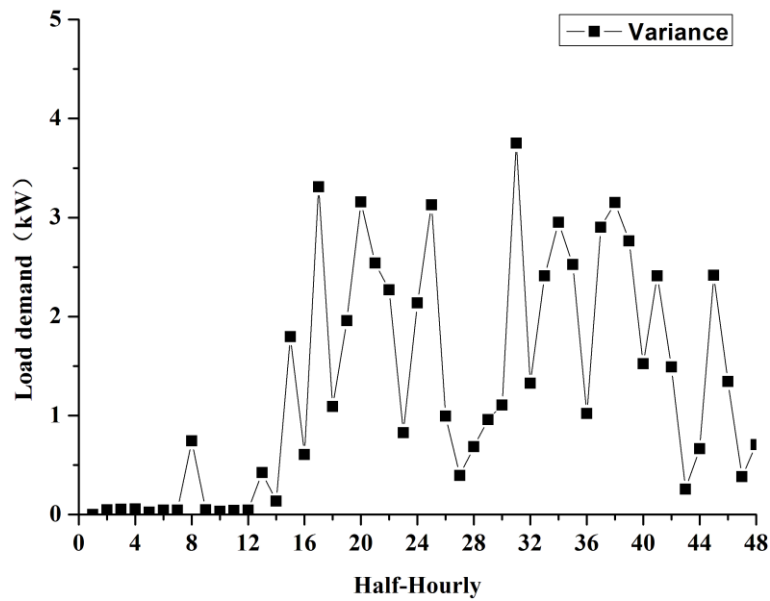


Fig. 6.12 Variance for load curves

Then, different types and number of distributed power sources are considered in different MGs to evaluate the variation of overall revenues. In MG A, the distributed solar systems, as the only energy resource, are installed. The data curves were derived from historical data of solar generation acquired from co-simulation system developed in chapter3. The half-hourly generation curves of 13 solar systems were

shown in Fig.6.13. The mean, μ_{AS} , and the variance, σ_{AS}^2 , were also shown in this figure. In MG B, two wind systems are assumed to be additionally installed with the same solar systems in MG A. The wind data curves are derived from [204] and we scale the generation curves of wind turbine by assuming the rated capacity of wind turbines is 20kW. Fig.6.14 shows that compared with photovoltaic power generation, the wind power generation is more stable and time domain is not obvious. MG C contains scheduled load and generation such as the AC vehicle charger ($5 \times 7\text{kW}$) and battery storage system ($4 \times 5\text{kW}$). The working schedules for charger and battery which based on statistical data of daily EV/PHEV arrival/departure probabilities [205] are shown in Fig.6.15. Due to the bidirectional nature of the battery, the battery systems were treated as prosumers who either supply or consume energy depend on the controlling strategy.

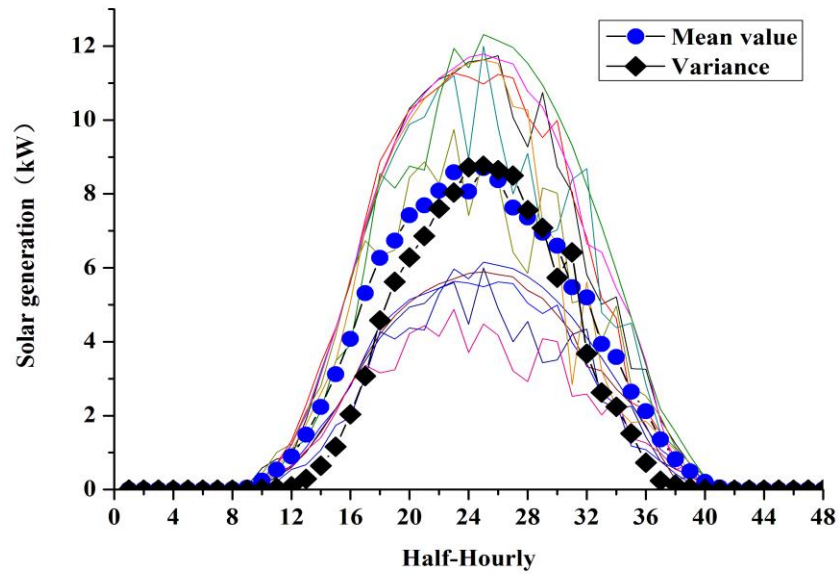


Fig. 6.13 Curves of solar generation

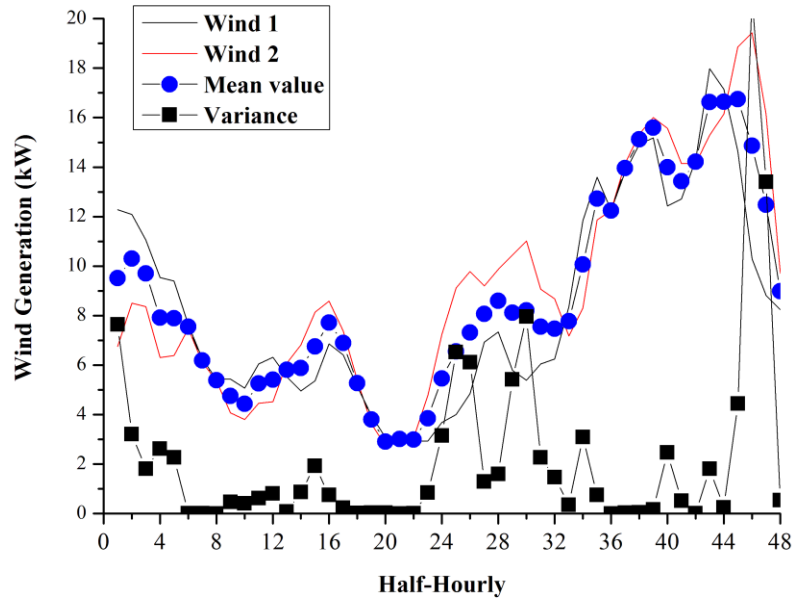


Fig. 6.14 Curves of wind generation

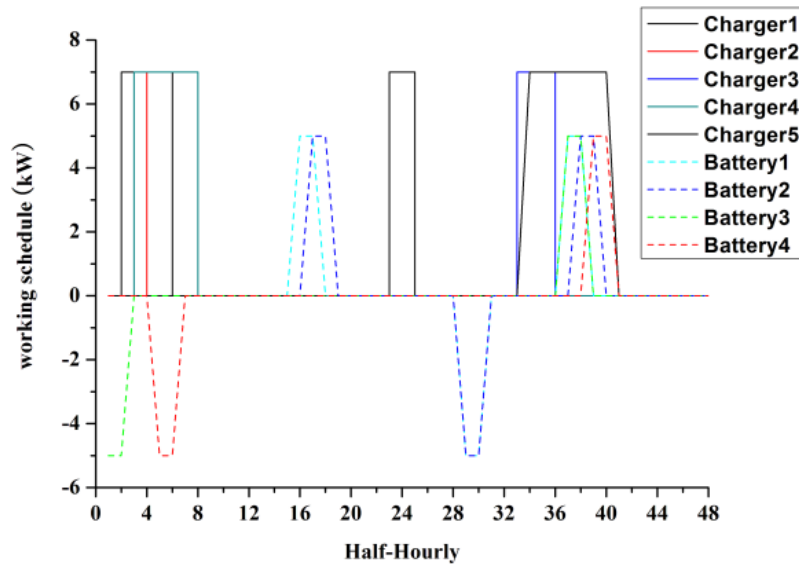
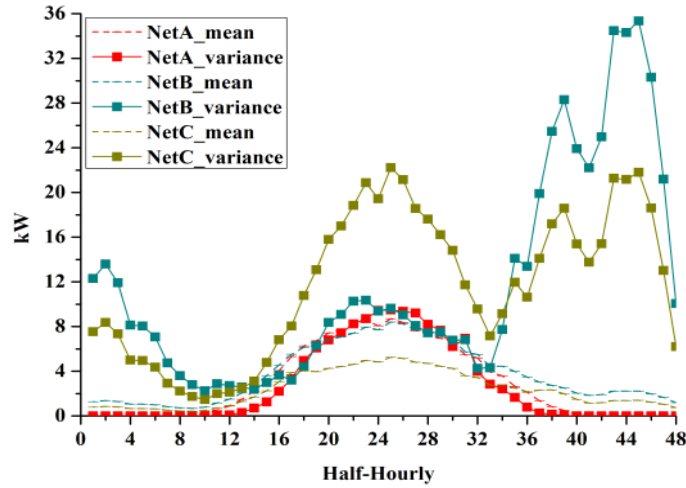


Fig. 6.15 Working schedule of EV chargers and Battery systems

In Fig.6.16, the mean value and variance of distributed power sources of each MG is listed. The mean value of MG C is much lower than the mean value of MG A and MG B since the battery systems do not work in most of time during the day. Apart from the peers of three MGs, there are two 100kW wind systems and three

commercial buildings existed in the gateway layer. The curves of wind generation are from the historical data in 2018 [203] and the curves of commercial buildings were acquired from local meter in Eston market of UK in 2018[203].



a

Fig. 6.16 Mean and variance in different networks

6.5.2.2 Results

As shown in Fig.6.17, it is observed that the trading price of each MG changed every half hour since the supply and demand changed every half hour. The price of MG A is close to upper limit when the time period is 0am-6am and 9pm-12pm due to the reasons that there were almost no solar generation during these periods and the customers need to consume electricity at the price of 14.2p/kwh which is the purchase price in DAM. In contrast, the price in all MGs is close to 4.7 p/kWh which is the selling price in DAM from 9am to 15pm, which was because power generated by solar or wind far exceeds the demand of demand raised from customers ($|\tau| > 100$), which further verified the results in Fig.6.10.

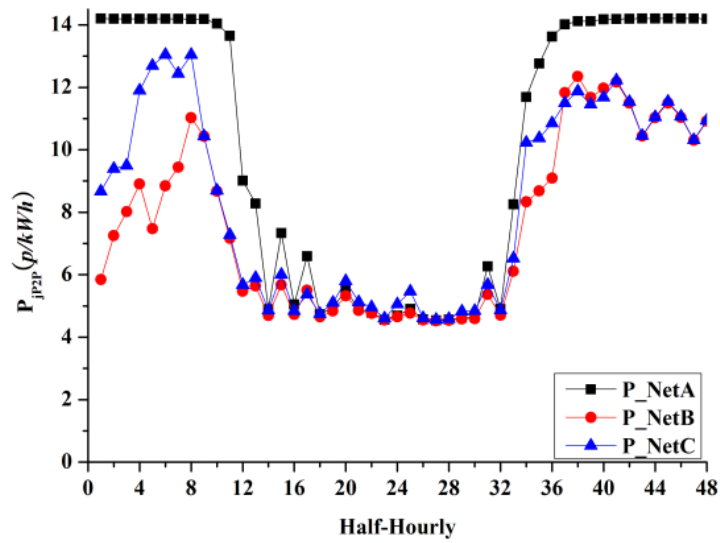


Fig. 6.17 P_{p2p} in different MG markets

After MG market is cleared, the gateway peers of each MG whose needs of trading remain outstanding will be packed and delivered to the gateway layer and continue its trading with other peers. As shown in Fig.6.18, the bidding price of gateway network fluctuates with τ and η . The variation of τ and η are determined by numbers of participants and the ratio of the total amount of electricity supplied by the sellers to the total amount of electricity consumed by the buyers. It is assumed that the participants will try to bid in gateway layer if the trading price is lower than 110 % of the selling price (4.5p/kwh) in DAM or the trading price is higher than 90 % of the purchase price (14.2p/kwh) in DAM. Table 6-1 shows the number of participants in different time period. In Eq.6.4, we could see the transition of P_{p2p} between P_{sDAM} and P_{bDAM} by varying τ is rapid when η is small. In practice, the P_{p2p} is expected to be stable even τ changes since η is likely to be large. From Fig.6.18, we observed that the prices fluctuated between 5p/kWh to 13p/kWh. Therefore, prosumers that did not make deal in MG are still able to get the chance to bid in gateway layer

Table 6-1 Number of participants from each MG in gateway layer

Time (half-hourly)	number of Sellers			Number of Buyers		
	MG_A	MG_B	MG_C	MG_A	MG_B	MG_C
1	54	0	0	0	2	2

2	54	0	0	0	1	2
3	54	0	1	0	1	0
4	54	0	19	0	1	0
5	54	0	11	0	1	0
6	54	0	16	0	1	0
7	54	0	21	0	1	0
8	54	34	28	0	0	0
9	54	23	4	0	0	0
10	54	0	0	0	1	1
11	38	0	0	4	5	5
12	24	0	0	4	5	6
13	0	0	0	4	5	6
14	0	0	0	8	10	10
15	0	0	0	8	10	10
16	0	0	0	8	10	10
17	0	0	0	8	10	10
18	0	0	0	8	10	11
19	0	0	0	8	10	11
20	0	0	0	8	10	10
21	0	0	0	8	10	12
22	0	0	0	8	10	12
23	0	0	0	8	10	13
24	0	0	0	8	10	12
25	0	0	0	8	10	12
26	0	0	0	8	10	12
27	0	0	0	8	10	13
28	0	0	0	8	10	13
29	0	0	0	8	10	13
30	0	0	0	8	10	14
31	0	0	0	5	7	11
32	0	0	0	9	11	12
33	0	0	0	9	11	11
34	9	0	4	0	3	0
35	20	0	10	0	1	0
36	24	0	12	0	1	0
37	40	19	42	0	0	0
38	46	25	55	0	0	0
39	48	22	43	0	0	0
40	54	25	40	0	0	0
41	54	29	33	0	0	0
42	54	23	22	0	0	0
43	54	13	11	0	0	0
44	54	18	18	0	0	0
45	54	23	26	0	0	0
46	54	20	18	0	0	0
47	54	12	7	0	0	0
48	54	19	10	0	0	0

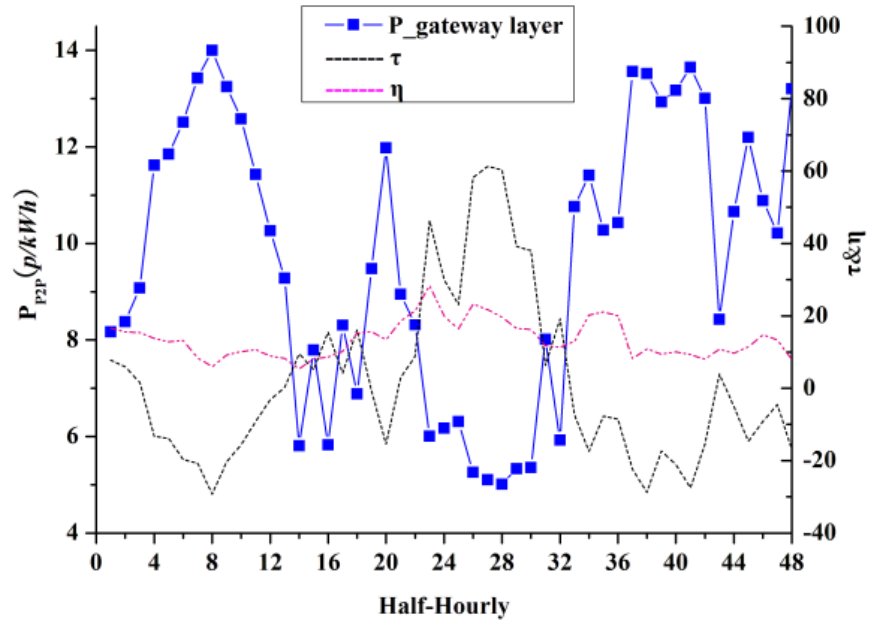
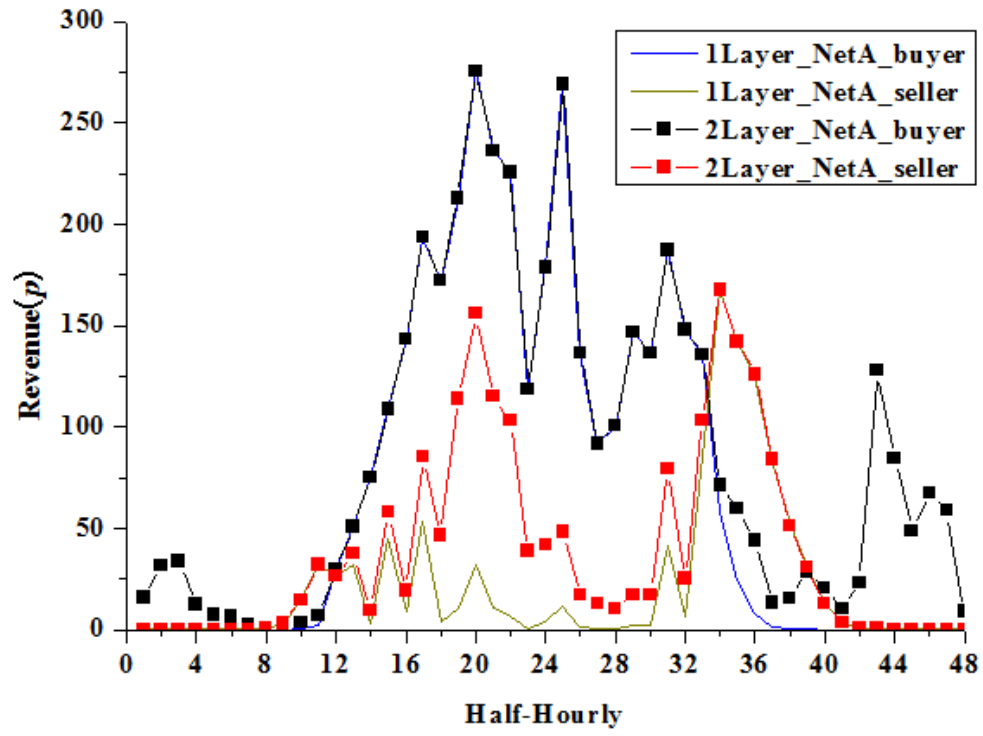
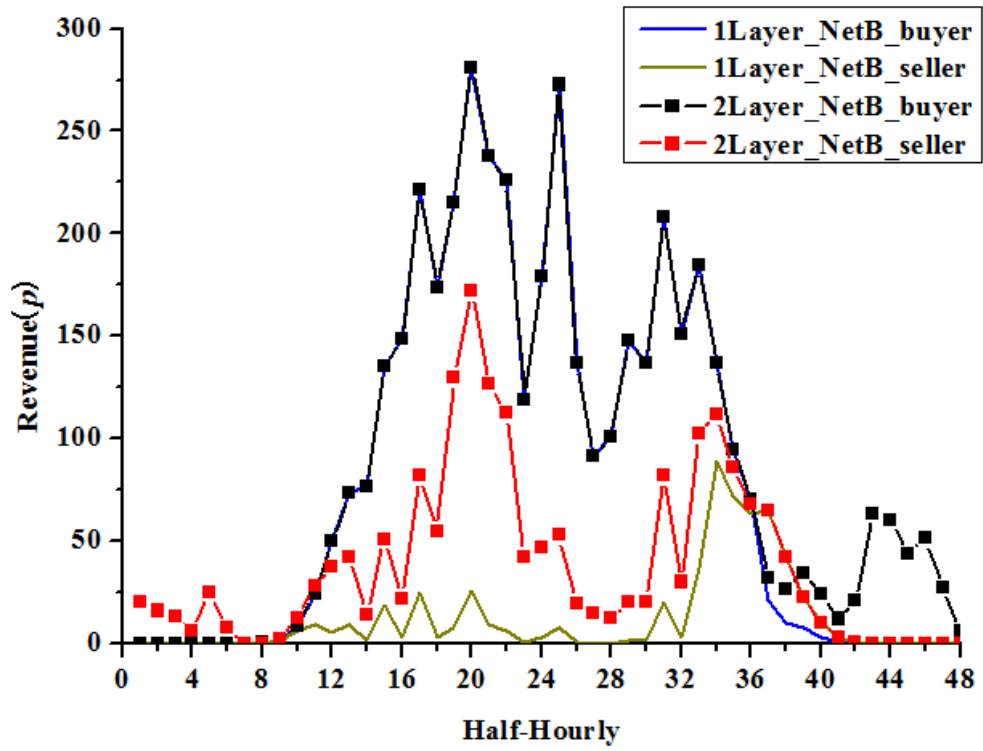


Fig. 6.18 P_P2Pvs τ & η in gateway layer

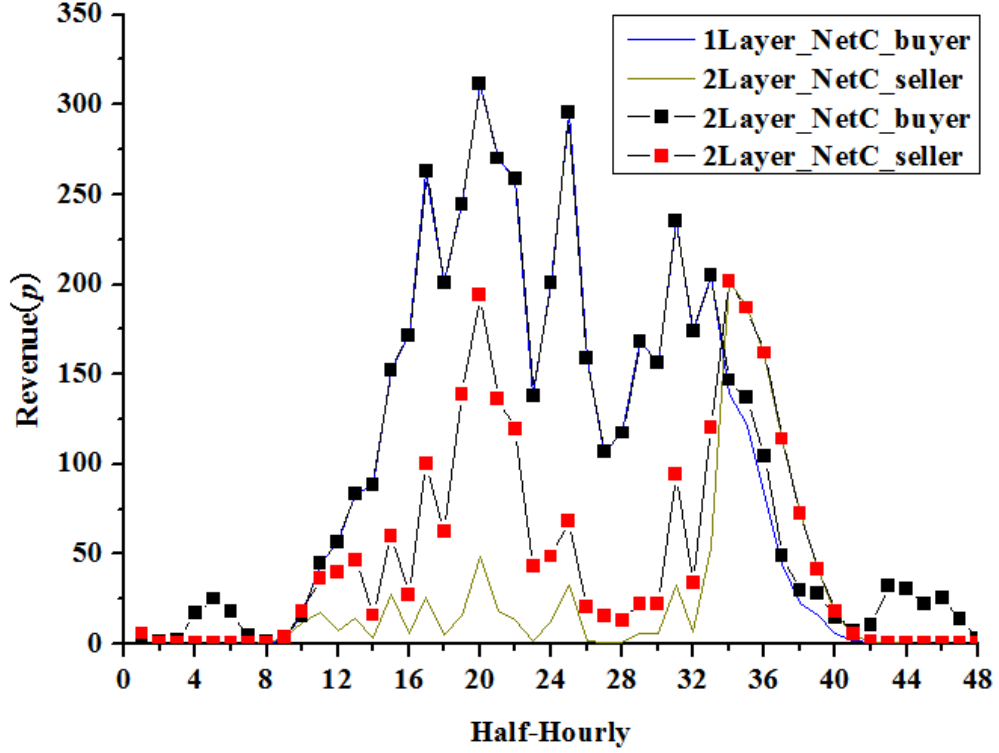
Given the price of electricity sold to the grid is lower than the price sold to peers, with the implementation of gateway layer, suppliers are offered an alternative option of selling its energy to other peers in the gateway layer where higher price could be obtained, instead of selling the exceeding supply of energy to the grid at lower price. For example, the sellers will sell the energy to grid at 4.5p/kwh from 13pm to 14pm if there is only one P2P layer in MG A. However, this energy could be sold at around 5.4p/kWh during the same period in gateway layer. Thus, we concluded that suppliers would be able to generate higher revenue with the implementation of gateway layer trading. For further verification, as shown at Fig 6.19 a, daily revenue generated by all sellers of MG A without any gateway-layer P2P network is £ 10.58 and the electricity cost for buyers is reduced from £ 41.79 to £ 34.68. While daily revenue generated by all sellers of network A with gateway-layer P2P network is £ 18.52, which shows a difference of up to 75 % of revenue. The revenue of MGs in every half hour generated from two kinds of P2P structure were shown in Fig.6.19, where we assumed that the loss of energy in transmission between each peer were ignored.



(a) Total revenues of MG_A



(b) Total revenues of MG_B



(c) Total revenues of MG_C

Fig. 6.19 Total revenues of different MGs: 1-layer P2P system vs 2-layer P2P system

6.6 Summary

In this chapter, we studied the process of energy trading in the wholesale market of UK and proposed a two-layer P2P structure to reduce the cost for end users and increase the revenue for suppliers. The two-layer P2P trading market is formulated based on the structured coalitional game theory and the Shapley value can be achieved by using the proposed pricing scenario. The theoretical analysis had proved the stability of P2P market when there are enough participants, the case study had further proved zero incentive of participants on rejecting the P2P trading, as case study had fully demonstrated that the two-layer networks had shown its advantageous by offering better system stability and profitability compare to the single-layer P2P networks. In the future we are to focus on the flexible trading in terms of the point-to-point energy prediction, where participants can decide whether to trade within the local MGs or participate in a higher-level platform by their own free will.

Chapter 7

Conclusions and Future work

This thesis focuses on analysis and optimisation of electrical power systems at the distribution network level and its cooperation with heat supply and local power generation. The main contributions include the development of power co-simulation platform for local multi vector energy system study , the optimal scheduling of CHP-based energy system, the techno-economic analysis of solar PV integration with existed electrical power system and the study of electrical power system with a P2P electricity trading mechanism.

Overview of power system evolution presented in Chapter 2 provides a clear picture to how the energy system changes with technology development, growth of renewable energy and impact from electrification of heating and transportation. The evolution has been driven by many factors; the current changes are driven by digitation – backed by IoT technology development. IoT technology enables the power network and energy systems becoming more flexible, active collaboration between the devices and systems, which will help improve energy efficiency, reduce costs, and improve stability. IoT has a positive impact on the evolution of the electrical power system in terms of power generation, power transmission and distribution, power consumption, electricity market and social impact. The overview clarified the challenges faced by power and energy sectors which motivate the studies in the thesis to address the challenges from modelling tool, optimization and operation scheduling methodology, local generation integration capacity, more efficient and flexible potential future energy trading at the distribution level.

These objectives have been achieved in the studies reported in Chapter 3,4, 5, and 6 of this thesis. The main contributions and conclusion from the work presented in the thesis are:

1) Establishment of a new co-simulation platform for local energy systems

This work described in chapter 3 is to extend the capability of HIL and IoT technologies to bring physical model, real system physical variables and operation data onto the same simulation system. This exploration is proven successful; a test system based on campus CHP dominant multi vector energy system is set up which demonstrate and experimented various methods and technology for communication, data storage, modelling operation, synchronization, algorithm implementation, computation speeding up and multi vector energy system optimisation. In chapter 3 and chapter 4, we further extended the function of co-simulation platform by adding the stability analysis in the power flow. In chapter 3, the operational optimisation of a CHP-based power system has been performed using a MILP formulation. Despite discrepancies in different metrics values between the optimisation results and measurement data, the overall shares of energy flows are similar between them. The results of an operational optimisation of this energy system can also be viewed as the reference boundaries of the real operation. In chapter 4, the simulation platform was used to evaluate the stability of campus energy system after different potential solar or battery system are considered. The platform also provided a fast evaluation tool to analyse the static economical analysis.

2) Exploration of optimisation method for local multi-energy system scheduling based on campus CHP dominant system

The two different optimization algorithms are studied and verified in chapter 4 and chapter 5. In chapter 4, In this chapter, a programming model was presented for optimising the annual operation cost in CHP-based energy system with hybrid energy resources under energy demand and supply uncertainties. To solve these uncertainties, A combined scenario generation method was introduced, where various PDF was handled and discretized conveniently. Then, SCENRED, which used Fast backward forward methods to reduce the scenarios, is proposed. A scheduling multi-objective linear programming problem was formulated with the consideration of practical constraints to minimize the energy operational cost, which included the electricity import cost from the main grid, cost of consumed natural gas, as well as the battery running cost, while satisfying time-varying demand. In chapter 4, Further optimisation is made into the installation of larger utility scale ground solar PV systems with the integration of battery systems. The installation cost for utility

solar PV is relatively small compared to rooftop solar system, so the large solar plant should be considered if the installation space is available. In the case that the surplus energy of solar system is produced and fed to the grid for free, the energy storage system may be an option. The payback years are studied and compared, which shows that the payback years of hybrid system is much longer than the solar PV installation alone without batteries.

3) Feasibility study of a P2P electricity trading mechanism in the current electricity market frame introduces game theory to the trading strategy

The P2P electricity trading mechanism with hierarchical P2P architecture is successful to enhance revenues of prosumers in proposed pricing competition algorithm. This trading mechanism is proven to be feasible to motivate prosumers to actively take part in the electricity market. In chapter 6, we studied the process of energy trading in the wholesale market of UK and proposed a two-layer P2P structure to reduce the cost for end users and increase the revenue for suppliers. The two-layer P2P trading market is formulated based on the structured coalitional game theory and the Shapley value can be achieved by using the proposed pricing scenario. The theoretical analysis had proved the stability of P2P market when there are enough participants, the case study had further proved zero incentive of participants on rejecting the P2P trading, as case study had fully demonstrated that the two-layer networks had shown its advantageous by offering better system stability and profitability compare to the single-layer P2P networks. In the future we are to focus on the flexible trading in terms of the point-to-point energy prediction, where participants can decide whether to trade within the local MGs or participate in a higher-level platform by their own free will.

This thesis proposed a co-simulation platform and various methods for the local energy system analysis and optimal operation. To this application, these ideas and platform can be applied to other power systems analysis and operation, such as wind-based power system, power system optimisation and microgrid applications. It is suggested the future work are focused on the following:

- 1) Extend the co-simulation system and enhance the flexibility of interface of platform to make it easy to integrate with other systems, such planning software, real-time simulator. Furthermore, the current co-simulation system

did not take the complex electricity market simulation into consideration so the integration of electricity market can be one part of platform to enhance the feasibility in real application. Finally, the coordination between real-time simulator and HIL system need to be further improved to reduce the data flow latency.

- 2) The planning of multi-power system is playing a crucial role in increasing system efficiency and emission reduction. Various constraints will highly affect the optimal results so the impact of various constraints on system operation cost and emission can be further analysed.
- 3) Extend the idea of scenario generation and reduction to long-term system planning, e.g., scenarios can be generated for unit commitment decisions, and with a receding time horizon approach, the scenarios can be improved as we approach the operating time. This approach has potential to deliver better results as the forecast tends to improve as the lead time decreases.
- 4) A novel P2P trading mechanism was proposed in this thesis with the consideration of increasing the willingness to participate into the electricity trading market. However, the clearance price including transmission loss and benefit margin of each parties need to be further discussed in the future.

Reference

- [1] International Energy Agency. World Energy Outlook; International Energy Agency: Paris, France, 2017.
- [2] United Nations Framework Convention of Climate Change (2015) United Nations Framework Convention on Climate Change: adoption of the Paris agreement (United Nations Framework Convention of Climate Change, ed.). United Nations, Paris. Oct 2018.
- [3] BEIS, "Energy Trend June 2020," 2020.
- [4] Chu S, Majumdar A, "Opportunities and challenges for a sustainable energy future," *Nature*, 488, 294–303, 2012.
- [5] Jenkins Nick, Long Chao, Jianzhong Wu. "An Overview of the Smart Grid in Great Britain," *Engineering*, Volume 1, Issue 4, pp.413-421, December 2015.
- [6] Pei Huang, Tao Xu, Yongjun Sun. "A genetic algorithm based dynamic pricing for improving bi-directional interactions with reduced power imbalance," *Energy and Buildings*, Volume 199, pp.275-286, September 2019.
- [7] B. Currie et al., "Flexibility Is Key in New York: New Tools and Operational Solutions for Managing Distributed Energy Resources," in *IEEE Power and Energy Magazine*, vol. 15, no. 3, pp. 20-29, May-June 2017.
- [8] Y. Yoldaş, A. Önen, S.M. Mueen, A.V. Vasilakos, İ. Alan, "Enhancing smart grid with micro-grids: challenges and opportunities," *Renew Sustain Energy Rev*, pp. 205-214, 2017.
- [9] P. Scott, D. Gordon, E. Franklin, L. Jones and S. Thiébaux, "Network-Aware Coordination of Residential Distributed Energy Resources," in *IEEE Transactions on Smart Grid*, vol. 10, no. 6, pp. 6528-6537, Nov. 2019.
- [10] M. Mao, X. Jiang, Y. Ding and J. Hu, "Hardware-in-Loop Real-Time Test Bed for Microgrid Systems with Multi-Level Control," *PCIM Asia 2019; International Exhibition and Conference for Power Electronics, Intelligent Motion, Renewable Energy and Energy Management*, pp. 1-6, 2019.
- [11] Konark Sharma, Lalit Mohan Saini, "Power-line communications for smart grid: Progress, challenges, opportunities and status," *Renewable and Sustainable Energy Reviews* Volume 67, pp. 704-751, January 2017.
- [12] Seyyed Mostafa Nosratabadi, Rahmat-Allah Hooshmand, Eskandar Gholipour, "A comprehensive review on microgrid and virtual power plant concepts

- employed for distributed energy resources scheduling in power systems,” Renewable and Sustainable Energy Reviews Volume 67, pp.341-363 January 2017.
- [13] W. Inam, D. Strawser, K. K. Afridi, R. J. Ram and D. J. Perreault, "Architecture and system analysis of microgrids with peer-to-peer electricity sharing to create a marketplace which enables energy access," 2015 9th International Conference on Power Electronics and ECCE Asia (ICPE-ECCE Asia), Seoul, pp. 464-469, 2015.
- [14] G. Migliavacca et al., "SmartNet: H2020 project analysing TSO–DSO interaction to enable ancillary services provision from distribution networks," in CIREN - Open Access Proceedings Journal, vol. 2017, no. 1, pp. 1998-2002, 10 2017.
- [15] M. Grubb, D. Newberry, "UK electricity market reform and the energy transition: emerging lessons," Energy J, pp. 2-25, 2018.
- [16] Prado, J.C, Qiao, W, Qu, L, Agüero, J.R, "The Next-Generation Retail Electricity Market in the Context of Distributed Energy Resources: Vision and Integrating Framework," Energies 2019.
- [17] Online,” <https://www.gov.uk/government/news/green-industrial-revolution-in-sight-as-government-sets-out-plans-for-more-clean-energy>”2020.
- [18] C. C. Chesney and C. F. Scott, "Early History of the A-C System in America," in Transactions of the American Institute of Electrical Engineers, vol. 55, no. 3, pp. 228-235, March 1936.
- [19] David L and Morton Jr,” Reviewing the history of electric power and electrification,” Endeavour, Pages 60-63, June 2002.
- [20] NationalGrid,”Future Energy Scenarios,”July,2020.
- [21] Europea The Climate Change Act 2008 (2050 Target Amendment) Order 2019 is available at www.legislation.gov.uk/uksi/2019/1056/contents/made.
- [22] J. Rogelj, M. Den Elzen, N. Höhne, T. Fransen, H. Fekete, H. Winkler, R. Schaeffer, F. Sha, K. Riahi, M. Meinshausen, “Paris agreement climate proposals need a boost to keep warming well below C,” Nature 534(7609), pp.631–639 2016.
- [23] W. Obergassel, C. Arens, L. Hermwille, N. Kreibich, F. Mersmann, H.E. Ott, H. Wang-Helmreich, “Phoenix from the ashes—an analysis of the paris

- agreement to the united nations framework convention on climate change,” Wuppertal Instit. Climate Environ. Energy, pp.1–54 2016.
- [24] EU Commission. ENERGY UNION PACKAGE – A Framework Strategy for a Resilient Energy Union with a Forward-Looking Climate Change Policy. Brussels; 2015.
- [25] European commission,”2030 climate & energy framework”, 2020.
- [26] A. Costa, P. Sanchez, E. Macron, M. Canete, “Lisbon Declaration,” Lisbon Accessed 5th Sep 2018.
- [27] International Renewable Energy Agency, “RENEWABLE POWER GENERATION COSTS IN 2018,” 2018.
- [28] P. Siano, “Demand response and smart grids—a survey,” *Renew. Sustain. Energy Rev.* 30, 461–478, 2014.
- [29] M.H. Albadi, E. El-Saadany, “A summary of demand response in electricity markets,” *Electric Power Syst. Res.* 78(11), 1989–1996, 2008.
- [30] Harleysville, Pennsylvania, “Consumer Attitudes About Renewable Energy: Trends and Regional Differences,” Natural Marketing Institute, 2011.
- [31] Anne Immonen, Jussi Kiljander, Matti Aro,” Consumer viewpoint on a new kind of energy market,” *Electric Power Systems Research*, Volume 180, 2020.
- [32] E. J. Palacios-Garcia, B. Arbab-Zavar, J. C. Vasquez and J. M. Guerrero, "Open IoT Infrastructures for In-Home Energy Management and Control," 2019 IEEE 9th International Conference on Consumer Electronics (ICCE-Berlin), Berlin, Germany, 2019, pp. 376-379.
- [33] A. Čolaković, M. Hadžialić, "Internet of Things (IoT): A review of enabling technologies challenges and open research issues", *Computer Networks*, vol. 144, pp. 17-39, oct 2018.
- [34] M. Mylrea and S. N. G. Gourisetti, "Blockchain for smart grid resilience: Exchanging distributed energy at speed, scale and security," 2017 Resilience Week (RWS), Wilmington, DE, pp. 18-23, 2017.
- [35] K. Christidis, M. Devetsikiotis, "Blockchains and Smart Contracts for the Internet of Things", *IEEE Access*, vol. 4, pp. 2292-2303, 2016.
- [36] Marinakis, V.; Doukas, H.; Koasidis, K.; Albuflasa, H,” From Intelligent Energy Management to Value Economy through a Digital Energy Currency: Bahrain City,” *Sensors*, 20, 1456, 2020.
- [37] International Energy Agency,” Digitalisation and Energy,” 2017.

- [38] Arthur Henriot, Jean-Michel Glachant."Melting-pots and salad bowls: The current debate on electricity market design for integration of intermittent RES," Utilities Policy, Volume 27, pp. 57-64, 2013.
- [39] Morstyn, T., Farrell, N., Darby, S.J. et al. "Using peer-to-peer energy-trading platforms to incentivize prosumers to form federated power plants," Nat Energy 3, 94–101, 2018.
- [40] Pudjianto, D. et al." Value of integrating distributed energy resources in the UK electricity system," In IEEE PES General Meeting IEEE, 2010.
- [41] Helena Lindquist."Chapter 1 - The Journey of Reinventing the European Electricity Landscape, Renewable Energy Integration (Second Edition)," Academic Press, pp. 3-13, 2017.
- [42] Q. H. Vu, M. Lupu, B. C. Ooi." Peer-to-peer computing: Principles and applications," 1st Edition, Springer, 2010.
- [43] P. Siano, G. De Marco, A. Rolán and V. Loia, "A Survey and Evaluation of the Potentials of Distributed Ledger Technology for Peer-to-Peer Transactive Energy Exchanges in Local Energy Markets," in IEEE Systems Journal, vol. 13, no. 3, pp. 3454-3466, Sept. 2019.
- [44] Hagiu, A. & Wright, J." Multi-sided platforms," Int. J. Ind. Organ. 43, pp.162–174 2015.
- [45] R. Rocha, J. Villar and R. J. Bessa. "Business models for Peer-to-Peer Energy Markets," 2019 16th International Conference on the European Energy Market (EEM), Ljubljana, Slovenia, pp. 1-6, 2019.
- [46] Moret F, Baroche T, Sorin E, Pinson P." Negotiation algorithms for peer-to-peer electricity markets: Computational properties," Accepted on 20th Power System Computation Conference, PSCC, 2018
- [47] Rouse Margaret, HYPERLINK
["https://internetofthingsagenda.techtarget.com/definition/Internet-of-Things-IoT"](https://internetofthingsagenda.techtarget.com/definition/Internet-of-Things-IoT). IOT Agenda. Retrieved 14 August 2019.
- [48] Miguel Angel Gonzalez-Salazar, Trevor Kirsten, Lubos Prchlik," Review of the operational flexibility and emissions of gas- and coal-fired power plants in a future with growing renewables," Renewable and Sustainable Energy Reviews, Volume 82, Part 1, Pages 1497-1513, 2018.

- [49] Ramamurthy A, Jain P, "The Internet of Things in the Power Sector: Opportunities in Asia and the Pacific; Asian Development Bank: Mandaluyong, Philippines, ", 2017.
- [50] Reid, Michael, and File, Tony, "Enhancement of an Equipment Reliability Program with Smart, Connected Power Plant Assets." Proceedings of the ASME 2017 Power Conference, pp.26–30, June 2017.
- [51] Immelt J.R, "The Future of Electricity Is Digital; Technical Report," MA, USA, 2015.
- [52] J Guo, C Chen, Z Lu and X Zheng, "Wind-Solar Power Consumption Strategy Based on Neural Network Prediction and Demand-side Response," 2020 Asia Energy and Electrical Engineering Symposium (AEEES), Chengdu, China, pp. 805-809, 2020.
- [53] Jianfeng Li, Dongxiao Niu, Ming Wu, Yongli Wang, Fang Li and Huanran Dong, "Research on Battery Energy Storage as Backup Power in the Operation Optimization of a Regional Integrated Energy System," *energies*, pp.1-20, 2018.
- [54] Victor Vega-Garita, Ali Hanif, Nishant Narayan, Laura Ramirez-Elizondo, Pavol Bauer, "Selecting a suitable battery technology for the photovoltaic battery integrated module," *Journal of Power Sources*, 2018.
- [55] Ahmed Hany Elgamal, Gudrun Kocher-Oberlehner, Valentin Robu, Merlinda Andoni, "Optimization of a multiple-scale renewable energy-based virtual power plant in the UK," *Applied Energy*, Volume 256, 2019.
- [56] D Tan and D Novosel, "Energy challenge, power electronics & systems (PEAS) technology and grid modernization," in *CPSS Transactions on Power Electronics and Applications*, vol. 2, no. 1, pp. 3-11, 2017.
- [57] Guneet bedi, Ganesh Kumar, Rajendra Singh and Richard R Brooks, "Review of Internet of Things (IoT) in Electric Power and Energy Systems," *IEEE INTERNET OF THINGS JOURNAL*, VOL. 5, NO. 2, April 2018.
- [58] Bin Wang, Jun Xu and Binggang Cao, "Design of a novel hybrid power for EV," 2014 IEEE Conference and Expo Transportation Electrification Asia-Pacific (ITEC Asia-Pacific), Beijing, pp. 1-5, 2014.
- [59] W. Wang and N. Yu, "A Machine Learning Framework for Algorithmic Trading with Virtual Bids in Electricity Markets," 2019 IEEE Power & Energy Society General Meeting (PESGM), Atlanta, GA, USA, pp. 1-5, 2019.

- [60] Bowley,Graham,"Preserving a Market Symbol," The New York Times. Retrieved August 7,2014.
- [61] EEX-Group," annual report 2018," Dec 2018.
- [62] McKinsey Global Institute," The Internet of Things: Mapping the Value Beyond the Hype," 2015.
- [63] World Economic Forum," World Economic Forum White Paper: Digital Transformation of Industries: Electricity—prepared in collaboration with Accenture," 2016.
- [64] General Electric. GE Power Digital Solutions.
<https://www.ge.com/digital/sites/default/files/GE%20Power%20Digital%20Solutions%20Brochure.pdf>
- [65] P. Bellagente, P. Ferrari, A. Flammini and S. Rinaldi, "Adopting IoT framework for Energy Management of Smart Building: A real test-case", Research and Technologies for Society and Industry Leveraging a better tomorrow (RTSI), 2015.
- [66] M. Cullinen, "Machine to machine technologies: Unlocking the potential of a \$1 trillion industry," AT&T Carbon War Room, Washington, DC, USA, Rep., Feb. 2013.
- [67] I. Mashal, O. Alsaryrah, T.-Y. Chung, C.-Z. Yang, W.-H. Kuo, and D. P. Agrawal, "Choices for interaction with things on Internet and underlying issues, Ad Hoc Networks," vol. 28, pp. 68–90, 2015
- [68] Sharma K, Mohan Saini L," Performance analysis of smart metering for smart grid: an overview," Renew Sustain Energy Rev;49:720–35. 2015.
- [69] Kiran Jot Singh, Divneet Singh Kapoor," Create Your Own Internet of Things: A survey of IoT platforms," IEEE Consumer Electronics Magazine. Volume: 6, Issue: 2, April 2017.
- [70] Mirjana Maksimović, Vladimir Vujović, Nikola Davidović, Vladimir Milošević and Branko Perišić," Raspberry Pi as Internet of Things hardware: Performances and Constraints," 2014.
- [71] Emmanuel Baccelli, Oliver Hahm, Mesut Günes, Matthias Wählich, Thomas Schmidt, "RIOT OS: Towards an OS for the Internet of Things,".11 Feb 2014.

- [72] G. MAURI et al, "State-of-the-Art Technologies & Protocols – Description of State-of-the-Art Communication Protocols and Data Structures: D 2.1/Part 4", Jun 2009.
- [73] J. Kethireddy and S. Suthaharan, "Visualization Teaching Tool for Simulation of OSI Seven Layer Architecture," *IEEE SoutheastCon, 2004. Proceedings.*, Greensboro, North Carolina, USA, pp. 335-34, 2004.
- [74] Online, available on <https://www.micrium.com/iot/internet-protocols>
- [75] Matteo Giacomo Prima, Matteo Lionetti, "Transition pathways optimisation methodology through EnergyPLAN software for long-term energy planning" *Applied Energy*, pp. 356-368, Feb 2019.
- [76] S. Bartha, T. Pusic, R. Anderluh, G. Krajacici, B. Vajda and L. Vlaicu, "Modelling and simulation of the energy demand and large scale integration of the electrical vehicles in "EnergyPLAN" model — Case of Romania," 2017 Electric Vehicles International Conference (EV), Bucharest, 2017, pp. 1-6. "EnergyPLAN" model — Case of Romania," 2017 Electric Vehicles International Conference (EV), Bucharest, pp. 1-6, 2017.
- [77] T. Sethi and W. Jewell, "Demand Response and Solar to Mitigate Peak Load," 2019 North American Power Symposium (NAPS), Wichita, KS, USA, pp. 1-5, 2019.
- [78] S. Eisele, P. Ghosh, K. Campanelli, A. Dubey and G. Karsai, "Demo: Transactive Energy Application with RIAPS," 2019 IEEE 22nd International Symposium on Real-Time Distributed Computing (ISORC), Valencia, Spain, pp. 85-86, 2019.
- [79] T. Duy Le, A. Anwar, R. Beuran and S. W. Loke, "Smart Grid Co-Simulation Tools: Review and Cybersecurity Case Study," 2019 7th International Conference on Smart Grid (icSmartGrid), Newcastle, Australia, pp. 39-45, 2019.
- [80] K. Hopkinson, X. Wang, R. Giovanini, J. Thorp, K. Birman, D. Coury, "EPOCHS: a platform for agent-based electric power and communication simulation built from commercial off-the-shelf components", *IEEE Transactions on Power Systems*, vol. 21, no. 2, pp. 548-558, 2006.
- [81] M. Maniatopoulos, D. Lagos, P. Kotsampopoulos, N. Hatziaargyriou, "Combined control and power hardware in-the-loop simulation for testing smart grid control algorithms", *IET Generation Transmission & Distribution*, vol. 11, no. 12, pp. 3009-3018, 2017.

- [82] David Murray-smith. "Modelling and Simulation of Integrated Systems in Engineering" Issues of Methodology, Quality, Testing and Application, Pages 269-290, 2012.
- [83] Bethany Sparn, Dheepak Krishnamurthy, Annabelle Pratt, and Mark Ruth. "Hardware-in-the-Loop (HIL) Simulations for Smart Grid Impact Studies" IEEE Power and Energy Society General Meeting Portland, Oregon August 5-9, 2018.
- [84] A. Meghwani, S. C. Srivastava and A. Srivastava, "Development of Real-Time Distribution System Testbed Using Co-Simulation," 2020 21st National Power Systems Conference (NPSC), Gandhinagar, India, 2020, pp. 1-6, doi: 10.1109/NPSC49263.2020.9331860.
- [85] Ravinder Kumar, Hari Om Bansal. "Investigations on shunt active power filter in a PV-wind-FC based hybrid renewable energy system to improve power quality using hardware-in-the-loop testing platform," electric power systems research, volume 177, Dec 2019.
- [86] Ramamurthy, A.; Jain, P. The Internet of Things in the Power Sector: Opportunities in Asia and the Pacific; Asian Development Bank: Mandaluyong, Philippines, 2017.
- [87] Shakerighadi B, Anvari-Moghaddam A, Vasquez, J.C, Guerrero, J.M. "Internet of Things for Modern Energy Systems: State-of-the-Art, Challenges, and Open Issues," Energies 2018.
- [88] Haseeb, K, Almogren A, Islam N.; Ud Din I, Jan Z. "An Energy-Efficient and Secure Routing Protocol for intrusion Avoidance in IoTBased WSN," Energies, 2019.
- [89] Beibei Xu, Diyi Chan. "Modeling a pumped storage hydropower integrated to a hybrid power system with solar-wind power and its stability analysis," Applied Energy Volume 248, Pages 446-462, 15 August 2019.
- [90] Chary, Dr. D. Venu Madhava, M. V. Subramanyam and Peddi Kishor. "P-V Curve Method for Voltage Stability and Power Margin Studies," 2017.
- [91] S. M. Said, B. Hartmann, M. M. Aly, M. Mosa and R. S. Balog, "Comparison between operating modes of distributed generation on voltage profile and stability of distribution systems," 2018 IEEE Texas Power and Energy Conference (TPEC), College Station, , pp. 1-6, 2018.
- [92] Sultan H.M, Diab A.A.Z, Kuznetsov O.N, Ali Z.M, Abdalla O, " Evaluation of the Impact of High Penetration Levels of PV Power Plants on the Capacity,"

- Frequency and Voltage Stability of Egypt's Unified Grid. *Energies* 12, 552, 2019.
- [93] Kamaruzzaman, Zetty Adibah, Azah Mohamed and Ramizi Mohamed. "Optimal placement of grid-connected photovoltaic generators in a power system for voltage stability enhancement." *Indonesian Journal of Electrical Engineering and Computer Science* 13: 339-346, 2019.
- [94] R. Zafar, J. Ravishankar, J. E. Fletcher and H. R. Pota, "Multi-Timescale Voltage Stability-Constrained Volt/VAR Optimization with Battery Storage System in Distribution Grids," *IEEE Transactions on Sustainable Energy*, vol. 11, no. 2, pp. 868-878, April 2020.
- [95] Elifuraha Reuben Mmary, Boonruang Marungsri." Integration of Renewable Energy Distributed Generation and Battery Energy Storage in Radial Power Distribution System," *International energy journal*, Jan 2019.
- [96] O.B. Adewuyi, M.S.S. Danish, A.M. Howlader, T. Senjyu, M.E. Lotfy." Network structure-based critical bus identification for power system considering line voltage stability margin," *J. Power Energy Eng.*, pp. 97-111, 2018.
- [97] W.Su, J.Wang, J Roh,"Stochastic energy scheduling in microgrids with intermittent renewable energy resources," *IEEE Trans. Smart Grid*, pp.1876-1883, 2014.
- [98] V. Davatgaran, M. Saniei, S.S. Mortazavi,"Smart distribution system management considering electrical and thermal demand response of energy hubs," *Energy*, pp. 38-49, 2019.
- [99] Shengming Tan, Xu Wang and Chuanwei Jiang," Optimal Scheduling of Hydro–PV–Wind Hybrid System Considering CHP and BESS Coordination," *applied science*, 2019.
- [100] Q.Zhu, X.Luo, B. Zhang, Y.Chen,"Mathematical modelling and optimization of a large-scale combined cooling, heat, and power system that incorporates unit changeover and time-of-use electricity price," *Energy Convers Manage*, pp. 385-398, 2017.

- [101] J.L.Mojica, D.Petersen, B.Hansen, K.M.Powell, J.D.Hedengren ,”Optimal combined log-term facility design and short-term operational strategy for CHP capacity investments,”Energy, pp.97-115,2017.
- [102] R.Yokoyama, K.Ito,”Optimal design of energy supply systems based on relative robustness criterion,” Energy Convers Manage, , pp.499-514, 2002.
- [103] K. Akbari, F. Jolai, S.F. Ghaderi,” Optimal design of distributed energy system in a neighborhood under uncertainty,” Energy , pp.567-582,2016.
- [104] G.Mavrotas, K.Florios, D.Vlachou,”Energy planning of a hospital using mathematical programming and Monte Carlo simulation for dealing with uncertainty in the economic parameters,” Energy Convers Manage, pp.722-731,2010.
- [105] C.Z.Li, Y.M.Shi, S.Liu, Z. Zheng, Y.Liu.”Uncertain programming of building cooling heating and power (BCHP) system based on Monte-Carlo method,”Energy Build, pp.1375,2010.
- [106] Michael Negnevisky, “An overview of forecasting problems and techniques in power systems, “IEEE Power and Energy Society General Meeting, pp. 1-6, July 2009.
- [107] Qia Ding, “Long-Term Load Forecast Using Decision Tree Method,” Power Systems Conference and Exposition, PSCE 06, “IEEE PES, Vol.1, pp.1541-1543, 2006.
- [108] Varadan S, Makram EB, “Harmonic Load Identification and Determination of Load Composition Using a Least Squares Method,” Electric Power Sys. Research, Vol.37, pp.203-208, 1996.
- [109] J. F. Chen, W. M. Wang and C. M. Huang, “Analysis of an Adaptive Time-Series Autoregressive Moving-Average (ARMA) Model for Short-Term Load Forecasting,” Electric Power Systems Research, Vol.34, pp.187-196, 1995.
- [110] Bengio Y, Courville A, and Vincent P, “Representation Learning: A Review and New Perspectives,” IEEE Transactions on Pattern Analysis and Machine Intelligence, vol. 35, pp. 1798-1828, 2013.

- [111] Hochreiter S and Schmidhuber J, “Long short-term memory,” *Neural computation*, vol. 9, pp. 1735-1780, 1997.
- [112] Weicong Kong, Zhao Yang Dong, Youwei Jia, “Short-Term Residential Load Forecasting based on LSTM Recurrent Neural Network,” *IEEE transactions on smart grid*, pp.1-11, Sep. 2017.
- [113] Diagne Maimouna, Mathieu. David, Philippe. Lauret, John. Boland, Nicolas. Schmutz, “Review of solar irradiance forecasting methods and a proposition for small-scale insular grids,” *Renewable and Sustainable Energy Reviews*, vol. 27, pp. 65-76, 2013.
- [114] Gamal Aburiyana, Mohamed E. El-Hawary, “An overview of forecasting techniques for load, wind and solar powers,” *IEEE Electrical Power and Energy Conference*, pp. 22-25, Oct.2017
- [115] S. X. Chen, H. B. Gooi, M. Q. Wang, “Solar radiation forecast based on fuzzy logic and neural networks,” *Renewable Energy*, vol. 60, pp. 195-201, 2013.
- [116] Jang Han, Seung Kuk, Yeol. Bae, Hong-Shik. Park, Dan Keun. Sung, “Solar power prediction based on satellite images and support vector machine,” *IEEE Transactions on Sustainable Energy*, vol. 7, no. 3, pp. 1255-1263, 2016.
- [117] Azadi Avenue, Ali Hajebrahimi, “A comprehensive review on uncertainty modelling techniques in power system studies,” *Elsevier*, pp.1078-1086, 2015.
- [118] Aien M, Rashidinejad M, Fotuhi-Firuzabad M,” On possibilistic and probabilistic uncertainty assessment of power flow problem: a review and a new approach,” *Renew Sustain Energy Rev*; 37:883–95, 2014.
- [119] Khosravi A, Nahavandi S, Creighton D, Atiya AF,” Lower upper bound estimation method for construction of neural network-based prediction intervals,” *IEEE Trans Neural Netw*, 2011.
- [120] M. Rahimiyan, “A statistical cognitive model to assess impact of spatially correlated wind production on market behaviors,” *Appl. Energy*, pp.62-72, 2014.

- [121] Aliasghar Baziar, Abdollah Kavousi-Fard," Considering uncertainty in the optimal energy management of renewable microgrids including storage devices," *Renew Energy*, pp.158-166, 2013.
- [122] H. Benchraa, A. Redouane, I. E. Harraki and A. E. Hasnaoui, "Techno-economic feasibility study of a hybrid biomass/PV/diesel/battery system for powering the village of Imlil in High Atlas of Morocco," 2018 9th International Renewable Energy Congress (IREC), Hammamet, pp. 1-6, doi: 10.1109/IREC.2018.8362541,2018.
- [123] C. Thammasorn, "Generation unit commitment in microgrid with renewable generators and CHP," 2013 10th International Conference on Electrical Engineering/Electronics, Computer, Telecommunications and Information Technology, Krabi, pp. 1-6, 2013.
- [124] M. Kia, M. S. Nazar, M. S. Sepasian, A. Heidari and P. Siano, "Optimal day ahead scheduling of combined heat and power units with electrical and thermal storage considering security constraint of power system", *Energy*, vol. 120, pp. 241-252, Feb. 2017.
- [125] W. Gu, S. Lu, Z. Wu, X. Zhang, J. Zhou, B. Zhao, et al., "Residential CCHP micro-grid with load aggregator: Operation mode pricing strategy and optimal dispatch", *Appl. Energy*, vol. 205, pp. 173-186, Nov. 2017.
- [126] A. Rong and R. Lahdelma, "An efficient model and algorithm for the transmission-constrained multi-site combined heat and power system", *Eur. J. Oper. Res.*, vol. 258, pp. 1106-1117, 2017.
- [127] D. Wei, Y. Cheng, S. Sun, J. Su and Y. Wang, "Optimal Design of Parameters and Coupling study on Multi-objective of a Combined Cooling Heating and Power System," 2018 International Conference on Power System Technology (POWERCON), Guangzhou, pp. 4238-4244, 2018.
- [128] References Hwantae Kim, Kangho Kim, et al." Co-Simulating Communication Networks and Electrical System for Performance Evaluation in Smart Grid," *Appl.Sci*, 2018.

- [129] M. Steurer, F. Bogdan, W. Ren, M. Sloderbeck, and S. Woodruff, "Controller and power hardware-in-loop methods for accelerating renewable energy integration," in Power Engineering Society General Meeting, 2007. IEEE, 2007, pp. 1–4.
- [130] Mayank Panwar, Blake Lundstrom," An Overview of Real Time Hardware-in-the-Loop Capabilities in Digital Simulation for Electric Microgrids," pp.1-5, Sep 2013.
- [131] Salwa Ben Said, Kamel BenSaad, Mohamed Benrejeb," HIL simulation approach for a multicellular converter controlled by sliding mode," International Journal of Hydrogen Energy, Volume 42, Issue 17, Pages 12790-12796, 27 April 2017.
- [132] C. Liu, H. Bai, S. Zhuo, X. Zhang, R. Ma and F. Gao, "Real-Time Simulation of Power Electronic Systems Based on Predictive Behavior," in IEEE Transactions on Industrial Electronics, vol. 67, no. 9, pp. 8044-8053, Sept. 2020.
- [133] Alireza Ghasempour," Internet of Things in Smart Grid: Architecture, Applications, Services, Key Technologies, and Challenges," Inventions, 26 March 2019.
- [134] Ahmed Egypt, "Internet of Things (IoT) System Architecture and Technologies, White Paper," Feb 2018.
- [135] Wang L, Zhang Y, Yin C, et al." Hardware-in-the-loop simulation for the design and verification of the control system of a series–parallel hybrid electric city-bus," Simulation Modelling Practice and Theory, pp.148-162, 2012.
- [136] Online:<http://docs.aws.amazon.com/iot/latest/developerguide/x509-certs>. April 2017.
- [137] Daki et al. J. Big," Data management in smart grid: concepts, requirements and implementation," Journal of Big Data.2017.
- [138] W. Lee, K. Nam, H.-G. Roh, and S.-H. Kim, "A gateway-based fog computing architecture for wireless sensors and actuator networks," in 2016 18th International Conference on Advanced Communication Technology (ICACT). pp. 210–213, IEEE, 2016.

- [139] M. Ringwelski, C. Renner, A. Reinhardt, A. Weigel, and V. Turau, "The Hitchhiker's guide to choosing the compression algorithm for your smart meter data," in Proc. IEEE Int. Energy Conf. Exhibit., Florence, Italy, 2012.
- [140] F. Zhang et al., "Application of a real-time data compression and adapted protocol technique for WAMS," IEEE Trans. Power Syst., vol. 30, no. 2, pp. 653–662, Mar. 2015.
- [141] J. Khan, S. Bhuiyan, G. Murphy, and M. Arline, "Embedded zerotree wavelet-based data compression for smart grid," in Proc. IEEE Ind. Appl. Soc. Annu. Meeting, Lake Buena Vista, FL, USA, 2013.
- [142] Nousdilis, Angelos & Chrysochos, Andreas & Papagiannis, Grigoris & Christoforidis, Georgios," The impact of Photovoltaic Self-Consumption Rate on voltage levels in LV distribution grids,"pp.650-655,2017.
- [143] J.-Ayubi and M.-Rezaei, "Lossy color image compression based on singular value decomposition and GNU GZIP," Adv. Comput. Sci. Int. J., vol. 3, no. 3, pp. 16–21, May 2014.
- [144] Network Simulator ns 3. <http://www.isi.edu/nsnam/ns/doc/index.html>.2011.
- [145] Selim Ciraci, Jeff Daily, Khushbu Agarwal," Synchronization Algorithms for Co-Simulation of Power Grid and Communication Networks," Analysis & Simulation of Computer and Telecommunication Systems. pp. 355-364, 2014.
- [146] Y. Chu, B. Urquhart, S. Gohari, H. Pedro, J. Kleissl, C. Coimbra," Short-term reforecasting of power output from a 48 MWe solar PV plant," Sol. Energy 112, 2015.
- [147] D. Larson, L. Nonnenmacher, C.F.M. Coimbra," Day-ahead forecasting of solar power output from photovoltaic plants in the American Southwest," Renew. Energy 91, 2016.
- [148] Hu W, Min Y. Zhou Y.; Lu Q,"Wind power forecasting errors modelling approach considering temporal and spatial dependence," J. Mod. Power Syst. Clean Energy, pp.489–498, 2017.
- [149] Duffy, Aidan & McLoughlin, Fintan & Conlon, Michael," The Generation of Domestic Electricity Load Profiles through Markov Chain Modelling," 2010.

- [150] Alessandrini S, Delle Monache L, Sperati S, Cervone G, “An analogue ensemble for short-term probabilistic solar power forecast,” *Appl. Energy* 157, pp.95-110, 2015.
- [151] Vaz A, Elsinga B, van Sark W, Brito M,” An artificial neural network to assessthe impact of neighbouring photovoltaic systems in power forecasting in Utrecht,” *The Netherlands, Renew.* pp.631-641, 2016.
- [152] Y. Wang, “Energy storage operation under uncertainty,” 2017.
- [153] G. Nicole, “Gams/scenred tutorial: Technical report,”
- [154] P. Ramsami, V. Oree,” A hybrid method for forecasting the energy output of photovoltaic systems,” *Energy Convers.* pp.406-413, 2015.
- [155] Genest C, Favre AC, “Everything you always wanted to know about copula modeling but were afraid to ask,” In: *symmetries in nuclear structure*, pp. 117–24, 2003.
- [156] Abdulkarim A, Abdelkader S.M, Morrow D.J, “Statistical analyses of wind and solar energy resources for the development of hybrid microgrid,” 2nd International Congress on Energy Efficiency and Energy Related Materials (ENEFM2014), Springer International Publishing, pp. 9-14, 2015.
- [157] Sepehry M, Heidari-Kapourchali M, Aravinthan V, “Modelling of uncertainty in distribution network reconfiguration using Gaussian Quadrature based approximation method,” *Power and Energy Society General Meeting (PESGM), IEEE*, pp. 1-5, 2016.
- [158] Guangta Tang, Zhao Xu,” A coordinated dispatch model for electricity and heat in a Microgrid via particle swarm optimization,” *Transactions of the Institute of Measurement and Control.* Pp.44-55, Feb 2013.
- [159] Parastegari M, Hooshmand R, Khodabakhshian A, Zare A,” Joint operation of wind farm, photovoltaic, pump-storage and energy storage devices in energy and reserve markets,”. *Int J Electr Power Energy Syst.*pp.75-84,2015,
- [160] Javier Silvente, Lazaros G. Papageorgiou, Vivek Dua, “Optimal management of microgrids under uncertainty using scenario reduction,”*Computer Aided Chemical Engineering*, Volume 40, pp. 2257-2262, 2017.
- [161] Bo Fu, Chenxi Ouyang, Chaoshun Li, Jinwen Wang and Eid Gul,” An Improved Mixed Integer Linear Programming Approach Based on Symmetry

- Diminishing for Unit Commitment of Hybrid Power System” energies, March 2019.
- [162] CHRISTODOULOS A FLOUDAS,” Mixed Integer Linear Programming in Process Scheduling: Modelling, Algorithms, and Applications,” *Annals of Operations Research*.pp.139-162,2005.
- [163] Benders J F,” Partitioning procedures for solving mixed-variables programming problems,” *Numer Math*, pp.238–252, 1962.
- [164] Shahabi M, Unnikrishnan A, Boyles S D,” An outer approximation algorithm for the robust shortest path problem,” *Trans Res Part E: Logist Trans Rev*. pp.52–66, 2013.
- [165] Quesada I, Grossmann I E,” An LP/NLP based branch and bound algorithm for convex MINLP optimization problems,” *Comput Chem Eng*, pp.937–947, 1992.
- [166] Padberg, Manfred, Rinaldi, Giovanni,” A Branch-and-Cut Algorithm for the Resolution of Large-Scale Symmetric Traveling Salesman Problems,” *SIAM Review*.1991.
- [167] John E. Mitchell,” Branch-and-Cut Algorithms for Combinatorial Optimization Problems,” *Mathematical Sciences*, September 1999.
- [168] Flener, Pierre & Pearson, Justin & Sellmann, Meinolf & Van Hentenryck, Pascal. (2006). Static and Dynamic Structural Symmetry Breaking. 4204. 695-699. 10.1007/11889205_53.
- [169] Alemany J, Magnago F, Moitre D, Pinto H,” Symmetry issues in mixed integer programming-based Unit Commitment,” *Int. J. Electr. Power Energy Syst*. Pp.86-90, 2014.
- [170] Christian Milan, Michael Stadler, Gonçalo Cardoso, Salman Mashayekh,” Modeling of non-linear CHP efficiency curves in distributed energy systems,” *Applied Energy*, Volume 148, 2015.
- [171] Online.https://www.globalpetrolprices.com/UnitedKingdom/natural_gas_prices.
- [172] Jianwei Li, Xudong Wang, Zhenyu Zhang, Simon Le Blond, Qingqing Yang, Min Zhang et al. Analysis of a new design of the hybrid energy storage system used in the residential m-CHP systems. *Appl Energy*, pp.167-179, 2017.

- [173] Baljinnnyam Sereeter, Cornelis Vuik, Cees Witteveen, "On a comparison of Newton–Raphson solvers for power flow problems," *Journal of Computational and Applied Mathematics*, Volume 360, pp.157-169, 2019.
- [174] H. Le Nguyen, "Newton-Raphson method in complex form [power system load flow analysis]," in *IEEE Transactions on Power Systems*, vol. 12, no. 3, pp. 1355-1359, Aug. 1997.
- [175] Hongbo Sun, "A Fast and Robust Load Flow Method for Distribution Systems with Distributed Generations," *ICSGCE 2011*: 27–30. 2011.
- [176] Deutsche Bank Markets Research, "Industry Solar," 27 February 2015.
- [177] Da Costa VM, Martins N, Pereira JLR, "Developments in the Newton-Raphson power flow formulation based on current injections," *IEEE Transactions on Power Systems*. 1999.
- [178] Erwin Nashrullah, Abdul Halim, "Polynomial Load Model Development for Analysing Residential Electric Energy Use Behaviour," *ICIEE*, 2018.
- [179] S Kamel , M Abdel-Akher , F Jurado, "Improved NR current injection load flow using power mismatch representation of PV bus" *Electrical Power and Energy Systems*, pp.64-68, 2013.
- [180] Ioannis Stavropoulos, "Study of Optimisation Strategy of the University Campus Energy System," 2018.
- [181] Y Wang, A Bermukhambetova, J Wang, M Donner, "Modelling of the whole process of a university campus CHP power plant and dynamic performance study," *International Journal of Automation and Computing*, pp.53-63. 2016
- [182] A. M. Neto, A. C. Victorino, I. Fantoni and D. E. Zampieri, "Real-time dynamic power management based on Pearson's Correlation Coefficient," 15th International Conference on Advanced Robotics (ICAR), Tallinn, pp. 304-309, 2011,
- [183] UK parliamentary office of science & technology, "Carbon Footprint of Electricity Generation," June, 2011.
- [184] Online. <http://www.solar mango.com/ask/2015/10/26/what-is-the-installation-cost-of-utility-scale-solar-power-plant-mw-in-the-uk/>. 2015.
- [185] Online. www.hesa.ac.uk/data-and-analysis/publications/estates-2014-15, 2016
- [186] IRENA, "Electricity storage and renewables: costs and markets to 2030," 2017.

- [187] Sungwook Kim, "Game Theory Applications in Network Design, "IGI Global, 2014.
- [188] Hasimoto-Beltran, R Lopez-Fuentes F & Vera-Lopez M," Hierarchical P2P architecture for efficient content distribution," Peer-to-Peer Netw. Appl. 12, 724–739,2019.
- [189] Olamide Jogunola, Augustine Ikpehai, Kelvin Anoh," Comparative Analysis of P2P Architectures for Energy Trading and Sharing," energies, pp.1-10, Dec.2017.
- [190] "Gnutella Protocol Development – RFC-Gnutella 0.6", <http://rfc-gnutella.sourceforge.net/developer/testing/index.html>, accessed April 2006.
- [191] LVQ, CAO P, COHEN E, LI K AND SHENKER S," Search and Replication in Unstructured Peer-to-Peer Networks," In Proceedings of 16th ACM International Conference on Supercomputing(ICS'02), June 2002.
- [192] Almasalma H, Engels J, Deconinck G," Peer-to-peer control of microgrids," In Proceedings of the IEEE Benelux PELS/PES/IAS Young Researchers Symposium, Eindhoven, The Netherlands, pp.12–13 May 2016.
- [193] Bin Wang, Qing-guo Shen,"An effective and practical design for hierarchical-structured P2P model,"Computer Communications,Volume 35, Issue 13,2012.
- [194] J. Li and S. Vuong, "Ontology-based Clustering and Routing in Peer-to-Peer Networks," Proc. International Conference on Parallel and Distributed Computing, Applications and Technologies (PDCAT '05), Dalian, China, pp. 791-79, Dec2005.
- [195] Werth A, Andre A, Kawamoto D, Morita T, Tajima S, Yanagidaira D, Tokoro M, Tanaka K," Peer-to-peer control system for DC microgrids," IEEE Trans. Smart Grid, 2016.
- [196] Saleh M. S, Althaibani A, Esa Y, Mhandi Y, Mohamed A.A," Impact of clustering microgrids on their stability and resilience during blackouts," International Conference on Smart Grid and Clean Energy Technologies (ICSGCE), pp.195–200.2015.

- [197] Office of the National Coordinator for Smart Grid Interoperability. NIST framework and roadmap for smart grid interoperability standards; 2012.
- [198] Hugo T.C. Pedro, Carlos F.M. Coimbra, "Assessment of forecasting techniques for solar power production with no exogenous inputs," Solar Energy, pp. 2017-2028, 2012.
- [199] E. Mengelkamp, J. Garttner and C. Weinhardt, "The role of energy storage in local energy markets," 2017 14th International Conference on the European Energy Market (EEM), pp. 1-6, 2017.
- [200] T. M. Liggett, S. A. Lippman, and R. P. Rumelt, "The asymptotic Shapley value for a simple market game," Econ. Theory, vol. 40, no. 2, pp. 333– 338, Aug. 2009.
- [201] Woongsup Lee, E, Lin Xiang, "Direct Electricity Trading in Smart Grid: A Coalitional Game Analysis" IEEE journal of selected areas communications, pp.1398-1411, JULY.2014.
- [202] Z. Han, D. Niyato, W. Saad, T. Basar, and A. Hjørungnes, "Game Theory in Wireless and Communication Networks," Cambridge, U.K.: Cambridge Univ. Press, 2012.
- [203] [Online].<https://www.nimblefins.co.uk/average-cost-electricity-kwh-uk#nogo>.
- [204] [Online]. <http://www.elia.be/en/grid-data/power-generation/wind-power>.
- [205] [Online].http://gridlabd.shoutwiki.com/wiki/Hybrid_Electric_Vehicle_Chargers.